GIS PLATFORM FOR MANAGEMENT OF SHALLOW GEOTHERMAL RESOURCES

PhD Thesis

Department of Geotechnical Engineering and Geosciences, ETCG
Technical University of Catalonia, UPC
Institute of Environmental and Water Research, IDAEA-CSIC
Barcelona, Spain

María del Mar García Alcaraz

Supervisors:

Enric Vázquez-Suñé
Violeta Velasco

February, 2016

This thesis was founded by the Spanish Ministry of Economy and Competitiveness project MEDISTRAES (CGL2013-48869-C2-1-R) and by the Generalitat de Catalunya (Grup Consolidat de Recerca: Grup d'Hidrologia Subterrània, 2009-SGR-1057).

A mis abuelos, Ana y María, y Emilio y Aurelio

Abstract

This thesis promotes an efficient use of shallow geothermal energy by means of an integrated management system to organize its exploitation. Shallow geothermal energy is a renewable resource based on thermal energy exchange with the ground. Due to the growth in demand for this energy, the development of management techniques to organize the exploitation of this resource is mandatory to protect both groundwater and the users' rights.

Shallow geothermal performance of underground is closely related to groundwater behavior, so it is necessary to understand and improve the knowledge about it. Thus, an integrated methodology is proposed for the 3D visualization of underground resources related to groundwater. A set of tools named *HEROS3D* was developed in a GIS environment to support the generation of 3D entities representing geological, hydrogeological, hydrochemical and geothermal features.

The GIS technology also gives a wide-ranging support to environmental modeling, either conceptual or numerical, especially to groundwater modeling. However, there is a scarcity of tools to implement the conceptual model in numerical modeling platforms. This transition needs of specific methodologies to adapt the geometries and alpha-numerical data from the conceptual model to the numerical model to get optimal numerical results. Although most necessities can be satisfied with inherent GIS tools, there are particular steps in the implementation of hydrogeological conceptual model into the numerical modeling software that have not been solved yet. To overcome this gap, a set of tools is presented, named

ArcArAz. It focuses on the configuration of geometry and parameterization for groundwater numerical models.

Once both the hydrogeological conceptual model and the numerical model are defined, a solid basis for management of Shallow Geothermal energy is available. This thesis proposes two methodologies for the management of this energy resource at two different scales: for a regional scale and for a metropolitan scale.

The first GIS methodology provides a response to the need for a regional quantification of the geothermal potential that can be extracted by Boreholes Heat Exchangers and its associated environmental impacts. For the first time, advection and dispersion heat transport mechanisms and the temporal evolution from the start of operation of the BHE are considered in the regional estimation of the variables of interest. A sensitivity analysis leads to the conclusion that the consideration of dispersion effects and temporal evolution of the exploitation prevent significant differences up to a factor 2.5 in the heat exchange rate accuracy and up to several orders of magnitude in the impacts generated.

To deepen the management of Shallow Geothermal Energy, this thesis proposes to establish a market of shallow geothermal energy use rights which would allow managing this resource at a metropolitan scale. This methodology is based on a GIS framework and is composed of a geospatial database to store the main information required to manage the installations and a set of GIS tools used to define, implant and control this use rights market. Thermal impacts derived from the exploitation of this resource can also be registered geographically, by taking into account the groundwater flow direction and adjusting the thermal impact to the available plot.

Resumen

Esta tesis promueve el uso eficiente de la geotermia somera a través de un sistema integrado de gestión de este recurso. La geotermia somera es un recurso renovable que se basa en el intercambio de energía con el suelo. Los Intercambiadores de calor, o Borehole Heat Exchangers (BHEs) se están popularizando como sistema para explotarla. Debido al crecimiento en la demanda de geotermia somera, es imprescindible establecer una gestión integrada de este recurso para organizar su explotación y proteger tanto a las aguas subterráneas como a los beneficiarios de esta energía renovable.

Debido a que la geotermia somera está íntimamente relacionada con el comportamiento de las aguas subterráneas, es imprescindible ahondar y mejorar su conocimiento. Para ello, se propone una metodología para la visualización tridimensional de los recursos subterráneos relacionados con la hidrogeología. Se ha desarrollado un conjunto de herramientas, llamado *HEROS3D*, en un entorno SIG. Estas herramientas facilitan la creación de entidades tridimensionales que representan datos geológicos, hidrogeológicos, hidrogeoquímicos y geotermales. Están relacionadas con una base de datos donde tanto la información bruta como la interpretada se encuentran almacenadas.

La tecnología SIG también da soporte, no sólo a la modelación conceptual, sino también a la numérica, especialmente en el caso de la hidrogeología. Para facilitar la implementación de los modelos conceptuales en las plataformas de modelación numérica, esta tesis presenta un segundo conjunto de herramientas,

llamado *ArcArAz*. Estas herramientas ofrecen soluciones a los problemas más comunes relacionados con la configuración de la geometría de entrada al modelo numérico, así como su parametrización.

Las bases para una gestión eficiente de la geotermia somera se establecen una vez que hemos definido y están disponibles tanto el modelo hidrogeológico conceptual como el modelo numérico. En relación a este aspecto, en esta tesis se proponen dos metodologías de gestión enfocadas a escalas diferentes: escala regional y escala metropolitana o local.

La primera metodología SIG ofrece una respuesta a la necesidad de una cuantificación regional del potencial geotérmico somero que puede extraerse con intercambiadores de calor o Borehole Heat Exchangers, así como sus impactos térmicos asociados. Por primera vez pueden tenerse en cuenta en la estimación regional de las variables de interés la advección y dispersión de calor, como mecanismos de transporte de calor, así como la evolución temporal desde el inicio de la explotación. Un análisis de sensibilidad demuestra que la consideración de los efectos de dispersión así como el régimen temporal de la explotación supone diferencias de hasta 2.5 veces el potencial extraído y hasta de varios ordenes de magnitud en los impactos térmicos generados.

Para profundizar en la gestión de la geotermia somera a escala local, esta tesis propone establecer un mercado de derechos de uso de este recurso. Esta metodología se ha implementado en un ambiente SIG y está compuesta de una base de datos donde se almacena la información principal necesaria para gestionar las instalaciones y de un conjunto de herramientas para definir, implantar y controlar este mercado de derechos de uso de geotermia somera. Los impactos térmicos derivados de la explotación de este recurso pueden quedar registrados geográficamente, teniendo en cuenta la dirección de flujo de las aguas subterráneas y ajustando estos impactos a la superficie de la parcela disponible.

Agradecimientos

Table of Contents

List of Figures

List of Tables

Acronyms

BHD	BoreHole Diagram
BHE	Borehole Heat Exchanger
DEM	Digital Elevation Model
GCHP	Ground-Coupled Heat Pump
GIS	Geographic Information System
GWHP	Ground Water Heat Pump
LTGE	Low Temperature Geothermal Energy
MILS	Moving Infinity Line Source model
RDBMS	Relatonal Database Management System
SC-SC	Stratigraphic Cross-Sections Correlation
SGP	Shallow Geothermal Potential
SGE	Shallow Geothermal Energy
SIG	Sistema de Información Geográfica
TIN	Triangular Irregular Network

I. INTRODUCTION

In the current scenario of global climatic change, sustainably meeting the need for energy is a worldwide goal. Several studies have been carried out to demonstrate the viability of substitute carbon when producing power and heat [1]–[3]. Thus, renewable energies are being promoted by public and private entities. As documented in [4] and [5], the European Union estimated that shallow geothermal energy (SGE), also known as Low Temperature Geothermal Energy (LTGE), would be the renewable energy resource with the most growth from 2009 to 2020 [6].

SGE is the renewable energy accumulated in the ground and available for heat exchange with an external medium at low temperature. The exploitation of SGE consists of exchanging heat between the ground in the first approx. 100 m depth and any installation or building that needs heat or to dissipate it. According to [7]–[10], it has been shown as a feasible option to satisfy the energy demand for heating and cooling, especially in combination with other energy sources.

SGE provides an alternative energy source with several advantages [11] over other renewable energies, such as: the lowest environmental impact of any renewable energy source, high availability regardless of weather conditions, decentralized and localized production and economic viability.

In this scenario, two common situations are usually found in European countries:

1. Energy strategies involving SGE are not yet sufficiently developed despite its advantages. To popularize the use of SGE, it would be necessary to provide

the decision-makers with suitable tools to facilitate the implementation of this energy resource. As starting point, the estimation of the Shallow Geothermal Potential (SGP) at a regional scale together with the assessment of the environmental impact produced by its exploitation should be available.

2. The use of SGE is expanding greatly during last years (for further details see [12]). In this case, an accurate management of SGE is paramount for the development of effective renewable energy strategies [13]–[15]. In fact, the rapid growth in the implementation of SGE exploitations is causing incipient thermal impacts which are affecting current users of SGE. This is due to the scarcity of management methodologies for this energy resource [16], [17]. Thus, it is obligatory to organize and manage the exploitation of this resource with appropriate methodologies.

1. BACKGROUND AND INITIAL REQUIREMENTS

The main methods for making use of Shallow Geothermal Energy (SGE) are the Ground Heat Pumps Systems, classified as open and closed-loop systems. Open-loop systems are pumping wells which extract groundwater from the aquifer to make the heat exchange. After that, the groundwater, whose temperature has been altered, is reinjected into the aquifer. By contrast, closed-loop systems are vertical boreholes with a heat exchanger inside them known as Borehole Heat Exchangers (BHE). The heat is extracted or dissipated directly with the ground, without varying the hydraulic regimen of the aquifer. In both cases, the exploitation of this energy resource adds a new physical impact to groundwater media by altering its temperature.

For any kind of the aforementioned exploitation systems, shallow geothermal resources are extremely dependent on groundwater behavior. The presence of groundwater determinates the heat transport mechanisms to be taken into account to suitably represent the thermal respond of underground media. Thus, the groundwater behavior must be analyzed and defined in order to elaborate accurate hydrogeological and geothermal conceptual models as well as numerical models.

To accomplish a thorough analysis and management of urban underground resources, especially of SGE and others, it is mandatory to improve the knowledge of groundwater flow processes. The efficiency and proper performance of underground services, such as dewatering systems or SGE exploitations, depend largely on the properties and conditions of the groundwater system [18], [19].

Groundwater modelling represents an essential tool to identify, conceptualize and quantify the different processes that occur in the subterranean media and allows evaluating the affections and interferences [20]–[22]. The construction of reliable hydrogeological conceptual models requires a solid geological characterization of the subsurface media (e.g., [23], [24]). Both the geometry and properties of the different geological bodies and their connectivity must be provided with the adequate scale. Moreover, according to the nature of the process of interest (e.g., geotechnical, hydraulic or geothermal problems), the definition of specific variables will be required.

2. GIS: THE MOST SUITABLE TOOL

Since the 80's, Geographical Information Systems (GIS) technologies have been applied to support environmental modeling. GIS have been demonstrated to be the most efficient tool to deal with geometric and alpha-numeric data to this purpose [25].

The construction of reliable hydrogeological conceptual models requires the integration of information from different type of formats (paper, ASCII files, Excel files, databases) and of diverse nature (geological, hydrochemical, geophysical, hydrogeological, hydrological or meteorological data, etc...). Moreover, data are usually available on incongruent scales.

Although GIS inherent capabilities provide of advanced tools for the study of underground resources, specific competences must be developed inside GIS platforms to meet the new challenges arising in the field of hydrogeology.

To deal with this situation, the Hydrogeology Group (GHS; CSIC-UPC) started to develop a GIS-based platform specially oriented to facilitate the hydrogeological modeling, termed *HEROINE* (for further information see [24], [26]–[28]), in the frame of a previous doctoral thesis [26]. This thesis continues this line of research, by extending

HEROINE with new methodologies and tools to give a solution to certain problems still unsolved.

3. OBJECTIVES AND THESIS OUTLINE

In light of the foregoing discussion, the main objective of this thesis is to give support and promote the efficient exploitation of shallow geothermal resources as energy supply through an integrated management system for underground resources.

Each chapter of this thesis responds to specific objectives proposed to achieve this main objective. These objectives are presented below along with a brief description of the corresponding chapter:

- To improve existing methodologies and develop new ones for data management during the construction of hydrogeological conceptual models to facilitate their construction and understanding.

Chapters II and III are focused on this objective. Chapter II presents the already existing GIS-based platform *HEROINE* and the developments implemented in this platform. They are illustrated with their application to the Great Basin of Calama, Chile. Chapter III describes the GIS-based methodologies and instruments generated for the analysis, visualization and creation of 3D geological models to be used in hydrogeological modeling. Moreover, these new methodologies allows for a 4D representation of hydrogeological, hydrochemical and geothermal data (taking the time as a fourth variable) along with the 3D geological model.

- To facilitate the implementation of hydrogeological conceptual models into numerical models.

To fulfill this goal, chapter IV presents GIS-based methods to adapt the hydrogeological conceptual model to numerical software platforms. The geometry and alpha-numerical data required for numerical model can be structured and pre-processed to be exported to numerical software. The automation of geometric processes saves time and resources when working with finite element meshes.

- To quantify shallow geothermal energy resources and environmental impacts in an accurate manner.

Chapter V describes a GIS-based methodology to estimate the shallow geothermal potential and its associated environmental impacts at regional scale. It is based on map-algebra, where the solution of the heat transport equation in porous media is solved for each raster cell. To achieve the most accurate results, this solution considers the main heat transport mechanisms: advection and dispersion.

- To establish management methodologies for shallow geothermal energy.

Chapter VI proposes a market of shallow geothermal energy use rights to arrange this resource among all interested participants with GIS techniques. This methodology facilitates the management of shallow geothermal energy at metropolitan scale, applying technical criteria to consider geological and hydrogeological characteristics of each plot.

4. SCIENTIFIC ARTICLES AND TECHNICAL REPORTS RELATED

This thesis is characterized for being the result of the intersection of two complementary aspects:

- Scientific: definition of new knowledge fields in the groundwater area and development of methodologies for its application.
- Technical: application of developed methodologies to several study sites in cooperation with water management public entities.

The development of this thesis was conditioned by this double viewpoint, which has enriched both aspects. As a result, articles and technical reports were written on the subject. A list of them is shown below.

4. 1. Scientific articles

Each chapter of this thesis is based on the following research articles:

2016	**M. Alcaraz**, A. García-Gil, E. Vázquez-Suñé, V. Velasco. Advection and dispersion heat transport mechanisms in the quantification of shallow geothermal resources and associated environmental impacts. *Science of the Total Environment.* DOI:10.1016/j.scitotenv.2015.11.022 IF: 4.099 Ranking in ENVIRONMENTAL SCIENCE category: 18/223, Q1
2016	**M. Alcaraz**, A. García-Gil, E. Vázquez-Suñé, V. Velasco. Use rights markets for shallow geothermal energy management. *Applied Energy*. Accepted with major revisions. IF: 5.613 Ranking in ENGINEERING, CHEMICAL category: 6/135, Q1
2016	**M. Alcaraz**, E. Vázquez-Suñé, V. Velasco. 3D GIS-based visualization of geological, hydrogeological, hydrogeochemical and geothermal models. *German Journal of Geosciences.* Submitted. Journal not indexed.
2016	**M. Alcaraz**, E. Vázquez-Suñé, V. Velasco, D. Fernández. Integrated hydrogeology framework for water management in arid zones exploited by mining. *Hydrogeology Journal*. In elaboration. IF: 0.743 Ranking in GEOSCIENCE, MULTIDISCIPLINARY category:22/83, Q2
2016	**M. Alcaraz**, E. Vázquez-Suñé, V. Velasco. GIS tools to optimize implementation of groundwater conceptual models into numerical modeling. *Environmental Modelling & Software*. In elaboration.

The scientific production in the frame of this thesis is complemented with the following research articles.

2015	R. Criollo, V. Velasco, E. Vázquez-Suñé, A. Serrano-Juan, **M. Alcaraz,** A. García-Gil. An integrated GIS-based tool for Aquifer Test Analysis. *Environmental Earth Sciences.* DOI: 10.1007/s12665-016-5292-3 IF: 1.765; Ranking in WATER RESOURCES category: 26/83, Q2
2015	A. García-Gil, E. Vázquez-Suñé, J. Sánchez-Navarro, J.M. Lázaro, **M. Alcaraz.** The propagation of complex flood-induced head wavefronts through a heterogeneous alluvial aquifer and its applicability in groundwater flood risk management. *Journal of Hydrology.* DOI: 10.1016/j.jhydrol. 2015.05.005

	IF: 3.053; Ranking in WATER RESOURCES category: 7/83, Q1
2015	A. García-Gil, E. Vázquez-Suñé, **M. Alcaraz**, A. Serrano-Juan, J.A. Sánchez-Navarro, M. Montleó, G. Rodriguez, J. Lao. GIS-supported mapping of low-temperature geothermal potential taking groundwater flow into account. *Renewable Energy.*DOI: 10.1016/j.renene.2014.11.096 IF: 3.476. Ranking in ENERGY & FUELS category: 20/89, Q1
2014	V. Velasco, I. Tubau, E. Vázquez-Suñé, D. Gaitanaru, R. Gogu, **M. Alcaraz**, A. Serrano, X. Sánchez, D. Fernandez, J. Fraile, T. Garrido. GIS based Hydrochemical Analysis Tools (QUIMET). *Computers & Geosciences.* DOI: 10.1016/j.cageo.2014.04.013 IF: 2.054; Ranking in COMPUTER SCIENCE, INTERDISCIPLINARY APPLICATIONS category: 25/102, Q1
2012	V. Velasco, R. Gogu, E. Vázquez-Suñé, A. Garriga, E. Ramos, J. Riera, **M. Alcaraz**. The use of GIS based 3d geological tools to improve hydrogeological models of sedimentary media in an urban environment. *Environmental Earth Sciences.* DOI: 10.1007/s12665-012-1898-2 IF: 1.765; Ranking in WATER RESOURCES category: 26/83, Q2

4. 2. Chapters in books

Violeta Velasco, Enric Vázquez-Suñé, **Mar Alcaraz**, Alejandro Serrano-Juan, Isabel Tubau, Xavier Sánchez-Vila, Daniel Fernández-García, Teresa Garrido, Josep Fraile.
GIS-based software platform for managing hydrogeochemical data in the book *Experiences from Ground, Coastal and Transitional Water Quality Monitoring. The EU Water Framework Directive Implementation in the Catalan River Basin District* (Vol. II. Chapter 4) The Handbook of Environmental Chemistry, pp. 91 - 118.
Springer International Publishing Switzerland, 2015.
DOI: 10.1007/698_2015_368

4. 3. Proceedings in congresses

2015	Velasco, V., Vázquez-Suñé, E., Criollo, R., **Alcaraz, M**., Serrano, A., García-Gil, A. GIS-based tools for facilitating the development of hydrogeological models. *42nd IAH CONGRESS. Rome, Italy. 13-18 September 2015.*
2015	**M. Alcaraz**. GIS-BASED TOOLS FOR QUANTIFICATION OF SHALLOW GEOTHERMAL RESOURCES. *Oral presentation*

1st Meeting of Young Researchers from IDAEA-CSIC. Barcelona, 22nd October 2015.

2015 **M. Alcaraz**, V. Velasco, E. Vázquez-Suñé.
GIS-Based 3D geological analysis tools. *Short article and oral presentation.*
EUREGEO, 8th European Congress on Regional Geoscientific Cartography and Information Systems, Barcelona, Catalonia, Spain. June 15th-17th 2015.
ISBN: 978-84-393-9292-7. Vol. 1, pp. 25-26.

2015 Velasco, V., **Alcaraz, M**., Vázquez-Suñé, E., Criollo, R., Serrano, A., García-Gil, A.
GIS-Based tools for facilitating the application of the groundwater related directives.
GEOProcessing 2015. February 22-27, 2015 - Lisbon, Portugal.

2014 **M. Alcaraz**, V. Velasco, E. Vázquez-Suñé (2014).
Desarrollo de herramientas en un entorno GIS para la creación de modelos geológicos en 3D. *Poster.*
II Congreso Ibérico de las Aguas Subterráneas (CIAS 2014) Valencia, España, Septiembre 2014.
ISBN: 978-84-9048-239-1. Volumen 1, 3-4.

2014 V. Mansilla, E. Vázquez-Suñé, R. Criollo, M. Alcaraz, A. Serrano-Juan, A. García-Gil.
Desarrollo de herramientas de análisis de datos hidrogeológicos en un entorno SIG.
II Congreso Ibérico de las Aguas Subterráneas (CIAS 2014), Valencia, España Septiembre 2014.

2014 R. Criollo, E. Vázquez-Suñé, V. Velasco, A. Serrano-Juan, **M. Alcaraz**, A. García-Gil (2014).
Herramientas de interpretación de ensayos hidráulicos en un entorno SIG.
II Congreso Ibérico de las Aguas Subterráneas (CIAS 2014), Valencia, España Septiembre 2014.
ISBN: 978-84-9048-239-1. Volumen 1, 43-44.

2013 Velasco, V., Vázquez-Suñé, E., Criollo, R., **Alcaraz, M.**, Serrano-Juan, A., García-Gil, A., Tubau, I., Gogu, R., Gaitanaru, D.
GIS-based Hydrogeological Database and Analysis Tools.
INFOCOMP2013. The Third International Conference on Advanced Communications and Computation. 17-22 Noviembre, Lisboa (Portugal).IARIA, 2013.
ISBN: 978-1-61208-310-0. Vol1, 105-109.

2013 V. Velasco, E. Vázquez-Suñé, R. Gogu, **M. Alcaraz**, D. Gaitanaru, A. Serrano, R. Criollo, A. García-Gil.

GIS-based hydrogeological analysis tools.
The Fifth International Conference on Advanced Geographic Information Systems, Applications, and Services. GEOProcessing 2013.February 24 - March 1, 2013 - Nice, France.

2012 V. Velasco, I. Tubau, E. Vázquez-Suñé, D. Gaitanaru, R. Gogu, **M. Alcaraz**, A. Serrano, X. Sánchez, D. Fernandez, J. Fraile, T. Garrido (2012).
GIS based Hydrochemical Analysis Tools (QUIMET).
7th EUREGEO, Bolonia, Italia, June, 12th - 15th. Volumen 1, 419-420.

4. 4. Technical reports

2011 Estudi sobre el comportament hydrològic de l'aqüífer del Besòs en l'entorn del campus de la Ciutadella per a la Universidad Pompeu Fabra. (IDAEA-UPC, 2012).

2012 Modelo numérico hidrogeológico del valle de Quito. Calibración y predicción de posibles afecciones causadas por la construcción del metro -Proyecto metro de Quito- (IDAEA-UPC, 2012).

2012 Estudio acuífero de Calama sector medio del río Loa, región de Antofagasta. Gobierno de Chile. Ministerio de Obras Públicas, Dirección General de Aguas. División de Estudios y Planificación. (Matraz /IDAEA-UPC, 2012).

2013 Mezcla de salmueras y evolución química durante la operación de los pozos (Integración y Upscaling). (Matraz/ IDAEA-UPC, 2013).

2014 Modelación hidrogeológica para el proyecto minero de Santa Este (Perú). (Hydro-Geo/IDAEA-UPC, 2014).

2014 Modelación hidrogeológica para el recrecimiento de la relaavera Chinchán (Perú). (Hydro-Geo/IDAEA-UPC, 2014).

2014 Estudio Hidrogeológico integral de la unidad minera Iscaycruz (Perú). (Hydro-Geo/ IDAEA-UPC, 2014).

2015 Avaluació de les possibilitats d'aprofitament de l'anomalia geotèrmica detectada al sector de Fondo de Santa Coloma de Gramanet. (IDAEA-UPC, 2015).

II. IMPROVEMENTS IN GIS HYDROGEOLOGICAL PLATFORM

With the use and application of existing tools in different hydrogeological projects (which can be consulted in Appendix A), new requirements arise to treat specific data of each project when working with *HEROINE* platform. The author of this thesis has contributed actively to the development of this platform, during the design, programming, debugging, deployment and diffusion of these tools as evidenced by the authorship in [24], [27]–[29]. In this chapter, the specific contribution to them is shown, centered in the programming aspects implemented.

1. BRIEF DESCRIPTION OF HEROINE GIS PLATFORM

HEROINE GIS platform has been developed to analyze and manage data for the construction of comprehensive hydrogeological conceptual models. This platform is composed of different toolsets available in *ArcMap (ESRI)*. They were created with *ArcObjects SDK*, the software development kit for *Microsoft .NET* framework.

HEROINE platform was initially composed of two main modules: *HEROS* tools, oriented to geological data, and *QUIMET* tools, focused on hydrochemical data. These tools rely on a spatial database named *HYDOR*, where raw and processed data are stored (See Figure II.1).

Figure II.1. Schematic view of initial HEROINE platform.

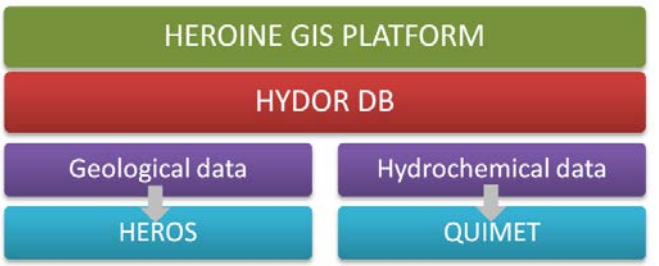

This thesis has enlarged the capabilities of *HEROINE* with new methodologies and tools, described in each chapter. In Figure II.2, the new modules added to *HEROINE* in the frame of this thesis are shown in bright color.

Figure II.2. Schematic view of current HEROINE platform with new added modules.

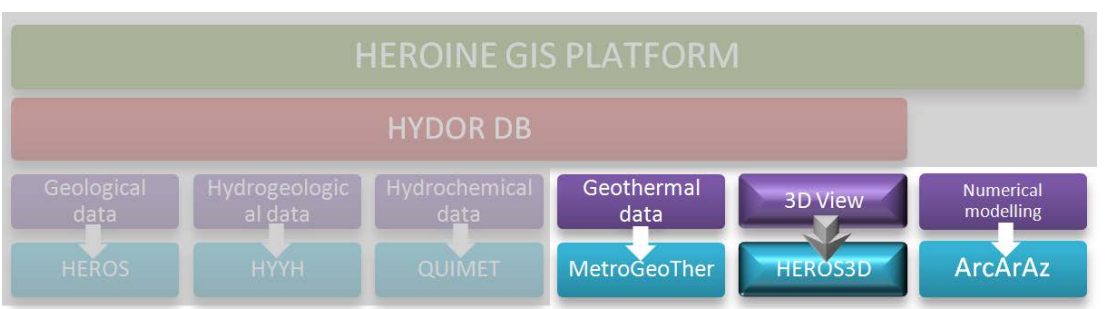

1. 2. Geospatial Data storage: *HYDOR* database

The geospatial database *HYDOR* follows the Personal Geodatabase structure provided by *ArcGIS (ESRI).* It is composed of several datasets that include a variety of geographical and alpha-numerical data necessary for a comprehensive geological and hydrogeological study. The main components include geological, hydrological, hydrogeological, hydrochemical, geophysical and geothermal features. This geodatabase allows us to store a very detailed geological description (e.g. lithology, geotechnical properties, fossils contents, etc…) that can be generalized and up-scaled. In order to ensure the standardization and the harmonization of the data, several code lists (e.g. list of lithology, fossils, age…) were created taking into account standard guidelines such us One Geology [30], OGC

Water ML [31] and INSPIRE [32], [33]. For further information about *HYDOR* geodatabase, the reader is referred to [26].

In addition, the geometry and attributes of the different interpretations derived from the geological data placed in the database can also be stored in *HYDOR*. Up to two different levels of interpretation can be stored as hydrogeological units and subunits. This allows for additional reinterpretation and feedbacks with the tools described below.

1. 3. Geological data management: HEROS tools

As stated above, *HEROS* is the set of instruments in the *HEROINE* platform oriented to perform geological analysis. The *HEROS* toolset allows the users to apply advanced techniques of interpretation to integrate all available geological information stored in *HYDOR*.

HEROS toolset allows us to work with 3D geological data in a bi-dimensional space and consists of two subcomponents: (1) *Borehole Diagram* Tools (*BHD*) and (2) *Stratigraphic Cross-Sections Correlation* tools (SC-SC). *BHD* tools allow us to visualize the detailed geological core description for each borehole from the database in order to define its geological and hydrogeological units and subunits. The interpretation generated individually is also stored in the database, so it can be further visualized and reinterpreted (Figure II.3).

Figure II.3. Borehole Diagram generated with BHD tool

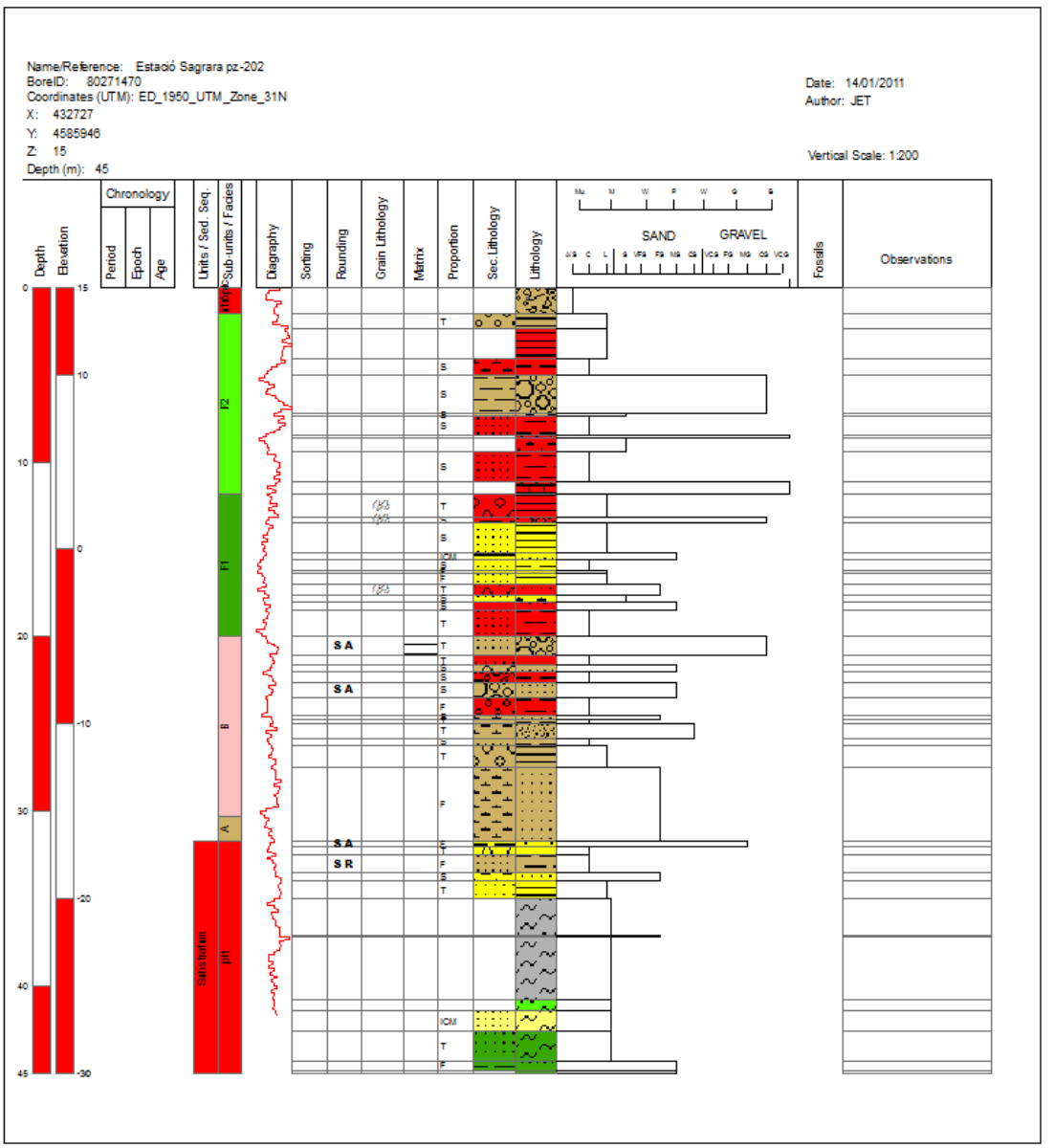

To merge these individual interpretations in an integrated regional hydrogeological model, *SC-SC* tools allow the generation of geological profiles that display the lithological columns of the boreholes together with the defined geological and hydrogeological units/subunits and the graphical results of in situ tests (e.g. diagraphy). Complementary information such as the surface terrain profile extracted from the DEM or the distance between the boreholes are shown (Figure

II.4). From the graphical representation of all this information, the geologist is able to define and construct a coherent geological model that serves as basis for a hydrogeological model.

Figure II.4. Stratigraphic Cross-Section generated with SC-SC tool

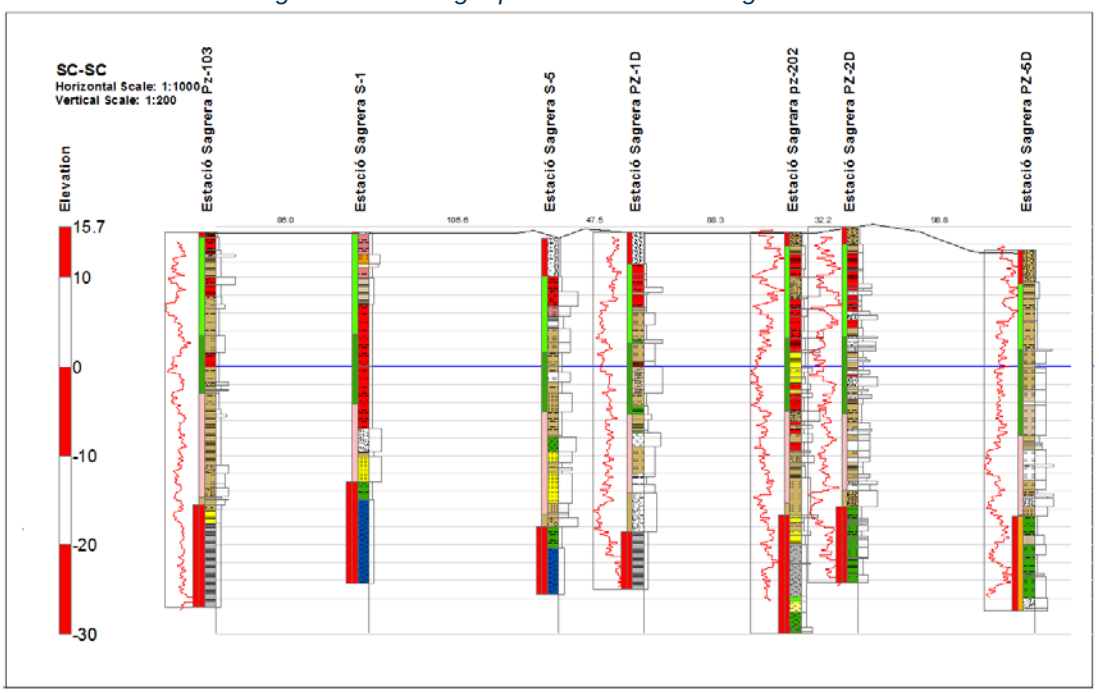

These geological cross-sections, besides representing the data stored in the database, create a bi-dimensional canvas that support drawing the geometry of the conceptual model defined by the geologist. The user defines the contact surface between geological units, and also faults and other discontinuities, as lines. The data created inside *SC-SC* canvas can be exported as three-dimensional data. Not only is the 3D geometry established, but attributes related to these lines can also be created, such as unit name, top and bottom units and other alpha-numeric information.

1. 4. Spatial and temporal Hydrogeochemical data management: QUIMET tools

The hydrochemical query module in 2D is named *QUIMET* [27] and allows for different interpretation techniques in 2D of hydrochemical data stored in *HYDOR*, such as the calculus of ionic balance, the creation of Piper, Schoeller-Berkaloff, SAR

or Stiff diagrams. *QUIMET* tools can apply spatial and temporal criteria in their queries: first, the user has to select on a map the points to be queried and then, specify a temporal interval for the chemical query. The spatial property of data can be studied by the creation of maps representing the spatial distribution of hydrochemical values of samples (Figure II.5). For instance, Stiff diagrams can be generated over a map for selected points (Figure II.6).

Figure II.5. Spatial representation of Chloride generated with QUIMET tools.

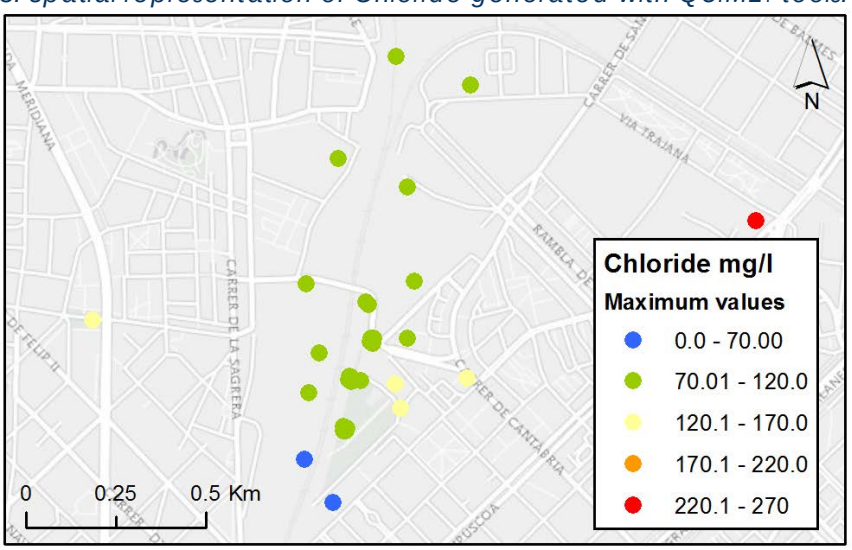

Figure II.6. Stiff diagrams generated with QUIMET tools.

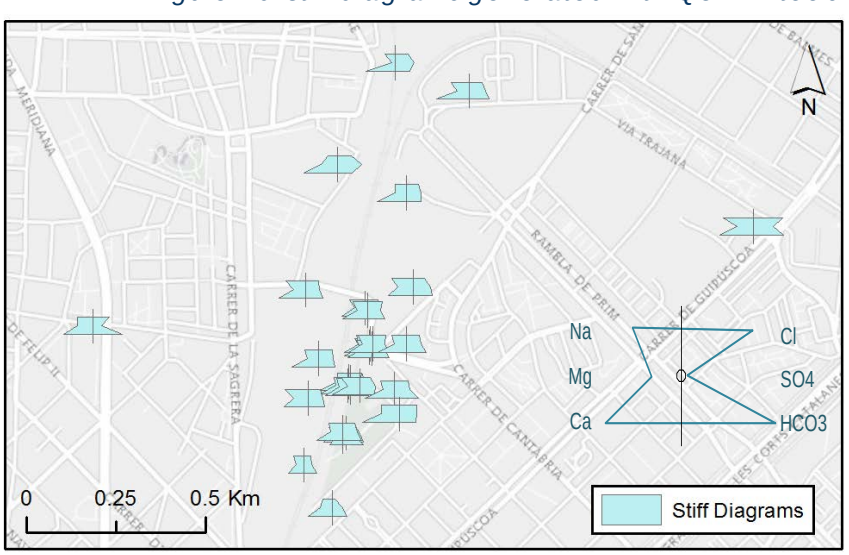

The hydrochemical data stored in *HYDOR* can also be queried outside of *ArcGIS* platform, without taking into account spatial characteristics.

A comprehensive statistical analysis can be accomplished over the selected data. It is comprised of the following capabilities: general univariable analysis, univariable and bivariable analysis, correlation matrix and correlation graphic, covariance matrix, and coefficient r^2 matrix.

2. IMPROVEMENTS AND NEW DEVELOPMENTS MADE IN THIS THESIS

The above mention tools were improved in several aspects that can be classified in four main groups:

- Update, optimization and automation advances.
- Improvements in data analysis, exportation and visualization.
- Improvements in data edition.
- Integration of new types of data.

2. 1. Update, optimization and automation advances

Before extending the capabilities of existing tools, *HEROS* and *QUIMET* were updated from *ArcGIS* 9.3 to the last version of *ArcMap*, *ArcGIS* 10. With this change, specific libraries were added and a slowdown in performance of tools appeared when executing *HEROS* tools. This is due to internal processes of *ArcGIS* 10. To revert this phenomenon, the *HEROS* tools code was analyzed and modified to improve the memory usage and management and avoid system resources to be exceeded.

Once the memory problem was solved, it was possible to automate the creation of Borehole Diagrams (BHDs) and Stratigraphic Cross-Section Correlations (SC-SCs) in a planned manner with *BHD Plan* tool and *SC-SC Plan* tool.

Previously, the user had to select one by one each borehole over the map and specify the scale and size of paper to create BHDs. With the new tool, *BHD* Plan tool, the user only has to select all boreholes of interest over the map and specify just once the scale and size of paper to create BHDs. The BHDs are stored as portable document format (.pdf extension) and as *ArcMap* document (.mxd extension).

The process to create SC-SC individually is also time consuming, because the user has to select all the boreholes that participate in the SC-SC one by one. With *SC-SC Plan* tool the user only has to draw and store in a shapefile the lines followed by SC-SCs. These lines must intersect the boreholes of interest for each SC-SC. The SC-SCs are stored as *ArcMap* documents with .mxd extension.

New templates of unlimited size were created to fit all BHDs and SC-SCs sizes.

2. 2. Improvements in data analysis, exportation and visualization

Errors were debugged in *QUIMET* queries to the geodatabase. Also, errors prompt when exporting queried data to Excel templates were solved to allow for the statistical analysis performed in these templates.

Two new capabilities were implemented to reuse the data stored in *HYDOR* and queried with *QUIMET* for further analysis. The Excel spreadsheets named *Easy-Quim* and *Mix* [34] can be filled with the data selected with *QUIMET*. *Easy-Quim* provides portability to data outside *ArcMap*. In this way, the ionic balance and diagrams such as Piper, Schoeller-Berkaloff, SAR or Stiff are available to *ArcGIS* unlicensed users. The Mix Excel Spreadsheet can be automatically filled with data queried by *QUIMET*. Mix performs statistical multivariate analyses for groundwater mixing ratio calculations [35].

Moreover, the temporal evolution of chemical compounds for selected points can be visualized in the same graphic for allowing comparisons (Figure II.7).

In addition to chemical parameters, hydrogeological variables (such as dropdown or water level depth) stored in *HYDOR* can also be queried and graphed. These initial tools for querying the hydrogeological data were the precursors of *HYYH* tools [28].

With relation to *HEROS* tools, the geological patterns for further lithologies were added to existing plots. Moreover, when creating BHDs with BHD tool, the geological type contact can be visualized between two lithological descriptions in a graphical manner.

The Regulatory Parameter Query Tools in *QUIMET* was adapted to represent parameters thresholds from different regulations in maps.

Figure II.7. Temporal Evolution graphic for well COLA and six chemical compounds and for two different wells (08245-0005 and 08281-0028) and two chemical compounds.

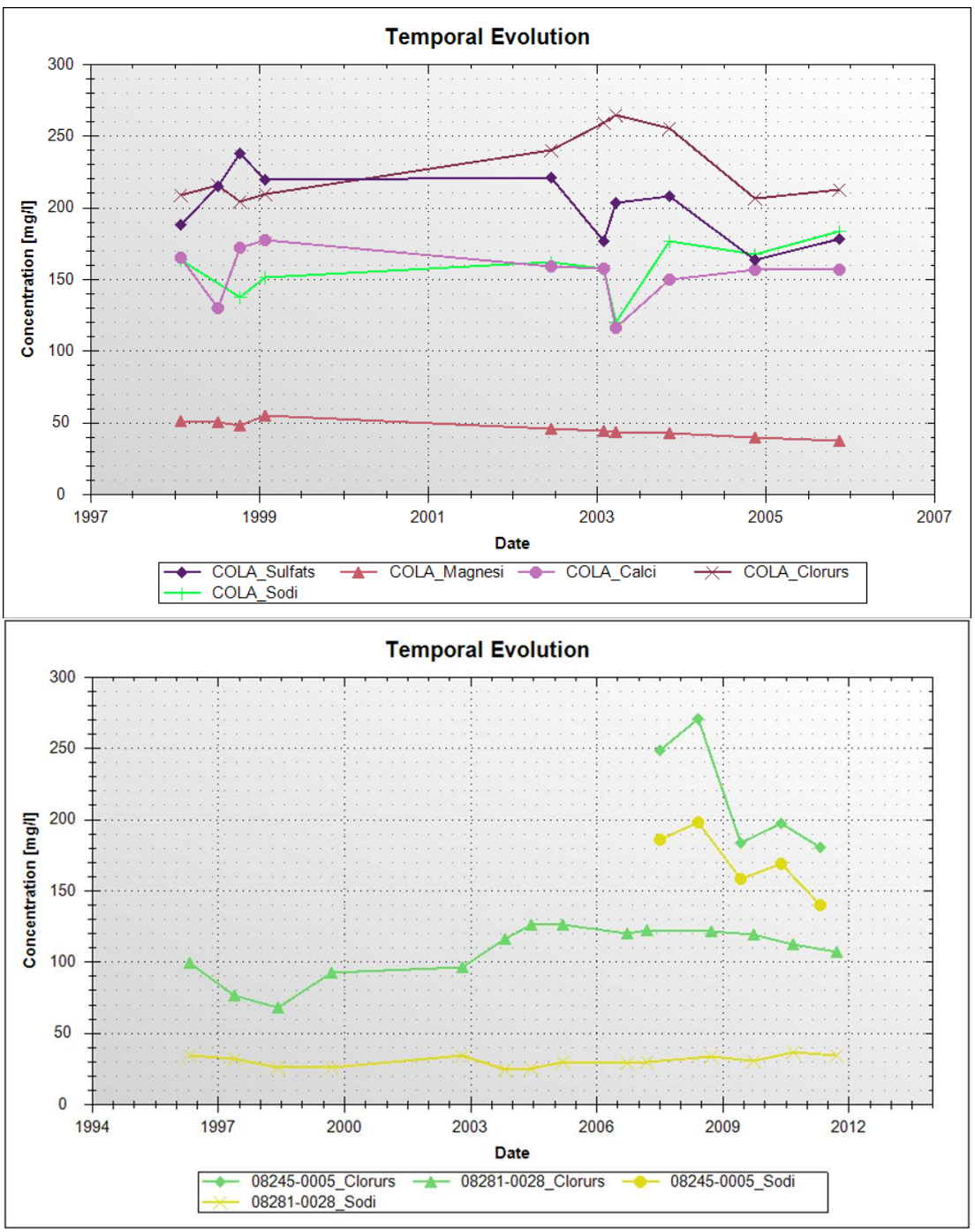

2. 3. Improvements in data edition

New capabilities were added to the canvas of *SC-SC* tools to facilitate the digitalization of geological and hydrogeological entities.

During the digitalization process, new snap capabilities were added to ensure consistency of final geometry. The geological lines and polygons drawn with the new tool can be snapped to lines representing the axes of boreholes, to marker points[1] or to other geological lines or polygons previously drawn.

It is possible to modify the geometry of lines and polygons once they have been created by the user by modifying their vertex.

The generation of polygons boding geological units was automated. If lines representing the top and bottom surface of the geological unit of interest have been previously drawn, a geological polygon between these two lines can be generated automatically.

Additional graphics without geological properties or attributes can be drawn.

The new appearance of SC-SC canvas evolutions with the new tools explained before as shown in Figure II.8.

Figure II.8. Evolution of SC-SC canvas, with new tools accessible from the panel.

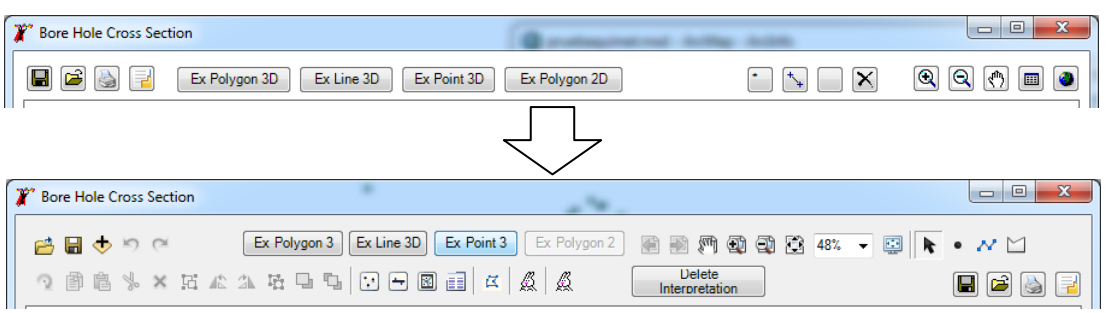

[1]Marker points are representations of previous interpretations of a specific geological surface in a SC-SC drawn previously.

2. 4. Integration of new types of data

Information contained in raster format, TIN format or alphanumeric format can be integrated with existing data in *HEROS* tools.

Georeferenced images with information about surface characteristics, such as geological outcrops or soil uses can be added to SC-SCs. Its topographical profile appears colored with the same colors than the image (Figure II.9).

Figure II.9. Geological outcrops over topographical profile and intersection with Substratum TIN in SC-SC.

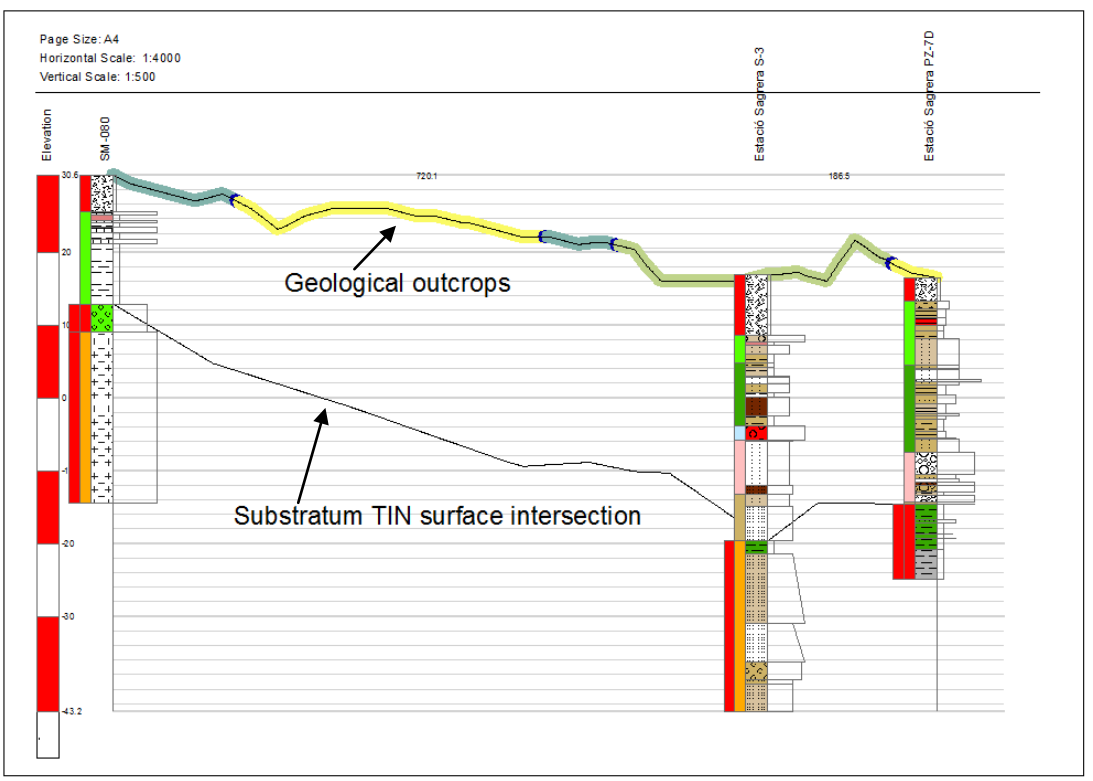

The intersection of existing TIN surfaces can be represented in SC-SCs (Figure II.9). These surfaces can correspond to piezometric surfaces or geological contact surfaces previously interpreted. In this way, prior versions of the geological model can be considered.

The visualization of seismic profiles or other images (such as previous interpreted geological profiles) can also be included as background in SC-SCs, to support digitalization processes of features contained in these images.

3. APPLICATION TO THE GREAT BASIN OF CALAMA (CHILE)[2]

The scarcity of water supplies in arid zones results in a water demand continuously growing under a scenario of industrial development [36]. This affects directly to groundwater resources, as an option to complement the supply [37]. In water management, the quantification of this affection is essential in the decision making process. To support it, the behavior of the hydrogeological system must be known and registered in a conceptual model.

Arid zones are also characterized by a low population density rate. This means that existing information about geology and hydrogeology is scarce and isolated, with different formats and details and limited to areas of interest, barely covering the whole system. Without an appropriate tool to process all this information, the key to define the conceptual model could remain unnoticed [38].

In view of this situation, the integration of all existing information in a unique database is needed [39]. The information should be homogenized, which would allow us to make specific consults and analysis over all available information. Implicitly, synergies between data will emerge only if data and their spatial and temporal relations are considered. The geographical characteristics of this kind of information made GIS (Geographic Information System) the best environment to manage this database [26], [40].

The Antofagasta Region, in northern Chile, presents extremely arid conditions with the Loa River as the main source of water resources [41]. This situation has been aggravated during the last decade, particularly due to growth of industrial uses [42], [43], in special the mining, which is one of the principal sectors of economy in Chile. Socio-cultural [42] and environmental [44] factors are also in a critical situation from a point of view of sustainability, as they all depend on water resources. An example of the overexploitation of water supplies is the medium sector of the Loa river, where the bigger open pit copper mine in the world, Chuquicamata mine, is located along

[2] This subchapter is based on *M. Alcaraz, E. Vázquez-Suñé, V. Velasco, D. Fernández., X. Sánchez-Vila (2016). Integrated hydrogeology framework for water management in arid zones exploited by mining. Hydrogeology Journal. In elaboration.*

with other holdings. In this area, groundwater resources represent a delocalized water supply source, which represents a supplement to superficial water supply.

This is a very sensitive situation in which, on the one hand, the Loa River has been declared overexploited, and on the other hand, the river-aquifer system is extremely interconnected with the Calama basin, thus an intensive exploitation of groundwater without control will necessarily impact on superficial water resources [44]. Not only quantity problems of water resource are present, also possible quality impacts (due to industrial and agricultural uses) have to be controlled.

Moreover, hydrogeological models have been performed, but none of them covers the entire basin. There is an important amount of hydrogeological data related to the study region because of recent research have been carried out by mining companies. They have contributed to enlarge the knowledge of the Calama Aquifer.

However, the detail and the analysis of this information is framed in the interests and commitments assumed individually by each mining company, whilst the scope of a global analysis must be regional, taking into account the whole system and integrating all available data. The DGA (Dirección General de Aguas, Civil Works Ministry of Chile) required elaborating a hydrogeological model integrating all available information to accomplish an appropriate water management. Therefore, these data as well as its interpretation must be available in the future for facilitating water management tasks.

In addition to the local and specific character of existing data, the hydrogeological limits of the basin (its geometry and structure) are unknown.

In this context, the main objective of this section is to define an optimal methodology based on GIS to integrate all available hydrogeological information in order to establish the hydrogeological conceptual model. It would represent the main tool to support an integrated management of water resources in Calama basin.

3. 1. METHODOLOGY

The following methodology to establish an integrated framework for water management is proposed (Source: [26]), in which the hydrogeological cycle is cared for extremely.

I. Recompilation of data that cover the entire study area through:
   I.a. Contact governmental agencies to ask for existing information
   I.b. Carry out geological, hydrological, hydrogeological and hydrochemical field campaigns to get new data in those areas with sparse information.
II. Storage and management of spatial entities and temporal data on a geospatial database, to support:
   II.a. The representation of diverse spatial-temporal scales of groundwater parameters.
   II.b. The incorporation of diverse types of information (e.g. hydrogeology, meteorology, hydrology, hydrogeochemistry).
   II.c. The option of the standardisation and harmonisation of raw data.
   II.d. The integration of previously interpreted data, such as existing geological and hydrogeological models.
III. Data processing and analysis using:
   III.a. Instruments to perform comprehensive geological analysis and creation of 3D models:
      i) specific techniques to execute accurate stratigraphic analysis, visualisation of stratigraphic columns and generation of cross-sections
      ii) techniques to generate 3D surfaces and
      iii) techniques to create fence-diagrams.
   III.b. Tools to carry out an accurate hydrogeochemical analysis by using quality standars, computation methods, statistical analysis and traditional graphical analysis techniques (e.g. Piper, Stiff and salinity diagrams).
   III.c. Instruments to query and analyse other hydrogeological data such as groundwater level, aquifer tests and well abstractions or injections.
   III.d. Tools that enable the hydraulic parameterisation based on hydraulic test interpretations (i.e. pumping and tracer tests) and based on the textural properties…
   III.e. GIS environment which provides:
      i) interpolation tools to estimate and validate the distribution of several parameters such as hydrogeological, hydrochemical, petrophysics, hydrological, hydrometeorological properties,
      ii) Index and overlay techniques and
      iii) a wide range of utilities for further analysis (e.g., Mapping tools, Spatial Analysis Tools, Geostatistical Tools, etc).
IV. All this sequence of steps is part of an iterative process in which the results at one point enhance the previous one. The set of tools used must offer the possibility of feedback between steps.

3. 2. GENERAL SETTINGS

The Calama basin is located in the Antofagasta region in northern Chile, between 1750 meters above sea level (masl) in the bottom of the basin located to

the western end, and about 3000 masl in the eastern part. The study area is surrounded by mountain peaks having different altitudes around 4000 meters. It is bounded to the north by Sierra del Medio and to the south by the Sierra Limón Verde (Figure II.10).

Figure II.10. Location of the study area in Chile. Ortograph of the study area: WGS 1984 Web Mercator (Auxiliary Sphere)

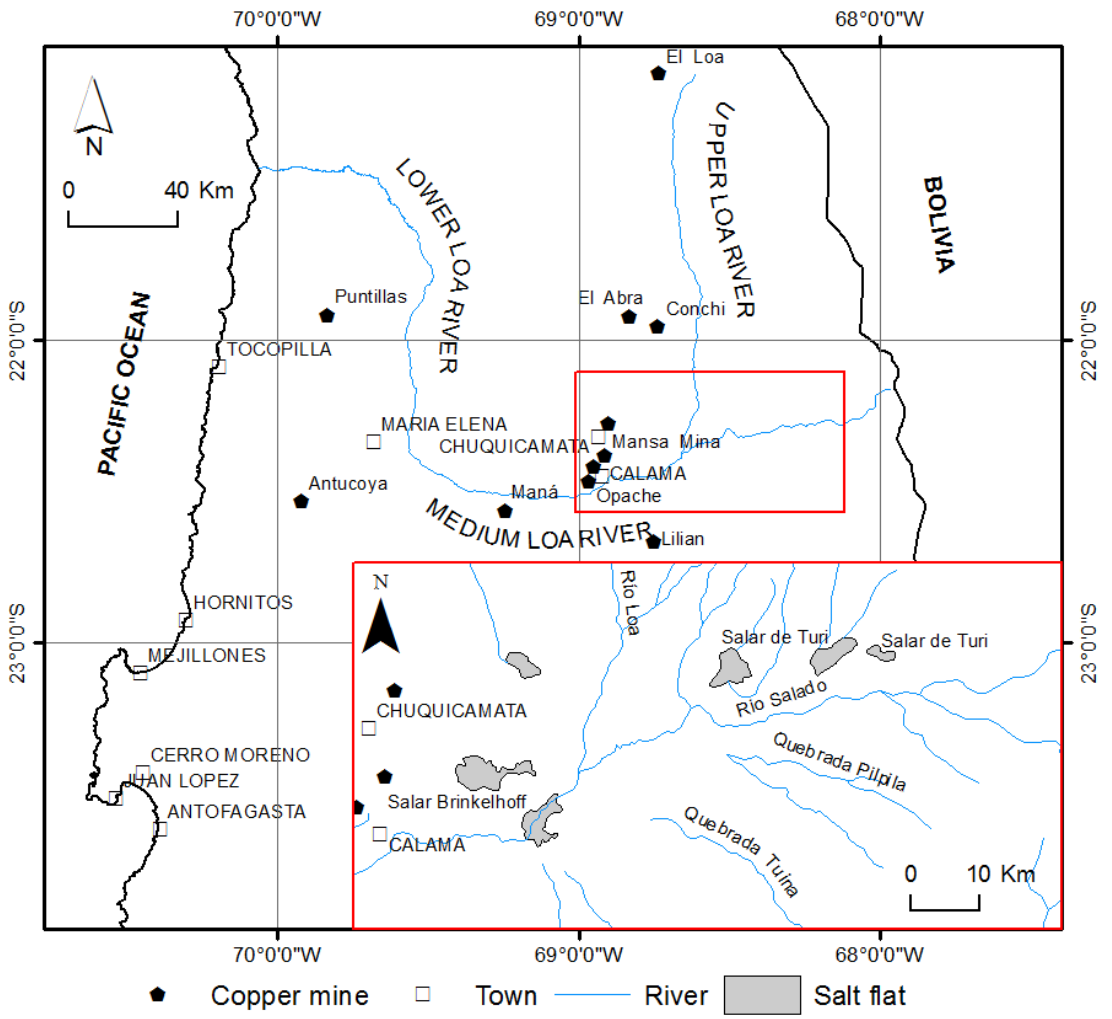

The average precipitation is 5 mm per year. Temperatures are moderate, reaching an annual average around 10 ° C.

The Loa River crosses the Calama Basin from North to West. It is sourced throughout most of the year by baseflow from a number of basin aquifers in the high Andes, the Precordillera, the Calama Basin and the Pampa Tamarugal (part of the

Longitudinal Valley). During the wet summer months of December to March on the Altiplano, multi-peak seasonal floods pass down the river, undergoing transmission losses that partly replenish the basin aquifers [45].

The geology of the study area has been described by several authors [46]–[50]. It consists of a series of sedimentary materials that have filled the Loa River basin during the past 50 million years. These materials have a variable thickness with an average of nearly 300 meters, and in some specific cases gaining thickness of up to 500 meters. Underlying these materials, an igneous-metamorphic basement is defined, on which all the aforementioned materials have been sedimented. This basement outcrops in the margins of the basin, as part of the higher peaks. In the study area seven main geological units composed mainly of igneous, metamorphic rocks and semi-consolidated sedimentary deposits have been defined, which are described in Table II.1, naming them from base to top:

Table II.1. Description of the different geological units of the study area.

Unit	Geologial Fm.	Geological description of materials
	Basament	Igneous, volcanic and metamorphic rocks
	Calama Fm.	Gravel and conglomerates deposits (GU-2a). Intercalations of lavas and andesitic breccias (GU-2b)
	Jalquinche Fm.	Siltstone and claystone (GU-3a) Tuffs, volcanic ashes, sands and silts (GU-3b) Calcarenites and limestones (GU-3c)
	Lasana Fm.	Sandstones, siltstones and conglomerates
	Chiquinaputo Fm.	Conglomerates and sandstones
	Opache Fm.	Shales and sandstones (GU-6a) Conglomerates and sandstones (GU-6b) Limestone, travertine and calcarenites (GU-6c)
	Chiu-Chiu Fm.	Sandstone, travertine and volcanic ashes

Structurally, geologic materials that shape the basin are affected by different sets of normal and reverse faults due to different tectonic episodes that have affected it, causing the combination of horst and graben structures. In many cases, the different geological units are faulted and displaced in the vertical plane. A detailed geological map can be consulted in Appendix B.

Hydrogeologically, 3 main aquifer units can be identified among the detrital material, as shown in Figure II.11. A first Shallow Aquifer nested in limestones and sandstones with variable thickness (30 to 60 meters) is separated by a formation of clay and silt of variable thickness (between 80 and 150 meters). Below it, the Deep Aquifer is nested in gravel and with a thickness of 30 to 130 meters. Samples from the Shallow Aquifer are mainly sodium chlorinated, with a small group with magnesium chloride-water. The Deep Aquifer has not samples in the sodium extreme, presenting sodium chlorinated and magnesium-calcium chlorinated facies.

Figure II.11. Profile of hydrogeological units. Source [51]

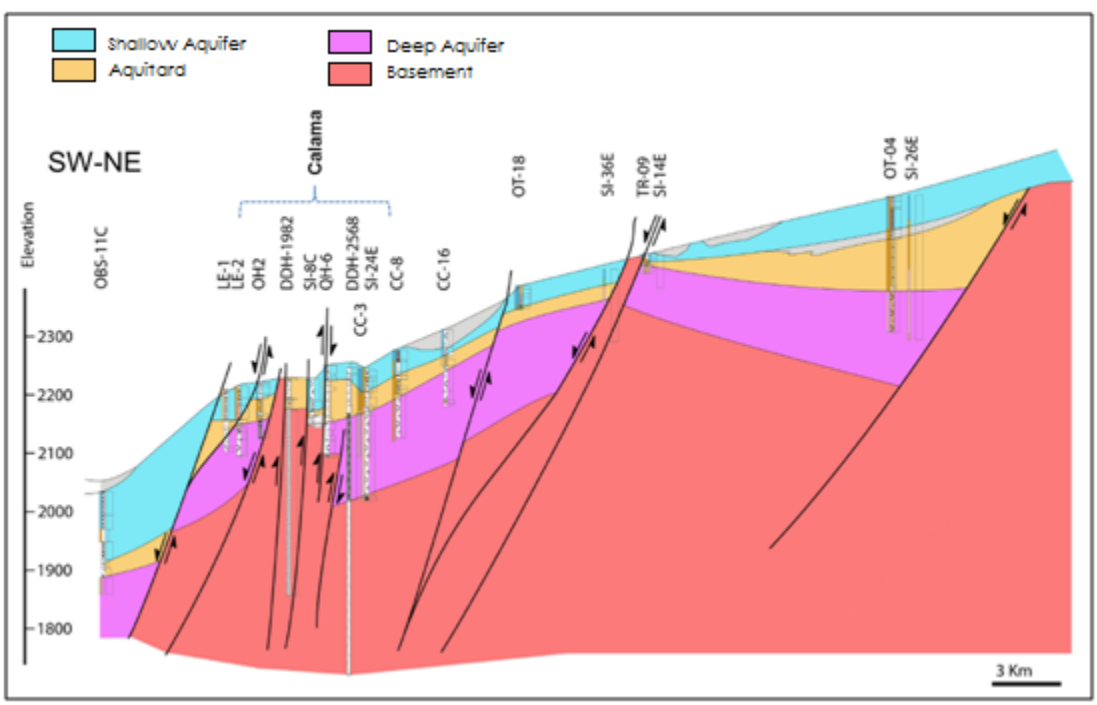

3. 3. RESULTS

3. 3. 1. GATHERING DATA

Firstly, existing information have been requested to the governmental authorities and privates entities, mainly mining enterprises located in the study area. More than 25 documents from different kind have been analyzed, among them, geological, hydrogeological and hydrogeochemical technical studies, water resources evaluations, monitoring reports of groundwater levels and hydraulic model

dossiers [51]. Information related to lithology descriptions, hydrochemical analysis, pumping tests, temporal measurements of groundwater level and existing conceptual and numerical models has been extracted from the above-mentioned documents, and digitalized, if it was not. All existing information is restricted to specific areas inside the whole aquifer system, as illustrated in Figure II.12., corresponding to Partial sectors as Calama-Pampa Llalqui Sector, El Tesoro Mine, Toki Sector, Talabre Dam or Loa River segments are the main locations with relevant information.

Figure II.12. Partial studied areas in Calama desert by three different existing models. Ortograph of the study area: South American 1969 UTM Zone 19N

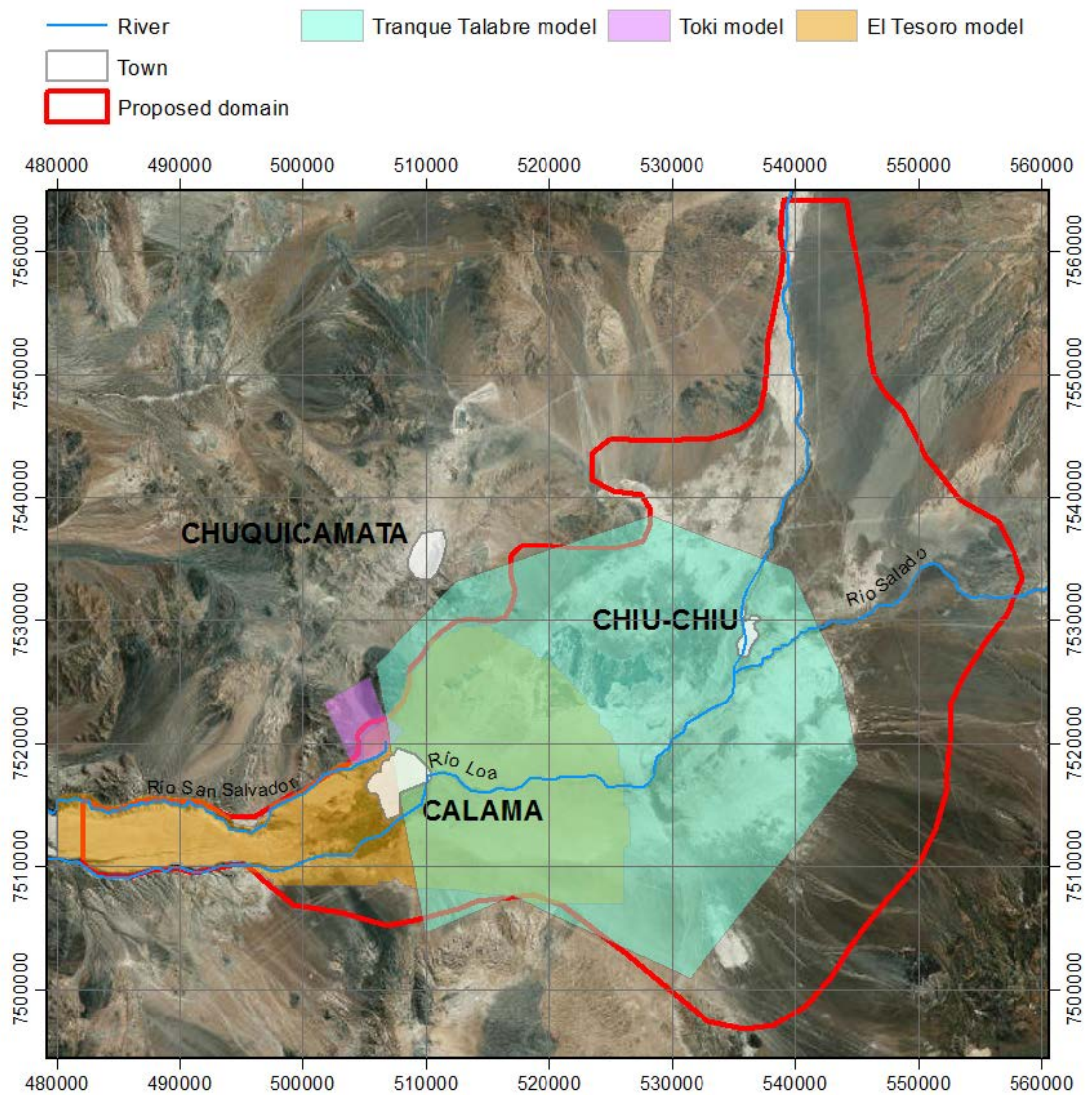

3. 3. 2. GENERATION OF NEW INFORMATION

The lack of information in certain parts of the domain forced to carry out a geophysical campaign in order to cover the sparse areas and to establish the aquifer layers (as non consolidated materials) as well as the basement depth in the eastern and western edges of the basin (only 33% of boreholes have information about the basement depth).

During September 2012, 14 sections were generated from 123 geophysical points. These gravimetric sections were radially distributed from points with known geology information (Figure II.13). Most of the points were concentrated in the eastern part of the basin, because this zone represents the incoming superficial and subsuperficial water. In the western part, two sections were planned in order to characterize the groundwater flux coming through the western contour.

3. 3. 3. HOMOGENIZATION AND STORAGE OF INFORMATION

In the next step, all available information was stored in a unique database. Raw data stored in this database share a common structure and nomenclature. This allows us to query all the data through the tools presented in previous sections. The information has been introduced directly in the database or imported from spreadsheets, after digitalization.

Lithology information from 427 boreholes has been adapted with term lists to the vocabulary of the database. The vocabulary of description has been standardized, pooled and stored in the database.

Regarding to geochemical data, 8956 samples have been analyzed and stored in the database, with a total of 26 physical and chemical parameters. So there are 141 boreholes with geochemical information associated to them. This data has been collected from 2003 to 2010 and the temporal evolutions of some parameters are available.

The database also stores hydrogeological information: 86 pumping tests, 44 recovery tests, 37 Lefranc tests, 23 Slug tests and 15 Packer tests (pumping rates and withdrawals and the interpretations). In summary, data about hydraulic conductivity

and storage coefficient for 115 wells in the Shallow Aquifer, 5 wells in the aquitard and 85 wells in the Deep Aquifer, for a total of 205 wells, were available.

Figure II.13. Gravimetric sections for field campaign. Ortograph of the study area: South American 1969 UTM Zone 19N. Source [51]

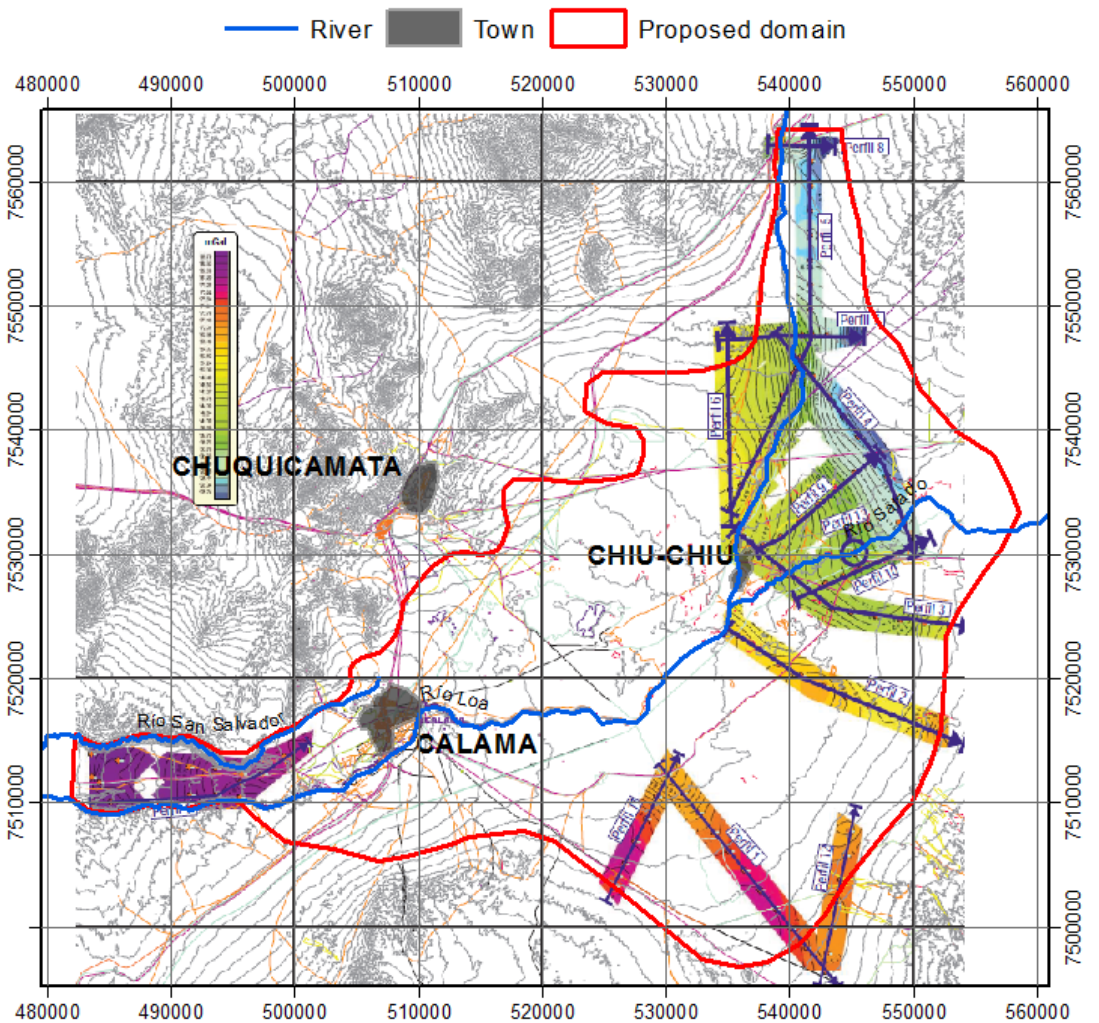

In general, this homogenization process represents an abstraction from detailed row data. To keep these details, references to original documents are included as metadata hyperlinks, so they can be queried at any time.

3. 3. 4. PROCESSING OF STORED INFORMATION

The lithological description was interpreted (in some cases, even reinterpreted) to define the main hydrogeological units described.

To cope with this amount of information, the hydrogeological GIS platform *HEROINE* [26] was used. *BHD* tools allow us to visualize the lithological information for each borehole from the database in order to define its geological and hydrogeological units. The interpretation generated was also stored in the database, and was available to a global interpretation at regional scale. This individual interpretation for each borehole can be modified attending to the regional information (mainly correlations with near boreholes, but also for previous model surfaces or outcrops). 338 boreholes were analyzed with *BHD* tools. Between the 83% and 88% of the boreholes had information related with the bottom layers of the shallow aquifer and the aquitard, respectively. Data about the bottom of the deep aquifer were identified in 73% of boreholes, while only the 33% of the boreholes had information about the basement extracted from lithology descriptions. 123 boreholes have geological interpretation deduced from the geophysical campaign.

To merge these individual interpretations in an integrated regional hydrogeological model, *SC-SC* tools created geological sections, which represent, not only the geological information, such as lithology and hydrogeological interpretations, but also topography and outcrops. Moreover, intersection of existing layers for previous geological models could be visualized in the geological section as surface lines. From the graphical representation of all this information, the modeler was able to construct a coherent geological model that serves as basis for a hydrogeological model.

These geological sections were a platform that supports drawing the geometry of the conceptual model defined by the geologist (Figure II.14). The modeler defined the layer contacts between geological units, and also faults and discontinuities, as lines. Not only the geometry was established, also attribute information related to these lines was created, such as unit name, SC-SC name, top and bottom units and others. Interpretation lines were not continuous for each unit: each line represented the contact between only one unit at the top of the surface, and only one unit at the bottom of the surface. Following this criterion, these interpretation lines will be easy to query in next step due to their attributes.

From the interpretation of existing boreholes, a total of 15 geological sections were studied with *SC-SC* tools, such as the one shown in Figure II.14. These geological

sections are available at Appendix C. Over the template of *SC-SC* tools, lines were drawn to identify the 3 main contact surfaces between the 4 main hydrogeological units. These lines represent the contact between the basement, the Shallow Aquifer, the Aquitard and the Deep Aquifer (Figure II.14).

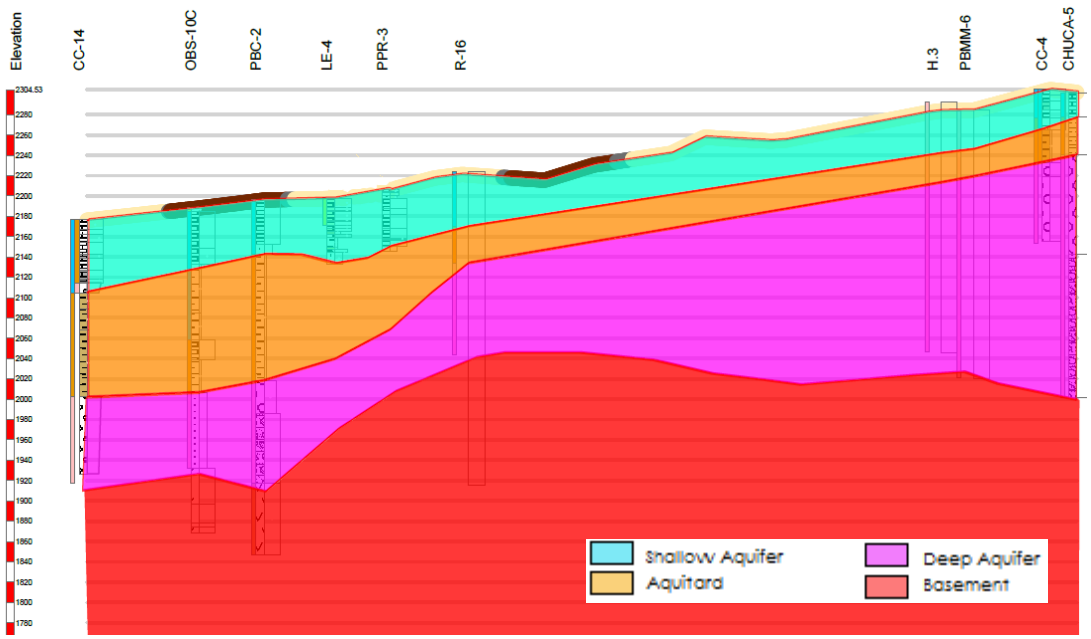

Figure II.14. SC-SC created by HEROS tools representing the 4 main hydrogeological units. Source [51]

These drawn lines were exported from the 2 dimensional section to a 3 dimensional schema, where tridimensional surfaces can be generated (Figure II.15). For instance, to generate the top surface of Deep Aquifer, lines with Bottom Unit Attributes equal to DeepAq. were selected.

Figure II.15. Contact surfaces between hydrogeological units.

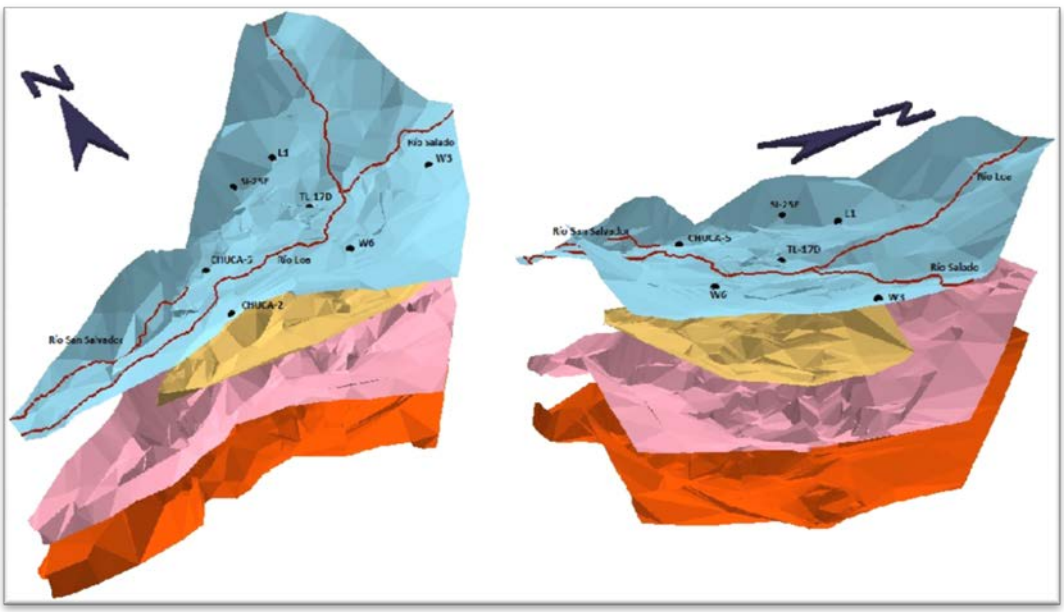

As an alternative 3D model representation, *HEROS* tools allow to generate vertical 3D polygons in SC-SC canvas. These 3D polygons can be visualized as fence diagrams, as in Figure II.16.

Figure II.16. Fence Diagrams created by HEROS tools.

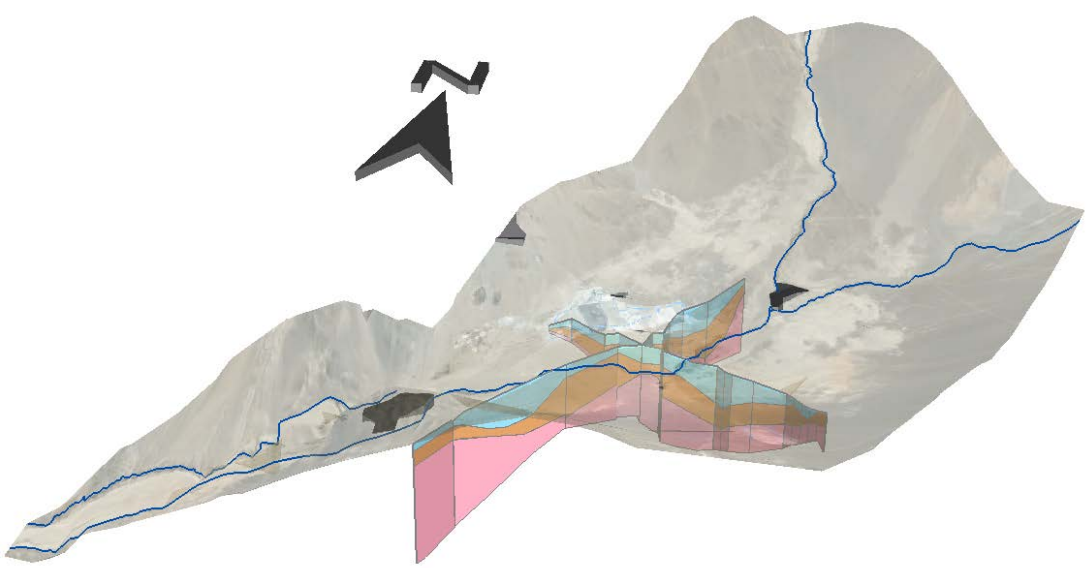

At this point, the main geometry characteristics of the hydrogeological conceptual model (both in terms of the limits as to the thickness of each unit) were

established with *HEROS* tools. In order to know other general aspects related to the behavior of the system, such as water origin, fluxes between hydrogeological units or their limits, a further analysis of data was carried out with *HYYH* tools and *QUIMET* tools.

A deep analysis about piezometric can be executed from the compendium of existing data with *HYYH* tools. This set of tools creates maps with punctual piezometric values. The hydrogeologist draws the piezometric surface over them, as shown in Figure II.17. *HYYH* tools can also represent the spatial distribution of hydraulic conductivity and storage coefficient values obtained from pumping test. This is very helpful to characterize each aquifer, in order to get initial values for a numerical hydrogeological model. This set of tools also facilitates the query of piezometric data under spatial and temporal criteria.

Further analysis related to hydrogeochemistry can be carried out from existing data. *QUIMET* tools allow querying all available hydrogeochemical data. This set of tools give support when working with hydrogeochemical information, generating distribution maps of parameters of interest, including temporal evolution graphs. As an example, Figure II.18 shows the Stiff graphs during the year 2006.Hydroquemical impacts from mining industries should come to light at this point. One important aspect of data integration is the enlargement of the temporal registry: the integration of all available information has increased the registry of data from different dates, so temporal queries may extract significant information from integrated data.

Figure II.17. Spatial distribution of piezometric values. Ortograph of the study area: South American 1969 UTM Zone 19N.

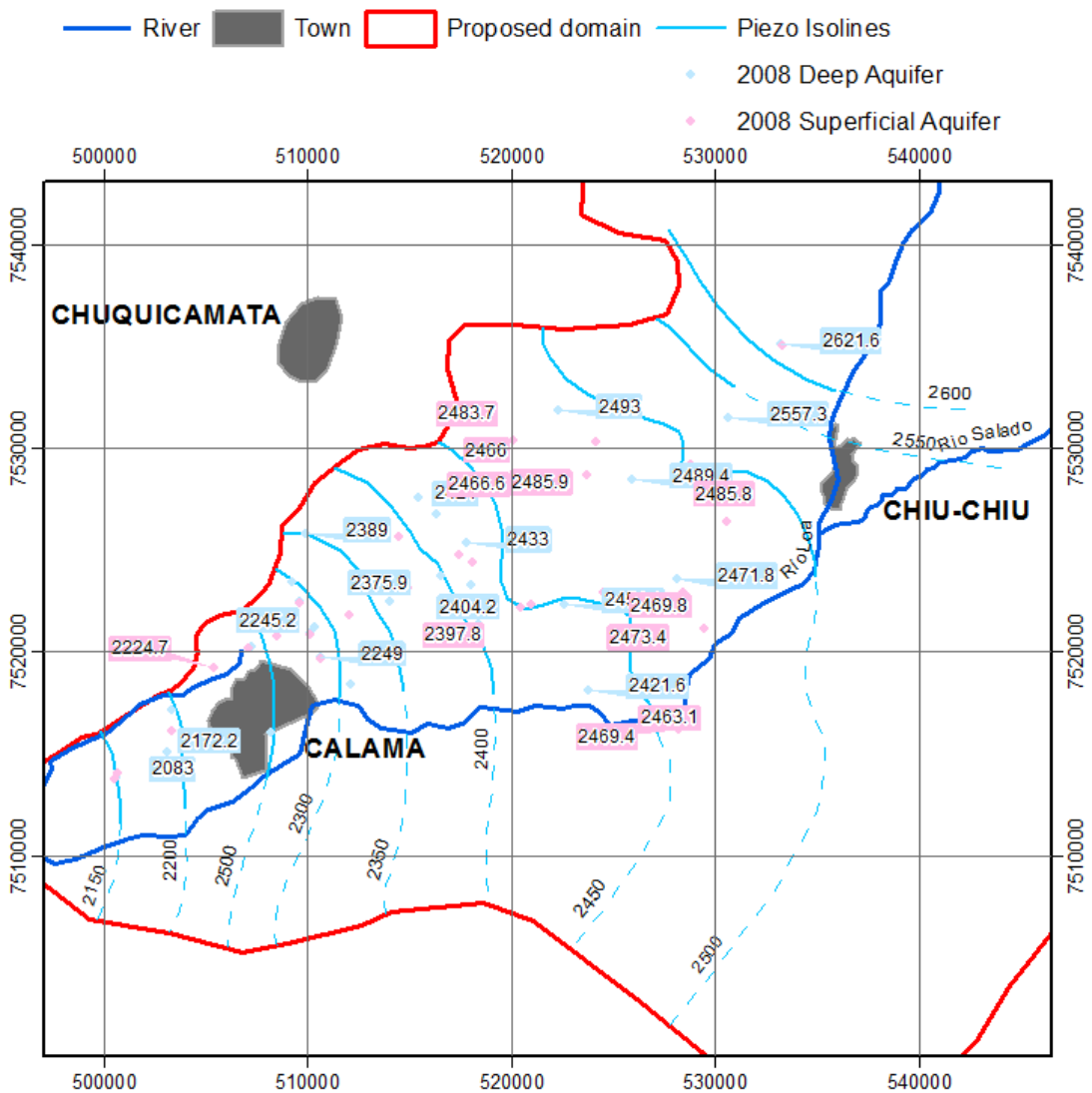

Figure II.18. Stiff graphs in 2006. Ortograph of the study area: South American 1969 UTM Zone 19N.

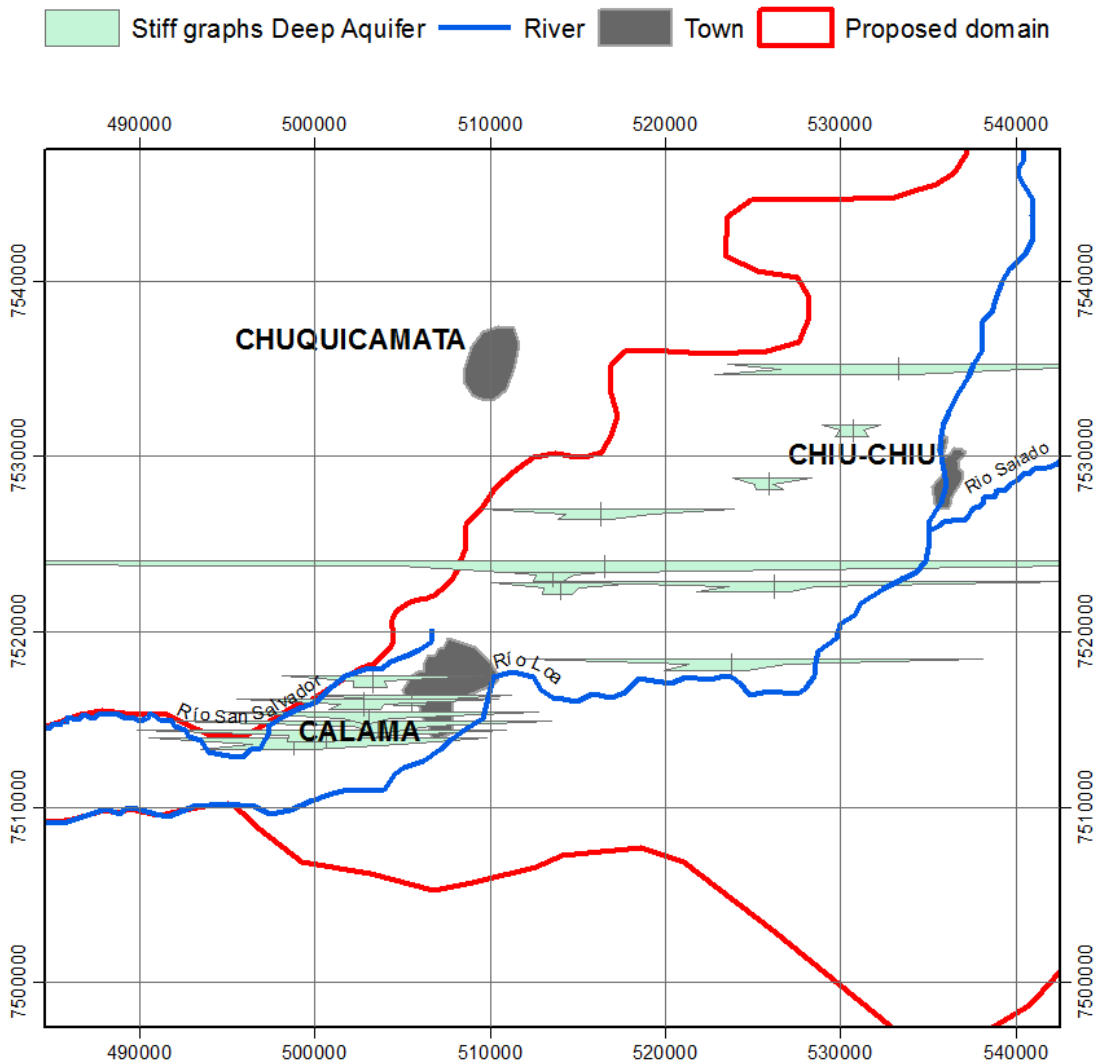

3. 4. CONCLUSIONS

The study area has been subjected to a number of studies that have approached the domain and sub-areas with different objectives. The study presented here has achieved the integration of all available data, developing an integrated framework to develop the conceptual model of the aquifer system of the Great Basin of Calama.

To accomplish this, in addition to compiling a vast amount of information, it has been necessary to raise new data where the knowledge of the aquifer system

was limited. This has been achieved by a gravimetric campaign, executed during the development of this project.

All existing data about geology, hydrogeology and hydrogeochemistry from different aims and scope generated during last years, were stored and harmonized in a geodatabase and now is accessible to decision-maker agents, through the development of an integrated framework which facilitates the management of all this heterogeneous information. This has been possible by using a complete set of tools developed in a GIS platform. These tools have allowed us to: store it in a unique database; homogenize it in order to compare data from different origins, scales and formats; and create new information from interpreting the treated data.

Merging geological and geophysical data allowed defining the hydrogeological basin limits where no data were initially available. Thus, a 3D hydrogeological model, that covered the entire study area, was proposed. That was the starting point to establish a conceptual model that supported the integrated water resources management in the Great Basin of Calama, due to unknown aspects of the basin have been clarified.

Upon this basis, further analysis can be supported in the future. Thus, a cross analysis of both watertable information and hydrochemical data can be now performed. These perspectives will allow postulating hypotheses about the main flow patterns and the presence of water with different hydrochemical footprints. With an appropriate data update, evolution of parameters can be queried and future impacts in quantity and quality analyzed.

III. 3D GIS VISUALIZATION OF UNDERGROUND MEDIA[3]

1. INTRODUCTION

Usually, geological representation and analysis are made on a 2D basis [52]. However, 3D analysis and visualization of geological models are required to understand and represent the heterogeneity of the aquifers in the three dimensions of the space [53], [54]. In fact, nowadays 3D geological modeling is not a goal, but a step in hydrogeological projects. Besides, the 3D visualization of geological model and hydrogeological conceptual model including the impacts produced by the exploitation of subterranean resources can help to define and establish particular management. Several authors have used 3D visualization of geological and hydrogeological models to face different situations as geotechnical problems [55], hydrochemical problems related to gypsum dissolution conditions [56] and groundwater management [57].

For the construction of comprehensive 3D geological models, a large amount of data must be taken into consideration. Usually, this data is of different kind, origin, format and scale. This complicates the integration, visualization and understanding of all available data for the definition of an accurate three-dimensional geological model. The improvements of 3D geographic information

[3] This chapter is based on *M. Alcaraz, E. Vázquez-Suñé, V. Velasco, M. Diviu. (2016) 3D GIS-based visualization of geological, hydrogeological, hydrogeochemical and geothermal models. German Journal of Geosciences. Submitted.*

systems (GIS) with query functionality and data management tools have considerably enhanced our ability to characterize subsurface conditions [58]. As a consequence, several methodologies and software have been developed upon the GIS technology, mainly oriented to generate and visualize 3D geological models. [59] present a new approach to deal with multi-scale geological data in GIS. [60]–[62] use GIS technology to manage geological information (mainly borehole logs and cross-sections) and rely on geomodeller software, such as Gocad [63], to give real 3D characteristics to geological features and build geological surfaces or volumes with complex geometry, such as folds and faulted structures. [64] complement the GIS capabilities with CAD software to construct the geological surfaces.

To avoid losing the advantages in data management of GIS platforms when changing to CAD platforms, a number of stand-alone GIS applications have been developed, such as Geotouch [65], GSIS [66] or GSI3D [67], specially oriented to 3D creation and visualization of geological models. These and many other software systems (commercial and non-commercial) and methodologies used for geological modelling are extensively documented elsewhere, for example in [24] and [66], and references therein.

However, the aforementioned methodologies and tools have been not designed to deal with some specifics aspects related with a comprehensive analysis and assessment of the groundwater system nor the analysis and visualization of specific impacts on this environment in a three-dimensional environment. To deal with this situation, some hydrogeological methodologies and software have been developed. For instance, *GVS* [68] is a stand-alone application oriented to visualize 3D geological (cross-section and surfaces) and hydrogeological data in a friendly user interface, including tools to query and visualize temporal evolution of hydrogeological variables. In spite of these advantages, previous geological and hydrogeological conceptual models must be carried out outside this platform, thus it needs of additional software for pre-processing of hydrogeological data. [69] developed a set of tools in a GIS environment (*Arc Hydro Groundwater* Tools) that support the creation and the storage of 3D objects such as hydrostratigraphy, cross-sections and volumetric objects. In addition, this platform includes a set of tools to facilitate the generation of 2D/3D modeling elements and its database structure

enables the generation of SQL queries to map time series. Additionally, [70] present an effective methodology to build a comprehensive database through the combination of a Relational Database management System (RDBMS) that incorporates instruments for data quality control and the aforementioned *Arc Hydro Groundwater* Tools. These platforms and methodologies allow the integration of the main hydrogeological characteristics, such as geological and hydrogeochemical models, but do not include other more specific characteristics, such as the geothermal.

Nevertheless, further procedures may be improved especially for the management, visualization, retrieval and understanding of detailed geological and hydrogeological data and parameterization in a 3D GIS environment [54]. During construction of 3D geological models, some relevant aspects must be taken into account related to data management. For instance, facilitating the creation and modification of geological surfaces or integrating the visualization of all the available hydrogeological data in an understandable manner. Once the media is properly characterized and an exhaustive geological, hydrogeological, hydrogeochemical and geothermal analysis has been carried out, the expected impacts obtained from this analysis must be available.

To overcome these gaps, this chapter presents a methodology that aims to integrate in a unique 3D GIS environment the whole process of hydrogeological modeling with 3D capabilities, by focusing on (1) the development of 3D geological models suitable for hydrogeological modeling and (2) the 3D validation and visualization of geological, hydrogeological, hydrogeochemical and geothermal models.

2. METHODOLOGY FOR 3D INTEGRATION OF DATA

The proposed methodology aims to analyze, visualize and integrate in the three-dimensional space the variables and properties required to define a comprehensive hydrogeological model. This is possible because it is embedded in a wider hydrogeological platform, *HEROINE*, which includes facilities to perform a complete hydrogeological analysis in a single GIS environment. The software platform *HEROINE* facilitates a detailed hydrogeological conceptual modeling by means of a geospatial database (*HYDOR*) and several sets of GIS–based analysis

tools developed in a two dimensional environment such as extensions of *ArcMap* (*ArcGIS; ESRI*). They are accessible by different toolbars. These toolsets manage the geological (*HEROS*), hydrogeological (*HYYH*), hydrochemical (*QUIMET*) and shallow geothermal (*MetroGeother*) data stored in *HYDOR* geodatabase (see Figure III.1). These instruments are briefly described in the previous chapter. More details can be found in [24], [26]–[28], [71]. To give three-dimensionality to all these data types, a set of tools is presented named *HEROS3D*. It allows 3D geological and hydrogeological analysis. This set of 3D analysis tools is accessible through a toolbar in *ArcScene*, the 3D environment of *ArcGIS* 10.X (*ESRI*) software package.

Figure III.1. Schematic view of extended HEROINE platform

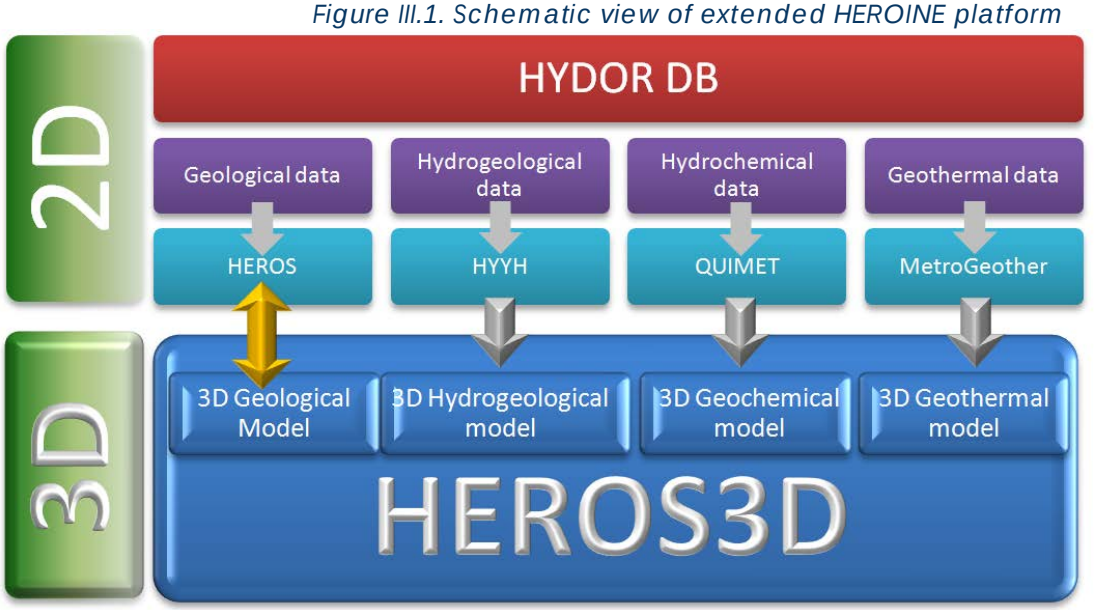

2. 2. 3D Geospatial Data storage: *HYDOR* geodatabase

The *HYDOR* geodatabase, as explained before in section II.1. 2, contains geological, hydrogeological and hydrochemical data. Most of this information is bidimensional; however, information about the height or depth of some features can be stored, e.g., topographic elevation or groundwater head levels. These data with three-dimensional characteristics will be queried to represent it in several forms by *HEROS3D* tools.

2. 3. 3D Geological data management

Two common situations are usually found. On one hand, it is common to find simplistic approximations of real aquifer geometry and spatial variability of geological and hydrogeological properties that show the lack of geological knowledge of the study site. Usually, this is because there is not enough resources (time or funds) to obtain the detailed geological interpretations [72]. On the other hand, there are studies where more complex geometries are defined for the geological structures such as detailed characterizations of faults and folds. These complex geometries do not fit to the multilayer character of most common software for hydrogeological numerical modeling, such as *FEFLOW* [73], *MODFLOW* [74] or *Visual TRANSIN* [75]. This implies a post-processing of the geological model to adapt the geometry to hydrogeological modeling process and then importing a proper geometry to the numerical software.

For groundwater, the layered structure of the system justifies the application of semi-3D GIS platforms. For instance, it is common to encounter a disposition of at least two aquifers, one deep and one shallow. The impacts on each of them together with the interrelation between them can only be represented simultaneously in 3D. However, these standard multi-layered systems are quite limited for modeling, visualizing, and editing subsurface data and geologic objects and their attributes. Here, we propose a methodology for improving the modeling of multi-layered systems.

HEROS3D extends the functionality of *HEROS* to work in the three-dimensional space. These analysis instruments cover a wide range of methodologies for visualizing, querying and interpreting geological data in a 3D environment. They include, among others, different commands that enable the user to: (1) query and visualize in 3D the different units/subunits interpreted for each borehole (Borehole Tubes); (2) create 3D surfaces (TINs) automatically for the specific units/subunits interpreted from the boreholes and recorded in the database; (3) perform further calculations with the aforementioned 3D surfaces (e.g. extension); (4) Create automatically fence diagrams. These facilities are explained below.

2. 3. 1. Borehole Tubes

The borehole data interpreted previously with *HEROS* as unit or subunits and stored in the geodatabase *HYDOR* is only visible in raw format inside the geodatabase table or in 2D dimension individually or jointly with related boreholes in cross-sections with *HEROS*.

HEROS3D creates *Borehole Tubes* entities, which are 3D visualizations of the borehole stored in *HYDOR* geodatabase. The *Borehole Tubes* represent the geological interpretation defined previously for the boreholes, such as geological or hydrogeological units or subunits. These representations allow us to understand the location of geological unit and subunits in the three-dimensional space as an additional information layer which can be displayed jointly with further information.

A Borehole Tube entity is composed of several colored cylinders, each one representing a defined geological unit or subunit lot. Its diameter can be adjusted to the scale of the model to make it visually compatible with other data (Figure III.2).

Figure III.2. Boreholes Tubes entities for the study area. The topography is shown in green with the main 3D structure of Sagrera-Meridiana station. Vertical exaggeration factor: 15. Diameter size of BoreholeTubes: 7 m.

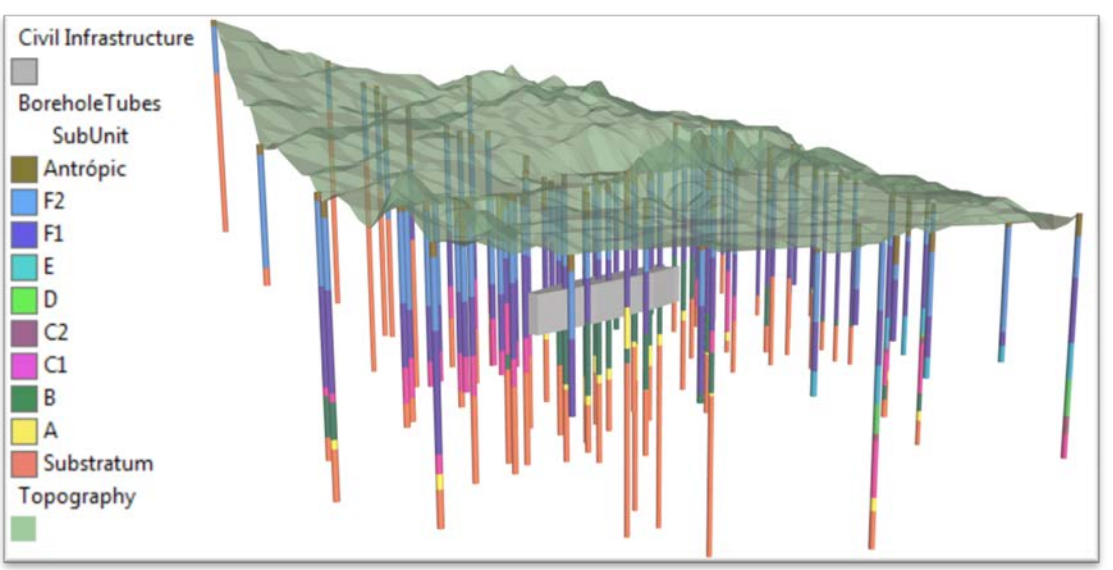

2. 3. 2. Geological surfaces

HEROS3D toolset expresses its maximum strength and capabilities when managing geological surfaces. It allows the user to create automatically the surfaces from the geological data stored in *HYDOR* and to modify them following different processes described below.

2. 3. 2. 1. Automatic creation of geological surfaces

HEROS3D generates automatically the surfaces of the selected geological units or subunits stored in the geodatase *HYDOR*. A Triangular Irregular Network (TIN) surface representing the bottom of the specified interpretation unit is added to the display. It is created as a linear interpolation from the punctual interpretation data of each unit or subunit stored in the geodatabase. These surfaces can represent the first simplified version of the 3D geological model. They can also be used in the iterative process during the definition of the 3D geological model with *HEROS* because their intersection can be visualized in cross-sections created with SC-SC to contribute with additional interpolated information where boreholes are sparse.

These surfaces can be modified by adding particular 3D data generated in *ArcScene* with its inherent tools or with SC-SC tools to develop the final version of the 3D geological model.

2. 3. 2. 2. Modification of existing geological surfaces by extension

Usually, the boundaries of geological and hydrogeological models are not properly defined because the scarcity of data in the margins is common. To overcome this problem, a set of instruments was created. It enables the user to extend the interpreted geological boundaries of the model by using three-dimensional extrapolation techniques. It is based on the extension of the surfaces created previously (or whatever surface saved as TIN) to cover the entire domain. This extension can be calculated by extending up to a specific distance the border line of the surface. New triangles are generated and added to the existing TIN. The slope of these triangles can be defined by the modeller in two ways: (1) maintaining the slope of the triangles located in the actual boundary or (2) defining a constant value as slope.

A polygon representing the entire domain of the geological or hydrogeological model can be used as a clip to delimit these extended surfaces and adjust them to the model boundary.

2. 3. 2. 3. Modification of existing geological surfaces by intersection

In order to be able to use the defined 3D geological surfaces generated in further processes of hydrogeological and geological modeling, they must be topologically valid. This means that in 3D meshes, edges and nodes of the intersecting surfaces must be shared. To date, these geometric problems associated with the intersection of 3D geological surfaces are not solved by using the default techniques offered by the inherent capabilities of *ArcGIS*. To overcome this, *HEROS3D* enables the user to obtain the 3D intersection line between two intersecting surfaces. Inherent *ArcGIS* tools can be then used to create the boundary of the surface of interest with this 3D line and clip the geological surface (Figure III.3). This methodology is based in the triangle to triangle intersection algorithm proposed by [76].

2. 3. 2. 1. Validation and Feedback between interpreted geological surfaces and *HYDOR* geodatabase

The information generated during the interpretation can be reintroduced in previous steps to validate, edit and correct, when necessary, the interpreted geological surfaces. In this way, successive version of the 3D model can be generated, stored and reused for reinterpretation. For instance, the 3D geological surfaces constituting the geological model can be visualized in the geological cross-section to check the agreement among all existing data. Additionally, the final 3D geological model can be stored in the geodatabase as depth values of each 3D surface for specific control points.

Figure III.3. Intersection of contact surfaces of interpreted geological units. Vertical exaggeration factor: 15

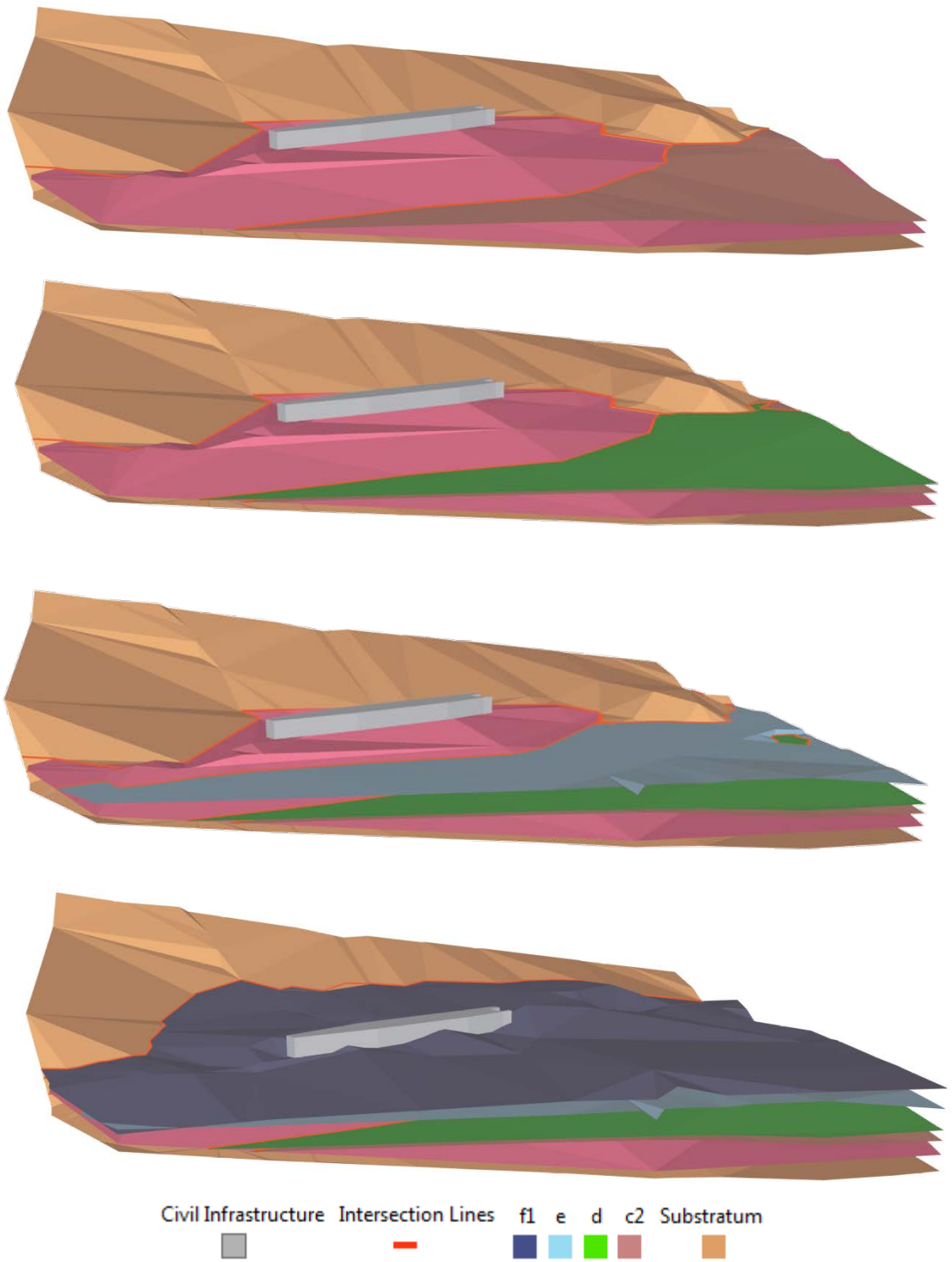

2. 3. 1. Fence Diagrams

To disseminate 3D geological models and make them accessible and easily understandable, it is common to visualize them through fence diagrams. The fence diagrams are vertical sections of geological units following specific lines over the domain. *HEROS3D* allows them to be created automatically from a geological surfaces defined previously by the modeler, e.g., the TIN surfaces generated automatically in the previous step. These surfaces must represent the bottom of the geological units. The lines defining the path of vertical sections must be available as geometrical entities. These lines are divided in segments of a specific distance defined by the modeler, creating vertices. This distance depends on the precision required and the scale of the geological model. The longer the distance, the lower the number of vertex used. Starting from the deepest/shallowest surface, this technique checks the vertical distance between this surface and the next surfaces over/below it for each vertex of the guide line. As a result, 3D vertical polygons are created for the unit selected following the guide lines (Figure III.4). The bottom surface corresponds entirely to only one unit while the top surface can represent the contact with different geological units.

This technique supposes an advance in the automatic generation of fence diagrams. Alternatively, the fence diagrams can also be obtained by exporting to 3D each of the different units/subunits defined as 2D polygons in each geological profile generated with *HEROS*. *HEROS3D* allows the creation of fence diagrams directly on a 3D environment from existing geological surfaces.

Figure III.4. Fence diagrams for geological model of the study area. Vertical exaggeration factor: 10

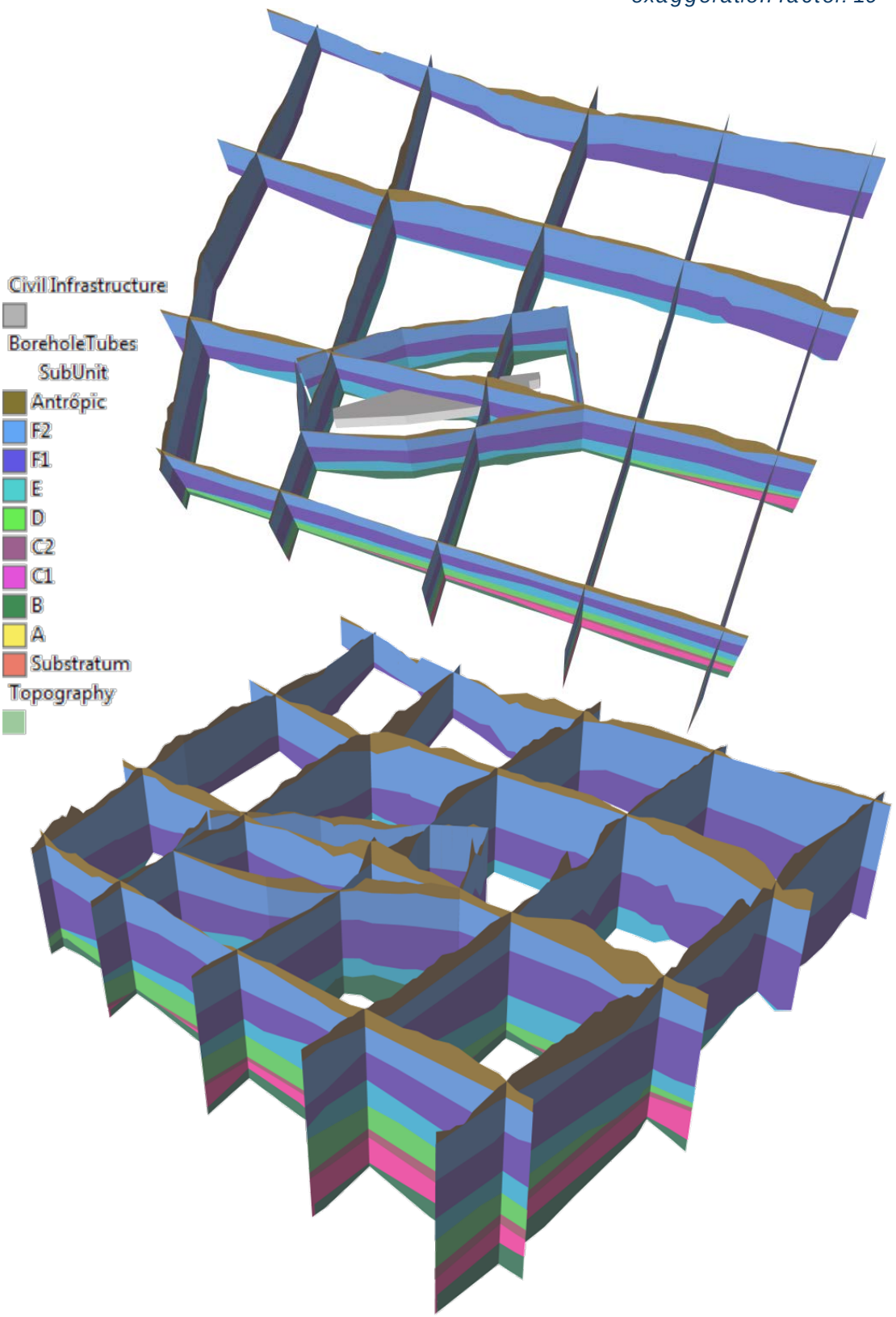

2. 4. 3D and temporal Hydrogeological data management: Piezo Tubes

The hydrogeological data can be analyzed in the same platform with *HYYH* [28]. These tools query the hydrogeological data stored in *HYDOR* such as groundwater levels registered over a period of time. *HEROS3D* represents in the three-dimensional space the temporal evolution of the groundwater table registered from field campaigns. A tube representing the groundwater level can be visualized whose diameter can be modified by the modeller to make it compatible with the additional geological or hydrochemical information (Figure III.5). The base of this tube starts on the bottom surface of the hydrogeological unit that is being studied and reaches the groundwater head. This tube can vary over time if a temporal evolution of the groundwater level has been registered.

Figure III.5. Piezo and Chem Tubes of the study area. Vertical exaggeration factor: 15

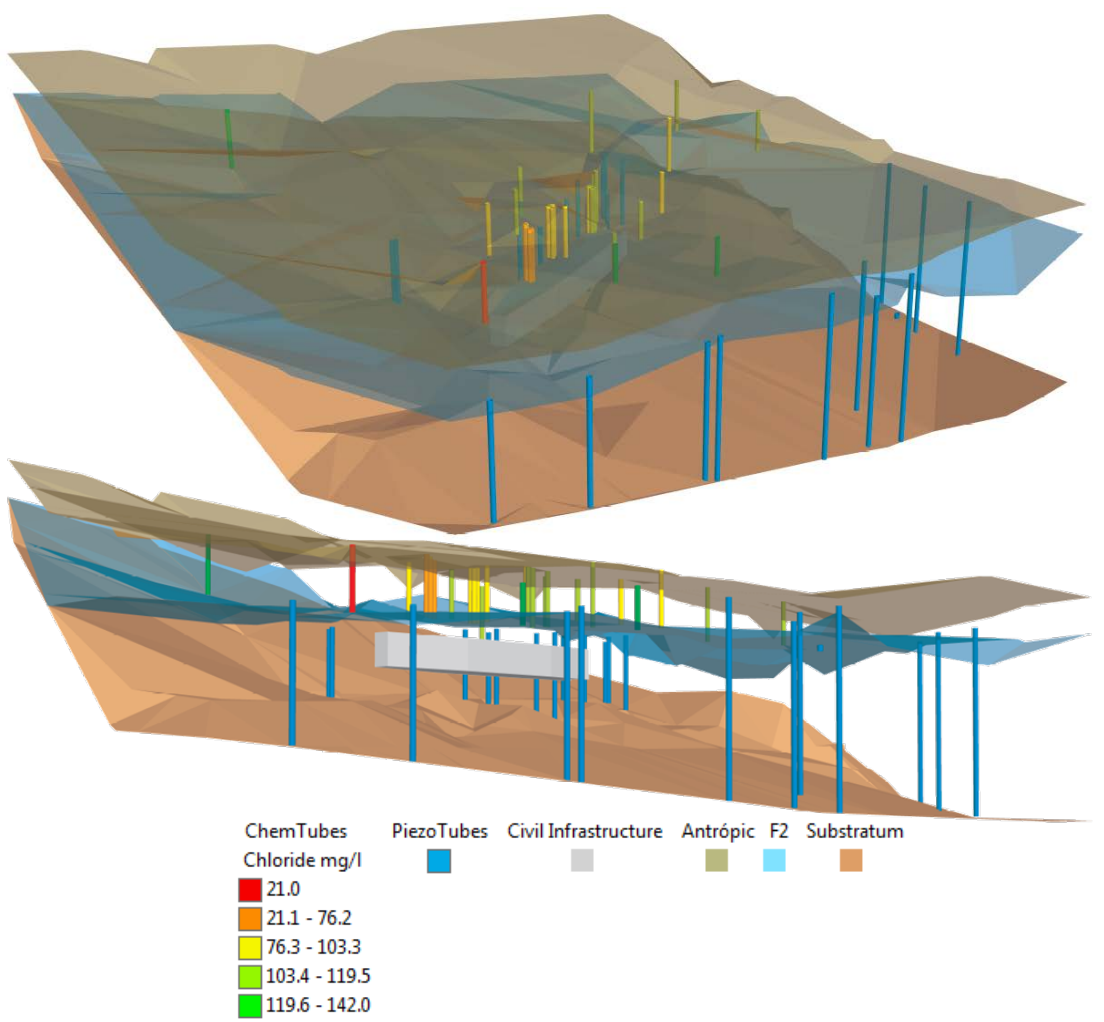

2. 5. 3D and temporal Hydrogeochemical data management

Once the hydrochemical analysis has been carried out in *QUIMET*, the results can be visualized with *HEROS3D*.

2. 5. 1. Chem Tubes

The well is represented as a cylinder inside the hydrogeological unit where the water sample has been extracted from. This representation is named Chem Tube. Its diameter can be adjusted to the global scale of the 3D model as all tubes entities generated with *HEROS3D* (Figure III.5). To visualize the temporal evolution of the chemical concentration of the parameter of interest, the symbology colour of Chem Tube can be adapted to the chemical value for each time interval.

2. 5. 2. Screen Tubes

Additionally, in multi-aquifer systems, *HEROS3D* enables us to visualize the screened interval of the well to show which aquifer has been sampled. Screen tubes are entities representing the depth and length of screens of each groundwater point.

2. 6. 3D Geothermal data management: Thermal Disturbance Plumes

The shallow geothermal analysis in the *HEROINE* platform is carried out with *MetroGeother* tools for closed-loop systems, which are described in chapter VI . This set of tools provides methodologies to facilitate the visualization and management of the geothermal data and thermal impacts generated in the two-dimensional space. The thermal plume produced by the exploitation of SGE can be drawn with these tools in the plane X-Y. In cases where the closed-loop system crosses units with different hydraulic and thermal properties, the thermal impacts will be different for each geological or hydrogeological unit. The 3D visualization of these thermal impacts (Figure III.6) can help to manage this resource, and distribute the thermal impact among existing exploitations and affected geological units.

Figure III.6. Synthetic analysis of several exploitations of SGE in the study area. These thermal plumes have been calculated for a Darcy velocity of 10-7m/s, a thermal conductivity of 2.6 W/K·m, a volumetric heat capacity of 3223000 J/K·m3 for a heat rate of 100 W/m after a period of exploitation of 6 months. Vertical exaggeration factor: 10

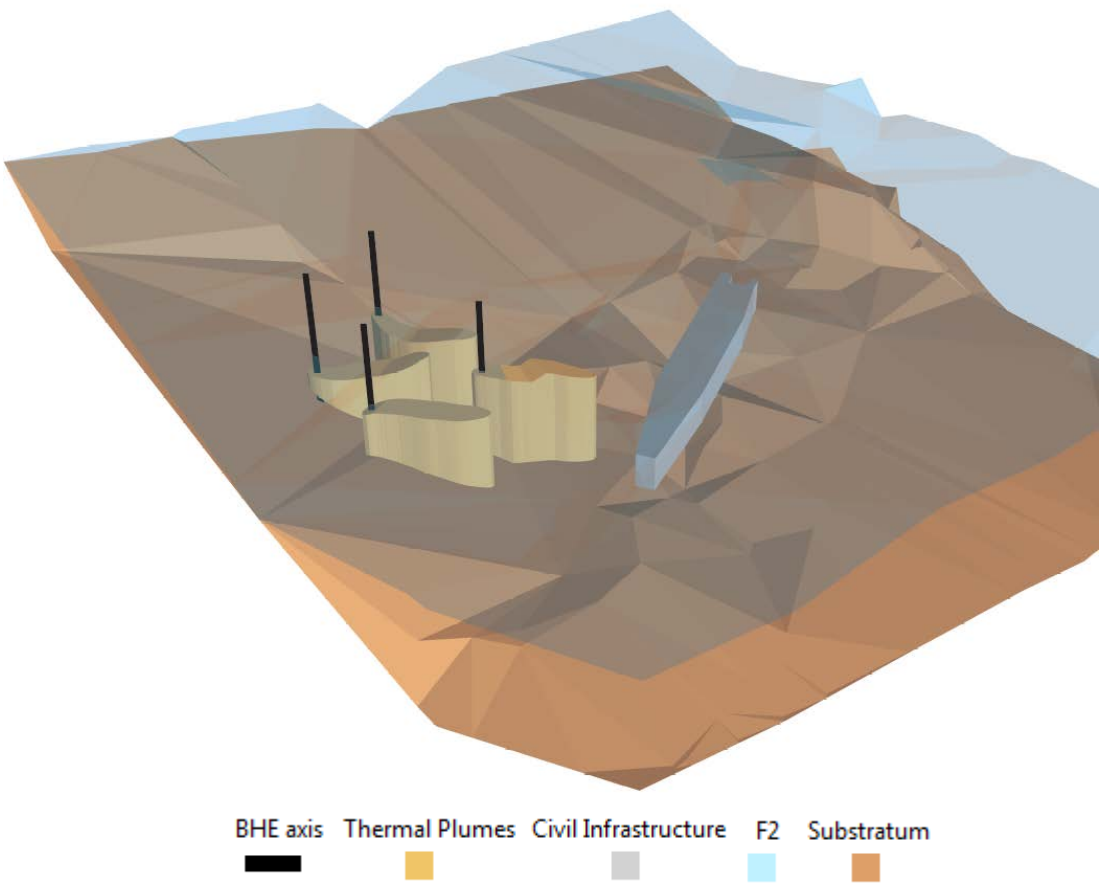

3. APPLICATION

The *HEROS3D* toolset was used in a case study involving an urban aquifer to illustrate its performance. The study area is located in a highly urbanized area in Barcelona, Spain. It is framed around the civil works related to the construction of the Sagrera-Meridiana Intermodal Transportation Hub, which will receive passengers of high speed and suburban trains, subway and buses. Its deepest base reaches the -6 m a.s.l. and is located below groundwater level (Figure III.7).

Geologically, the study area is mainly characterized by the presence of Quaternary sucession of the Besòs Delta that rest unconformably over a substratum of Paleozoic rocks. The main features of the geological units in this area are summarized in Table III.1[77]. The geospatial database *HYDOR* includes 87 points with lithological descriptions that were interpreted with *HEROS* to define contact points for each of the nine hydrogeological units defined (Table III.1). 2061 hydrogeochemical data of 239 chemical compounds are also available from 138 groundwater points, from which 29 points have geological descriptions. Finally, 1368 piezometric measurements are also stored for the groundwater points.

Figure III.7. Location map of the study area along with groundwater points, geological points and path lines for fence diagrams. Ortograph of the study area: UTM, ED-50, 31N.

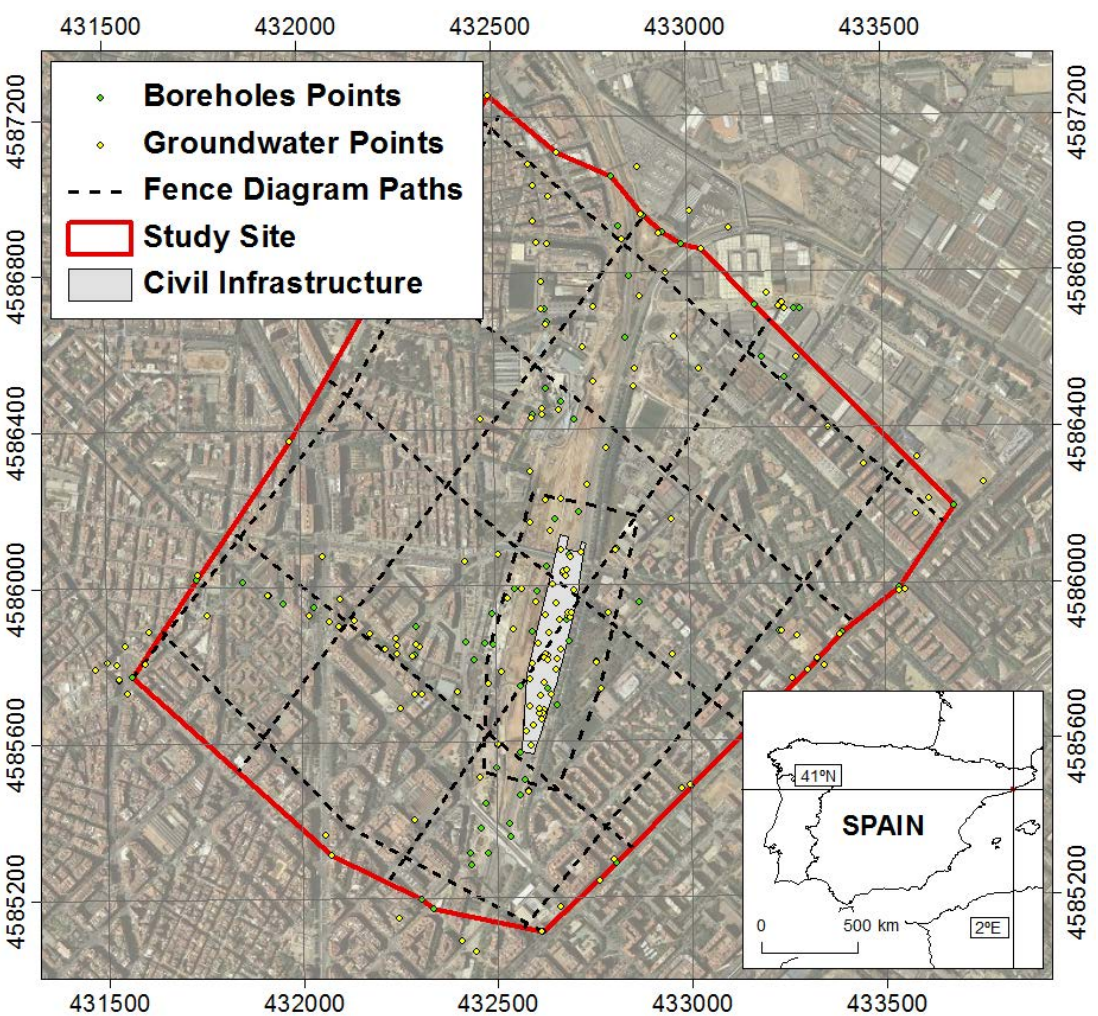

Table III.1. Lithological, hydrogeological and chronological description of the different geological units of the study area.

Age	Unit	Lithological description	Hydrogeological description
Post Glacial - Holocene	F2	Local heterometric and massive deposits of clast supported and very coarse-grabels with clay-sandy matrix into high series of lutitic units with some sandstone beds	Partially permeable (permeable in areas with less silt)
	F1		Less permeable (only permeable in areas with less silt and clay
	E	Well sorted gravels and sandstones with some traces of fossiliferous content	Aquifer
	D	Yellow to gray coarse grained facies belt made up by sands and gravels (from distal to proximal). Some traces of shell fragments	Aquitard
	C2	Well rounded to angular clast supported pebbles with sand	Aquifer
	C1	Poorly sorted gravels, occasionally with sandy matrix and some lenses of organic matter. Pebbles are well rounded and polymictic and the structure is clast supported.	Partially permeable (permeable in areas with less silt)
Pleistocene	B	Massive red/brown lutites with isolated poorly sorted gravels and pebbles which are passing to interlayered sandstones and clays in a finning-upward succession.	Less permeable (only permeable in areas with less silt and clay
	A	Poorly sorted gravels, occasionally with sandy matrix and some lenses of organic matter. Pebbles are well rounded and polymictic and the structure is clast supported.	Aquifer
Pliocene	Substratum	Gray marls in some places interbeded with sandstones and gravels	Less permeable (only permeable in areas with less silt and clay
Paleozoic	Substratum	Granite	Less permeable (only permeable in fractured areas)

A comprehensive geological analysis was carried out in Diviu et al. (2015) that comprises the complete geological methodology proposed of feedback and validation. Here, only the output and methodologies of *HEROS3D* are shown.

After the geological analysis in the two dimensional space with *HEROS* tools, the geological interpretation is available in *HYDOR* and ready to be queried by *HEROS3D*. The Boreholes Tubes representing the three-dimensional visualization of this interpretation is shown in Figure III.2. The geological surfaces generated automatically are shown in 0. Most of them were extended up to the boundary of the model or up to their intersection with other surfaces. Once these geological surfaces are available, the fence diagrams can be generated automatically following the paths of Figure III.7 (Figure III.4). The methodology shown here generates an initial version of the geological model. Further details must be checked and validated using both *HEROS* and *HEROS3D* in an iterative process.

Temporal evolution of hydrogeochemical and piezometric values for groundwater points was created for the study site. Figure III.5 contains the Chem Tubes entities for concentration of chloride and also Piezo Tubes which reflect the piezometric level variations for each groundwater point.

Finally, a synthetic exploitation of SGE with a closed-loop system was generated. The SGE exploitation goes across the F2 unit, whose thermal impacts can be visualized in Figure III.6. This can help to optimize the depth of heat exchangers and to allocate this resource among users in an efficient manner.

4. CONCLUSIONS

HEROS3D offers a working environment for managing, querying and interpreting geological, hydrogeological, hydrogeochemical and geothermal data in a 3D GIS environment, along with additional data, such as 3D urban infrastructures.

The geospatial database allows us to store and manage data from most hydrogeological and geological studies. Additionally, the possibility of querying and visualizing all the available information in the same 3D environment gives us the possibility of integrating the geological and hydrogeological information with other

relevant data (e.g., hydrogeochemical or geothermal data) and thus to obtain further information.

Apart from the database, the presented platform offers a great variety of automatic tools developed in *ArcScene* (*ArcGIS;ESRI*) designed to exploit the stored data. Using these tools in conjunction with the rest of *ArcScene* capabilities increases the functionality of the software, which provides a 3D geological modelization and a subsequent a comprehensive geological and hydrogeological analysis. 3D visualization of geological interpretation can be generated automatically in different entities, such as Borehole Tubes, geological surfaces and Fence Diagrams. In addition, hydrogeochemical and geothermal impacts can be visualized in three-dimensional space along with the geological and hydrogeological models.

The three-dimensional visualization of input and output data generated in each step of hydrogeological modeling supports and improves the management and understanding of available data to achieve its integration and validation during the construction of comprehensive hydrogeological models.

IV.IMPLEMENTATION INTO NUMERICAL MODELLING[4]

1. INTRODUCTION

GIS techniques are required along the whole modeling process as a support tool [78] [79]. Environmental modelers can take advantage of the synergies leveraged by GIS and numerical modeling [80]. GIS is used from the initial data management [81], which they are originally intended for, to complex modeling techniques. The modeling process can be divided in two main steps: the conceptual modeling and the numerical modeling (Table IV.1).

Table IV.1. GIS as support tool in groundwater modeling phases. Source: [78]

Phases		GIS functions	Modeling Steps
Conceptual modeling	Pre processing Data colection Conceptualization	Data input, Digitalization, Data conversion (impor/export), Coordinate transformation, Map retrieval	Collection of required data
		Conversion of vector and raster layers, Data integration, Image processing, buffering, Surface generation,	Model conceptualization

[4] This chapter is based on *M. Alcaraz, E. Vázquez-Suñé, V. Velasco. (2016 GIS tools to optimize implementation of groundwater conceptual models into numerical modeling.Environmental Modelling & Software. In elaboration.*

		Linking of spatial and attribute data	
Numerical modeling	Model design	Map calculations, Neighborhood operations, Interpolation, Theissen polygons, Surface generation	Boundary delineation, Mesh generation, 3-dimensional layering of the aquifer
	Calibration and Verification	Data layers integration	Parameter zonation, Recharge estimation, Water balance
		Overlay analysis	Steady state and transient state simulations
		Statistical analysis	Parameter estimation
	Post processing, Predictions, Data presentation	Data retrieval	Prediction, Scenarios
		Data visualization, Presentation of simulated results	Map composition

The conceptual modeling process involves management, query, visualization and analysis of spatially referred information available. Its goal is to understand and define the behavior of the environmental systems. Numerous GIS applications for different environmental disciplines have been developed to deal with all kind of data [25], such as geological, hydrogeochemical or meteorological data for oceanography, hydrology or hydrogeology.

Once the conceptual model has been defined, the numerical modeling process aims to reproduce its behavior and simulate the system response under specific situations. Different numerical methodologies can be applied, such as finite elements or finite differences, where analytical methodologies are also of interest. Traditionally, there has been a general effort to integrate GIS techniques in the numerical modeling. For instance, [82] merge GIS techniques with numerical modeling to generate maps of artificial recharge suitability. In this second step, the GIS integration has been achieved in different grades as stated in [83], [84].

GIS and numerical modeling can be loose/tightly coupled or embedded in each other (fully coupled). According to the process of interest and its associated data, one of these three formulae can be applicable, whose advantages and disadvantages are described in Table IV.2.

Figure IV.1. Schema of coupling strategies for GIS and numerical modeling software. Source: [83], [84]

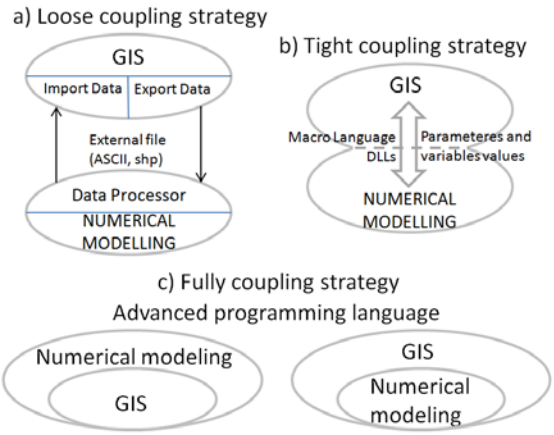

Table IV.2. Advantages and disadvantages of three coupling strategies between GIS and numerical modeling codes. Modified from [85]

Strategy	ADVANTAGES	DISADVANTAGES
Loose coupled	GIS and Groundwater numerical capabilities are completely available. Geometric and alphanumeric data can be reused in other numerical modeling software. Conceptual model is available for further analysis apart from hydrogeology. Independent development of GIS platform and numerical software can be accomplished.	Advanced knowledge for both platforms. Manual file exchange between both platforms.
Tightly coupled	Groundwater numerical capabilities are completely available. Geometric and alphanumeric data can be reused in other models with adaptation to third platforms. Automatic data exchange between both platforms.	Migration to new platform is time-cost. Inherent GIS capabilities are limited for standard users. Data model shared by both platforms, which limits exchanges with a third one due to its fix structure.
Fully coupled or embedded	Changes in parameters or processes are possible while simulating. Just one platform for the entire modeling process.	Learning new platform is time-cost. Specially designed platforms have not the same number of capabilities of GIS or Numerical modeling platforms. Changes to base code are difficult due to large source code structure.

The integration of GIS and numerical modeling has been extensively described for hydrological modeling. For instance, hydrology processes have been largely treated with tight [86] or full coupling [84]; for an updated stated of the art, see [85]. This is possible because the relevant variables in hydrological processes are based on topography, which has been traditionally managed by GIS. Similarly, software developed for numerical hydrogeological modeling [87] and other environmental processes can also be classified according these statements. However, each discipline has its own peculiarities referred to data requirements, thus each one must be analyzed individually [88].

In this work we are going to focus on hydrogeological modeling. Numerous data models have been developed to store, manage and access easily all information needed [69], [70], [89]. This information is mainly relating to hydrogeology (spatial zonation of hydrogeological parameters such as hydraulic conductivity, storage coefficient, dispersivity, etc...) but also to geology (spatial distribution of hydrogeological parameters such as porosity, thermal conductivity, etc...), meteorology (rainfall, evapotranspiration) or surface hydrology (runoff).

Several applications have been developed as tightly coupled relations between GIS and hydrogeological numerical modeling. This relation is based on the feedback of geometry and alpha-numerical data between GIS and numerical software. This feedback is accomplished through the automatic generation and exchange of structured files (usually ASCII files) generated by GIS platform with tools designed specially for this purpose. These files are read by groundwater numerical software as input files to perform numerical calculations. A detail state of the art about the existing GIS applications for groundwater modeling can be consulted in [90]. Some recent examples of tightly coupled applications are described below.

Governmental water management agencies have developed specific software to satisfy its necessities. For instance, the State of California, through the California Natural Resources Agency, have developed a tight-coupled model, IWFM (Integrated Water Flow Model), that simulates groundwater, surface water, stream-groundwater interaction and other components of the hydrologic system. It solves

the governing flow equation using the Galerkin finite element method. As a support tool, they developed IWFM GIS/GUI [5], where the finite element grid, stream network, stratigraphy and initial conditions can be visualized in a GIS environment (*ArcGIS* v10.0). They also developed another GIS application to create finite element meshes inside *ArcGIS*, assign the hydrogeological parameters to each element and export them to IWFM as text files.

The Pacific Northwest Regional Office of Boise (Idaho) offers TimML [91], an analytical model which can be complemented with *MODFLOW* [74] in some cases to define boundary conditions. They have developed a toolbar inside *ArcMap*, name *ArcTim* [92], with tools to manage shapefiles and grids and configure the geometry and parameters to run the analytical model.

Private companies also extend GIS capabilities to lead with meshing generation in hydrogeological numerical modeling. [93] described *MODFLOW USG Tools for ArcGIS*, a set of tools to create unstructured meshes in *ArcGIS* that can be exported to numerical modeling platforms such as *MODFLOW*.

Arc Hydro Groundwater is the development supported by *ESRI* to deal with groundwater numerical modeling [69]. This platform is highly efficient to define the conceptual model. Relating to the numerical model, the mesh and general configuration of the numerical model is generated with *MODFLOW*. Then, *Arc Hydro* imports the spatial discretization and settings defined with *MODFLOW*. The data can be visualized and modified to go back to *MODFLOW*, where numerical calculations are performed.

OpenGeoSys [94] also suggest to manage data in a GIS platform [95] as pre and post processing tool, along with *ParaView*.

SID&GRID [96] is tightly coupled application within *GvSIG*. *MODFLOW* is the numerical code to perform the hydrogeological numerical model. [97] presented a Graphical User Interface for *MODFLOW* as a module of *Argus*[6]. *ArcEngine* has also

[5] http://baydeltaoffice.water.ca.gov/modeling/hydrology/IWFM/SupportTools/index_SupportTools.cfm accessed on November, 13th 2015.
[6] http://www.argusone.com/ accessed on November, 17th 2015.

given support for tightly applications such as the one proposed by [98]. They implemented SUTRA in a GIS platform developed with *ArcEngine*.

Fully coupled or embedded applications are less frequent. Numerical modeling software have implemented GIS applications, which are limited for visualization purposes. Conversely, GIS platforms have become the most common framework where the numerical modeling is integrated. *ArcFem* [99] can be considered as a embedded application, where the numerical calculations are carried out inside the GIS software. Again, data must follow a data structure adapted to this software.

However, it is a common trend that hydrogeological numerical modeling software are able to import and read shapefiles, such as last versions of *Visual MODFLOW* or *FEFLOW*. The shapefile is a widespread structured vector file, which can be managed easily from GIS. This is a gateway to loose coupled applications which has not been specifically developed to optimize hydrogeological modeling until now. Loose coupled applications have been used frequently to prepare the conceptual model and the input data required to numerical modeling process ([78], [79], [89], [100]–[102]). But all of them relay on inherent GIS capabilities to prepare the defined conceptual model to be used in numerical modeling. These GIS loosed coupled applications resort to advanced tools inherent to GIS platforms. However, these inbuilt GIS capabilities are insufficient, because hydrogeological data requires specific treatment in order to be used in numerical modeling. These preprocessing is mainly related to geometry characteristics to facilitate mesh generation in finite element numerical software. The mesh creation is usually a troublesome, labor-intensive and time-consuming process [103] for mesh generators due to inconsistencies of input geometries. Moreover, suitable meshes must accomplish specific requirements [104] for an optimal numerical modeling.

In this situation, this work presents the development and structure of *ArcArAz*, a set of GIS-based tools specially oriented to adapt hydrogeological data to be used for numerical modeling. These tools are focused on improving the geometry of input features that configure the model geometry, thus avoiding obstacles when creating the finite element mesh and configuring the boundary conditions and other aspects of numerical modeling.

2. ArcArAz SOFTWARE DESCRIPTION

2. 1. GIS-MODEL COUPLING STRATEGY

One of the three coupling strategies presented above, loose/tightly/fully coupled, can be used to integrate numerical modeling and GIS. In this work, a loose coupled approach was selected to integrate *Visual TRANSIN* in *ArcGIS* framework.

The main advantage of loose coupled applications relays in the flexibility of data model upon they work. There is no need of sharing a common data model, as in tightly coupled applications. This has favorable consequences listed below:

Any data model structure can be processed with *ArcArAz* and the selected numerical modeling software. This is very profitable because each project has different data with different structures, so it is desirable to be able to adapt the methodology to whatever data model structure.

Loose coupling strategy allows for independent development of both hydrogeological model and GIS.

This advantage allows reuse the hydrogeological conceptual model defined in GIS with alternative numerical software. This can be also very useful to study other environmental processes, apart from hydrogeology, such as surface hydrology. By maintaining the access to both platforms, GIS and numerical modeling platforms, all the advanced capabilities of both platforms are available to enhance the modeling process.

The loose coupled approach gives enough flexibility to modelers to decide which platform use to face specific steps, such as parameter assignation. Therefore, data can be managed for both GIS and numerical software, according to modeler's preferences. This is possible due to the ability of numerical software to link parameters to entities' attributes stored in shapefile format.

2. 1. 1. Exchange file format

Both platforms, GIS and numerical software, support shapefile format, so shapefile was selected to exchange data between the different platforms, thanks to

- the versatility of shapefile format
- the general standardization of its use

- *Visual TRANSIN*, as well as other numerical software, can import both geometries and attributes of entities

It is not necessary to export to third formats, avoiding data redundancy and improving accuracy when processing in both platforms.

2. 1. 2. GIS platform

ArcGIS (*ESRI*) was used as the GIS platform to perform GIS-model integration. *ArcGIS* allows visualizing, editing, creating and analyzing geographical information, in both raster and vector format. The selection of *ArcGIS* was based on several factors including:

- widely used across all science disciplines;
- strongly rooted in the market to ensure its durability and permanence;
- well supported by active developer and user communities;
- powerful software developer kit available.

The *ArcMap* is one of the main components of *ArcGIS* to explore and manage bi-dimensional data. It hosts the hydrogeological platform *HEROINE* ([24], [26], [27]) which *ArcArAz* is part of. This specialized platform allows for the management, analysis and interpretation of geological and hydrogeological data to elaborate the hydrogeological conceptual model.

The data exchange between GIS and modeling software is accomplished with shapefiles, due to the above-mentioned advantages of this format.

2. 1. 3. Framework for hydrogeological numerical modeling

The numerical modeling software selected was *Visual TRANSIN*, a finite element code that, among other functions, solves coupled flux and mass transport equations in porous media and the inverse problem (the estimation of model parameters from measurements of the respond system, groundwater levels and chemical concentrations). Its mesh generator is *2DUMG* [105], which constructs unstructured triangular meshes.

Although *ArcArAz* was oriented to solve problems when meshing with *2DUMG*, similar circumstances usually prompt with other mesh generators. Thus, *ArcArAz* can be applicable when meshing and working with other numerical software apart from *Visual TRANSIN*, thanks to the loose coupled strategy selected.

2. 2. DESIGN: ARQUITECTURE AND PROCEDURAL DETAILS

Functions accomplished by *ArcArAz* tools can be classified in three main sections: file organization, entity setup and mesh creation. File organization includes capabilities to keep controlled (traced) the input and output shapefiles used for numerical modeling. Entity setup is oriented to configure the geometry and attributes of each entity to make them valid for importing into numerical software. Finally, mesh creation tools provide the ability to adjust entities' geometry to facilitate and control mesh generation.

ArcArAz tools are organized as a sequence of procedural tools to (a) manage input/output shapefiles for/from *Visual TRANSIN*, (b) set initial shapefiles in a well organized manner, according to each model version along the iterative process, (c) rescale entities' geometries according to numerical modeling purpose, (d) modify entities' shape to adapt it to meshing process, and (e) adjust alpha-numeric attributes to make easy their manage and assignment as parameters in the numerical modeling software.

2. 3. DEVELOPMENT

ArcArAz user interface is integrated with the *ArcMap*, as a based toolbar. It was developed with *ArcObjects SDK for .NET*, the customization framework provided by *ArcGIS*. This framework enables the development of form and menu systems within *ArcGIS* to configure the user interface of *ArcArAz*. These tools are accessible from ten dropdown menus of the toolbar, whose structure is shown in Figure IV.2.

Figure IV.2. Schematic representation of ArcArAz menus with all capabilities implemented. Use of bold indicates the new tools implemented. The remaining tools are shortcuts to already existing GIS tools.

Input Data	Entity Properties	Temporal Series
Set Project and WorkFolder	**Remove Interior Holes**	Simplify Graphic
Add Shapefile to TOC and Workfolder	Line to Polygon	**Domain**
Remove shapefile from TOC and Workfolder	Multipart to Singlepart	**Convex domain**
Safety copy of shapefiles	Start Edit Session	**Spatial Fields**
Import from AutoCAD	**Rename Entities**	DEM from AutoCAD
Split Shapefile	**Copy/Paste features**	Assign Altitude to entities
Set Coordinate System	**Vertex**	**Vertex Coordinates to ASCII**
Output Data	Select entity to submit	Raster to Element Mesh
Shapefile with mesh nodes	**Visualize Vertex Entities**	**Raster/TIN to ASCII**
Shapefile with mesh elements	**Vertex Count**	**Rivers**
Raster / TIN Piezo	Reduce vertex number	**Reorganize Rivers Network**
Raster / TIN with Descensos	**Vertex at Intersection**	**Ever Increasing Height Rivers**
PLT Viewer	**Increase Vertex Number:**	**Delete Duplicate Segments**
Parameters Nodes	**Vertices at specific distance Maximum distance between vertex**	**To VT**
Parameters Elements	**Wells**	**Topology**
Particle Track	**Auxiliar lines for Meshing**	**Central Coordinates**

ArcMap offers the display and editing of geometric and alpha-numeric data, facilitates the visualization of additional relevant data and supports *HEROINE* (the GIS platform specifically oriented to hydrogeological conceptual modeling described in Chapter II). Therefore, the complete hydrogeological model, from the conceptual to the numerical processes, is integrated in the *ArcMap*.

The main functions of *ArcArAz* tools can be classified as *Input Data Processing* tools and *Output Data Visualization* tools. They are accessible following the same procedural flow as in *Visual TRANSIN*, although the menus' names are intuitive enough to alter this flow according particular needs of different software platforms for numerical modeling. The tools are classified according the modeling entity they are focused on, such as Rivers or Wells.

In addition to new and specific tools, *ArcArAz* also offers shortcuts to most common inherent GIS tools. In this way, the most powerful GIS characteristics are available not only for advanced users, but also for standard GIS users.

3. ArcArAz APPLICATION

To demonstrate the applicability of *ArcArAz* tools, we present the configuration of the groundwater numerical model carried out for Matanza-Riachuelo basin, in the metropolitan Area of Buenos Aires, Argentina (Figure IV.3). This area has been studied in detail in last years [106] due to its strategic role in water management for this highly populated region. Next subsections provide detailed description of the study area and of *ArcArAz* tools. For here onwards use of italics indicates a reference to *ArcArAz* tools or toolset.

3. 1. Study area description and numerical model discretization

A total of three hydrogeological units had been conceptualized to represent the groundwater behavior in this area, the upper and bottom aquifers separated by an aquitard. With a modeled area of 4.500 Km^2, the parameter zonation is determinant to achieve an optimal calibration of the model. The superficial aquifer corresponds to sandy and clayey silt sediments with more accurately defined geology. The aquitard is formed by plastic clays and the bottom aquifer corresponds to sand and sand with interbedded clay and silty formations [107].

Figure IV.3. Location and detail of multilayer mesh for ACUMAR hydrogeological model.

The finite element mesh is defined as a quasi-three dimensional mesh. Two bidimensional layers represent the aquifers. They both are connected by vertical elements of one dimension simulating the aquitard [108]. The finite element mesh is adapted to the geometry of upper layer, more complex due to the variety of boundary conditions (rivers, recharge areas and geological zonation), whilst the bottom aquifer is conceptualized as homogeneous for all hydraulic and transport parameters (Figure IV.3).

It is noted that the scope of this chapter is limited to demonstrating the capability and effectiveness with which *ArcArAz* tools enable the configuration of the groundwater numerical model. The model results shown in this chapter were neither calibrated nor validated against field observations. Readers are referred to [108] for details about numerical simulations.

3. 2. File structure and project configuration

This set of tools allows for organization of input and output shapefiles. During the calibration process, both the value of the parameter and the shape of its zonation can be modified to achieve better adjustment to observed values [109]. This represents an iterative process in which the conceptual model is altered according to the results of the numerical simulations. It has a high relevance when optimizing the shape or geometry of each parameter zonation. Several versions of the conceptual hydrogeological model can be stored and available for further analysis or been reincorporated again in the modeling process. To facilitate this task, *Set Project and Workfolder* tool was developed to configure a workspace where shapefiles for each successive version must be stored. *Add Shapefile to TOC and Workfolder* tool creates a copy of an original shapefile into the workspace folder and automatically adds this shapefile as a layer to the map. Conversely, *Remove Shapefile from TOC and Workfolder* tool deletes the specified shapefile from the map and simultaneously from the workfolder. Before accomplish any modification to shapefiles, the creation of a safety copy is recommended with *Safety Copy of Shapefiles* tool. This allows keeping track of the evolution of entities' shape and attributes.

Additionally, to make accessible some initial processes previous to the setup of the numerical model, tools oriented to specific actions where developed. Assignment of the spatial coordinate system (*Set Coordinate System* tool) and import of geometries from CAD files (*Import from AutoCAD* tool) are examples. The last tool of this toolset, *Split Shapefile* tool, divides an original shapefile in several shapefiles containing a specified number of entities. This is necessary if original files are too large and may have problems when importing them to the numerical platform.

3. 3. Entity setup

This set of tools prepares the geometry and attributes of entities and other alpha numeric data to assist the process of importation into the numerical software platform. Related to the attributes properties, *Rename Entities* tool assigns univocal names for each entity to be used as ID in the numerical software. The new name is generated from a selected attribute of type text, e.g. the location. Symbols which could not be recognized by the numerical software are substituted or removed.

Because a location can be shared by different entities, a unique ID number is added to difference between them. The character length is also limited.

The *Convex Domain* tool creates a polygon which encloses all features of interest and serves as a base polygon to elaborate the numerical model domain (Figure IV.4). This convex hull can be edited to adapt the final boundary to border entities with GIS inherent edit tools.

Figure IV.4. Convex domain generated with Convex Domain tool taking into account the geometries of geological, hydrological and areal recharge entities.

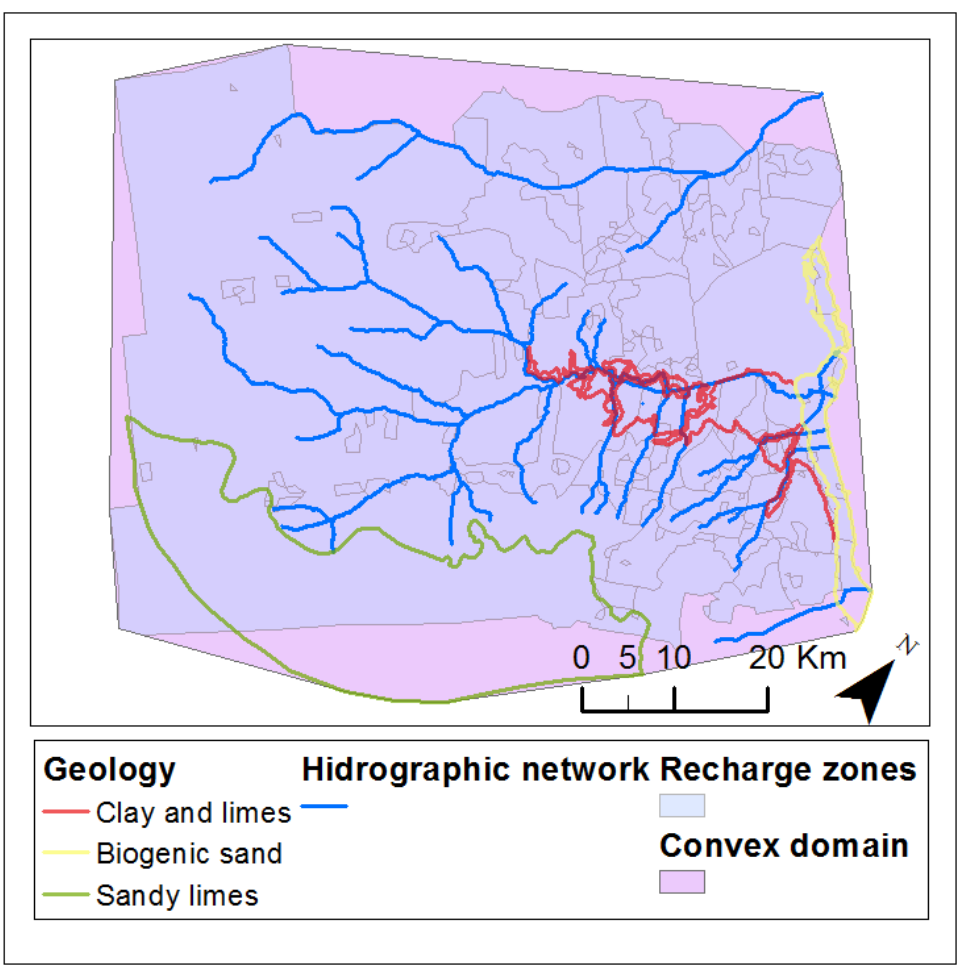

With relation to rivers entities, two tools were developed specifically oriented to this kind of entity when defining the boundary conditions of the system. The *Assign Altitude to Entities* tool converts a two-dimensional shapefile in a three-dimensional

one getting the heights from a DEM. Another relevant alphanumerical data is the elevation of rivers. When the hydrographic network is not obtained from the DEM (for instance, by digitalizing over a map) the rivers may present pits zones when assigning elevation. These segments must be filled with the *Ever Increasing High* tool. This tool calculates a new elevation value for each vertex of river entities based on the average slope of each entity. The Figure IV.5 shows in red the rivers without modifications and in green, the ones with the corrected slope.

Figure IV.5. 3D detailed view of two rivers (Arroyo Rey and Arroyo Catalina). The red lines correspond to original rivers shapefile used as input file for Ever Increasing High tool. The blue lines are obtained as output. The new slopes have been smoothing to avoid pits.

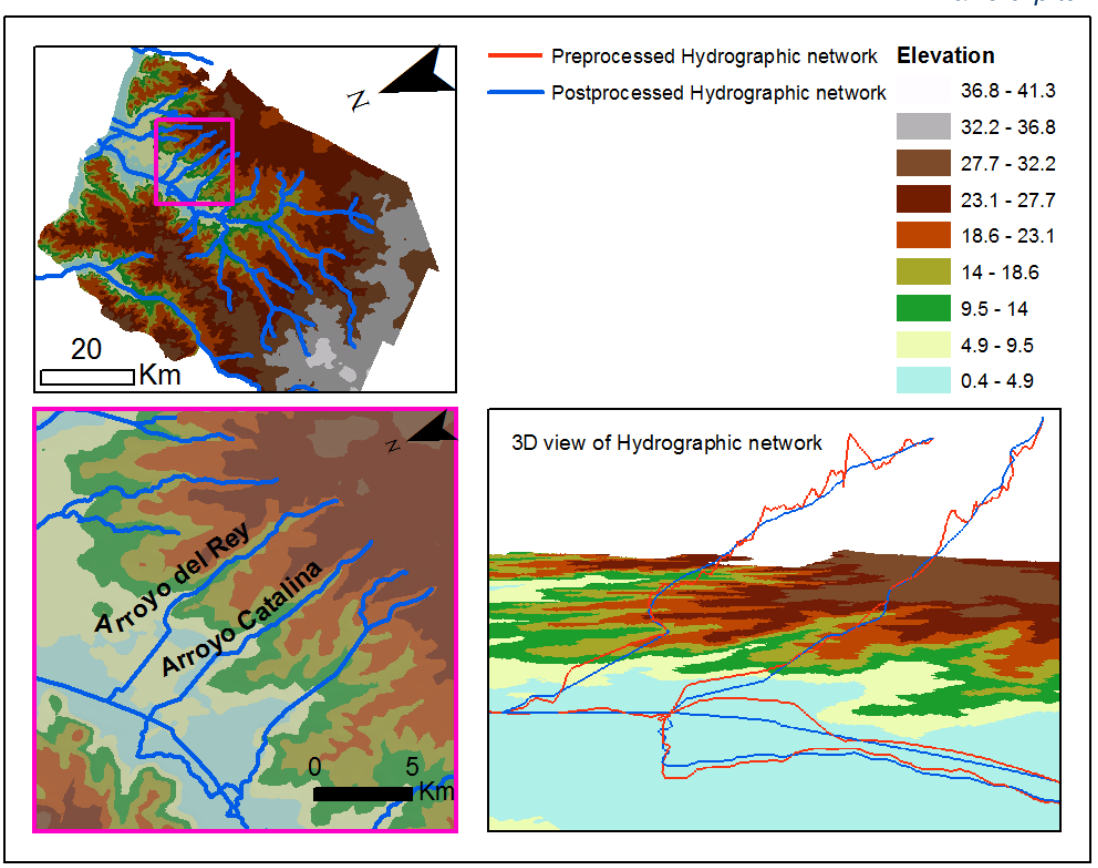

Also, this toolset supports tools to generate spatial fields to be exported as ASCII files into *Visual TRANSIN* or other numerical platforms. Spatial fields are used in numerical modeling to reproduce the spatial variation of hydraulic and transport parameters. According to these spatial fields, the properties can be assigned to each mesh element. These spatial fields can have their origin in CAD files (*DEM from CAD* tool), raster or TIN surfaces (*Raster/TIN to ASCII* tool), and even vector files (*Vertex Coordinates to ASCII* tool). The text files generated contain the X and Y coordinates and the elevation of TIN nodes, central points of raster cells and entities' vertices respectively.

In addition to the afore-mentioned tools for alphanumerical data, the following tools are oriented to improve the geometry or shape of geographical entities to import them into the numerical modeling platform. Multipart entities can be split into single part entities with *Multipart to Single Part* tool. As new entities are created, the *Rename tool* should run after this tool. Continuous polygons without holes can be acquired with *Remove Interior Holes* tool. Conversely to this tool, *Non-overlapping Polygons* tool generates polygons from the geometric union of input features; output features could have interior rings and could constitute multipart features. *Line to Polygon* tool converts closed lines in polygons in a new shapefile. This tool is required when the digitalization process generates lines instead polygons for areal parameters. Finally, the last tool, *Central Coordinate* tool, displaces the coordinate origin to the geometric center of all features.

3. 4. Mesh creation

This set of tools is oriented to prepare the geometries for mesh generation inside the numerical software in order to generate more suitable meshes for finite element modeling. When elaborating finite element meshes, some consideration must be taken into account related to number and shape of nodes and elements:

- All vertices of geometries involved in meshing are going to participate in the mesh as nodes.
- Mesh must be refined where more variations of state variable were expected.
- Triangular elements should be equilateral whenever possible [110].

The tools located under the Vertex menu allow managing the number and position of entity geometries. By selecting a feature on the map, its number of vertices can be known with *Vertices Count* tool. Moreover, these vertices can be

visualized as graphics elements by using Vertices *Visualizer* tool. This tool was used in next figures to show how the vertices of specific entities were treated. The number of vertices can be increased to control the mesh refinement in an area of interest with *Densifier* tools. There are two methods to perform the vertex densification. A constant distance between vertices can be defined and new vertices will be placed at this distance from the origin of the line (or border line for polygons). In this case, last vertex can remain too near the end vertex of the line (*Vertices at Specific Distance* tool). Alternatively, a maximum distance between vertices can be defined so all new vertices will be equidistributed (Maximum Distance between Vertices tool). Due to the scale of ACUMAR model, it was not necessary to densify the vertices number; however, an example of these two methodologies is shown in Figure IV.6, although these geometries were not implemented in the numerical model.

Figure IV.6. Detail of finite element mesh before and after run Maximum Distance between Vertices tool. The new mesh generated has a higher number of elements around the processed entities. Colored areas represent different recharge areas. Red and greed dots represent entities' vertices visualized with Vertices Visualizer tool.

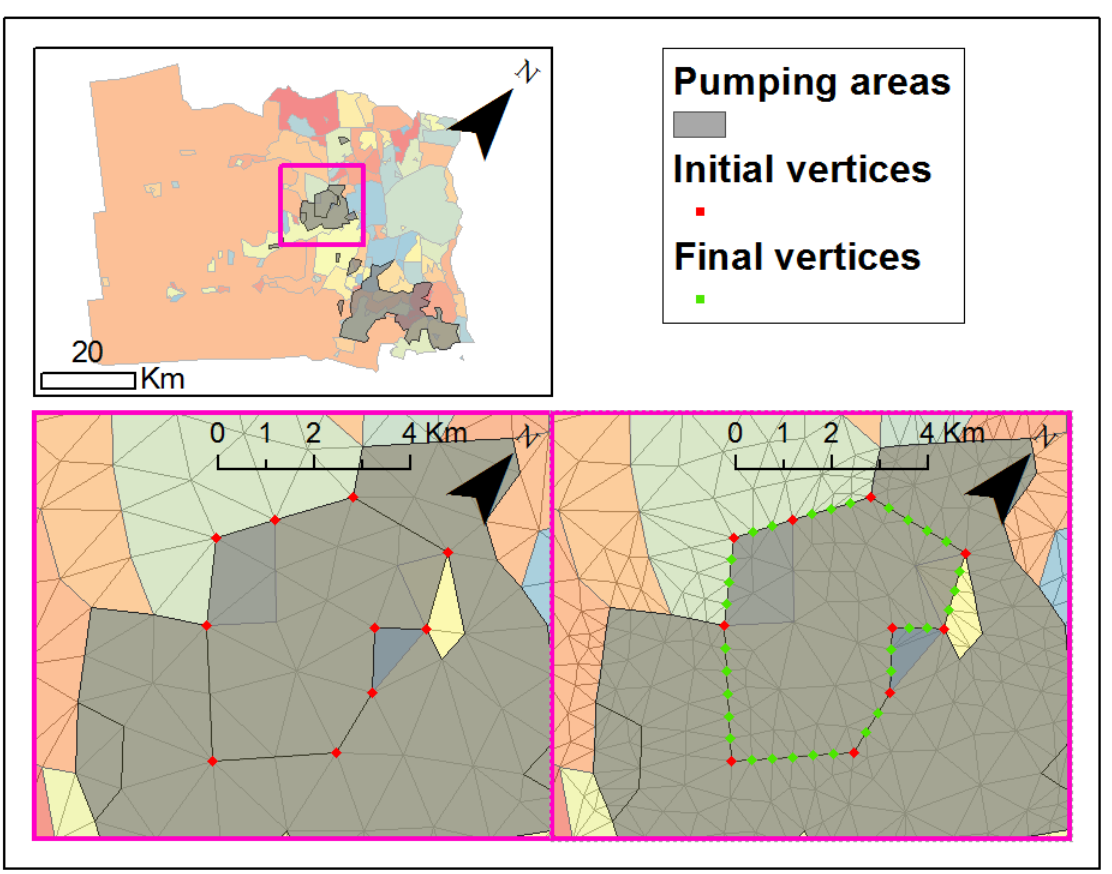

Conversely, it is possible to reduce the number of vertices with *Generalizer* tool up a specific distance tolerance. The Figure IV.7 represents a detail of Arroyo Pantano, whose geometry was simplified to reduce the number of vertices. A tolerance distance of 250 m was used to reduce the number of vertices from 101 to 7 vertices. This implies a reduction of element number required for this river (from 207 elements to 78 elements).

Figure IV.7. Detail of finite element mesh before and after run Simplify tool. The new mesh generated after run Simplify tool has a minor number of elements due to the reduction in the number of vertices participating in entities' geometry. Colored areas represent different recharge areas. Red dots represent entities' vertices visualized with Vertices Visualizer tool.

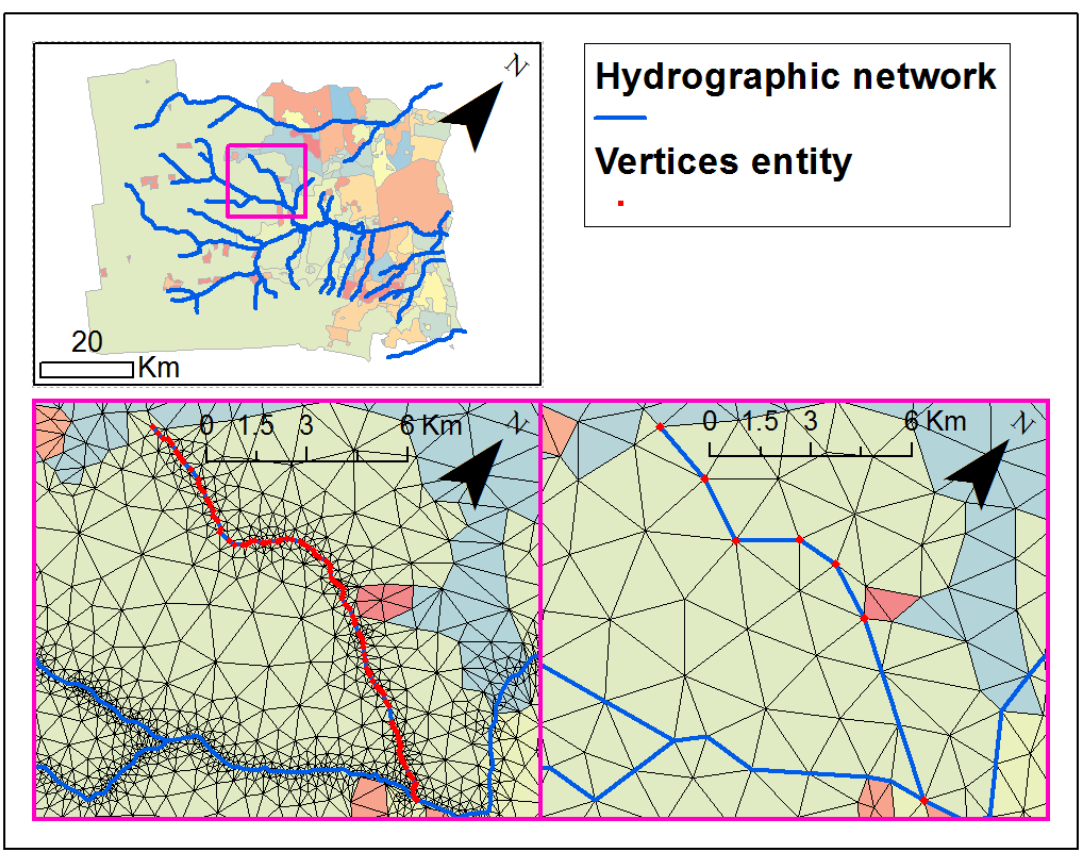

Additionally, *Vertex at Intersection* tool generates a common vertex where two entities intersect. This facilitates convergence process while meshing. Finally, the vertices can be organized in the space with *Topology* tool. This tool snaps entities' vertices together when they fall within the distance tolerance defined. So,

coincident vertices will be coalesced in a single one. This tool works by arranging the vertices to a fictitious grid of points which are distributed in horizontal and vertical coordinates according to the precision of data.

To control mesh refinement, the *Auxiliary Lines for Meshing* tool was created. This tool generates concentric lines from selected features (which can be points, lines and polygons) where pumping wells or groundwater level depressed areas are expected (Figure IV.8). The initial and final distance must be defined previously. This tool generates concentric lines following a logarithmic distribution, to adjust the element size to the logarithmic variation of groundwater level in level depressed areas.

Figure IV.8. Detail of finite element mesh with refinement around pumping wells. Colored areas represent different recharge areas.

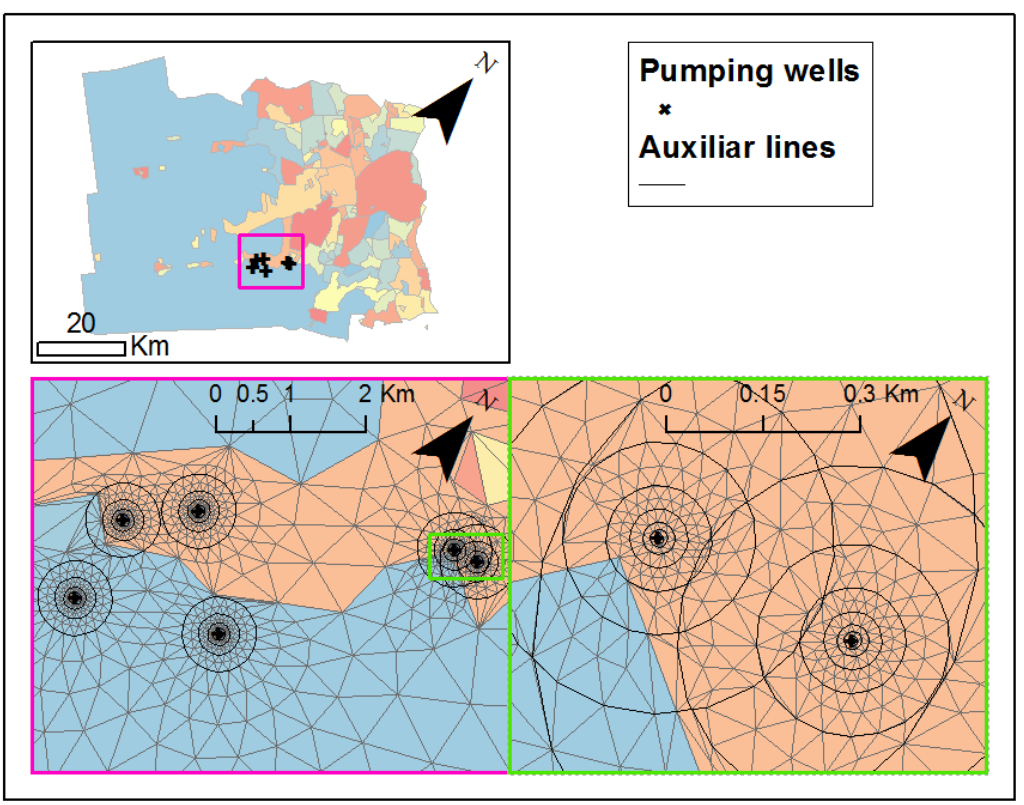

The creation of thin elements in the mesh must be avoided [111]. Usually, mesh generators circumvent thin elements by densifying the mesh in this area. This

can be a disadvantage if no variation of state variable is expected there, because additional and unnecessary computational cost will be required. The *Sharp Edges Location* tool locates those entities whose edges shape acute angles and highlights them with red circles (Figure IV.9). Once the maximum angle value is defined by the modeler, this tool also locates and remarks the acute angles between the edges of two entities.

Figure IV.9. Detail of output data generate with Sharp Edges Location tool. Colored areas represent different recharge areas.

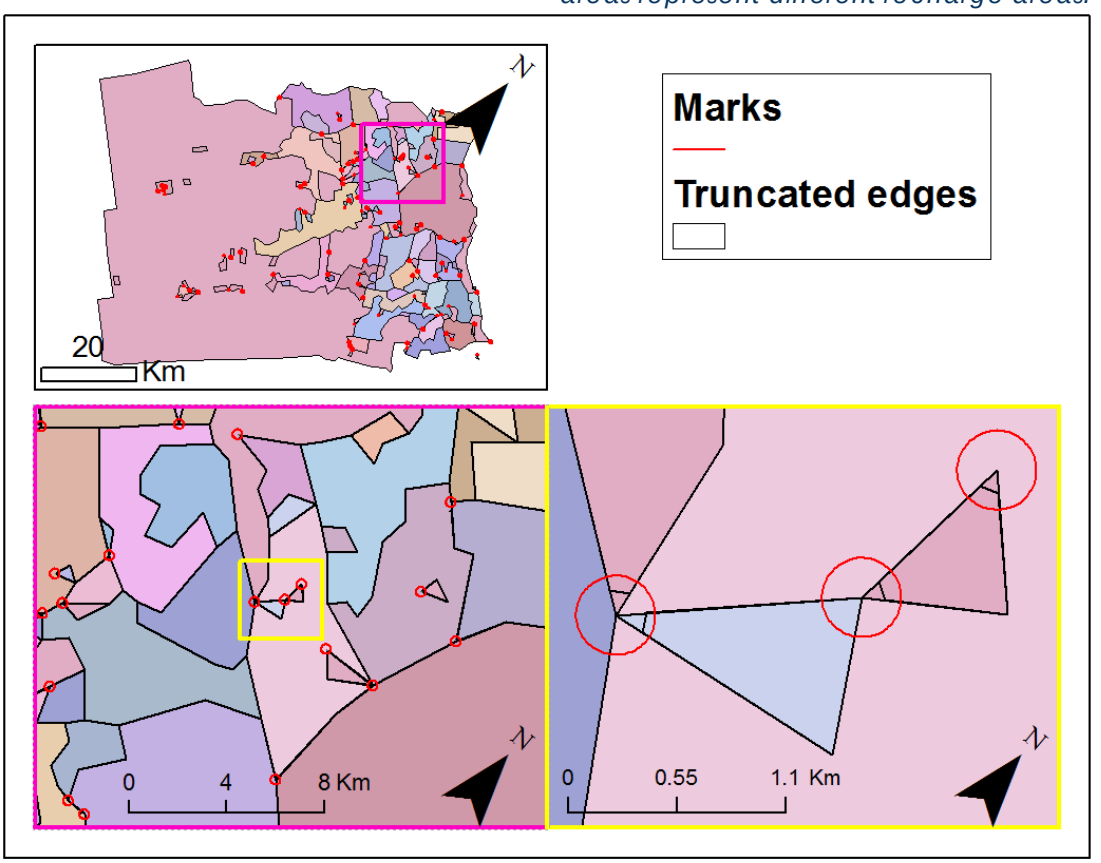

Automatic reshape of features will be accomplished *with Anti-Sharp Edges* tool (in elaboration). This tool faces the problem of acute angles by modifying the feature's shape with two possible options, by cutting or eliminating angles minor than a specific value. The angle will be cut at a distance such that the opposite side measure a specific distance defined previously by the modeler. If this distance is bigger than the maximum possible, the vertex is deleted so the angle will be eliminated.

4. CONCLUSIONS

The set of tools *ArcArAz* is oriented to guide standard GIS users during different steps in data management and configuration of groundwater numerical models once the conceptual model is defined. It concentrates in a single toolbar advanced GIS capabilities to cope with geometric and alpha-numeric complexity of data.

ArcArAz contains both inherent tools from GIS platform and new tools developed to solve specific conflicts during groundwater modeling setup. The main gap solved by *ArcArAz* is related to finite element mesh generation, which represents the innovation of these tools. New tools were developed to create most favorable meshes for numerical modeling. Additional tools were developed to lead with input and output files from numerical modeling with *Visual TRANSIN*, as well as to improve quality of geometrical and alpha-numerical data.

ArcArAz allows meshing the groundwater numerical modeling for ACUMAR with high time saving by simplifying the geometries involved in the area according to the scale of the model. Moreover, the configuration of boundary conditions, as Dirichlet conditions for rivers, was appropriately implemented and corrected.

Thanks to the loose coupled strategy, these tools can be applied to other sciences branches which require finite element modeling.

V. QUANTIFICATION OF SHALLOW GEOTHERMAL POTENTIAL[7]

1. INTRODUCTION

To assess the potential energy exchange of the ground, the main heat transport mechanisms should be considered: advection and dispersion. In general terms, many authors have highlighted the relevance of groundwater flow when estimating SGP ([62], [112]–[114]). Ignoring the contribution of advection in heat transport may lead to oversized shallow geothermal exploitation systems ([115]). In addition, [116] and [117] remarked on the importance of dispersion when estimating thermal impacts at regional scales, especially for medium sand to gravel aquifers.

Numerical modeling is an optimal solution that takes the main heat transport mechanisms into consideration. However, such models usually involve high computational costs ([114], [118]–[120]). Additionally, these models often solve the heat problem only for particular configurations of a thermal exploitation. Only [121] used the numerical modeling to generate a regional map of SGP. Their methodology was based on calculating SGP for several locations in their study area. They accomplished their calculations by generating individual numerical models for each location. Following spatial interpolation, a spatial distribution map of SGP was generated.

---

[7] This chapter is based on *M. Alcaraz, A. García-Gil, E. Vázquez-Suñé, V. Velasco. Advection and dispersion heat transport mechanisms in the quantification of shallow geothermal resources and associated environmental impacts. Science of the Total Environment. DOI:10.1016/j.scitotenv.2015.11.022*

As an alternative to numerical modeling, several analytical models have been developed assuming different boundary conditions (for an update on this technique, see [122]). Nevertheless, as usually occurs with numerical models, analytical models aim to solve the geothermal problem for specific local-scale applications.

At a regional scale, Geographic Information Systems (GIS) are an effective platform for managing existing geological, hydrogeological and renewable energy data ([69], [123], [124]). The GIS environment is also useful for developing an integrated geological and hydrogeological conceptual model, required for the estimation of SGP. As [125] remarked, GIS-supported maps of shallow geothermal systems may help to characterize the subsurface media when dimensioning exploitations, to avoid under- or oversizing.

However, the GIS-based applications and methodologies developed for the estimation of SGP have an empirical character. [126] proposed a GIS methodology for evaluating the suitability of SGP exploitation that created qualitative maps based on underground thermal properties and groundwater characteristics. [127] developed a GIS-based methodology to empirically calculate the SGP at a regional scale. Their methodology is based on the average specific heat extraction values for each material. Similarly, [12] established a GIS methodology to estimate the economic exploitability of SGP. In addition to the ground properties, [128] consider the efficiency of the technology and the energy demand to estimate empirically the SGP. However, none of these authors have considered the effects of groundwater flow. Moreover, these approximations are valid when the geological and hydrogeological models are unreliable or not very precise. With these data available and comprehensive, [129] generated a GIS methodology to assess the SGP at a regional scale, taking into account groundwater flow, but without considering dispersion. Despite these advantages, none of the aforementioned GIS methodologies consider the temporal evolution of the thermal system, which is especially relevant when geothermal exploitations have a cooling mode in summer and a heating mode in winter.

To overcome the above limitations in estimating SGP, this chapter presents a new methodology integrated in a GIS environment. It focuses on the quantification

of SGP at a regional scale. When necessary, the main heat transport mechanisms—advection and dispersion—can be taken into account to calculate the transient thermal state. A set of maps representing the main variables in shallow geothermal systems can be created, including SGP maps and maximum distances of thermal disturbance. These maps represent a powerful tool to support decision-making processes concerning shallow groundwater energy resources [130].

2. METHODOLOGY

2. 1. SHALLOW GEOTHERMAL ENERGY EXPLOITATION SYSTEMS

Two main types of shallow geothermal exploitation designs are used to exchange heat with the subsurface medium; the first involves closed loop systems, or Ground-Coupled Heat Pumps (GCHP), and the second consists of open loop systems, or Ground Water Heat Pumps (GWHP). The application of Borehole Heat Exchangers (BHEs) in closed systems (for further details, see [131], [132]), is increasingly being used to draw on SGE, so the proposed methodologies focus on closed loop vertical borehole heat exchangers. Horizontal shallow geothermal installations are beyond the scope of this research.

BHEs typically consist of one or more 50-100 m deep vertical boreholes with a heat exchanger circuit inside them. This type of exploitation system exchanges heat directly with the ground and immobile groundwater in pores through conduction. When groundwater flow exists, advection and dispersion heat transport mechanisms favor the heat exchange. In the range of temperature variations produced by shallow geothermal energy (±10K), the effects on groundwater flow due to variations of kinematic viscosity and density of water can be neglected [133]. So, it is possible to assume that the hydraulic state of the aquifer remains unchanged. However, the thermal regime is disturbed. BHEs are widely used in heating and cooling of commercial and domestic buildings and other facilities.

2. 2. Analytical modeling of SGP and its impacts

This section proposes a new approach to modeling maps of SGP and the thermal impacts of its exploitation at a regional scale. An accurate estimation of SGP and its impacts is based on the implementation of analytical solutions of the heat transport equation in porous media [134].

To achieve more conservative results, the dispersion effects are ignored when estimating the SGP. However, the dispersion mechanism has to be taken into account to represent more accurately the thermal affections in the underground, as suggested by [116].

The analytical solution proposed by [135] and [136] is applied when estimating the SGP. This solution considers only advection as heat transport mechanism to solve the heat transport equation. By contrast, to include the dispersion mechanism as well, the solution developed by [137] is used when estimating the thermal impacts.

Both of the previous solutions incorporate the response of a constant heat line source with infinite length along the z-direction (which gives a two-dimensional character to the solutions) with a continuous heat flow rate, known as the Moving Infinity Line Source model (MILS). This constant heat line source representing the BHE is assumed to be in the point (0, 0) with groundwater flow in the x direction. The MILS model neglects vertical groundwater fluxes, which has shown to be negligible when reproducing the behavior of BHE [131].

These equations have four degrees of freedom that have to be settled. They are the temperature increment (1) at a specific distance (2) produced by an extracted potential (3) at an elapsed time (4) from the start of the operation. The equations must be constrained by defining 3 of them to obtain the fourth.

2. 2. 1. Calculation tools

The methods for the quantification of the spatial distribution of the SGP and its environmental impacts are based on map algebra [138]. These methods require working with raster data[8], so that both input and output variables are constant for each pixel. This methodology is an efficient way to work with georeferenced information at a regional scale. The equations solved by map algebra are given

[8] Raster data represent the heterogeneity of geological media by discretizing it in cells, so the parameter values are homogeneous within each cell. This allows solving the analytical solutions for each cell of raster data, because analytical solutions assume homogeneous media.

below. These expressions are numerically solved for each variable of interest and for each pixel of output raster.

The numerical engine used to perform SGE analysis is the open source programming language Python 2.6[9]. This language is used across a wide range of disciplines and has been widely adopted in the environmental science community. The main site package used was SciPy Stack 0.7.1[10], a collection of open source software for scientific computing in Python. The SciPy Library contains a set of numerical algorithms and domain-specific toolboxes.

This methodology was implemented in a set of tools, GeoTherTools, written in Python language. It is integrated into *ArcGIS* 10.0, as a set of script tools known as geoprocessing tools in ArcToolBox. Regarding the Graphical User Interface (GUI), tool dialog boxes were generated following the same structure as all geoprocessing tools in *ArcGIS*, so that end users will be familiar with its appearance.

GeoTherTools is part of an ongoing effort to create a software platform ([26], [27], [77]), which facilitates the management, analysis and interpretation of geological and hydrogeological data for additional modeling. In particular, GeoTherTools belongs to this GIS-platform focused on hydrogeological settings, which favors feedback and consistency between geological, hydrogeological, hydrogeochemical and geothermal conceptual models. Although GeoTherTools operates independently of this platform, synergies can be leveraged through its integration. This allows successful data management of the input and output data required by GeoTherTools.

GeoTherTools allows for the quantification of the main variables required in the proposed methodology, the SGP and the thermal impacts. Moreover, it contains a set of auxiliary tools to define the input data, such as the Darcy velocity, the bulk and effective thermal conductivity and the heat capacity, which are described below. The complete set of tools can be downloaded from the internet: http://www.h2ogeo.upc.es/

[9] https://www.python.org/, accessed April 29th 2015.
[10] https://www.scipy.org/, accessed April 29th 2015.

2. 2. 2. Input data

A thorough geological and hydrogeological characterization of the study area must be available in order to obtain reliable results. The input data must be derived from this characterization. Required input data are briefly described below. A detail description of the origin and definition of input data can be consulted in [129].

The main hydraulic parameter is the groundwater velocity $[v_D]$. This can be obtained from hydrogeological numerical models. However, to avoid the numerical modeling process, groundwater velocity can be derived from the piezometric surface and the hydraulic conductivity $[K]$ for each aquifer layer, by applying Darcy's Law (Eq. 1). In this case, the hydraulic gradient $[i_H]$ can be obtained from the piezometric surface with inherent GIS capabilities to calculate the slope of a surface:

$$[v_D] = [K] + [i_H] \quad \text{Eq. 1}$$

The following thermal properties are required: the heat capacity $[c_0]$ and the thermal conductivity $[\lambda_0]$ of the media, ideally obtained from thermal tests. Alternatively, these parameters can be estimated as weighted averages of the saturated water and solid matrix, using lithological descriptions from borehole logs and thermal properties ($[\lambda_s]$ and $[c_s]$) values for each lithology from literature ([139], [140]). In this case, for the estimation of bulk thermal properties ($[\lambda_0]$ and $[c_0]$) of saturated geological layers it is necessary to use the material's porosity $[\phi]$ and water thermal properties (k_w and c_w). Finally, water and solid densities (ρ_w and ρ_s) are also required to calculate the thermal conductivity $[\lambda_0]$ and the volumetric specific heat $[\rho c_0]$ of the media, according to equations 2 and 3.

$$[\lambda_0] = [\phi] \cdot k_w + (1 - [\phi]) \cdot [\lambda_s] \quad \text{Eq. 2}$$

$$[\rho c_0] = [\phi] \cdot \rho_w c_w + (1 - [\phi]) \cdot [\rho_s c_s] \quad \text{Eq. 3}$$

When considering thermal dispersion due to terrain heterogeneity, an effective thermal conductivity $[\lambda_{x,y}]$ is used. This quantity is the sum of the bulk thermal conductivity $[\lambda_0]$ and a kinematic thermal dispersion term based on the thermal dispersivity $[\alpha_{x,y}]$. This term represents the influence of the heterogeneous velocity field according to the following expression:

$$[\lambda_{x,y}] = [\lambda_0] + [\alpha_{x,y}] \cdot \rho_w c_w \cdot [v_D] \quad \text{Eq. 4}$$

In addition to the hydraulic and thermal parameters of the terrain, geometry is also necessary to estimate SGP. The thickness of geological layers is indispensable in estimating SGP up to a certain depth. Therefore, a comprehensive 2D or 3D geological characterization of the media must be available.

Integration and validation of all existing data must be accomplished along with a parameterization over the entire domain. To integrate so much information with differing sources and scales, the most efficient method is to use a GIS platform specifically oriented towards groundwater management.

Finally, constraints imposed by legislation or other criteria must be considered. Countries have defined groundwater temperature thresholds for heating and cooling, and minimum distances between such geothermal systems to avoid detrimental environmental impacts or thermal interference between exploitation systems. International legislation can be consulted for several countries in [141].

2. 2. 3. Quantification of SGP

The Low Temperature Geothermal Potential (SGP, [W/m]) is estimated as the maximum energy per unit time that can be extracted from the ground per unit length of BHE, without exceeding a certain temperature increment at a specific distance from the BHE axis. The calculated heating rate is characteristic of the ground and independent of the BHE resistance and the heat pump coefficient of performance (COP).

To take into account advection to estimate SGP, the expression for transient state proposed by [136] was adapted (Eq. 5) so that the heating rate does not exceed the maximum temperature increment (ΔT_{Max}) at the influence distance (x_0) up to a specific time from the start of operation (t):

$$[SGP_{Max}] = \frac{\Delta T_{Max} \cdot 4 \cdot \pi \cdot [\lambda_0]}{exp\left(\frac{[v_T]}{2 \cdot [a]} \cdot x_0\right) \int_0^{\left({}^{4[a]t}/_{x_0^2}\right)} \frac{1}{\varphi} exp\left(-\frac{1}{\varphi} - \left(\frac{[v_T] \cdot x_0}{4 \cdot [a]}\right)^2 \varphi\right) d\varphi} \quad \text{Eq. 5}$$

where φ is the integration variable.

The influence distance x_0 is defined as the radius of the BHE, where the ΔT_{Max} will be the maximum value technically admissible for a proper working of the BHE

(usually not bigger than 10K). The specific time from the start of operation depends on the cycles of heating and cooling, closely linked with the climatic conditions. Its value remains the same for further calculations.

2. 2. 4. Quantification of environmental impacts

The environmental thermal impacts are calculated as the sum of the maximum distances upstream and downstream from the BHE where the SGP_{Max} obtained previously generates a specific temperature increment.

To consider the main heat transport mechanisms, advection and dispersion, the equation developed by [137] and applied to BHEs by [116] for transient state was adjusted and implemented (Eq. 6). The maximum thermal distance upstream and downstream (x_{Max}) are calculated by inverting numerically Eq. 6 for x_{Max}, assuming a minimum temperature increment (ΔT^*) produced by the SGP_{Max}.

$$[SGP_{Max}] = \frac{\Delta T^* \cdot 4 \cdot \pi \cdot \sqrt{[\lambda_x] \cdot [\lambda_y]}}{exp\left(\frac{[v_D] \cdot \rho_w c_w \cdot [x_{Max}]}{2 \cdot [\lambda_x]}\right) \int_0^{Limit} \frac{1}{\varphi} exp\left(-\varphi - \frac{1}{\varphi}\left(\frac{[x_{Max}]^2}{[\lambda_x]}\right)\frac{([v_D] \cdot \rho_w c_w)^2}{16 \cdot [\lambda_x]}\right) d\varphi} \quad \text{Eq. 6}$$

$$Limit = \frac{([v_D] \cdot \rho_w c_w)^2 t}{4 \cdot [\rho c_0][\lambda_x]}$$

The minimum temperature increment ΔT^* represents the threshold from which it is assumed that there is thermal affection, e.g., 0.5K-1K.

2. 2. 5. Quantification of volumetric SGP and SGP per area

Because extracting a SGP at two points with different thermal and hydrogeological properties produces different thermal plumes, it is necessary to normalize the SGP within the affected thermal area to compare the potential independently of thermal effects.

The affected thermal area, named as thermal plume, is defined as the surface characterized by a temperature increment ΔT bigger than ΔT^* produce by SGP_{Max}. The thermal plume area, A_{plume}, is calculated numerically from equation 7 :

$$[SGP_{Max}] = \frac{\Delta T^* \cdot 4 \cdot \pi \cdot \sqrt{[\lambda_x] \cdot [\lambda_y]}}{exp\left(\frac{[v_D] \cdot \rho_w c_w \cdot x}{2 \cdot [\lambda_x]}\right) \int_0^{Limit} \frac{1}{\varphi} exp\left(-\varphi - \frac{1}{\varphi}\left(\frac{x^2}{[\lambda_x]} + \frac{y^2}{[\lambda_y]}\right)\frac{([v_D] \cdot \rho_w c_w)^2}{16 \cdot [\lambda_x]}\right) d\varphi} \quad \text{Eq. 7}$$

$$Limit = \frac{([v_D] \cdot \rho_w c_w)^2 t}{4 \cdot [\rho c_0][\lambda_x]}$$

The equipotential line can be obtained by inversion of $[SGP_{Max}] = f(x, y)$. This expression represents the set of points (x, y) characterized by the same value of SGP_{Max} and ΔT^*, which defines the thermal plume. The inversion is performed numerically to state y as a function of x. Integration over x provides the area of the thermal plume. The upper and lower limits of integration are calculated numerically from Eq.6, as the maximum distances upstream and downstream.

To normalize the SGP and therefore obtain the volumetric SGP (VSGP, [W/m3]), it is necessary to divide the SGP values by the thermal plume area. Additionally, the VSGP can be multiplied by the thickness of each geological layer or by the length of the BHE to obtain the SGP per unit area [W/m2].

2. 3. Assumptions and limitations

Analytical solutions used in this methodology are applicable under predetermined specific boundary conditions ([116], [136]), i.e., where the ground is regarded as a homogeneous and semi-infinite medium with a uniform initial temperature and physical properties independent of temperature, the heat flow is constant, the upper and lower boundaries are impermeable to heat transfer (adiabatic) and the finite length of the BHE is not taken into account. The vertical integration of SGP for several layers can produce errors of up to 10%, as shown by [129].

Limitations of this methodology do not derive solely from analytical assumptions. They are also related to the accuracy of input data. As long as input data do not reflect the heterogeneity of geological and hydrogeological media, this uncertainty will be transferred to output variables. Thus, modeling criteria are crucial when deciding on pixel size. These criteria should ensure that the analytical solutions respect the geological heterogeneity at the scale established.

2. 4. Validation and application ranges

To illustrate the application range of the analytical solutions used in sections 3 and 4, a schematic model has been designed with synthetic maps for input variables, shown in Figure V.1: the spatial distribution of thermal diffusivity increases along the X coordinate of the fictitious maps from left (10-7 m2/s) to right (10-6 m2/s) and the Darcy velocity decreases in the Y coordinate from 10-5 to 10-11 m/s from top to bottom logarithmically.

Figure V.1. Input maps for synthetic model used in validation process. Control pixels values used for validation are marked. Properties for control pixel 1: Darcy velocity, 10-6.6 m/s; thermal diffusivity, 1.2E-6 m2/s. Properties for control pixel 2: Darcy velocity, 10-7.2m/s; thermal diffusivity, 2.2E-6 m2/s. For both pixels: Longitudinal thermal dispersivity, 10 m and transverse thermal dispersivity, 1m.

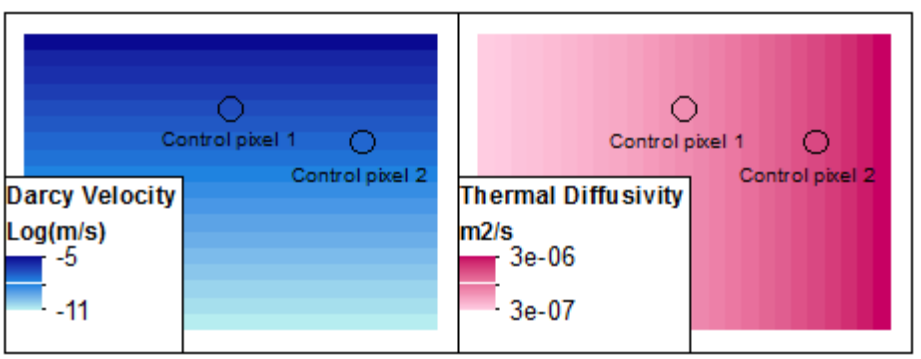

Four scenarios have been proposed for the validation: they combine the steady and transient thermal state with the consideration or neglect of dispersion effects (See Table V.1).

Table V.1. Configuration of scenarios for sensitivity analysis of SGP and its environmental impacts for the study site. Advection heat transport mechanism is taken into account for all scenarios.

	Steady Thermal State	**Transient Thermal State**
Without dispersion	Scenario 1	Scenario 2
With Dispersion	Scenario 3	Scenario 4

Figure V.2 and Figure V.3 contain the output variable maps for the synthetic model: shallow geothermal potential varies from 25.4 W/m to 279.7 W/m and thermal plume area ranges from 32.5 m2 to 2555.5 m2 for the different scenarios. Due to numerical limitations, the proposed methodology was designed for an upper limit on the Darcy velocity of 10-5 m/s, which is generally a high velocity in most aquifers.

Figure V.2. Output maps of shallow geothermal potential (SGP) for the synthetic model and for the four scenarios proposed. Stretch method for raster display: histogram equalized.

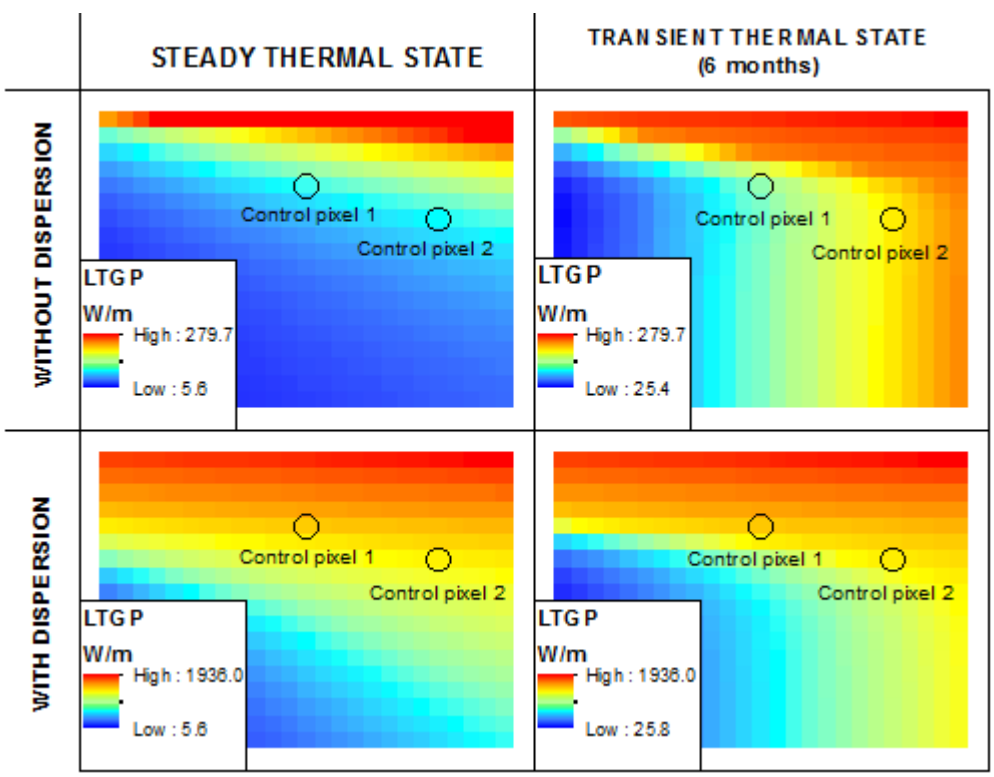

Figure V.3. Output maps of thermal plume area for the synthetic model and for the four scenarios proposed. Stretch method for raster display: histogram equalized.

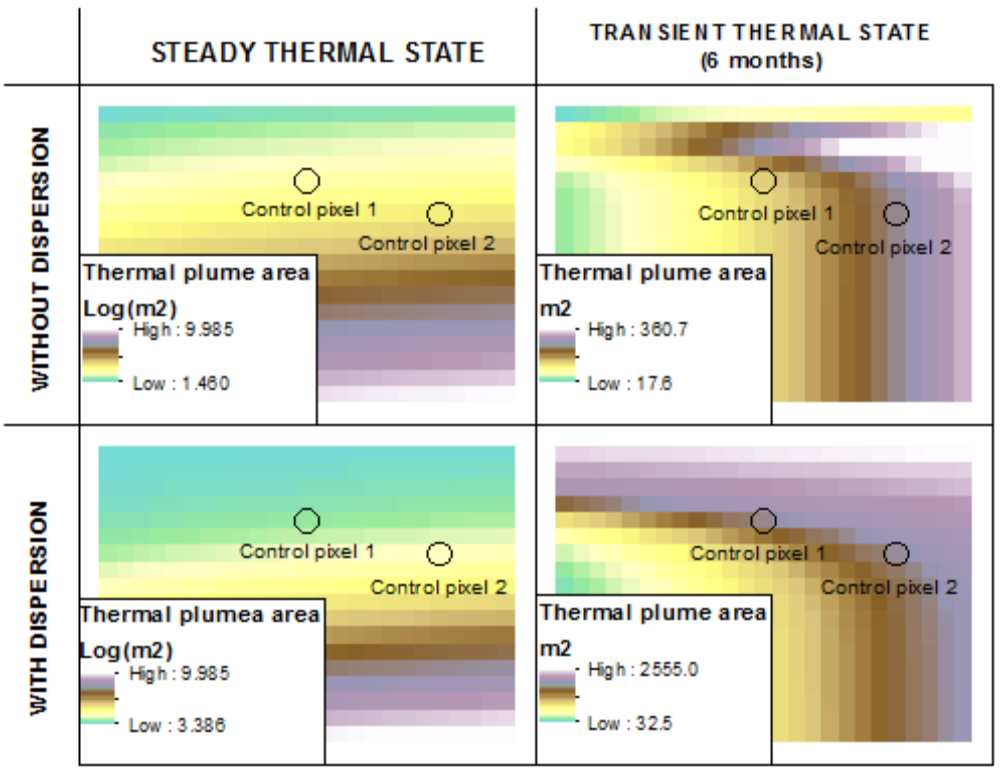

Appropriate implementation of the governing equations was verified by numerical modeling with *FEFLOW*, for two control pixels (marked in Figure V.1, Figure V.2 and Figure V.3) with satisfactory results. Table V.2 contains the thermal plume area for a heat rate that produce a temperature increment of 10K at 0.25 m from the BHE and for a temperature disturbance of 1K calculated numerically by *FEFLOW* and analytically by the proposed methodology. The errors were under 5% in all cases.

Table V.2. Validation of calculated areas by FEFLOW. Properties for control pixel 1: Darcy velocity, 10-6.6 m/s; thermal diffusivity, 1.2E-6 m2/s; longitudinal thermal dispersivity, 10 m; transverse thermal dispersivity, 1m. Properties for control pixel 2: Darcy velocity, 10-7.2 m/s; thermal diffusivity, 2.2E-6 m2/s; longitudinal thermal dispersivity, 10 m; transverse thermal dispersivity, 1m.

		Heat Rate (W/m)	Thermal Plume Area (analytical analysis) (m2)	Thermal Plume Area (numerical analysis, FEFLOW) (m2)	Relative error (%)
Steady State without dispersion	Pixel 1	55.9	1554.1	1556.3	-0.1
	Pixel 2	53.3	17141.9	17102.9	0.2
Transient State without dispersion	Pixel 1	60.6	106.6	101.5	5.0
	Pixel 2	62.9	170.2	175.5	-3.0
Steady State with dispersion	Pixel 1	97.32	5889.6	5868.3	0.4
	Pixel 2	76.4	26467.5	26389.6	0.3
Transient State with dispersion	Pixel 1	117.4	199	205.5	-3.2
	Pixel 2	92.2	202.4	209	-3.2

3. APPLICATION AND RESULTS

The proposed methodology was successfully applied in a highly urbanized sector of the Metropolitan Area of Barcelona (AMB) on the Mediterranean coast in northeast Spain (Figure V.4), where the local and regional authorities have promoted the use of shallow geothermal resources [142].

3. 1. Geological, hydrogeological and geothermal settings

Geologic and hydrogeologic models for this area come from previous studies ([20]; [143], [144] and references therein). Specifically, the area of interest is mainly composed of highly transmissive porphyritic dikes in a fractured medium made up of granodiorite (Figure V.4). The granodiorite is petrographically homogeneous, equigranular and of medium grain size. The porphyritic dikes are vertical and subparallel, kilometers in length and meters thick, and are oriented northeast-southwest. Subvertical strike-slip faults, with a regional Variscan (late Carboniferous) orientation (north-northwest–south-southeast), displace the porphyritic dikes, which are more resistant to erosion than the granodiorite, allowing identification.

Relating to the hydrogeological model, the piezometric surface has higher hydraulic gradients in the north where the effective hydraulic conductivity is greater due to the density of porphyritic dikes (Figure V.4). As a consequence, the greater values of Darcy velocity (10-5 m/s) are located in this area.

The geothermal properties were obtained from literature ([139], [140], [145]) due to observed geothermal data are not available for the study site. Their values are summarized in Table V.3.

Figure V.4. Geological map of the Metropolitan Area of Barcelona (AMB) and detailed geology of the study site. Coordinate System: UTM European Datum 1950, Zone 31N

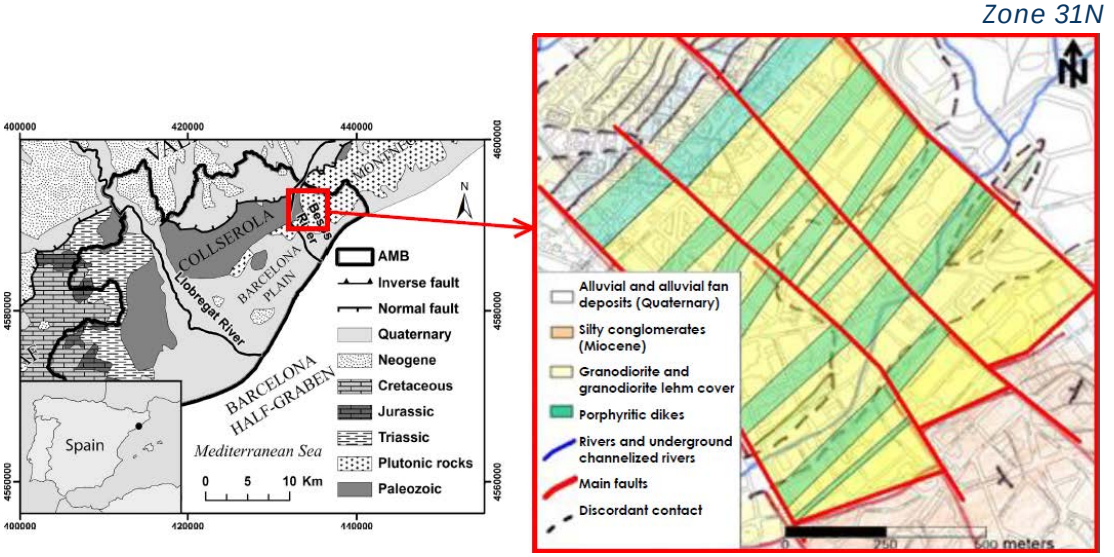

The input variable raster maps derived from the geological and hydrogeological models are shown in Figure V.5, and their parameter values are defined in Table V.3.

Figure V.5. Piezometric surface and spatial distribution of Darcy velocity and geological classification zones for the study site. The geological, hydrogeological and geothermal input parameters for each zone are described in Table 1.

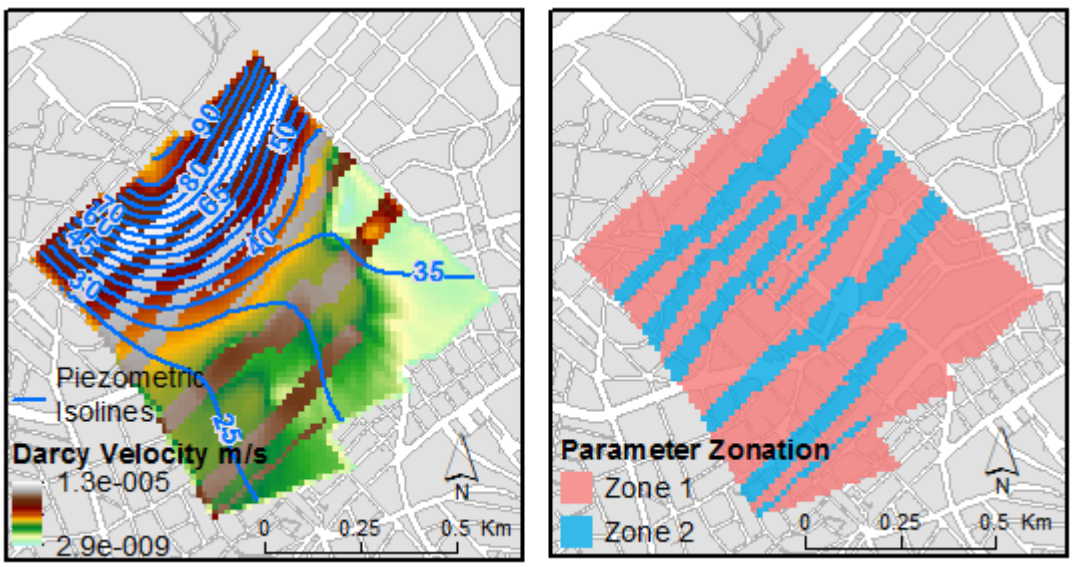

Table V.3. Hydrogeological and geothermal input parameter values for zones 1 and 2 described for the study site.

PARAMETER ZONATION		
Hydraulic Conductivity		
Zone 1	5.80E-06	m/s
Zone 2	2.30E-05	m/s
Thermal Conductivity		
Zone 1	2.65	W/m/K
Zone 2	2.8	W/m/K
Volumetric Heat Capacity		
Zone 1	2.83	MW/m3/K
Zone 2	2.86	MW/m3/K
Long/Trans Thermal Dispersivity		
Zone 1	10/1	m
Zone 2	10/1	m

3. 2. Results

Once the required input data has been obtained from the geological, hydrogeological and geothermal conceptual models described in the previous section, the SGP can be calculated per unit length by taking advection into account. Ignoring dispersion effects in aquifers leads to more conservative estimations. Figure V.6 shows the SGP map per unit length of BHE. This maximum potential was calculated so as not to exceed a temperature increment of 10K at 0.25 m from the BHE axis after 6 months from start of operation (assuming that cooling and heating mode alternate equally each year). The values obtained do not consider the technical limitations when extracting the SGP. The maximum SGP raster is required to calculate the environmental impacts. Figure V.7 contains a map with the distance affected thermally by the maximum SGP for a temperature increment threshold of 1K. It was obtained considering dispersion effects to avoid underestimation.

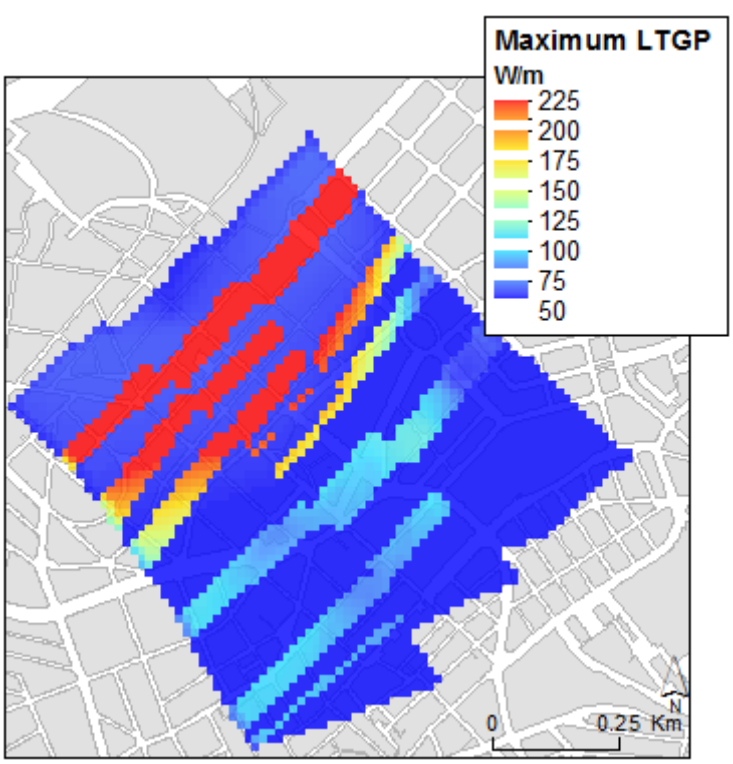

Figure V.6. Spatial distribution of maximum low temperature geothermal potential per unit length of the BHE for the study site. This maximum potential was calculated so as not to exceed a temperature increment of 10K at 0.25 m from the BHE axis after 6 months from start of operation.

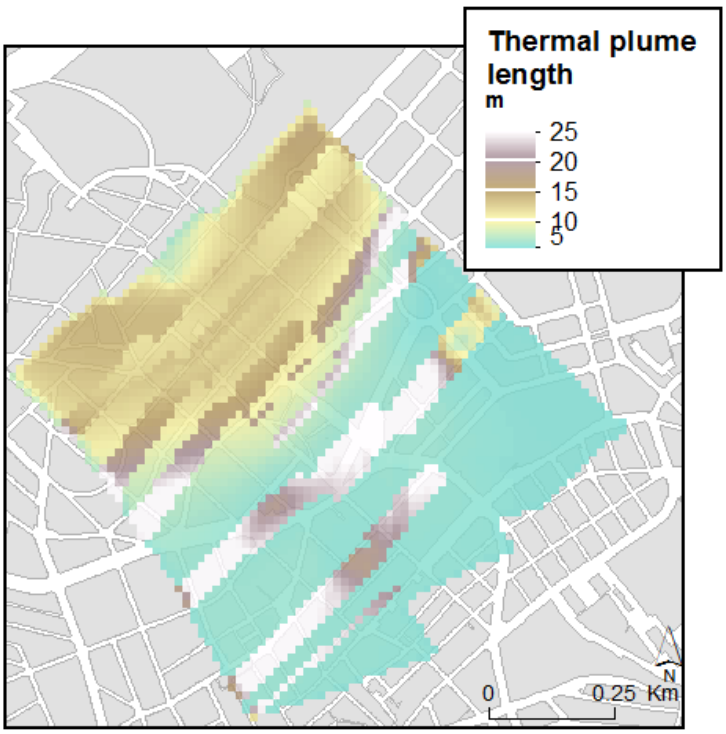

Figure V.7. Spatial distribution of thermal plume length produce by the maximum SGP (Figure V.6) for a temperature increment threshold of 1K. It was obtained considering dispersion effects to avoid underestimation.

The raster of the thermal plume area was obtained with the same parameters as the distance affected thermally (Figure V.8) and used to calculate the volumetric SGP represented in Figure V.9. Finally, assuming a BHE length of 100 m, the SGP that can be extracted per square meter is shown in Figure V.10. Based on these maps, decision-makers should promote the use of SGE in areas with the highest values of SGP per area. Moreover, SGP and impact maps can be used as guidelines or recommendations for initial dimensioning of the exploitations.

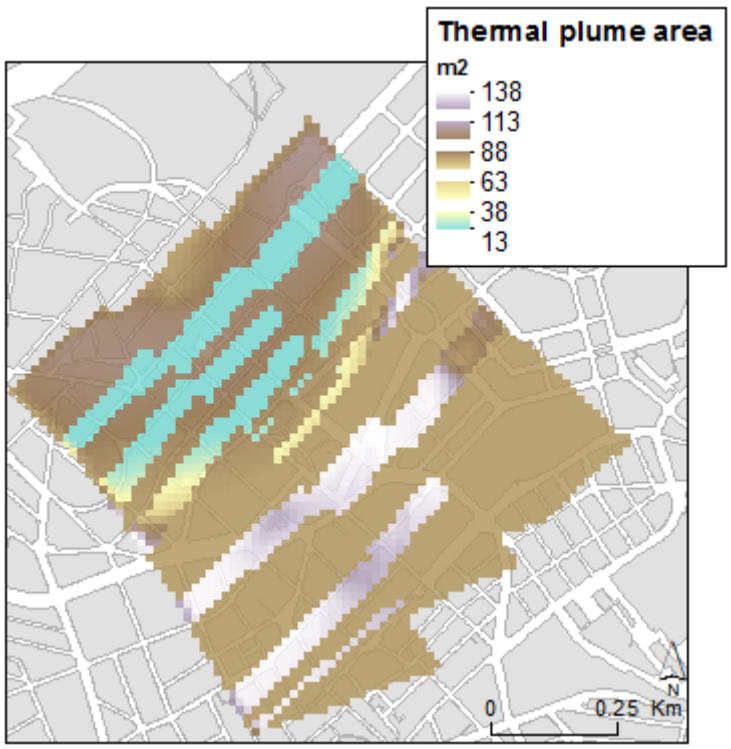

Figure V.8. Spatial distribution of thermal plume area produce by the maximum SGP (Figure V.6) for a temperature increment threshold of 1K. It was obtained considering dispersion effects to avoid underestimation.

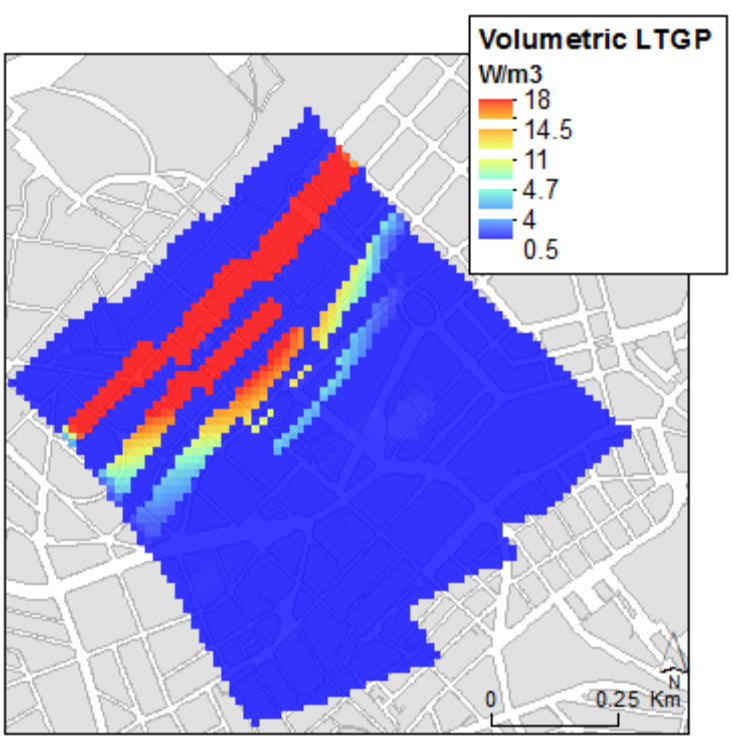

Figure V.9. Spatial distribution of volumetric shallow geothermal potential for the study site (VSGP). It is the maximum potential that can be extracted per unit volume of soil without exceeding a temperature increment of 10K at 0.25 m from the BHE axis after 6 months from start of operation and considering the thermal area affected with a temperature disturbance greater than 1K.

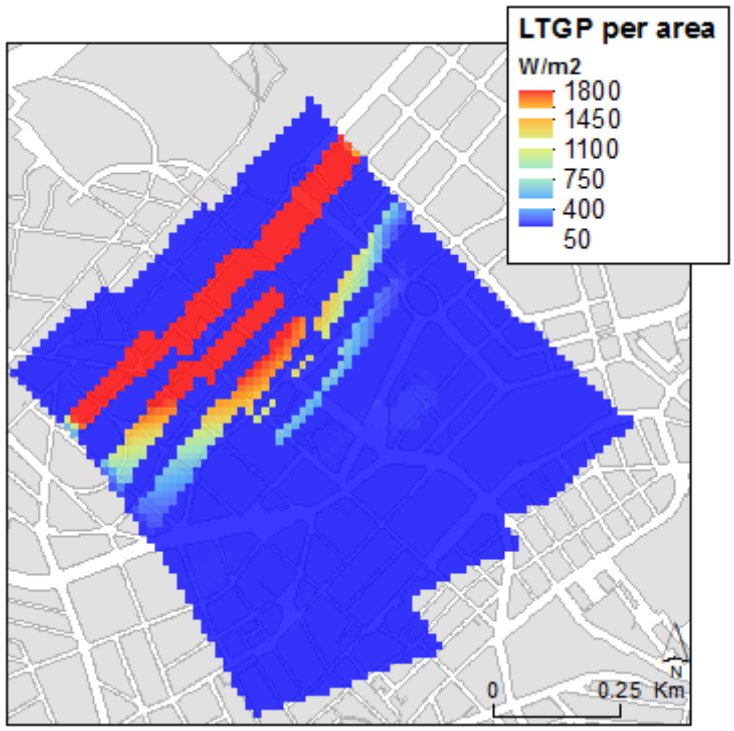

Figure V.10. Spatial distribution of shallow geothermal potential per area for the study site. It has been obtained assuming a drilling depth of 100 m.

4. DISCUSSION

These results show the significance of taking into account both the dispersion effects and the transient condition of the heat transport regimen. To quantify the relevance of these processes, a sensitivity analysis was carried out by calculating the SGP and its impacts for different scenarios, shown in 0. They combine the steady and transient thermal state with the consideration or neglect of dispersion effects.

The analytical solutions proposed by [136] and [116] were implemented to evaluate the different scenarios for the study site. The pixel values for each scenario and variable (SGP and thermal plume length) were plotted to facilitate comparisons.

The study site can be classified in four zones, according to the Darcy velocity, which is the most sensitive parameter ([116]): the porphyritic dikes in the north (zone 1) with the highest values of Darcy velocity (≈ 10-5m/s), the ones in the south (zone 2) with high values of Darcy velocity (in the range of 10-6-10-7 m/s), the granodiorite area in the north (zone 3) with Darcy velocity values similar to zone 2 and the granodiorite area in the south (zone 4) with the lowest groundwater velocity (≈ 10-8

m/s). The scatter plots in Figure V.11, Figure V.12 and Figure V.13 represent the Darcy velocity against the SGP or the thermal plume length for the different scenarios.

For the estimation of the maximum SGP, the proposed methodology recommends ignoring the dispersion effects, but taking into account the transient state of the system. As Figure V.11 shows, steady state conditions underestimate the SGP for low velocities by reducing it up to 2.5 times. For high velocities, calculations of SGP taking into account the dispersion effects lead to extremely high potentials that duplicate the values obtain without dispersion. This high SGP would exceed the technical limitation of extraction and would generate very large thermal impacts.

Figure V.11. Shallow geothermal potential as a function of the Darcy velocity for the pixels of the study site, showing the relevance of considering the transient thermal state for low velocities.

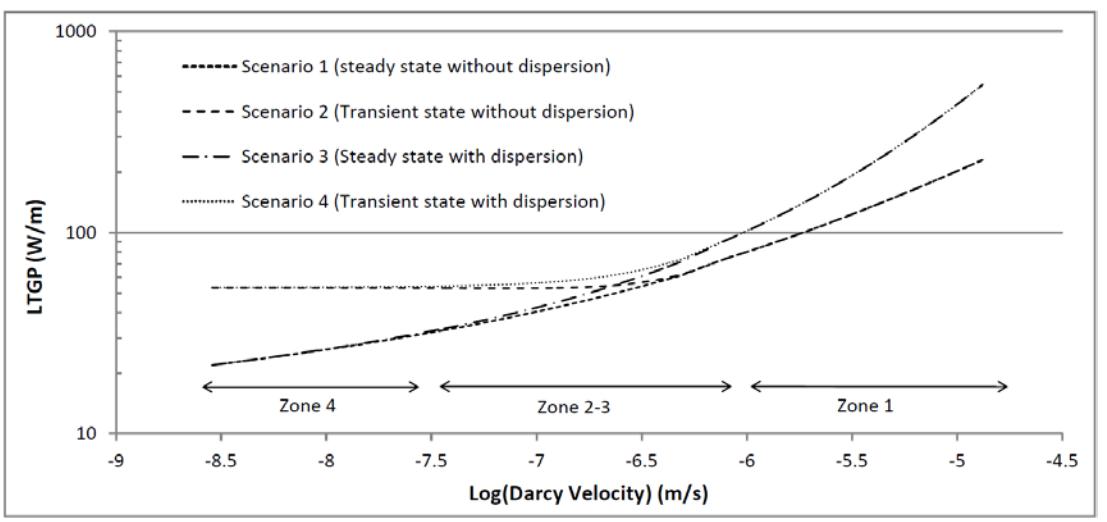

For the evaluation of the environmental impacts, this methodology proposes considering the dispersion effect for the transient thermal state of the system, as [116] suggest. To consider the transient state of the heat transport becomes relevant for lower velocities, when the steady state has not been reached at the defined time interval. Considering steady state conditions would imply an overestimation (up to several orders of magnitude) of the thermal plume for lower velocities. Figure V.12 shows the affected thermal distance against the Darcy velocity of each pixel of the study site under steady and transient states after 6 months and 2 years from the start of operation. As the time taken from the start of operation increases, more pixels

arrive at the steady state and reach their maximum plume size. For instance, in zone 4 the thermal plume is smaller than in zones 2 and 3 after 6 months of exploitation because it grows more slowly due to low velocities. Conversely, for higher velocities, when the steady state has already been reached, as in zone 1, the transient analysis does not improve the results with respect to the calculations in steady state.

Figure V.12. Plume length as a function of the Darcy velocity for the pixels of the study site, showing the relevance of considering the transient thermal state for low velocities.

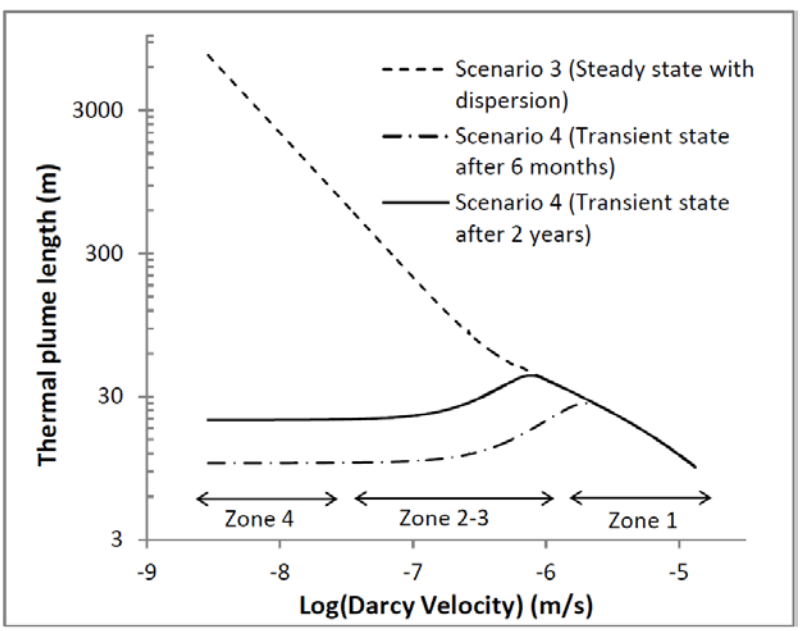

With respect to the effects of thermal dispersion, they are significant for high Darcy velocities when the steady state has been reached. The effects of thermal dispersion are closely related to the transient conditions of the system. As [116] remark, depending on the examined transient times, longitudinal dispersivity can dominate over transverse; by contrast, for steady state conditions, longitudinal dispersivity is not as relevant as transverse. This means that at steady state the heat spreads in the transverse direction to the flow. This causes dissipation of energy which reduces the temperature changes close to the BHE, resulting in smaller thermal plumes. The behavior of the thermal plume length as a function of the Darcy velocity is shown in Figure V.13 for the pixels of the study site with and without dispersion effects. For velocities in the range from 10-7 to 10-6, the thermal plume length would

be underestimated (up to one meter) if dispersion effects are neglected. This is because there are still transient conditions when the longitudinal dispersion prevails over the transverse. By contrast, for high velocities the dispersion reduces notably the size of the thermal plume, by almost up to a factor 3. This is revealed in zone 1, which has already got the steady condition of heat transport, when longitudinal and transverse dispersion effects have been developed entirely. The length of thermal plumes is the smallest of the domain. In the zones 2 and 3 there are still transient conditions and the longitudinal dispersivity dominates over the transverse. In zone 4, the dispersion effects are irrelevant for the calculations.

Figure V.13. Plume length as a function of the Darcy velocity for the pixels of the study site, showing the relevance of considering dispersion effects for high velocities.

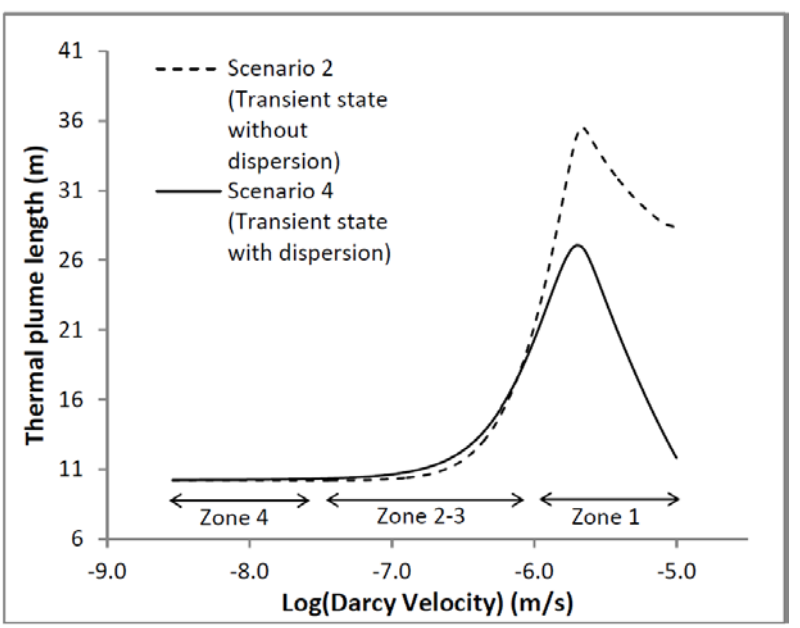

5. CONCLUSIONS

The proposed methodology provides support for decision making concerning shallow geothermal energy management policies. Maps with regional SGP distribution can be easily generated. These maps together with maps representing the environmental impacts represent a powerful decision support tool that can help promote the use of SGE and offer investors a regional estimation of SGP.

This methodology is integrated in a GIS environment, which allows users to include georeferenced data from different sources in an efficient manner. This GIS-based methodology estimates SGP at a regional scale for closed source heat pump systems for a wide range of Darcy velocities. Analytical solutions have been implemented to offer maximum accuracy in results, considering advection and dispersion heat transport mechanisms for transient exploitation regimes. The inclusion of dispersion effects and the consideration of the temporal evolution of the exploitation have been shown to be significant for achieving accurate results: up to a factor 2.5 in the SGP accuracy and up to several orders of magnitude in the environmental impacts.

The reliability of the results and the possibility of further downscaling depend on the amount of data available, its accuracy and its spatial distribution.

VI.USE RIGHTS MARKETS FOR SHALLOW GEOTHERMAL ENERGY MANAGEMENT[11]

1. INTRODUCTION

The continuous growth in the number of SGE installations is leading to conflicts between users due to thermal influences between shallow geothermal exploitations, as is already happening in cities like Berlin [146], Basel [14] or Zaragoza [15] among others. [147] analyzed the impact of housing patterns on the utilization of shallow geothermal energy for opened systems by considering the thermal and hydraulic influence distance of each installation. They estimated that this thermal interference can reduce the supply to meet only 10 -70% of the demand, according to different scenarios proposed.

In this situation, it is mandatory to establish a management system to control the exploitation of this resource in the most efficient manner [16]. Nevertheless, there is a scarcity of SGE management methodologies due to several aspects. Unlike solar or wind energies, that can be easily regulated by administration entities because their benefits and impacts are easily measurable and controlled [148], SGE is difficult to manage because this resource and its impacts are neither visible nor accessible for quantification. Moreover, there exists a great variety in control parameters and

[11] This chapter is based on *M. Alcaraz, A. García-Gil, E. Vázquez-Suñé, V. Velasco. (2016) Use rights markets for shallow geothermal energy management. Applied Energy. Accepted with major revisions (January 17th, 2016).*

thresholds in regulations and legislation which are not scientifically grounded [141]. As a common practice, international legislation defines different parameters to protect this resource, such as the minimum distance from the exploitation point to the next exploitation or the maximum temperature difference for heating and cooling. Most of the time, the given values are merely recommended and constant, which are supposed to apply over a vast territory.

There have been few efforts to define an integrated methodology which overcomes these aspects. The first attempt to manage this resource geographically was developed in Stockholm in 2010 through a website where users can apply for a domestic drilling permit for vertical single borehole closed loop systems [149]. When applying, the user can visualize on a map the protected circular areas for existing exploitations, according to an influence radius defined in legislation. Despite this advance, this method does not consider the thermal properties of the geological and hydrogeological media.

To take into account the thermal behavior of the underground media, current management methodologies draw upon the numerical modeling, with high time and resources costs [17], [150], [151]. The implementation of such numerical models is complicated and requires the definition of boundary conditions and vertical heat fluxes, which are usually unknown. These disadvantages limit the systematic application of this methodology for use in small exploitations or in poorly defined thermo-hydrogeological conceptual models. As [16] remark in the legal framework they suggest, only complex exploitation systems where thermal influence is expected require numerical simulations.

All above mentioned circumstances make it difficult to establish a widespread methodology of management which fits all regulations and legislation, and complicate the definition of a common framework to efficiently manage SGE resources. Thus, in most urban areas regulations for geothermal energy use are limited to the rule "first come, first served" [14].

To solve this situation, we present a methodology based on the application of use rights markets for geothermal energy, taking the water markets as a reference [152], [153]. This would manage this resource in an efficient way by allocating and

sharing the shallow geothermal potential between neighboring plots, avoiding thermal affections between users.

To support the implementation and management of a market of SGE use rights, a set of tools was developed based on Geographical Information System (GIS) technology. These tools support the decision-making process upon technical criteria based on analytical solutions of the energy transport equation in porous media. This provides city managers with an alternative solution to the problem of choosing between the empirical or weakly justified criteria currently followed by the administrations and the advanced numerical modeling techniques to simulate the heat transport.

The GIS technology allows decision makers to work with geospatial information distributed in large domains at different scales. GIS also facilitates the integration of additional information relevant to the exploitation of shallow geothermal resources, such as protected areas, poorly controlled old underground infrastructures, zones where existing underground services (telecoms, gas, electricity or water) may be present, archaeological remains, thermal sensible geological materials (Karst areas, gypsum formations) or thermal interferences calculated for existing systems with alternative software.

2. BASIS FOR A MARKET OF SGE USE RIGHTS

Traditionally, the use rights markets aim to reallocate the supply of a heavily exploited resource in a context of continuously growing demand, which is the current situation with the geothermal energy resource. In this section the need to establish a SGE market is highlighted and the main concepts for its definition and implementation are developed.

2. 1. Comparisons with others use rights markets

Nowadays, different kinds of use rights markets are strongly rooted and consolidated, e.g., gas-emission markets [154], water markets [155] and urban and rural soil markets [156].

The first kind looks for an agreement between the secondary sector and the environment and aims to potentiate the economic development of less industrialized countries in the current context of global warming, as in the European

Union emission trading system [157]. The water markets aim to control water resources supply mainly for the primary sector, respecting environmental needs. Markets for water use rights have been developed extensively in Australia [158], California [159] or Spain [160]. The soil markets define a tenure regime of the surface, and it is more articulated and less flexible than the others, as in China [161].

These markets apply at various organization levels: the gas-emission market involves private enterprises and stakeholders at a high administrative level, and can include the allocation of rights as well as economic transactions at all levels, including between separate countries; by contrast, the water markets have been developed at water basin scales, comprising administration and individual users, usually grouped into cooperatives or associations [162]. Similarly, the urban soil market is oriented to individual users or condominiums, coordinated by local administrators.

The tradable unit is also different from each use-rights market and with specific mechanisms of quantification and allocation. Water resources are easily reallocated, by simply adapting the flow or volume of water assigned to the final user. The water supply infrastructures are usually promoted and financed by the administration or are already constructed. The soil market is clearly controlled, due to its superficial nature; the boundaries and affections are easily measured and the surface available does not change substantially in quantity or quality when adjacent plots are exploited.

The differences with a prospective SGE market are notable, which requires the reformulation of the concept and management techniques to adjust it to this energy resource. The main parties in a SGE market would be the local administration and individual stakeholders. The installation to exploit SGE proceeds from private initiatives, although it can be promoted with subsidies by the administration. Furthermore, the SGE exploitation can exceed the boundaries of the superficial plot, so it requires additional tools to represent the behavior of underground media in order to evaluate and allocate this energy resource in the most efficient way.

In spite of the differences with a likely SGE use rights market, these examples of use rights markets have demonstrated and validated the application of this concept in situations where the supply and demand of the resource is unbalanced

[163]. As a consequence, the concept of SGE use-rights market must be adapted to the peculiarities of this resource.

2. 2. Market of SGE use rights

In the light of the previous discussion, we present a set of measures, proposals and original concepts aiming to define SGE use rights market. The objective of this SGE market is to assign the resource in a fair and sustainable way among the entities involved, including environmental protection issues.

A SGE market must satisfy the following issues: (1) promote the use of SGE, avoiding obstacles to its implementation; (2) offer the most suitable decision to all of the parties involved, by following principles of equity, efficiency and transparency; (3) consider the spatial implications of this resource, related to the thermal impacts which should be defined upon technical criteria; (4) facilitate the communication between the parties involved to achieve an agreement; and (5) pursue an equilibrium between a strong control of the market and the facilitation of transactions.

The main concepts of the proposed SGE market - the parties involved in it, the allocation of the resources and its management unit - are described below.

2. 2. 1. Parties involved

The principal parties are the local administration and land owners. The local administrator would be in charge of the unitary management of the resource, the registering, following and processing of the data generated by existing and new exploitations. As backup, a thermal monitoring network for vigilance purposes of the system should be considered. This entity should also promote the development of the SGE exploitations but at the same time should guarantee its sustainability. The local administrator should also provide information about the SGE potential and state of the plots to land owners, both individual users and residents' committees, to make this resource accessible.

2. 2. 2. Allocation of SGE

The main principle of allocation of the resource would be based on the land property. The SGE exploitation should be limited to the boundary of the owner's plot. In cases when the available area would not be enough to extract or dissipate the

required energy, the stakeholder could ask for a rights cession to affect an adjacent plot.

In order to promote the SGE, mainly in countries with lower SGE exploitations, penalty prices for consuming more than one's allocation should be avoided. If the reallocation of the resource is not possible, alternative benefits to affected parts could be offered.

The SGE use-rights market is oriented to manage the resource in a metropolitan level at hectometric or decametric scales in order to facilitate the evaluation and control of thermal affections.

2. 2. 3. Management unit: the thermal plot

In order to asses quantitatively the SGE, a basic exchange unit is proposed: the thermal plot. The thermal plot was defined as the portion of terrain from where the stakeholder can extract or dissipate the SGE. A similar concept was applied by [164] at a regional scale.

The measurable unit of the thermal plot is the surface area. However, the thermal plot is not characterized by this area, but by the SGE potential stored in the subsurface. This is due to the fact that thermal plots with the same superficial area can store different amounts of SGE, according to their geological and hydrogeological properties, the shape and orientation of the plot with respect to the piezometric surface and the position and number of exploitations.

As a result, each thermal plot must be analyzed individually in order to define the optimal SGE potential, whose thermal disturbances will remain inside the thermal plot. To accomplish this task, specialized methodologies and tools must be available to evaluate the possible scenarios of SGE consumption.

Initially, thermal plot could match the cadastral plot owned by the stakeholder, although it can be extended by adding adjacent public areas (e.g., streets, parks, squares). Public areas could be distributed among nearby thermal plots following principles of efficiency. For instance, when the cadastral plot borders with a street, the thermal plot boundary could be extended up to the axis of the street. This boundary will be shared by the thermal plot located in the other side of the street. The final shape of the thermal plot depends on the piezometric surface

and the direction of the groundwater flow in order to optimize the exploitation of the resource.

We propose to classify the thermal plot status as active or passive. An active thermal plot is the exploited thermal plot whose extracted energy meets the demand of its owner. If the SGE supplied by an active thermal plot does not meet the demand, stakeholders could make use of the SGE use rights market and get an agreement to obtain a use right on adjacent thermal plots. These thermal plots, whose SGE potential is transferred, were defined as passive plots. The loss of SGE potential of passive plots must be recognized and accepted by yielding its use rights to the active plot owner. This transaction must be regulated; the benefits and damages of each part, as well as the duration of the transfer, must be registered and quantified. To potentiate the sharing of SGE use rights, the passive land owner could receive compensation such as improvements on energy performance certificates [165] or other advantages.

3. METROGEOTHER GIS-BASED PLATFORM

3. 1. Design specifications

MetroGeother platform was designed bearing in mind the different methodologies used to evaluate, integrate and analyze the geological, hydrogeological and geothermal resources needed to facilitate the implementation of a SGE use rights market. Consequently, the following technical requirements were taken into consideration to design the GIS-based platform.

(1) A geospatial database with appropriate data storage and management. The database structure should enable the storage and management of geographically referenced geological, hydrogeological and geothermal data. Moreover, its structure should facilitate standardization and harmonization of available data. This environment should include specific mechanisms for facilitating data transcription (i.e., “one by one”, “massive”), managing different data formats, editing, and management of measurements reported in different units.

(2) Data processing and spatial analysis. The inclusion in a GIS environment meets the general requirements and it has proven to be a reliable method to analyze and visualize the different parameters needed for the management of SGE

resources [12], [29], [125], [127], [129]. Integration into a platform specially oriented to lead with geological and hydrogeological information is also advisable. For the effective processing of the data stored in the aforementioned database, the following methodologies should be available:

- Exploitation of a vast range of capabilities including: creation of spatio-temporal queries and calculations; integration of geological, hydrogeological and geothermal data sets; creation of interactive mapping; and effective assessment of the consistency of input data.
- Estimation and interpolation procedures to generate the spatial distribution of the geological, hydrogeological and geothermal properties needed, such as groundwater velocity, thermal conductivity or heat capacity.
- Estimation of energy supply for particular locations upon technical criteria.
- Prediction of the effects and consequences of existing and future geothermal exploitations relying on scientific or technical criteria.
- Support decision processes to establish threshold values to control the energy demand and supply according to legislation.
- Update of input and output data.

(3) Interaction with external software. The results obtained from external platforms should be easily exported or imported for pre and post-processing, e.g., to support numerical modeling proposes. A GIS environment facilitates these tasks.

3. 2. MetroGeoTher platform

The *MetroGeoTher* platform is composed of a geospatial database plus a set of tools, named *MetroGeoTherTools*, specifically designed for analytical and graphical support of SGE management. The characteristics of this platform are listed below.

3. 2. 1. Input data

The main required parameter is the piezometric surface (1). It can be obtained from a conceptual or numerical model. The groundwater or Darcy velocity (2) is also essential to obtain an accurate estimation of the geothermal potential

and the thermal impacts on the aquifer. It can be calculated with the piezometric surface and the hydraulic conductivity raster (3). The transmissivity raster (4) and the aquifer depth (5) are possible alternatives for estimating the hydraulic conductivity. To define the thermal behavior of the ground, the thermal conductivity (6), the thermal dispersivity in the longitudinal (7) and transverse (8) direction and the heat capacity (9) are required. Specific details about how to obtain these variables can be consulted in [29], [116], [129].

These required parameters should be provided in raster format, although the user can specify numerical values for some of them (see Table VI.1) when the parameter is considered constant within the whole domain.

Table VI.1. Required variables and type of data for each tool.

Variables	**Thermal Characteristic Curve**	**Thermal plume**
Piezometric surface (m asl)	Raster data	Raster data
Darcy velocity (m/s)	Raster / numeric data	Raster / numeric data
Effective Thermal conductivity (W/m K)	Raster / numeric data	Raster / numeric data
Volumetric heat capacity of aquifer (J/kg K)	Raster / numeric data	Raster / numeric data
Volumetric heat capacity of water (J/kg K)	Numeric data	Numeric data
Temperature threshold (K)	Numeric data	Numeric data
Shallow geothermal Potential (W/m)	--	Raster / numeric data
Time (s)	Numeric data	Numeric data
Thermal plot	Vector data	Vector data

3. 2. 2. Technical criteria

The quantification of the SGE potential of a thermal plot as well as the thermal impact generated by its exploitation are calculated based on analytical solutions of the heat transport equation in porous media [166]. The Moving Infinite Line Source model is considered to solve this equation. It describes the thermal field of a uniform medium that moves through a fixed heat linear source. This analytical approach has been widely used to solve the temperature variations caused by

Boreholes Heat Exchangers (BHE), the most common Ground Source Heat Pump (GSHP) system[12] [131].

The equations developed by [137] and applied for BHE by [116] for steady (Eq. 1) and transient (Eq. 2) state were implemented in *MetroGeoTherTools*. These analytical solutions consider the main heat transport mechanisms in porous media, advection and dispersion. The variables of interest are calculated numerically from these equations.

$$[SGP] = \frac{\Delta T \cdot 2 \cdot \pi \cdot \sqrt{[\lambda_x] \cdot [\lambda_y]}}{Exp\left(\frac{[v_D] \cdot \rho_w c_w \cdot x}{2 \cdot [\lambda_x]}\right) \cdot K_0\left(\frac{[v_D] \cdot \rho_w c_w}{2} \cdot \sqrt{\frac{[\lambda_x] \cdot x^2 + [\lambda_y] \cdot y^2}{[\lambda_x]^2 \cdot [\lambda_y]}}\right)} \quad \text{Eq. 1}$$

where $K_0(z)$, is the modiffied Bessel function of the second kind of order zero.

$$[SGP] = \frac{\Delta T \cdot 4 \cdot \pi \cdot \sqrt{[\lambda_x] \cdot [\lambda_y]}}{exp\left(\frac{[v_D] \cdot \rho_w c_w \cdot x}{2 \cdot [\lambda_x]}\right) \int_0^{Limit} \frac{1}{\varphi} exp\left(-\varphi - \frac{1}{\varphi}\left(\frac{x^2}{[\lambda_x]} + \frac{y^2}{[\lambda_y]}\right)\frac{([v_D] \cdot \rho_w c_w)^2}{16 \cdot [\lambda_x]}\right) d\varphi} \quad \text{Eq. 2}$$

$$Limit = \frac{([v_D] \cdot \rho_w c_w)^2 t}{4 \cdot [\rho c][\lambda_x]}$$

where φ is the integration variable.

These equations have four variables whose values have to be settled by the administrator. They are the temperature increment (ΔT) at a specific distance ($r = \sqrt{x^2 + y^2}$) produced by an extracted potential (SGP) at an elapsed time (t) from the start of operation. The administrator has to constrain the equation by defining three of them to obtain the fourth.

3. 2. 3. Geospatial database

The geospatial database represents information based on the Personal Geodatabase structure provided by the *ArcGIS* concept (*ESRI*).

[12] Ground Source Heat Pumps (GSHP) exploit the soil as a thermal source or sink, through the circulation of a heat carrier fluid in a closed pipe loop. GSHP consist of a conventional heat pump unit coupled with different pipe arrangements, such as Borehole Heat Exchangers (BHE), vertical pipe loops reaching depths of 50-200m. (for further details, Florides, G. and Kaligorou, S., 2007)

To ensure an optimal integration of information related to the underground medium, the following entities form part of a comprehensive database presented in [26]. This database stores geological, hydrogeological, hydrochemical and hydrophysical data, as well as their interpretations. Some details of the components of the database directly related to shallow geothermal management and the main characteristics of its structure are given below, in order to better illustrate the current platform. A sketch of the components of the database is shown in Figure VI.1.

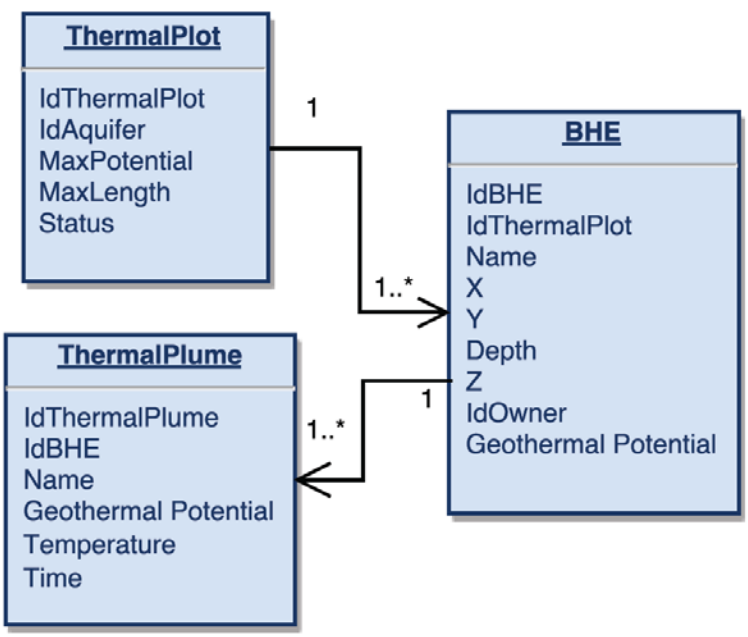

Figure VI.1. Geodatabase model structure.

In the geospatial database, each exploitation is correctly represented by a point-type entity termed BHEs. Its main attributes are the geographical coordinates, the nominal shallow geothermal potential (SGP) and other administrative information.

Regarding the affected area of each exploitation, two entities must be taken into account, both of polygon-type. On the one hand, the exploitation must not produce thermal affections outside the plot boundary of the owner, so the plot registered in a cadastral survey can be considered initially; this entity is named *ThermalPlots*. On the other hand, the entity named *ThermalPlumes* represents the

estimated thermal plume of the exploitation which should be stored to reflect a first evaluation of thermal affections.

The aforementioned datasets are vector data. The geospatial database also stores the input data required by *MetroGeoTherTools* as raster data which reflect the spatial distribution of hydrogeological and geothermal properties, such as piezometric surface, groundwater velocity, porosity, thermal conductivity and heat capacity.

3. 2. 4. MetroGeoTherTools

This set of instruments enables the administrator to perform a spatial analysis of the possible characteristics of the geothermal exploitations, such as the maximum shallow geothermal potential (SGP), and also to predict the thermal affection geographically. This represents a support toolset to achieve an optimal management of SGE use rights markets.

The type of input variables for these tools can be both raster data and numeric values introduced by the administrator through their respective input window. For both cases, a raster representing the piezometric surface is needed. For further information of the required input variables see Table VI.1. The developed tools are described below.

3. 2. 4. 1. Thermal Characteristic Curve tool

This tool gives support during the generation of possible scenarios of SGE consumptions, when deciding the position and potential of BHE inside a thermal plot. It generates the thermal characteristic curve (TCC) for the thermal plot of interest. This graph represents the relation between the length and width of thermal influence and the required shallow geothermal potential (SGP) extracted by one BHE, e.i., SGP vs. distance. To obtain this relation, the other two degrees of freedom must be constrained: the maximum temperature increment (1) and the time interval (2). Additionally, the TCC represents the maximum SGP which induces a specific thermal increment at the BHE wall. The steady thermal state of the thermal disturbance is also shown as maximum values of distances and shallow geothermal potentials.

The administrator has to define this temperature threshold and the time from the start of operation. By selecting the thermal plot on the map, additional hydraulic and thermal parameters are extracted from raster data to generate the TCC.

The TCC can be used in both directions. On the one hand, the maximum SGP which does not affect the neighboring plots can be obtained if the maximum dimensions available inside the thermal plot, length and width, are known. These distances can be obtained with native GIS tools over the map, according to the direction of groundwater and the orientation of the plot. Further restrictions must be considered regarding the feasibility of the BHE location. On the other hand, the TCC shows the length and width of the thermal disturbance caused by a specific SGP.

For instance, Figure VI.2 represents a sketch of a TCC with a maximum allowed temperature increment of 0.5K after a period of 6 months from start of operation where only the affected thermal length is shown.

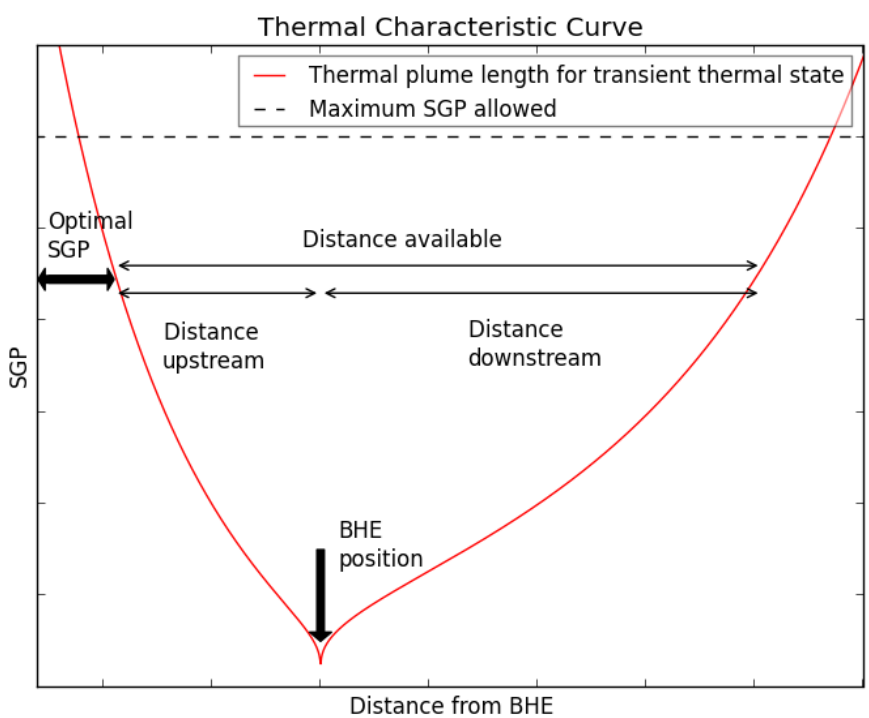

Figure VI.2. Synthetic example of Thermal Characteristic Curve.

3. 2. 4. 2. Thermal Plume tool

This tool draws over the map the thermal plume originated by one BHE for the scenario of the proposed exploitation regimen. Three variables must be established

to calculate the shape of the thermal plume: the temperature (1) increment caused by a specific SGP (2) at a particular time (3) interval.

Once the administrator establishes these three variables, a possible location for the BHE must be selected. The central axis of the thermal plume drawn is adapted to the streamline of groundwater flow starting in the BHE.

The administrator is able to reproduce different scenarios for evaluating the interferences between future and existing exploitations. After a decision is taken and the BHE is in operation, this thermal plume must be stored in the *ThermalPlume* entity of the geospatial database, along with the point representing the BHE.

The platform also supports the update of these entities because the influence of thermal plumes can change due to alterations of several factors. For instance, the piezometric surface could suffer modifications due to pumping regimen changes or to readjustments of the geological and hydrogeological conceptual models; alternatively, the heating rate initially expected for an exploitation can be adjusted to the real rate exchanged, if an adequate feedback exists between the owner and the administrator.

4. APPLICATION

In this section, an application of the *MetroGeoTher* platform is shown to illustrate the implementation and control of a SGE use-rights market. The selected area is located in the Metropolitan Area of Barcelona, a highly urbanized area in the NE of Spain. Geologically, the study area is characterized by porphyritic dykes intruded in a fractured granodiorite, which configures a heterogeneous urban aquifer. The main features of the geological units in this area are summarized in Figure VI.3.

Figure VI.3. Thermal properties of the study site and cadastral plots analyzed. Coordinate System: UTM European Datum 1950, Zone 31N.

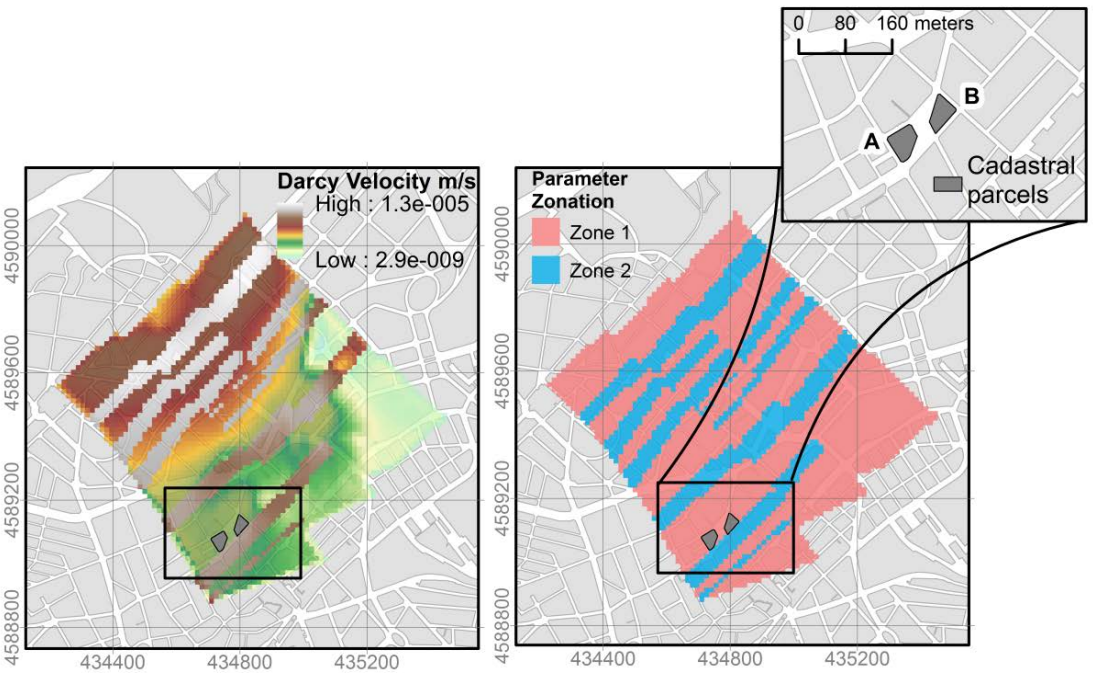

A synthetic scenario of management was created for the cadastral plot A, shown in 0. In this setting, a new concession is requested for the cadastral subplot A-01. First, the groundwater direction is shown (dashed blue lines). The cadastral subplot (cross hatch area), A-01, was redefined to create the thermal plot (simple hatch area) by extending its boundary in the direction of the groundwater flow over a public area. The maximum distance available inside this thermal plot is 30 m.

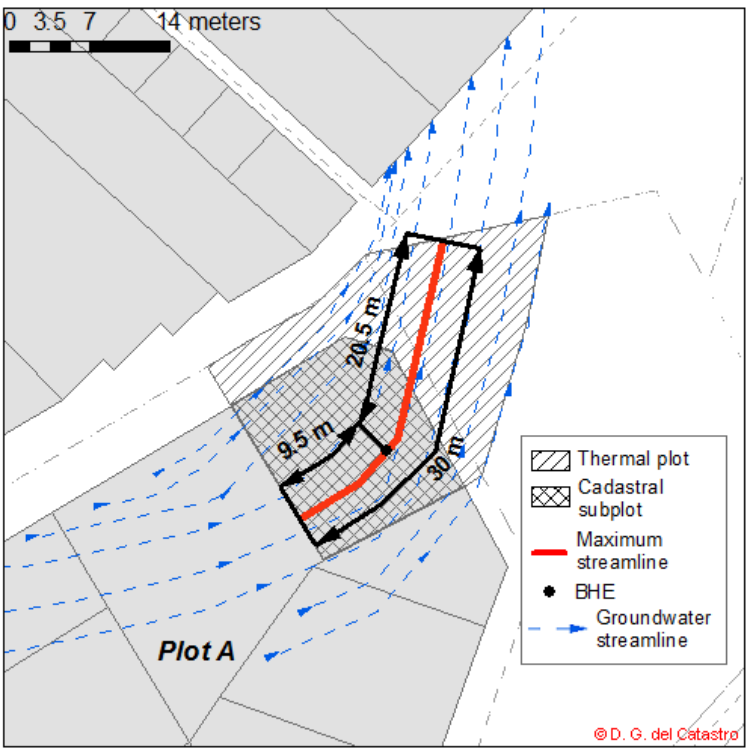

Figure VI.4. Definition of thermal plot taking into account the groundwater flow and the cadastral subplot.

The maximum SGP for a BHE inside this plot can be obtained with the Thermal Characteristic Curve (TCC) (Figure VI.5) generated with the TCC tool for a temperature increment of 0.25K and assuming an operating period of 6 months. The horizontal line representing a distance of 30 m fixes a maximum SGP of 46 W/m. The distance upstream and downstream of the BHE are also graphically defined (9.5 and 20.5 m). Once the maximum SGP has been established, the thermal plume can be drawn for different temperature increment thresholds, as shown in Figure VI.6. The thermal plume representing a temperature disturbance greater than 0.25K is completely allocated inside the thermal plot. This allows the evaluation of the thermal disturbance in neighboring plots, e.g., it can be seen that the thermal plume for 0.1K reaches the front plot.

Figure VI.5. Thermal Characteristic Curve for thermal plot A-01

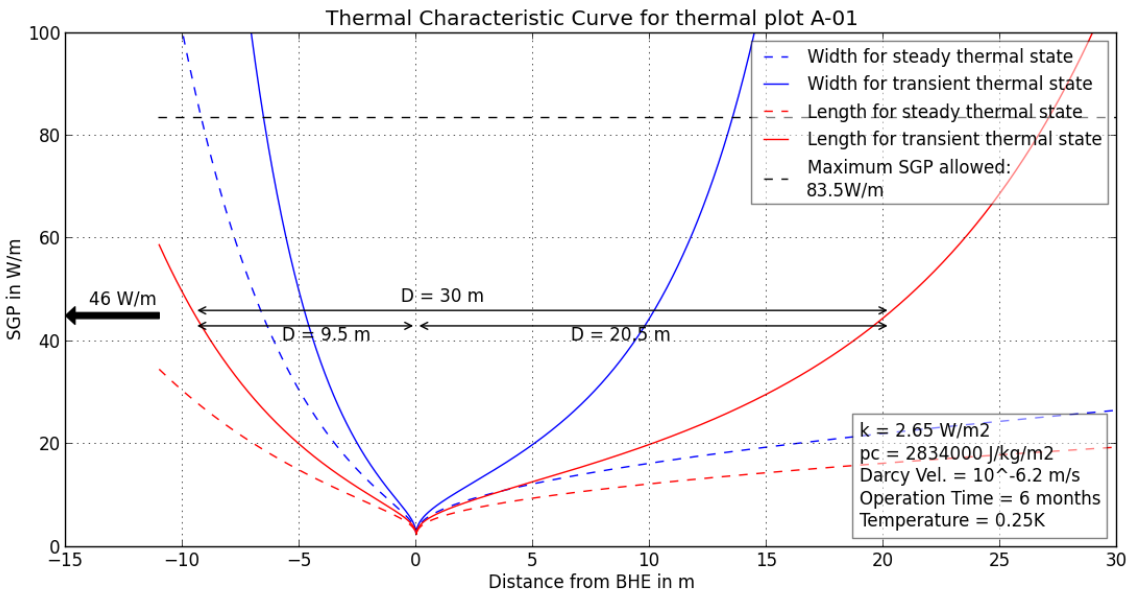

Figure VI.6. Thermal plumes for several temperature thresholds produced by a SGP of 46 W/m in thermal plot A-01

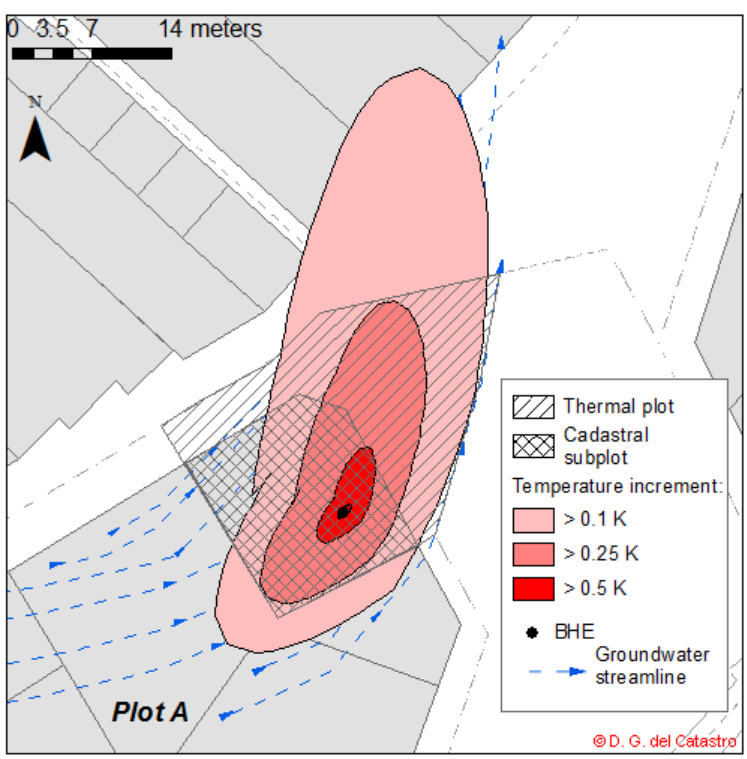

To illustrate the possibilities of this platform, a theoretical scenario was designed for the cadastral plot B to simulate its exploitation and analyze its optimization (Figure VI.7). The complete area is exploited; thermal plumes were created for a temperature increment greater than 0.25K, assuming an operation time of six months per year. The SGP extracted by each BHE was obtained in order to cover the maximum distance available inside the plot.

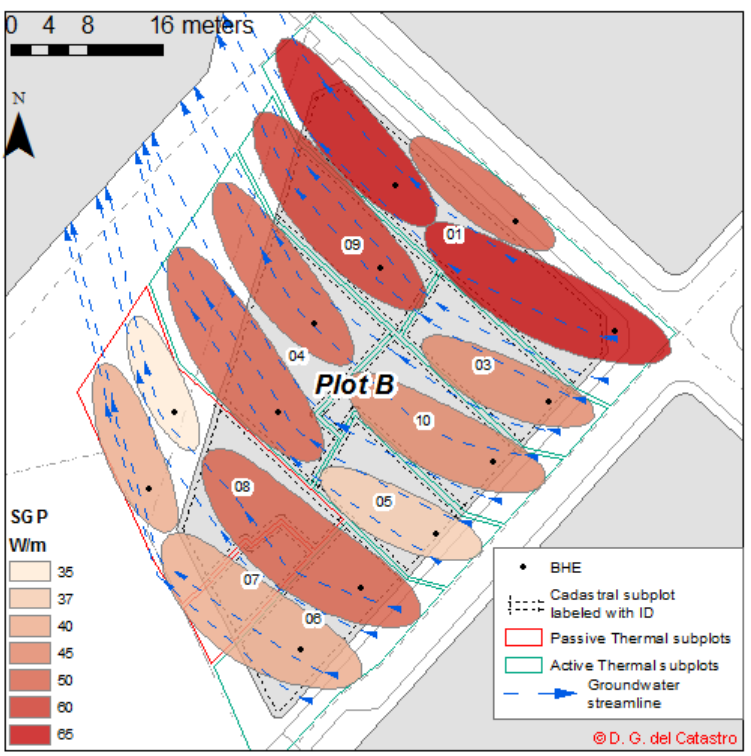

Figure VI.7. Optimized scenario of exploitation for cadastral plot B and its subplots; thermal plumes representing 0.25K for an operation time of six months per year

The conditions of the thermal subplot B-06 limit the SGP for this plot, so the owner could ask for permit to exploit the thermal subplots B-07 and B-08, which would become passive plots. The thermal disturbances would remain inside the thermal plots for all subplots, except for the thermal subplot B-06. The final depth of the BHE would be defined to cover the energy demand.

5. DISCUSSION

The administrator criteria is crucial when approaching several aspects, e.g., when calculating the geometry of thermal plumes generated and its space distribution within the thermal plot, which is conditioned by the piezometric surface.

Moreover, by overlaying additional information, the administrator can optimize the exploitation schema; areas not exploited by stakeholders could be reclassified as passive thermal plots and reassigned to the neighboring active thermal plots. The public entity also has to interpose for the establishment of temperature thresholds when defining the protection areas for each exploitation, choosing between more or less conservative positions.

For further development in the management of this resource and design of complex geothermal installations, such as Borehole/Aquifer Thermal Storage (B/ATES) systems, the numerical approach is essential to consider specifically the characteristic of the geological and hydrogeological media which are not simulated with the analytical solutions, such as the wide range of boundary conditions, the interactions between BHE and also temporal variations of thermal extractions.

To achieve an optimal management of SGE resources, there must be a feedback between the users and the administration. Once the owner has drilled the BHE, information about the final location and the heating rate measured should be notified. Using the techniques presented in this work, the information obtained from the stakeholder could be stored in the geospatial database and displayed along with other data.

6. CONCLUSIONS

As a response to the scarcity of SGE management systems, the proposed methodology establishes a general framework for the management of this resource based on the implementation of a market of SGE use rights. This methodology constitutes a powerful tool to accomplish an optimal management of SGE resources during the implementation of a SGE use rights market. It helps to cope with the spatial characteristic of this resource and represents a straightforward way of facilitating the distribution and assignment of SGE. The administrator can offer to the future stakeholders feasible locations for the BHE inside the thermal plot together with a first estimation of the heating rate expected as well as the thermal disturbance generated.

To develop this kind of use-rights market, this methodology is implemented in a GIS platform. The first element of this platform is the geospatial database that enjoys the following advantages: (1) an effective management of a large number of different types of geological, hydrogeological and geothermal data, (2) the possibility of querying and visualizing data simultaneously, facilitating further geothermal analysis, (3) a synoptic view of the thermal regime of the subsurface system, and (4) an efficient pre-processing of data.

The second element of this platform is a set of GIS tools. It allows the generating and storing of different scenarios for the consumption of shallow geothermal resources, by representing geographically the geothermal affections of existing and future exploitations through the implementation of different analytical solutions. An innovation which proved essential was the addition of geographic considerations to these analytical solutions to adapt the shape of the thermal plume to the groundwater direction. Thus, the optimal position, length and potential for new BHEs can be obtained based on the geometry of the thermal plot, the direction and velocity of groundwater, the initial energy demand estimation and the shape of the thermal plume generated by the new and existing BHEs. As a result, the thermal disturbances can be drawn easily on the map in a simple way. Therefore, these techniques allow the assessment of the affection perimeter of a given exploitation system, making an improvement in the development of SGE management policies. This methodology reduces the cost of managing SGE resources at a city scale for numerous small exploitations.

With this methodology, a SGE use rights market has been successfully defined, according to the energy demand of users and SGP available in the subsurface. On this basis, the approval of future installation must satisfy the requirement of sustainability, thereby avoiding the thermal disturbance between users.

Additional scenarios of shallow geothermal consumption generated with external software (such as numerical simulations executed for complex installations like open systems, ATES, BTES) can be added to the GIS application for visualizing thermal interferences.

VII. GENERAL CONCLUSIONS

The general conclusions and innovations obtained from the elaboration of this thesis are summarized here:

- An integrated GIS system for shallow geothermal energy management was developed to support the control, organization and supervision of the exploitation of this energy resource.
- Two complementary methodologies for the management of shallow geothermal energy were described for different spatial scales: regional and local or metropolitan scales.
- Scientific and technical criteria can be considered in both methodologies for the management of shallow geothermal energy.
- These criteria are based on a comprehensive hydrogeological conceptual model. This allows considering the main heat transport mechanisms in porous media, advection and dispersion when estimating the shallow geothermal potential that can be extracted as well as the thermal impacts produced.
- The regional methodology for management of shallow geothermal energy can be applied with a GIS toolset named GeoTherTools. This allows for the creation of thematic maps of: (1) shallow geothermal potential, (2) area and length of thermal impacts and (3) volumetric shallow geothermal potential.

- The local methodology for the administration of shallow geothermal energy is based on the implementation of a use rights market of shallow geothermal energy.
- The proposed use rights market of shallow geothermal energy can be established with a GIS toolset termed MetroGeoTherTools. This set of tools enables the administrator to take into account the specific characteristics of the site, such as the direction of groundwater flow, the underground thermal properties and the shape of the available plot. Taking in consideration these aspects, the thermal affections between neighboring exploitations can be avoided.
- Existing methodologies were improved and new ones were developed to define the hydrogeological conceptual model upon which shallow geothermal energy can be controlled.
- The three-dimensional integration of all available information related to the groundwater media were accomplished in a GIS environment. The GIS toolset named HEROS3D facilitates the visualization in a 3D scheme, as well as the management of different types of geological, hydrogeological, hydrochemical and geothermal data. It allows validating and improving the knowledge about the groundwater behavior.
- The interaction between the hydrogeological conceptual model and the numerical model was facilitated with new methodologies developed in a GIS environment. The GIS toolset termed ArcArAz was designed with specific techniques for implementing the hydrogeological conceptual model into numerical software platforms. The geometric and alphanumeric characteristics can be adapted to particular requirements for numerical modeling.

Bibliography

[1] K. Tokimatsu, S. Konishi, K. Ishihara, T. Tezuka, R. Yasuoka, and M. Nishio, "Role of innovative technologies under the global zero emissions scenarios," *Appl. Energy*, 2015.

[2] M. Z. Jacobson, M. a Delucchi, G. Bazouin, Z. a F. Bauer, C. C. Heavey, E. Fisher, S. B. Morris, D. J. Y. Piekutowski, T. a Vencill, and T. W. Yeskoo, "100% clean and renewable wind, water, and sunlight (WWS) all-sector energy roadmaps for the 50 United States," *Energy Environ. Sci.*, vol. 8, p. -, 2015.

[3] H. Safaei and D. W. Keith, "How much bulk energy storage is needed to decarbonize electricity?," *Energy Environ. Sci.*, 2015.

[4] J. W. Lund, D. H. Freeston, and T. L. Boyd, "Direct utilization of geothermal energy 2010 worldwide review," *Geothermics*, vol. 40, no. 3, pp. 159–180, Sep. 2011.

[5] J. W. Lund and T. L. Boyd, "Direct Utilization of Geothermal Energy 2015 Worldwide Review," in *Proceedings World Geothermal Congress 2015*, 2015.

[6] European Renewable Energy Council (EREC), "Mapping Renewable Energy Pathways towards 2020," Brussels, Belgium, 2011.

[7] O. Ozgener and L. Ozgener, "Modeling of driveway as a solar collector for improving efficiency of solar assisted geothermal heat pump system: a case study," *Renew. Sustain. Energy Rev.*, vol. 46, pp. 210–217, 2015.

[8] A. Buonomano, F. Calise, A. Palombo, and M. Vicidomini, "Energy and economic analysis of geothermal–solar trigeneration systems: A case study for a hotel building in Ischia," *Appl. Energy*, vol. 138, pp. 224–241, 2015.

[9] P. Pärisch, O. Mercker, J. Warmuth, R. Tepe, E. Bertram, and G. Rockendorf, "Investigations and model validation of a ground-coupled heat pump for the combination with solar collectors," *Appl. Therm. Eng.*, vol. 62, no. 2, pp. 375–381, 2014.

[10] S. Rosiek and F. J. Batlles, "Shallow geothermal energy applied to a solar-assisted air-conditioning system in southern Spain: Two-year experience," *Appl. Energy*, vol. 100, pp. 267–276, 2012.

[11] S. K. Soni, M. Pandey, and V. N. Bartaria, “Ground coupled heat exchangers: A review and applications,” *Renew. Sustain. Energy Rev.*, vol. 47, pp. 83–92, 2015.

[12] A. Gemelli, A. Mancini, and S. Longhi, “GIS-based energy-economic model of low temperature geothermal resources: A case study in the Italian Marche region,” *Renew. Energy*, vol. 36, no. 9, pp. 2474–2483, Sep. 2011.

[13] J. Busby, M. Lewis, H. Reeves, and R. Lawley, “Initial geological considerations before installing ground source heat pump systems,” 2009.

[14] J. Epting and P. Huggenberger, “Unraveling the heat island effect observed in urban groundwater bodies – Definition of a potential natural state,” *J. Hydrol.*, vol. 501, pp. 193–204, Sep. 2013.

[15] A. García-Gil, E. Vázquez-Suñe, E. G. Schneider, J. Á. Sánchez-Navarro, and J. Mateo-Lázaro, “The thermal consequences of river-level variations in an urban groundwater body highly affected by groundwater heat pumps.,” *Sci. Total Environ.*, vol. 485–486, pp. 575–87, Jul. 2014.

[16] S. Hähnlein, P. Bayer, G. Ferguson, and P. Blum, “Sustainability and policy for the thermal use of shallow geothermal energy,” *Energy Policy*, vol. 59, pp. 914–925, 2013.

[17] A. García-Gil, E. Vázquez-Suñe, E. G. Schneider, J. Á. Sánchez-Navarro, and J. Mateo-Lázaro, “Relaxation factor for geothermal use development – Criteria for a more fair and sustainable geothermal use of shallow energy resources,” *Geothermics*, vol. 56, pp. 128–137, 2015.

[18] A. Capozza, M. De Carli, and A. Zarrella, “Investigations on the influence of aquifers on the ground temperature in ground-source heat pump operation,” *Appl. Energy*, vol. 107, pp. 350–363, 2013.

[19] a. Angelotti, L. Alberti, I. La Licata, and M. Antelmi, “Energy performance and thermal impact of a Borehole Heat Exchanger in a sandy aquifer: Influence of the groundwater velocity,” *Energy Convers. Manag.*, vol. 77, pp. 700–708, Jan. 2014.

[20] E. Vázquez-Suñé, X. Sánchez-Vila, and J. Carrera, “Introductory review of specific factors influencing urban groundwater, an emerging branch of hydrogeology, with reference to Barcelona, Spain,” *Hydrogeol. J.*, vol. 13, no. 3, pp. 522–533, 2005.

[21] N. G. Tait, R. M. Davison, J. J. Whittaker, S. a. Leharne, and D. N. Lerner, “Borehole Optimisation System (BOS) - A GIS based risk analysis tool for optimising the use of urban groundwater,” *Environ. Model. Softw.*, vol. 19, no. 12, pp. 1111–1124, 2004.

[22] M. Schirmer, S. Leschik, and A. Musolff, “Current research in urban hydrogeology – A review,” *Adv. Water Resour.*, vol. 51, pp. 280–291, 2013.

[23] M. Ross, M. Parent, and R. Lefebvre, “3D geologic framework models for regional hydrogeology and land-use management: A case study from a Quaternary basin of southwestern Quebec, Canada,” *Hydrogeol. J.*, vol. 13, pp. 690–707, 2005.

[24] V. Velasco, R. Gogu, E. Vázquez-Suñè, a. Garriga, E. Ramos, J. Riera, and M. Alcaraz, "The use of GIS-based 3D geological tools to improve hydrogeological models of sedimentary media in an urban environment," *Environ. Earth Sci.*, vol. 68, no. 8, pp. 2145–2162, Aug. 2012.

[25] M. Diepenbroek, H. Grobe, M. Reinke, U. Schindler, R. Schlitzer, R. Sieger, and G. Wefer, "PANGAEA - an information system for environmental sciences," *Comput. Geosci.*, vol. 28, no. 10, pp. 1201–1210, 2002.

[26] D. V. Velasco Mansilla, "GIS-based hydrogeologica platform for sedimentary media," Universitat Politecnica de Catalunya (UPC), 2013.

[27] V. Velasco, I. Tubau, E. Vázquez-Suñè, R. Gogu, D. Gaitanaru, M. Alcaraz, a. Serrano-Juan, D. Fernàndez-Garcia, T. Garrido, J. Fraile, and X. Sanchez-Vila, "GIS-based hydrogeochemical analysis tools (QUIMET)," *Comput. Geosci.*, vol. 70, pp. 164–180, Sep. 2014.

[28] R. Criollo, V. Velasco, E. Vázquez-Suñé, A. Serrano-Juan, M. Alcaraz, and A. García-Gil, "An integrated GIS-based tool for Aquifer Test Analysis," *Environ. Earth Sci.*, 2016.

[29] M. Alcaraz, A. García-Gil, E. Vázquez-Suñé, and V. Velasco, "Advection and dispersion heat transport mechanisms in the quantification of shallow geothermal resources and associated environmental impacts," *Sci. Total Environ.*, vol. 543, pp. 536–546, 2016.

[30] ONEGeology, "ONE Geology," 2013. [Online]. Available: www.onegeology.org. [Accessed: 13-Oct-2015].

[31] Open Geospatial Consortium (OGC), "OGC," 2012. [Online]. Available: http://www.opengeospatial.org/standards. [Accessed: 21-Dec-2015].

[32] INSPIRE, *D2.9 Guidelines for the use of Observations & Measurements and Sensor Web Enablement-related standards in INSPIRE Annex II and III data specification development*, no. Directive 2007/2/EC of the European Parliament and of the Council of 14 March 2007 establishing an Infrastructure for Spatial Information in the European Community (INSPIRE) Project. 2011, p. 32.

[33] INSPIRE, *D2.8.II.4 Data Specification on Geology – Technical Guidelines*, no. Directive 2007/2/EC of the European Parliament and of the Council of 14 March 2007 establishing an Infrastructure for Spatial Information in the European Community (INSPIRE). 2013.

[34] A. Serrano-Juan, E. Vázquez-Suñé, M. Alcaraz, C. Ayora, V. Velasco, and R. Criollo, "Using MS Excel and VBA to reuse , customize and extend current hydrogeological software .," pp. 1–20, 2013.

[35] J. Carrera, E. Vázquez-Suñé, O. Castillo, and X. Sánchez-Vila, "A methodology to compute mixing ratios with uncertain end-members," *Water Resour. Res.*, vol. 40, no. 12, p. n/a–n/a, 2004.

[36] M. a. Dawoud, "The development of integrated water resource information management system in arid regions," *Arab. J. Geosci.*, vol. 6, no. 5, pp. 1601–1612, 2011.

[37] K. Rina, C. K. Singh, P. S. Datta, N. Singh, and S. Mukherjee, "Geochemical modelling, ionic ratio and GIS based mapping of groundwater salinity and assessment of governing processes in Northern Gujarat, India," *Environ. Earth Sci.*, vol. 69, no. 7, pp. 2377–2391, Nov. 2012.

[38] Z. Şen, S. a. Al Sefry, S. a. Al Ghamdi, W. a. Ashi, and W. a. Bardi, "Strategic groundwater resources planning in arid regions," *Arab. J. Geosci.*, pp. 4363–4375, 2012.

[39] K. L. Jacobs and J. M. Holway, "Managing for sustainability in an arid climate: lessons learned from 20 years of groundwater management in Arizona, USA," *Hydrogeol. J.*, vol. 12, no. 1, pp. 52–65, Feb. 2004.

[40] M. F. Goodchild, "Editorial: Citizens as Voluntary Sensors: Spatial Data Infrastructure in the World of Web 2.0," *Int. J. Spat. Data Infrastructures Res.*, vol. 2, pp. 24–32, 2007.

[41] L. Romero, H. Alonso, P. Campano, L. Fanfani, R. Cidu, C. Dadea, T. Keegan, I. Thornton, and M. Farago, "Arsenic enrichment in waters and sediments of the Rio Loa (Second Region, Chile)," *Appl. Geochemistry*, vol. 18, no. 9, pp. 1399–1416, Sep. 2003.

[42] F. M. Camacho, "Competing rationalities in water conflict: Mining and the indigenous community in Chiu Chiu, El Loa Province, northern Chile," *Singap. J. Trop. Geogr.*, vol. 33, no. 1, pp. 93–107, Mar. 2012.

[43] A. Pérez-carrera and A. F. Cirelli, "Water and Sustainability in Arid Regions," 2010.

[44] I. D. Jolly, K. L. McEwan, and K. L. Holland, "A review of groundwater–surface water interactions in arid/semi-arid wetlands and the consequences of salinity for wetland ecology," *Ecohydrology*, vol. 130, no. February, pp. 43–58, 2008.

[45] J. Houston, "The great Atacama flood of 2001 and its implications for Andean hydrology," *Hydrol. Process.*, vol. 20, no. 3, pp. 591–610, Feb. 2006.

[46] A. J. Hartley and G. May, "Miocene Gypcretes from the Calama Basin, northern Chile," *Sedimentology*, vol. 45, no. 2, pp. 351–364, Mar. 1998.

[47] G. May, a. J. Hartley, F. M. Stuart, and G. Chong, "Tectonic signatures in arid continental basins: an example from the Upper Miocene–Pleistocene, Calama Basin, Andean forearc, northern Chile," *Palaeogeogr. Palaeoclimatol. Palaeoecol.*, vol. 151, no. 1–3, pp. 55–77, Jul. 1999.

[48] G. MAY and A. J. Hartley, "Oligocene-Recent Sedimentary and Tectonic Evolution of the Calama Basin, N.Chilean Forearc," no. I, pp. 17–19, 1996.

[49] G. MAY and A. J. Hartley, "Eocene to Pleistocene lithostratigraphy , chronostratigraphy and tectono-sedimentary evolution of the Calama Basin , northern Chile," *Rev. geológica Chile*, pp. 1–26, 2005.

[50] J. A. Naranjo and R. P. Paskoff, "Estratigrafia de los depositos cenozoicos de la region de chiuchiu-calama. desierto de atacama," *Rev. geológica Chile*, no. 13, pp. 79–85.

[51] MATRAZ CONSULTORES ASOCIADOS and UPC, "ESTUDIO ACUÍFERO DE CALAMA SECTOR MEDIO DEL RÍO LOA, REGIÓN DE ANTOFAGASTA," Santiago

de Chile, 2012.

[52] D. Gàmez Torrent, "Sequence Stratigraphy as a tool for water resources management in alluvial coastal aquifers: application to the Llobregat Delta (Barcelona, Spain)," Technical University of Catalonia (UPC), 2007.

[53] D. Koller, P. Lindstrom, W. Ribarsky, L. F. Hodges, N. Faust, and G. Turner, "Virtual GIS: A Real-Time 3D Geographic Information System," in *VIS '95 Proceedings of the 6th conference on Visualization '95*, 1995, p. 94.

[54] a. K. Turner, "Challenges and trends for geological modelling and visualisation," *Bull. Eng. Geol. Environ.*, vol. 65, no. 2, pp. 109–127, 2006.

[55] F. de Rienzo, P. Oreste, and S. Pelizza, "Subsurface geological-geotechnical modelling to sustain underground civil planning," *Eng. Geol.*, vol. 96, no. 3–4, pp. 187–204, 2008.

[56] P. Thierry, A. M. Prunier-Leparmentier, C. Lembezat, E. Vanoudheusden, and J. F. Vernoux, "3D geological modelling at urban scale and mapping of ground movement susceptibility from gypsum dissolution: The Paris example (France)," *Eng. Geol.*, vol. 105, no. 1–2, pp. 51–64, 2009.

[57] B. Gill, D. Cherry, M. Adelana, X. Cheng, and M. Reid, "Using three-dimensional geological mapping methods to inform sustainable groundwater development in a volcanic landscape, Victoria, Australia," *Hydrogeol. J.*, vol. 19, no. 7, pp. 1349–1365, 2011.

[58] F. C. Conde, S. G. Martínez, J. L. Ramos, R. F. Martínez, and A. Mabeth-Montoya Colonia, "Building a 3D geomodel for water resources management: case study in the Regional Park of the lower courses of Manzanares and Jarama Rivers (Madrid, Spain)," *Environ. Earth Sci.*, vol. 71, no. 1, pp. 61–66, Aug. 2013.

[59] R. R. Jones, K. J. W. McCaffrey, P. Clegg, R. W. Wilson, N. S. Holliman, R. E. Holdsworth, J. Imber, and S. Waggott, "Integration of regional to outcrop digital data: 3D visualisation of multi-scale geological models," *Comput. Geosci.*, vol. 35, no. 1, pp. 4–18, 2009.

[60] A. Bistacchi, M. Massironi, G. V. Dal Piaz, G. Dal Piaz, B. Monopoli, A. Schiavo, and G. Toffolon, "3D fold and fault reconstruction with an uncertainty model: An example from an Alpine tunnel case study," *Comput. Geosci.*, vol. 34, no. 4, pp. 351–372, Apr. 2008.

[61] O. Kaufmann and T. Martin, "3D geological modelling from boreholes, cross-sections and geological maps, application over former natural gas storages in coal mines," *Comput. Geosci.*, vol. 34, no. 3, pp. 278–290, Mar. 2008.

[62] W. Baojun, S. Bin, and S. Zhen, "A simple approach to 3D geological modelling and visualization," *Bull. Eng. Geol. Environ.*, vol. 68, no. 4, pp. 559–565, 2009.

[63] J. L. Mallet, "Mallet, J.-L., 2003. Geomodelling: Shared-Earth-Model and SGrids. Report," Nancy, France, 2003.

[64] A. Tonini, E. Guastaldi, G. Massa, and P. Conti, "3D geo-mapping based on surface data for preliminary study of underground works: A case study in Val Topina (Central Italy)," *Eng. Geol.*, vol. 99, no. 1–2, pp. 61–69, 2008.

[65] J. M. Lees, “Geotouch: Software for three and four dimensional GIS in the earth sciences,” *Comput. Geosci.*, vol. 26, no. 7, pp. 751–761, 2000.

[66] J. Ming, M. Pan, H. Qu, and Z. Ge, “GSIS: A 3D geological multi-body modeling system from netty cross-sections with topology,” *Comput. Geosci.*, vol. 36, no. 6, pp. 756–767, Jun. 2010.

[67] H. Kessler, S. Mathers, and H.-G. Sobisch, “The capture and dissemination of integrated 3D geospatial knowledge at the British Geological Survey using GSI3D software and methodology,” *Comput. Geosci.*, vol. 35, no. 6, pp. 1311–1321, Jun. 2009.

[68] M. E. Cox, A. James, A. Hawke, and M. Raiber, “Groundwater Visualisation System (GVS): A software framework for integrated display and interrogation of conceptual hydrogeological models, data and time-series animation,” *J. Hydrol.*, vol. 491, pp. 56–72, 2013.

[69] G. Strassberg, N. L. Jones, and A. Lemon, “Arc Hydro Groundwater Data Model And Tools : Overview and Use Cases,” *AQUA mundi*, vol. Am02014, pp. 101–114, 2010.

[70] R. Chesnaux, M. Lambert, J. Walter, U. Fillastre, M. Hay, A. Rouleau, R. Daigneault, A. Moisan, and D. Germaneau, “Building a geodatabase for mapping hydrogeological features and 3D modeling of groundwater systems: Application to the Saguenay–Lac-St.-Jean region, Canada,” *Comput. Geosci.*, vol. 37, no. 11, pp. 1870–1882, 2011.

[71] M. Alcaraz, E. Vázquez-Suné, and V. Velasco, “Use rights markets for shallow geothermal energy management,” *Appl. Energy*, 2016.

[72] P. Wycisk, T. Hubert, W. Gossel, and C. Neumann, “High-resolution 3D spatial modelling of complex geological structures for an environmental risk assessment of abundant mining and industrial megasites,” *Comput. Geosci.*, vol. 35, no. 1, pp. 165–182, 2009.

[73] M. G. Trefry and C. Muffels, “FEFLOW: A Finite-Element Ground Water Flow and Transport Modeling Tool,” *Ground Water*, vol. 45, no. 5, pp. 525–528, 2007.

[74] M. G. McDonals and A. W. Harbaugh, “The History of MODFLOW,” *Ground Water*, vol. 41, no. 2, pp. 280–283, 2003.

[75] GHS-UPC, “Visual-Transin Code 1.1 R65.” Developed in the Department of Geothechnical Engineering and Geosciences (ETCG), UPC, 2003.

[76] O. Tropp, A. Tal, and I. Shimshoni, “A fast triangle to triangle intersection test for collision detection,” *Comput. Animat. Virtual Worlds*, vol. 17, no. 5, pp. 527–535, 2006.

[77] V. Velasco, P. Cabello, E. Vázquez-Suñé, M. López-Blanco, E. Ramos, and I. Tubau, “A sequence stratigraphic based geological model for constraining hydrogeological modeling in the urbanized area of the Quaternary Besòs delta (NW Mediterranean coast, Spain),” *Geol. Acta*, vol. 10, pp. 373–393, 2012.

[78] A. Ashraf and Z. Ahmad, “Integration of Groundwater Flow Modeling and GIS,” in *Water Resources Management and Modeling*, P. Nayak, Ed. InTech,

2012, pp. 239–262.

[79] I. Chenini and A. Ben Mammou, “Groundwater recharge study in arid region: An approach using GIS techniques and numerical modeling,” *Comput. Geosci.*, vol. 36, no. 6, pp. 801–817, Jun. 2010.

[80] N. Kresic and A. Mikszewski, *Hydrogeological Conceptual Site Models: Data Analysis and Visualization*. CRC Press, 2012.

[81] K. E. Kolm, “Conceptualization and characterization of ground-water systems using Geographic Information Systems,” *Elsevier Sci. B.V*, vol. 42, pp. 111–118, 1996.

[82] R. Sengupta, D. Bennett, and G. Wade, “Agent mediated links between GIS and spatial modeling software using a model definition language,” *GIS/LIS ’96 - Annu. Conf. Expo. Proc.*, pp. 295–309, 1996.

[83] D. Sui and R. Maggio, “Integrating GIS with hydrological modelling: Practices, problems and prospects,” *Comput. Environ. Urban Syst.*, vol. 23, no. 1, pp. 33–51, 1999.

[84] B. Huang and B. Jiang, “AVTOP: A full integration of TOPMODEL into GIS,” *Environ. Model. Softw.*, vol. 17, no. 3, pp. 261–268, 2002.

[85] G. Bhatt, M. Kumar, and C. J. Duffy, “A tightly coupled GIS and distributed hydrologic modeling framework,” *Environ. Model. Softw.*, vol. 62, pp. 70–84, 2014.

[86] S. H. Kang, “Tight coupling UFMArcGIS for simulating inundation depth in densely area,” *Nat. Hazards Earth Syst. Sci.*, vol. 10, no. 7, pp. 1523–1530, 2010.

[87] D. W. Watkins, D. C. McKinney, D. R. Maidment, and M.-D. Lin, “Use of Geographic Information Systems in Ground-Water Flow Modeling,” *J. Water Resour. Plan. Manag.*, vol. 122, no. 2, pp. 88–96, Mar. 1996.

[88] L. T. Steyaert and M. F. Goodchild, “Integration Geographic Information Systems and Environmental Simulation Models: A Status Review,” in *Environmental Information Management and Analysis: Ecosystem To Global Scales*, W. K. Michener, J. W. Brunt, and S. G. Stafford, Eds. Francis & Taylor, 1994, pp. 333–355.

[89] R. C. Gogu, G. Carabin, V. Hallet, V. Peters, and A. Dassargues, “GIS-based hydrogeological databases and groundwater modelling,” *Hydrogeol. J.*, vol. 9, no. 6, pp. 555–569, 2001.

[90] P. H. Martin, E. J. LeBoeuf, J. P. Dobbins, E. B. Daniel, and M. D. Abkowitz, “Interfacing GIS with water resource models: A state-of-the-art review,” *J. Am. Water Resour. Assoc.*, vol. 41, no. 6, pp. 1471–1487, 2005.

[91] M. Bakker, “TimML A Multiaquifer Analytic Element Model,” Delft, The Netherlands, 2010.

[92] M. Bakker, “User ’ s Manual for ArcTim ML A GIS based interface for Tim,” no. December. Boise, Idaho, p. 17, 2010.

[93] S. E. Silver, “Getting Out of Squaresville: MODFLOW USG Tools for ArcGIS,” in *ESRI International User Conference 2014 Paper Sessions*, 2014.

[94] O. Kolditz, S. Bauer, L. Bilke, N. Böttcher, J. O. Delfs, T. Fischer, U. J. Görke, T. Kalbacher, G. Kosakowski, C. I. McDermott, C. H. Park, F. Radu, K. Rink, H. Shao, H. B. Shao, F. Sun, Y. Y. Sun, A. K. Singh, J. Taron, M. Walther, W. Wang, N. Watanabe, Y. Wu, M. Xie, W. Xu, and B. Zehner, "OpenGeoSys: an open-source initiative for numerical simulation of thermo-hydro-mechanical/chemical (THM/C) processes in porous media," *Environ. Earth Sci.*, vol. 67, no. 2, pp. 589–599, 2012.

[95] A. Sachse, K. Rink, W. He, and O. Kolditz, *OpenGeoSys-Tutorial: Computational Hydrology I: Groundwater Flow Modeling*. Springer International Publishing, 2015.

[96] I. Borsi, R. Rossetto, and C. Schifani, "The SID&GRID project: developing GIS embedded watershed modeling," in *21st Century Watershed Technology: Improving Water Quality and the Environment Conference Proceedings, May 27-June 1, 2012, Bari, Italy*, 2012.

[97] A. M. . Shapiro, J. Margolin, S. Dolev, and Y. Ben-Israel, "A Graphical-User Interface for the U . S . Geological Survey Modular Three-Dimensional Finite-Difference Ground-Water Flow Model (MODFLOW-96) Using Argus Numerical Environments," Reston, Virginia, 1997.

[98] X. Xue, X. Chen, and H. He, "A visualized numerical modeling system for SUTRA based on ArcGIS Engine," in *Proceedings of Information Technology and Environmental System Sciences 2008*, 2008, vol. 2, pp. 760–765.

[99] A. Khomsi, J. Chao, B. El Mansouri, and M. Sbai, "ArcFem: New Software Module in ArcGIS for Numerical Modeling.," *International Journal on Information Technology (IREIT)*, vol. 2, no. 3. Praise Worthy Prize, pp. 70–79, 01-Jul-2014.

[100] S. Qiu, X. Liang, C. Xiao, H. Huang, Z. Fang, and F. Lv, "Numerical Simulation of Groundwater Flow in a River Valley Basin in Jilin Urban Area, China," *Water*, vol. 7, no. 10, pp. 5768–5787, 2015.

[101] X. Yang, D. R. Steward, W. J. de Lange, S. Y. Lauwo, R. M. Chubb, and E. a. Bernard, "Data model for system conceptualization in groundwater studies," *Int. J. Geogr. Inf. Sci.*, vol. 24, no. 5, pp. 677–694, 2010.

[102] S. Wang, J. Shao, X. Song, Y. Zhang, Z. Huo, and X. Zhou, "Application of MODFLOW and geographic information system to groundwater flow simulation in North China Plain, China," *Environ. Geol.*, vol. 55, no. 7, pp. 1449–1462, Nov. 2007.

[103] T. J. Heinzer, M. D. Williams, E. C. Dogrul, T. N. Kadir, C. F. Brush, and F. I. Chung, "Implementation of a feature-constraint mesh generation algorithm within a GIS," *Comput. Geosci.*, vol. 49, pp. 46–52, 2012.

[104] D. a Field, "Qualitative measures for initial meshes," *Int. J. Numer. Methods Eng.*, vol. 47, pp. 887–906, 2000.

[105] G. Bugeda, "Utilización de técnicas de estimación de error y generación automática de mallas en procesos de optimización estructural," Universidad Politécnica de Cataluña, 1990.

[106] M. E. Zabala, S. Martínez, M. Manzano, and L. Vives, "Groundwater chemical

baseline values to assess the Recovery Plan in the Matanza-Riachuelo River basin, Argentina," *Sci. Total Environ.*, vol. 541, pp. 1516–1530, 2016.

[107] C. Mancino, L. Vives, A. Funes, M. Zárate, and S. Martínez, "Modelación del flujo subterráneo en la cuenca Matanza-Riachuelo , provincia de Buenos Aires. 1. Geología y geometría del subsuelo," in *Temas actuales de la hidrología subterránea 2013*, 2013.

[108] L. Vives, C. Scioli, C. Mancino, and S. Martínez, "Modelación del flujo subterráneo e n la cuenca Matanza - Riachuelo, Provincia de Buenos Aires. 3. Modelo numérico de flujo," in *Temas actuales de la hidrología subterránea 2013*, 2013, pp. 101–108.

[109] J. Heredia, A. Medina Sierra, and J. Carrera, "Estimation of parameter geometry," in *Computational Methods for Flow and Transport in Porous Media*, vol. 17, J. M. Crolet, Ed. Dordrecht: Springer Netherlands, 2000, pp. 53–81.

[110] P.-O. Persson and G. Strang, "A Simple Mesh Generator in MATLAB," *SIAM Rev.*, vol. 46, no. 2, pp. 329–345, 2004.

[111] K. Ho-Le, "Finite element mesh generation methods: a review and classification," *Comput. Des.*, vol. 20, no. 1, pp. 27–38, Jan. 1988.

[112] A. D. Chiasson, S. J. Rees, and J. D. Spitler, "Preliminary assessment of the effects of groundwater flow on closed-loop ground-source heat pump systems," *ASHRAE Trans.*, vol. 106, no. 1, pp. 380–393, 2000.

[113] J. C. Choi, J. Park, and S. R. Lee, "Numerical evaluation of the effects of groundwater flow on borehole heat exchanger arrays," *Renew. Energy*, vol. 52, pp. 230–240, Apr. 2013.

[114] a Angelotti, L. Alberti, I. La Licata, and M. Antelmi, "Borehole Heat Exchangers: heat transfer simulation in the presence of a groundwater flow," *J. Phys. Conf. Ser.*, vol. 501, p. 012033, Apr. 2014.

[115] R. Fan, Y. Jiang, Y. Yao, D. Shiming, and Z. Ma, "A study on the performance of a geothermal heat exchanger under coupled heat conduction and groundwater advection," *Energy*, vol. 32, no. 11, pp. 2199–2209, Nov. 2007.

[116] N. Molina-Giraldo, P. Bayer, and P. Blum, "Evaluating the influence of thermal dispersion on temperature plumes from geothermal systems using analytical solutions," *Int. J. Therm. Sci.*, vol. 50, no. 7, pp. 1223–1231, Jul. 2011.

[117] J. J. Hidalgo, J. Carrera, and M. Dentz, "Steady state heat transport in 3D heterogeneous porous media," *Adv. Water Resour.*, vol. 32, no. 8, pp. 1206–1212, 2009.

[118] C. K. Lee and H. N. Lam, "A modified multi-ground-layer model for borehole ground heat exchangers with an inhomogeneous groundwater flow," *Energy*, vol. 47, no. 1, pp. 378–387, Nov. 2012.

[119] S. C. P. Pearson, S. a. Alcaraz, and J. Barber, "Numerical simulations to assess thermal potential at Tauranga low-temperature geothermal system, New Zealand," *Hydrogeol. J.*, vol. 22, no. 1, pp. 163–174, Dec. 2013.

[120] T. Y. Ozudogru, C. G. Olgun, and a. Senol, "3D numerical modeling of vertical

geothermal heat exchangers," *Geothermics*, vol. 51, pp. 312–324, Jul. 2014.

[121] H. Fujii, T. Inatomi, R. Itoi, and Y. Uchida, "Development of suitability maps for ground-coupled heat pump systems using groundwater and heat transport models," *Geothermics*, vol. 36, no. 5, pp. 459–472, Oct. 2007.

[122] S. L. Abdelaziz, T. Y. Ozudogru, C. G. Olgun, and J. R. Martin, "Multilayer finite line source model for vertical heat exchangers," *Geothermics*, vol. 51, pp. 406–416, Jul. 2014.

[123] J. Domínguez and J. Amador, "Geographical information systems applied in the field of renewable energy sources," *Comput. Ind. Eng.*, vol. 52, pp. 322–326, 2007.

[124] D. Voivontas, D. Assimacopoulos, a. Mourelatos, and J. Corominas, "Evaluation of renewable energy potential using a GIS decision support system," *Renew. Energy*, vol. 13, pp. 333–344, 1998.

[125] P. Blum, G. Campillo, and T. Kölbel, "Techno-economic and spatial analysis of vertical ground source heat pump systems in Germany," *Energy*, vol. 36, no. 5, pp. 3002–3011, May 2011.

[126] Y. Hamada, K. Marutani, M. Nakamura, S. Nagasaka, K. Ochifuji, S. Fuchigami, and S. Yokoyama, "Study on underground thermal characteristics by using digital national land information, and its application for energy utilization," *Appl. Energy*, vol. 72, no. 3–4, pp. 659–675, Jul. 2002.

[127] J. Ondreka, M. I. Rüsgen, I. Stober, and K. Czurda, "GIS-supported mapping of shallow geothermal potential of representative areas in south-western Germany—Possibilities and limitations," *Renew. Energy*, vol. 32, no. 13, pp. 2186–2200, Oct. 2007.

[128] A. Galgaro, E. Di Sipio, G. Teza, E. Destro, M. De Carli, S. Chiesa, A. Zarrella, G. Emmi, and A. Manzella, "Empirical modeling of maps of geo-exchange potential for shallow geothermal energy at regional scale," *Geothermics*, vol. 57, pp. 173–184, 2015.

[129] A. García-Gil, E. Vázquez-Suñe, M. M. Alcaraz, A. S. Juan, J. Á. Sánchez-Navarro, M. Montlleó, G. Rodríguez, and J. Lao, "GIS-supported mapping of low-temperature geothermal potential taking groundwater flow into account," *Renew. Energy*, vol. 77, pp. 268–278, May 2015.

[130] T. V. Ramachandra and B. V. Shruthi, "Spatial mapping of renewable energy potential," *Renew. Sustain. Energy Rev.*, vol. 11, pp. 1460–1480, 2007.

[131] H. Yang, P. Cui, and Z. Fang, "Vertical-borehole ground-coupled heat pumps: A review of models and systems," *Appl. Energy*, vol. 87, no. 1, pp. 16–27, Jan. 2010.

[132] S. J. Self, B. V. Reddy, and M. a. Rosen, "Geothermal heat pump systems: Status review and comparison with other heating options," *Appl. Energy*, vol. 101, pp. 341–348, Jan. 2013.

[133] F. Stauffer, P. Bayer, P. Blum, N. Molina Giraldo, and W. Kinzelbach, *Thermal Use of Shallow Groundwater*. CRC Press. Taylor & Francis Group, 2013.

[134] J. Bear, *Dynamics of Fluids in Porous Media*. Dover Mineola New York, 1972.

[135] M. Sutton, D. Nutter, and R. Couvillion, “A ground resistance for vertical bore heat exchangers with groundwater flow,” *J. Energy Resour. Technol.*, vol. 125 (3), pp. 183–189, 2003.

[136] N. Diao, Q. Li, and Z. Fang, “Heat transfer in ground heat exchangers with groundwater advection,” *Int. J. Therm. Sci.*, vol. 43, no. 12, pp. 1203–1211, Dec. 2004.

[137] T. Metzger, S. Didierjean, and D. Maillet, “Optimal experimental estimation of thermal dispersion coefficients in porous media,” *Int. J. Heat Mass Transf.*, vol. 47, pp. 3341–3353, 2004.

[138] C. Tomlin, *Geographic Information Systems and Cartographic Modeling*. Prentice Hall College Div, 1990.

[139] C. Clauser and E. Huenges, *Thermal conductivity of rocks and minerals*. American Geophysical Union, 2013.

[140] J. Schön, *Physical Properties of Rocks: A Workbook*. Amsterdam: Elsevier B.V., 2011.

[141] S. Haehnlein, P. Bayer, and P. Blum, “International legal status of the use of shallow geothermal energy,” *Renew. Sustain. Energy Rev.*, vol. 14, no. 9, pp. 2611–2625, Dec. 2010.

[142] E. Vázquez-Suñé, R. Criollo, and A. Serrano-Juan, “Evaluación de las posibilidades de aprovechamiento de la anomalía geotérmica detectada en el sector de Fondo de Santa Coloma de Gramanet,” Barcelona, Spain, 2015.

[143] J. Font-Capó, E. Vázquez-Suñé, J. Carrera, D. Martí, R. Carbonell, and A. Pérez-Estaun, “Groundwater inflow prediction in urban tunneling with a tunnel boring machine (TBM),” *Eng. Geol.*, vol. 121, pp. 46–54, 2011.

[144] D. Martí, R. Carbonell, I. Flecha, I. Palomeras, J. Font-Capó, E. Vázquez-Suñé, and a. Pérez-Estaún, “High-resolution seismic characterization in an urban area: Subway tunnel construction in Barcelona, Spain,” *Geophysics*, vol. 73, no. 2, p. B41, 2008.

[145] L. W. Gelhar, C. Welty, and K. R. Rehfeldt, “A critical review of data on field-scale dispersion in aquifers,” *Water Resour. Res.*, vol. 28, no. 7, pp. 1955–1974, 1992.

[146] K. Menberg, P. Bayer, K. Zosseder, S. Rumohr, and P. Blum, “Subsurface urban heat islands in German cities.,” *Sci. Total Environ.*, vol. 442, pp. 123–33, Jan. 2013.

[147] C. Urich, R. Sitzenfrei, M. Möderl, and W. Rauch, “Einfluss der Siedlungsstruktur auf das thermische Nutzungspotential von oberflächennahen Aquiferen,” *Osterr. Wasser- und Abfallwirtschaft*, vol. 62, pp. 113–119, 2010.

[148] E. Koutroulis and K. Kalaitzakis, “Development of an integrated data-acquisition system for renewable energy sources systems monitoring,” *Renew. Energy*, vol. 28, pp. 139–152, 2003.

[149] F. Jaudin, “Overview of shallow geothermal legislation in Europe,” 2013.

[150] M. Bloemendal, T. Olsthoorn, and F. Boons, “How to achieve optimal and sustainable use of the subsurface for Aquifer Thermal Energy Storage,” *Energy Policy*, vol. 66, pp. 104–114, 2014.

[151] A. Herbert, S. Arthur, and G. Chillingworth, “Thermal modelling of large scale exploitation of ground source energy in urban aquifers as a resource management tool,” *Appl. Energy*, vol. 109, pp. 94–103, 2013.

[152] V. I. Danilov-Danilyan, a. P. Demin, V. G. Pryazhinskaya, and I. V. Pokidysheva, “Markets of water and water management services in the world and the Russian Federation: Part I,” *Water Resour.*, vol. 42, no. 2, pp. 260–268, 2015.

[153] V. I. Danilov-Danilyan, a. P. Demin, V. G. Pryazhinskaya, and I. V. Pokidysheva, “Markets of water and water management services in the world and the Russian Federation: Part II,” *Water Resour.*, vol. 42, no. 2, pp. 260–268, 2015.

[154] F.-P. Chiu, H.-I. Kuo, C.-C. Chen, and C.-S. Hsu, “The energy price equivalence of carbon taxes and emissions trading—Theory and evidence,” *Appl. Energy*, vol. 160, pp. 164–171, 2015.

[155] R. Q. Grafton, G. Libecap, S. McGlennon, C. Landry, and B. O’Brien, “An integrated assessment of water markets: A cross-country comparison,” *Rev. Environ. Econ. Policy*, vol. 5, no. 2, pp. 219–239, 2011.

[156] Y. P. Chen, “Land use rights, market transitions, and labour policy change in China (1980-84),” *Econ. Transit.*, vol. 20, no. 4, pp. 705–743, Oct. 2012.

[157] J. Crossland, B. Li, and E. Roca, “Is the European Union Emissions Trading Scheme (EU ETS) informationally efficient? Evidence from momentum-based trading strategies,” *Appl. Energy*, vol. 109, pp. 10–23, 2013.

[158] R. Q. Grafton and J. Horne, “Water markets in the Murray-Darling Basin,” *Agric. Water Manag.*, vol. 145, pp. 61–71, 2014.

[159] J. M. Carey and D. L. Sunding, “Emerging Markets in Water. A Comparative Institutional Analysis of the Central Valley and Colorado-Big Thompson Projects,” *Nat. Resorces J.*, vol. 41, no. 2, pp. 284–327, 2001.

[160] N. Hernández-mora and L. Del Moral, “Geoforum Developing markets for water reallocation : Revisiting the experience of Spanish water mercantilización,” vol. 62, pp. 143–155, 2015.

[161] N. H. Koroso, P. van der Molen, A. M. Tuladhar, and J. a. Zevenbergen, “Does the Chinese market for urban land use rights meet good governance principles?,” *Land use policy*, vol. 30, no. 1, pp. 417–426, 2013.

[162] E. Custodio, “Comentarios sobre el comercio y mercados del agua subterránea en Canarias,” in *El conocimiento de los Recursos Hídricos en Canarias: Cuatro Décadas después del Proyecto SPA–15*, M. C. Cabrera, J. Jiménez, and E. Custodio, Eds. Las Palmas de Gran Canaria: Asociación Internacional de Hidrogeólogos–Grupo Español, 2011.

[163] J. D. Connor, B. Franklin, A. Loch, M. Kirby, and S. A. Wheeler, “Trading water to improve environmental flow outcomes,” *Water Resour. Res.*, vol. 49, no. 7, pp. 4265–4276, 2013.

[164] K. Schiel, O. Baume, G. Caruso, and U. Leopold, “GIS-based modelling of

shallow geothermal energy potential for CO2 emission mitigation in urban areas," *Renew. Energy*, vol. 86, pp. 1023–1036, 2016.

[165] *Directive 2010/31/EU of the European Parliament and of the Council of 19 May 2010 on the energy performance of buildings*. 2010, pp. 13–35.

[166] H. S. Carslay and J. C. Jaeger, *CONDUCTION OF HEAT IN SOLIDS*, Second edi., vol. XXXIII, no. 2. Oxford University Press 1959, 1959.

APPENDIX A. HYDROGEOLOGICAL PROJECTS

SCIENTIFIC PROJECTS

Febrero-Septiembre 2013	**"Estudios de mezcla de aguas y evolución de química durante la operación de los pozos."** Entidad Financiadora: SQM Salar, S.A. Investigador Principal: Enric Vázquez-Suñé
Enero-Junio 2013	**"Estudi complementari de les afeccions hidrogeològiques degudes a l'explotació de les aigües subterrànies per a usos energètics a l'àmbit de la Universitat Pompeu Fabra (Jaume I i Roger de Llúria)."** Entidad Financiadora: Universitat Pompeu Fabra Investigador Principal: Enric Vázquez-Suñé
Junio 2012-Junio 2013	**"Evaluación de aspectos hidrogeológicos y geoquímicos en Santiago de Chile."** Entidad Financiadora: MATRAZ Consultores Investigador Principal: Daniel Fernández
Junio-Julio 2012	**"Actualització del model hidrogeològic de les aigües subterrànies al Pla Tècnic d'aprofitament de recursos hídrics alternatius."** Entidad Financiadora: Ajuntament de Barcelona Investigador Principal: Enric Vázquez
Enero 2012-Enero 2013	**"Estudios hidroquímicos e hidrogeológicos en la explotación de Cobre de las Cruces."** Entidad Financiadora: Fundación Migres Investigador Principal: Carlos Ayora / Enric Vázquez
Enero 2011-Enero 2015	**"Proyecto de Aguas Subterráneas en la Cuenca Matanza Riachuelo". Entidad Financiadora: Autoridad de Cuenca Matanza Riachuelo a través de un Convenio con la Comisión de Investigaciones Científicas de la Provincia de Buenos Aires.** Investigador Principal: Luis S. Vives Vergara

Enero 2011-Diciembre 2013	**“Mejora del proceso de construcción de túneles incorporando información geológica e hidrogeológica en tiempo real.”** Entidad Financiadora: MICINN Investigador Principal: Enric Vázquez
Diciembre 2010	**“Estudi del comportament hidrológic de l’aqüífer del Besós en l’entorn del Campus de la Ciutadella per la Universitat Pompeu Fabra.”** Entidad Financiadora: Universitat Pompeu Fabra Investigador Principal: Enric Vázquez Suñé
Enero 2007 - Enero 2009	**“HEROS”** Entidad Financiadora: MCYT Investigador Principal: Enric Vázquez, Radu Gogu
Mayo 2007 - Junio 2009	**"Eïnas d'interpretació de dades hidroquímiques"** Entidad Financiadora: ACA (Agència Catalana de l'Aigua) Investigador principal: Xavier Sànchez Vila
Octubre 2007 - Octubre 2010	**“Herramientas de modelación hidrogeológicas 3D en medios sedimentarios.”** Entidad Financiadora: CGL2007-66748 Investigador Principal: Radu Gogu
Noviembre 2007-Abril 2009	**"Realització del desenvolupament d’eines de interpretació de dades hidroquímiques"** Entidad Financiadora: ACA (Agència Catalana de l'Aigua) Investigador principal: Xavier Sànchez Vila

TECHNICAL PROYECTS

Sept-Dic 2014	**"Estudio geológico integral de la unidad minera Iscaycruz".** Entidad Financionadora: Hydro-geo Consultores Investigador Principal: Enric Vázquez-Suñé
Abril-Mayo 2014	**"Modelación Hidrogeológica Numérica para el Proyecto de Recrecimiento de la Relavera Chinchán, Perú."** Entidad Financiadora: Hydro-Geo Consultores Invertigador Principal: Enric Vázquez-Suñé
Diciembre 2013 - Enero 2014	**"Modelación Hidrogeológica Numérica para el Proyecto Minero de Santa Este, Perú"** Entidad Financiadora: Hydro-Geo Consultores Invertigador Principal: Enric Vázquez-Suñé
Enero-Febrero 2012	**"Modelación de los Impactos Hidrogeológicos del Metro de Quito (Ecuador)"** Entidad Financiadora: EVREN Evaluación de Recursos Naturales, S.A. Investigador Principal: Enric Vázquez Suñé

APPENDIX B. SUPERFICIAL GEOLOGY AT CALAMA STUDY SITE (CHILE)

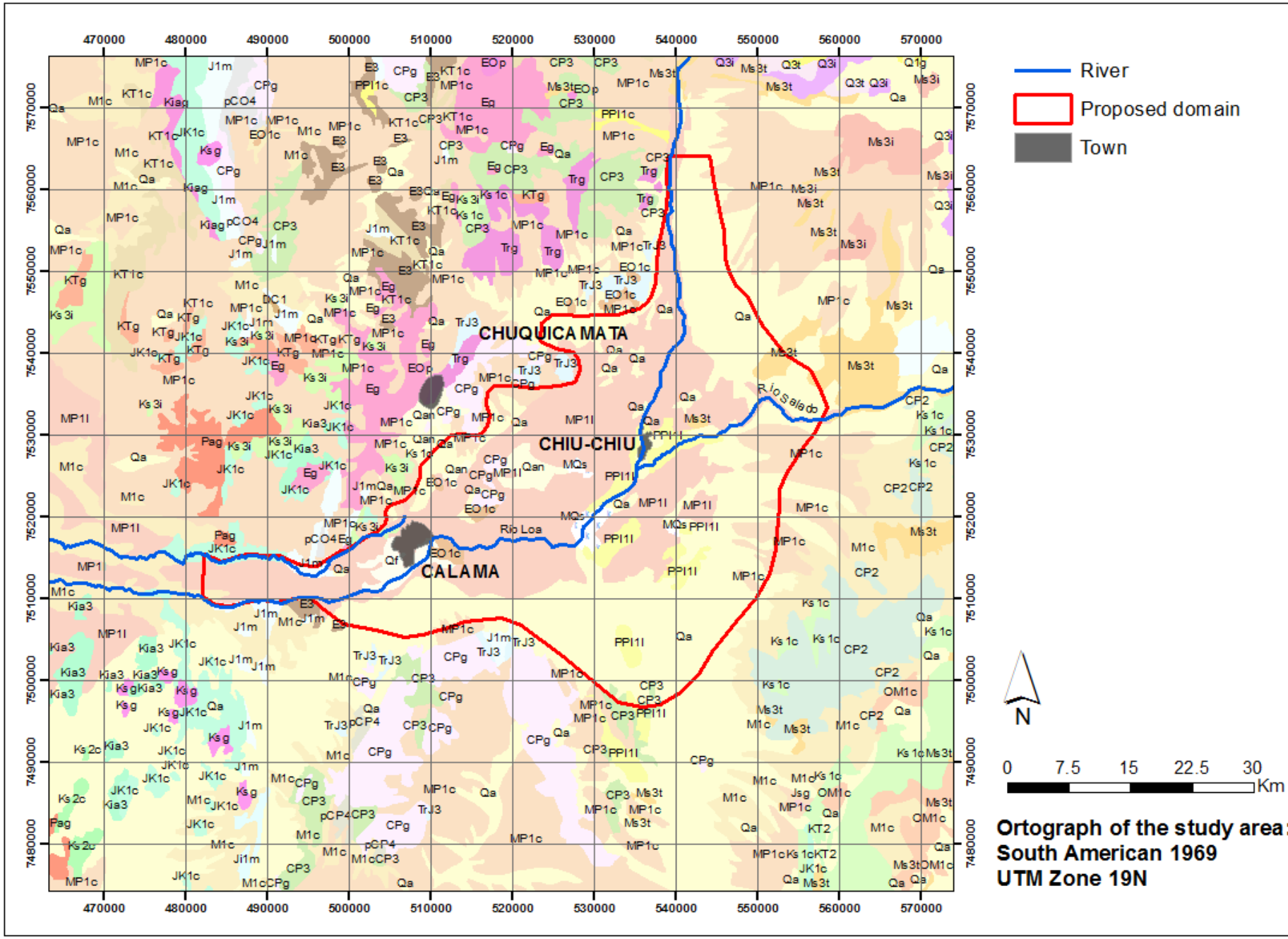
River
Proposed domain
Town
CHUQUICAMATA
CHIU-CHIU
CALAMA
Rio Salado
Rio Loa
N
0 7.5 15 22.5 30
Km
Ortograph of the study area:
South American 1969
UTM Zone 19N

SECUENCIAS SEDIMENTARIAS

Qan / Holoceno: Depósitos de origen antrópico: tranques de relave y depósitos de material estéril de la gran minería de cobre; rellenos sanitarios.

Qf / Pleistoceno-Holoceno: Depósitos fluviales: gravas, arenas y limos del curso actual de los ríos mayores o de sus terrazas subactuales y llanuras de inundación.

Qa / Pleistoceno-Holoceno: Depósitos aluviales, subordinadamente coluviales o lacustres: gravas, arenas y limos. En la Depresión Central, regiones I a III: abanicos aluviales.

Q1g / Pleistoceno-Holoceno: Depósitos morrénicos, fluvioglaciales y glacilacustres: diamictos de bloques y matriz de limo/arcilla, gravas, arenas y limos. En la Depresión Central, regiones IX, X, XI y XII: lóbulos morrénicos en el frente de los lagos proglaciales, abanicos fluvioglaciales frontales o varves en la ribera de lagos o cursos fluviales, asociados a las principales glaciaciones del Pleistoceno donde son indiferenciados o relativos a las glaciaciones Llanquihue.

Qe / Pleistoceno-Holoceno: Depósitos eólicos: arenas finas a medias con intercalaciones bioclásticas en dunas y barjanes tanto activos como inactivos.

PPl1c / Plioceno-Pleistoceno: Conglomerados, areniscas, limolitas y arcillolitas, generalmente consolidados, de facies principalmente aluviales, subordinadamente lacustres y eólicas.

PPl1l / Plioceno-Pleistoceno Secuencias sedimentarias lacustres: limos y arcillas con intercalaciones de niveles calcáreos, conglomerádicos o piroclásticos. En la Cordillera Principal, regiones I y II: formaciones Lauca, Chiuchiu y El Tambo.

SECUENCIAS VOLCANOSEDIMENTARIAS

SECUENCIAS VOLCANICAS

Q3i / Cuaternario Estratovolcanes y complejos volcánicos: lavas basáticas a riolíticas, domos y depósitos piroclásticos andesítico-basálticos a dacíticos; principalmente calcoalcalinos; adakíticos al sur de los 47ºS. En la Cordillera Principal, regiones I a III: volcanes Taapaca, Parinacota, Láscar y Ojos del Salado. Principalmente holocenos en la Cordillera Principal, regiones Metropolitana a X: volcanes San José, Peteroa, Antuco, Llaima, Villarrica, Osorno y Calbuco, entre otros; en la Cordillera Patagónica, regiones XI a XII: volcanes Hudson, Lautaro y Monte Burney. En Antártica: isla Decepción.

Q3t / Cuaternario Depósitos de flujo piroclástico, localmente soldados. En la Cordillera Principal, regiones I a III: ignimbritas Tuyajto, Cajón, Chato Aislado.

Q3av / Cuaternario Depósitos de avalancha volcánica, asociados a colap- so parcial de edificios volcánicos. En la Cordillera Principal, regiones I a VI: avalanchas de Parinacota, Ollagüe, Socompa, Colón-Coya y Teno.

ROCAS INTRUSIVAS

SECUENCIAS SEDIMENTARIAS

MQs / Mioceno-Cuaternario
Depósitos evaporíticos: sulfatos, cloruros, carbonatos y niveles detríticos finos, localmente con bórax y/o litio. En los salares, regiones I a III: salares de Surire, Huasco, Coposa, Pintados, Bellavista, Grande, Atacama, Pedernales y Maricunga.

MP1c / Mioceno Superior-Plioceno
Secuencias sedimentarias clásticas de piedemonte, aluviales, coluviales o fluviales: conglomerados, areniscas y limolitas. En las regiones I a IV: formaciones Huaylas, Lauca y Pastos Chicos, Gravas del Copiapó; en la región XI: Formación Galeras.

MP1l / Mioceno Superior-Plioceno
Secuencias sedimentarias lacustres, en parte fluviales y aluviales: limos, arenas, conglomerados, calizas y cenizas volcánicas. En las regiones I y II: formaciones El Loa, Quillagua y Vilama.

M1c / Mioceno Inferior-Medio
Secuencias sedimentarias de abanicos aluviales, pedimento o fluviales: gravas, arenas y limos con ignimbritas intercaladas. En las regiones I a III: formaciones Diablo, Chucal, Altos de Pica (superior) y Gravas de Atacama; en las regiones VIII a IX: Formación Cura-Mallín (superior); en la región XI: Formación Las Dunas.

OM1c / Oligoceno-Mioceno
Secuencias sedimentarias continentales parálicas o aluviales: conglomerados, areniscas, lutitas, calizas y mantos de carbón. En la Cordillera Principal y Precordillera, regiones I y II: formaciones Altos de Pica (inferior) y San Pedro; en la Cordillera de la Costa, región X: Estratos de Pupunahue y Parga, Frm. Cheuquemó; en la región XII: Formación Loreto.

SECUENCIAS VOLCANOSEDIMENTARIAS

SECUENCIAS VOLCANICAS

P3t / Plioceno
Depósitos piroclásticos dacíticos a riolíticos parcial- mente soldados. Principalmente en la Cordillera Principal, regiones I a III: ignimbritas Lauca, Puripicar, Atana, Tucúcaro, Patao y Laguna Verde.

P3i / Plioceno
Centros volcánicos: lavas, domos y depósitos piroclásticos andesíticos a dacíticos, conos de piroclastos y lavas basálticas a andesítico-basálticas. En la Cordillera Principal, regiones I a III: volcanes Larancagua, Miño, Peñas Blancas y Laguna Escondida; en la región XI: centros volcánicos de la península de Taitao

Ms3t / Mioceno Superior
Ignimbritas dacíticas a riolíticas y depósitos piroclásticos asociados a estratovolcanes. En la Cordillera Principal, regiones I a IV: ignimbritas Ujina, Sifón, San Andrés, Grande y Formación Vallecito.

Ms3i / Mioceno Superior
Centros y secuencias volcánicas: lavas, domos y depósitos piroclásticos, andesíticos a dacíticos, con intercalaciones aluviales, asociados a depósitos epitermales de Au-Ag. En la Cordillera Principal, regiones I a IV: volcanes Choquelimpie, Copiapó, Wheelwright y Formación Vacas Heladas.

ROCAS INTRUSIVAS

SECUENCIAS SEDIMENTARIAS

EO1c / Eoceno-Oligoceno
Secuencias sedimentarias continentales aluviales y fluviales: conglomerados, areniscas y limolitas con intercalaciones menores de yeso, tobas y lavas. En las regiones I a II: formaciones Azapa, Sichal, y Calama.

KT1c / Cretácico Superior-Terciario Inferior
Secuencias sedimentarias continentales aluviales y fluviales: conglomerados, areniscas y limolitas rojizas. En la Precordillera de la región II: formaciones Tolar y Tambillo, estratos de Quepe y Barros Arana.

Ks1c / Cretácico Superior
Secuencias sedimentarias continentales aluviales y lacustres: conglomerados, brechas, areniscas y limolitas rojas con intercalación de tobas riolíticas y lavas andesíticas. En la Precordillera, regiones I a III: formaciones Guaviña, Cerro Empexa (inferior) y Purilactis (inferior); Estratos del Leoncito

SECUENCIAS VOLCANOSEDIMENTARIAS

E2c / Eoceno
Secuencias volcanosedimentarias: brechas sedimentarias y volcánicas, areniscas e intercalaciones de tobas. En la Precordillera, regiones II a IV: Estratos de Loma Amarilla, formaciones Pircas y Astaburuaga, Gravas del Torín.

KT2 / Cretácico Superior-Terciario Inferior
Secuencias volcanosedimentarias: areniscas, paraconglomerados, lavas andesíticas y dacíticas, intercalaciones de ignimbritas, limolitas y calizas. En la Precordillera, regiones II y III: Estratos Cerro Totola y Formación Venado.

Ks2c / Cretácico Superior
Secuencias volcanosedimentarias continentales: rocas epiclásticas y piroclásticas riolíticas, lavas andesíticas y traquíticas. En la Precordillera, región I a III: formaciones Quebrada Mala, Llanta, Hornitos; en las regiones IV a Metropolitana: formaciones Quebrada Seca, Viñita (oriental), Los Elquinos y Lo Valle

SECUENCIAS VOLCANICAS

E3 / Eoceno
Secuencias y centros volcánicos continentales: lavas y brechas basálticas a andesíticas con intercalaciones de rocas piroclásticas y domos riolíticos. En la Precordillera, regiones I y II: Formación Icanche y Estratos del Cerro Casado; en la Cordillera Patagónica, región XI: domos de Lago Chacabuco y alto Río Cisnes.

PE3a / Paleoceno-Eoceno Inferior
Secuencias y complejos volcánicos continentales ácidos: domos y rocas piroclásticas dacíticas a riolíticas asociados a calderas de colapso. En la Precordillera, región III: calderas El Salvador, San Pedro de Cachiyuyo y Lomas Bayas.

Ks3i /Cretácico Superior
Secuencias volcánicas continentales: lavas, domos y brechas basálticos a dacíticos con intercalaciones piroclásticas y epiclásticas. En la Precordillera, regiones I a IV: Formación Cerro Empexa (superior), Estratos del Estanque, Cerro Los Carneros; en la Cordillera Patagónica, región XI: Grupo Ñireguao.

Kia3 / Cretácico Inferior alto
Secuencias y complejos volcánicos continentales: lavas y brechas basáticas a andesíticas, rocas piroclásticas andesíticas a riolíticas, escasas intercalaciones sedimentarias. En las regiones I y II: formaciones Suca, Punta Barranco y Estratos de Quebrada San Cristóbal.

ROCAS INTRUSIVAS

EOp / Eoceno-Oligoceno (42-31 Ma):
Pórfidos granodioríticos, monzoníticos, dioríticos, dacíticos y riolíticos de biotita y hornblenda, portadores de mineralización de tipo 'Pórfido cuprífero gigante'. En la Precordillera, regiones I a III: Collahuasi, El Abra, Chuquicamata, La Escondida.

Eg / Eoceno (52-33 Ma): Granodioritas, tonalitas y dioritas cuarcíferas de hornblenda y biotita, dioritas y monzodioritas de piroxeno y biotita; pórfidos dacíticos y riolíticos

Pag / Paleoceno (65-53 Ma): Monzodioritas de piroxeno y biotita, granodioritas y granitos de hornblenda y biotita; pórfidos dacíticos y riolíticos, asociados a mineralización tipo pórfido cuprífero y chimeneas de brechas.

KTg / Cretácico Superior-Terciario Inferior:
Granodioritas, dioritas y pórfidos graníticos. Entre las cordilleras de la Costa y Principal, regiones I a IV; en la Cordillera Patagónica, regiones XI y XII: granitoides y pórfidos de Puerto Ibañez e islas Evans.

Ksg / Cretácico Superior (90-65 Ma)
Monzodioritas, granodioritas, gabros y dioritas de piroxeno, biotita y hornblenda; pórfidos andesíticos y dioríticos. En la Precordillera, regiones I a III y entre las cordilleras de la Costa y Principal, reg. IV, V y Metropolitana; en la región XII: granitoides de las islas Wollaston y Navarino, Cordillera Darwin.

Kiag / Cretácico Inferior alto-Cretácico Superior bajo (123-85 Ma)
Dioritas y monzodioritas de piroxeno y hornblenda, granodioritas, monzogranitos de hornblenda y biotita.

SECUENCIAS SEDIMENTARIAS

JK1c / Jurásico Superior-Cretácico Inferior
Secuencias sedimentarias continentales aluviales, fluviales y eólicas, en parte transicionales: areniscas, limolitas, lutitas y conglomerados rojos. En la Precordillera, regiones I a III: formaciones Chacarilla, Quinchamale y Quehuita (superior), Cerritos Bayos, Llanura Colorada y Quebrada Monardes; en la Cordillera de la Costa, regiones I a II: formaciones Atajaña y Caleta Coloso.

J1m / Jurásico-Neocomiano
Secuencias sedimentarias marinas carbonatadas y clásticas: calizas, lutitas, areniscas calcáreas, para-conglomerados, niveles de yeso e intercalaciones volcánicas subordinadas. En la Precordillera, regiones I a III: formaciones Livilcar, Sierra del Cobre, Quehuita (inferior), Quinchamale (inferior) y El Profeta (superior).

Ji1m / Jurásico Inferior-Medio
Secuencias sedimentarias marinas litorales o de plataforma: calizas, areniscas calcáreas, lutitas, conglomerados y areniscas con intercalaciones volcanoclásticas y lávicas; basaltos almohadillados.

DC1 / Devónico-Carbonífero
Secuencias sedimentarias marinas, en parte transicionales: areniscas cuarzo-feldespáticas, lutitas micáceas, conglomerados. En la Precordillera, regiones II a III: formaciones Lila y Chinches; en la Cordillera Principal, regiones II y IV: formaciones Zorritas y Hurtado.

SECUENCIAS VOLCANOSEDIMENTARIAS

CP2 / Carbonífero-Pérmico
Secuencias sedimentarias y volcánicas continentales: rocas epiclásticas con intercalaciones de lavas andesíticas y tobas riolíticas. En Precordillera, región II: formaciones Tuina y Peine; en la Cordillera Principal, región IV: Formación Matahuaico.

SECUENCIAS VOLCANICAS

J3i / Jurásico
Secuencias volcánicas continentales y marinas: lavas y aglomerados basálticos a andesíticos, tobas riolíticas, con intercalaciones de areniscas, calizas marinas y conglomerados continentales. En la Cordillera de la Costa, regiones I a III: formaciones Camaraca y La Negra; en la Cordillera Principal, región VIII: Formación Nacientes del Biobío (Miembro Icalma).

TrJ3 / Triásico-Jurásico Inferior
Secuencias volcánicas continentales y transicionales: lavas, domos, brechas, basálticos a riolíticos con intercalaciones de areniscas y conglomerados. En la Precordillera, regiones II y III: Estratos Las Lomas y Formación La Ternera; en la Cordillera Principal, región IV: Estratos de los Tilos; en la Cordillera de la Costa, región IV: Formación Pichidangui.

CP3 / Carbonífero-Pérmico
Secuencias volcánicas continentales: lavas, domos, tobas y brechas andesíticas a riolíticas con intercalaciones de areniscas, conglomerados y calizas. Incluye cuerpos hipabisales riolíticos. En la Precordillera y Cordillera Principal, regiones I a IV: formaciones Quipisca, Collahuasi, Cas y La Tabla.

ROCAS INTRUSIVAS

JKg / Jurásico-Cretácico (150-100 Ma)
Granodioritas, dioritas, monzodioritas y granitos; pórfidos dacíticos y andesíticos. En la Cordillera de la Costa, regiones I y II: batolitos Punta Negra y Huara-Pozo Almonte.

Jsg / Jurásico Medio-Superior (180-142 Ma)
Monzodioritas cuarcíferas, dioritas y granodioritas de biotita, piroxeno y hornblenda. En la Cordillera de la Costa, regiones I a VI; en la Cordillera Principal, regiiones X y XI: Plutón Panguipulli y borde oriental del Batolito Norpatagónico; en la península Antártica.

Trg / Triásico (240-205 Ma)
Granitos leucocráticos, monzo y sienogranitos de biotita y muscovita, granodioritas y dioritas de biotita y hornblenda, pórfidos hipabisales. En la Cordillera de la Costa y Precordillera, regiones II y III: cerros de Paqui, granodioritas Este y Elena, Plutón Cerros del Vetado; en la Cordillera Principal, región IV.

CPg / Carbonífero-Pérmico (328-235 Ma)
Granitos, granodioritas, tonalitas y dioritas, de (a) hornblenda y biotita, localmente de muscovita. En la Precordillera y Cordillera Principal, regiones I a IV: Batolitos compuestos, 'stocks' y cuerpos hipabisales (b) (Sierra Moreno, Cordillera de Domeyko, Batolito Elqui-Limarí); en la Cordillera Principal, regiones X y XI: Batolito Panguipulli-Riñihue y 'Stock' Leones

ROCAS METAMÓFICAS

pCP4 / Precámbrico-Pérmico

Esquistos micáceos, metabasitas, anfibolitas, ortoneises y, en menor proporción, cuarcitas y mármoles con protolitos de probable edad desde Precámbrico a Paleozoico temprano y metamorfismo del Carbonífero al Pérmico. En la Precordillera, regiones II y III: complejos metamórficos Limón Verde y El Tránsito, Neises de la Pampa.

pCO4 / Precámbrico-Ordovícico

Esquistos micáceos, neises, migmatitas y, en menor proporción, anfibolitas, ortoneises, cuarcitas y filitas con protolitos de edades desde el Precámbrico a Paleozoico temprano y de metamorfismo del Cámbrico-Ordovícico. En la Precordillera y Cordillera de la Costa, regiones I y II: Esquistos de Belén, Formación Choja, metamorfitas de sierra Moreno y Mejillones.

.

APPENDIX C. GEOLOGICAL CROSS SECTIONS FOR CALAMA STUDY SITE (CHILE)

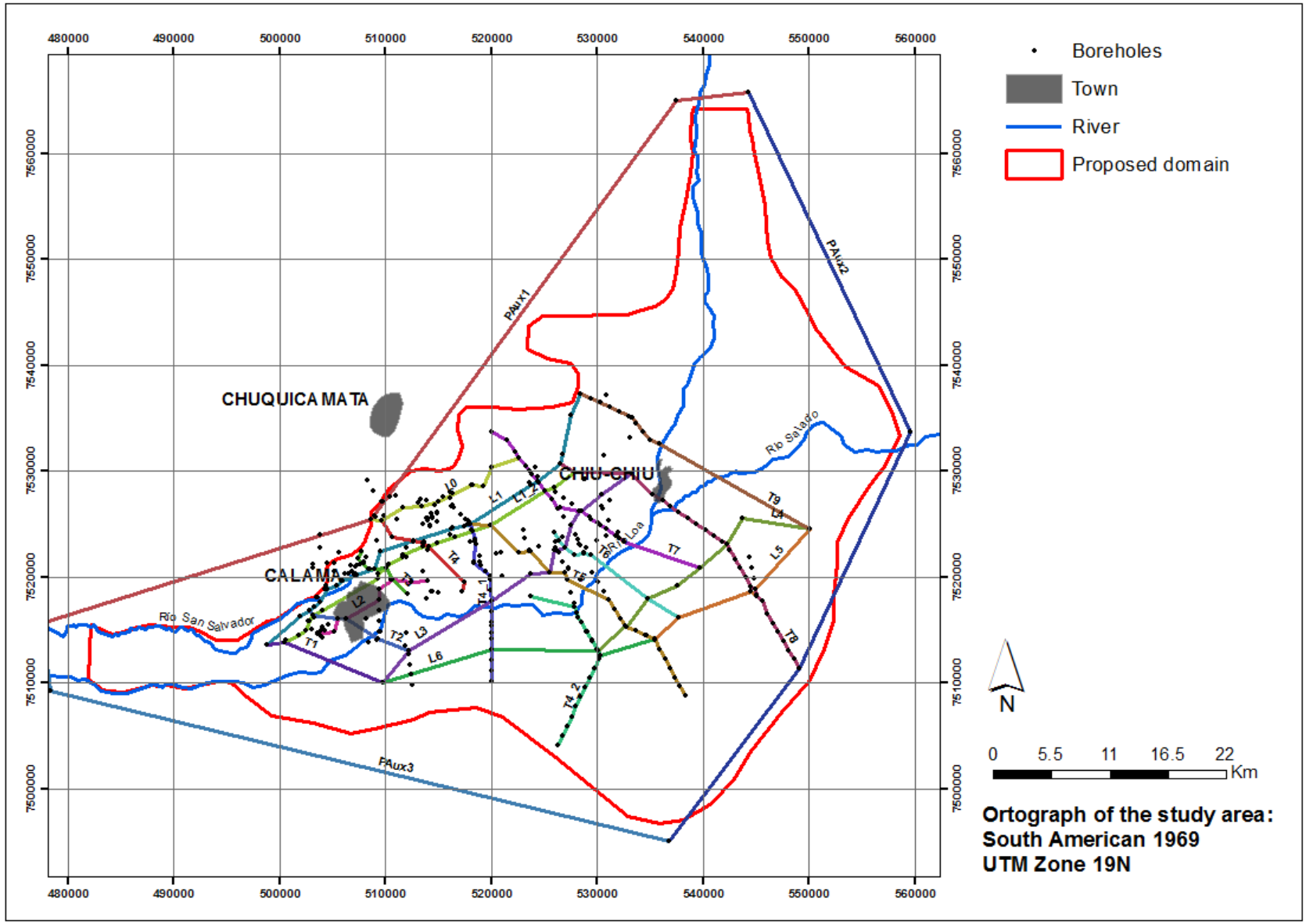
480000
490000
500000
510000
520000
530000
540000
550000
560000
7560000
7550000
7540000
7530000
7520000
7510000
7500000
CHUQUICA MATA
CHIU-CHIU
CALAMA
Río San Salvador
Río Salado
Río Loa
PAux1
PAux2
PAux3
L0
L1
L1.1
L2
L3
L4
L5
L6
T1
T2
T3
T4
T4.1
T4.2
T5
T5R
T6
T7
T8
T9
Boreholes
Town
River
Proposed domain
N
0
5.5
11
16.5
22
Km
Ortograph of the study area:
South American 1969
UTM Zone 19N

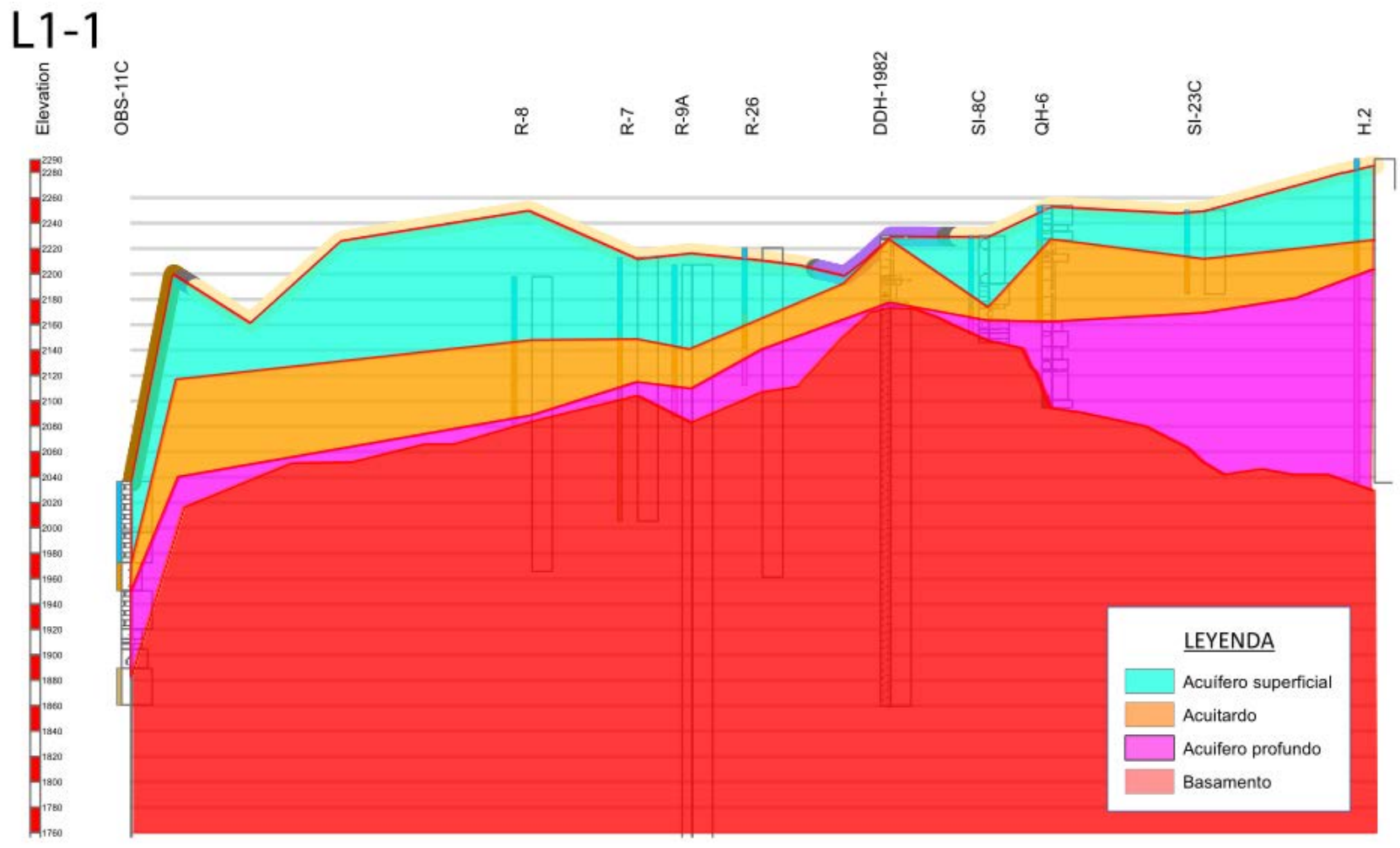
L1-1
Elevation
OBS-11C
R-8
R-7
R-9A
R-26
DDH-1982
SI-8C
QH-6
SI-23C
H.2
2290
2280
2260
2240
2220
2200
2180
2160
2140
2120
2100
2080
2060
2040
2020
2000
1980
1960
1940
1920
1900
1880
1860
1840
1820
1800
1780
1760
LEYENDA
Acuífero superficial
Acuitardo
Acuífero profundo
Basamento

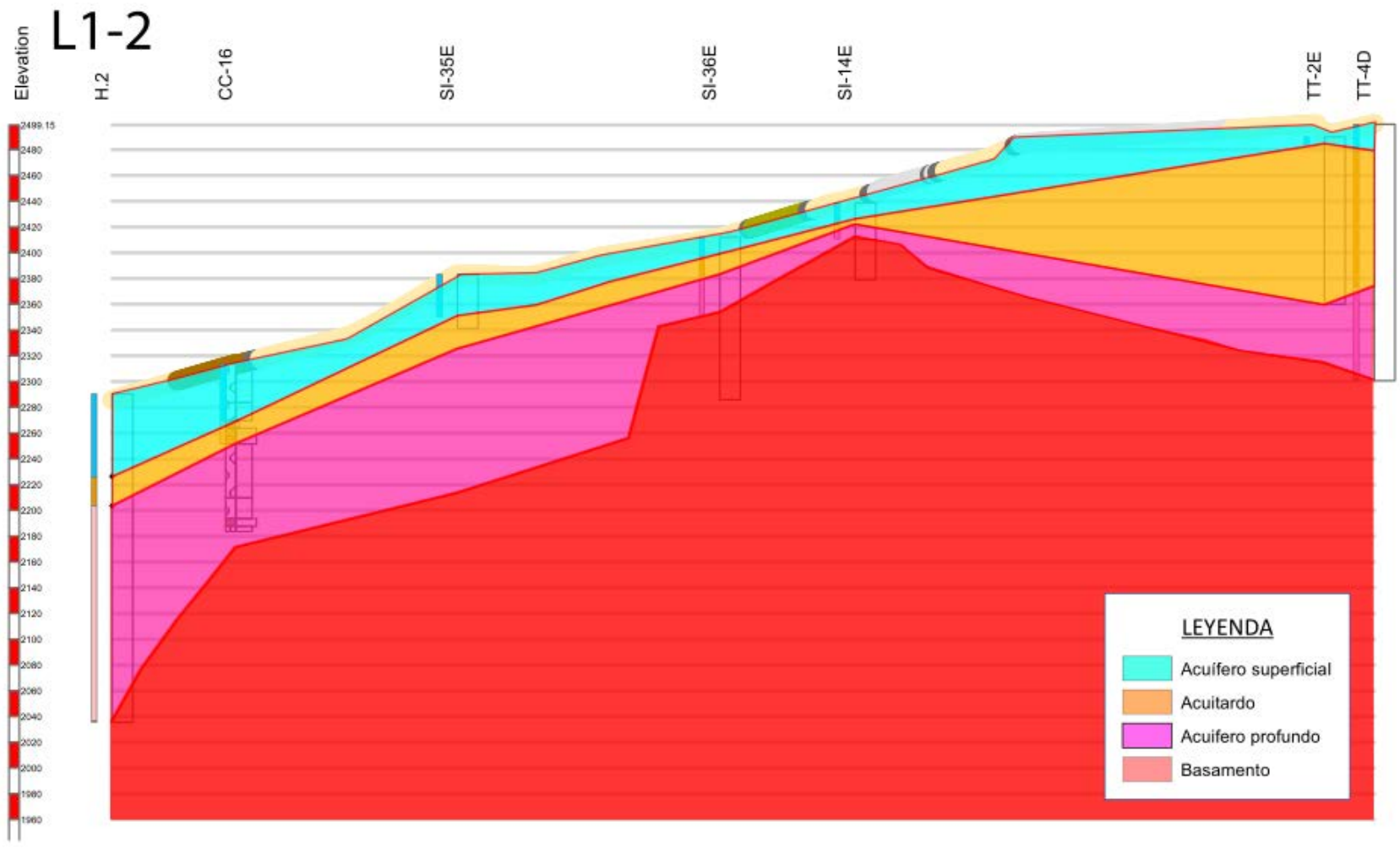
L1-2
Elevation
H.2
CC-16
SI-35E
SI-36E
SI-14E
TT-2E
TT-4D
2499.15
2480
2460
2440
2420
2400
2380
2360
2340
2320
2300
2280
2260
2240
2220
2200
2180
2160
2140
2120
2100
2080
2060
2040
2020
2000
1980
1960
LEYENDA
Acuífero superficial
Acuitardo
Acuifero profundo
Basamento

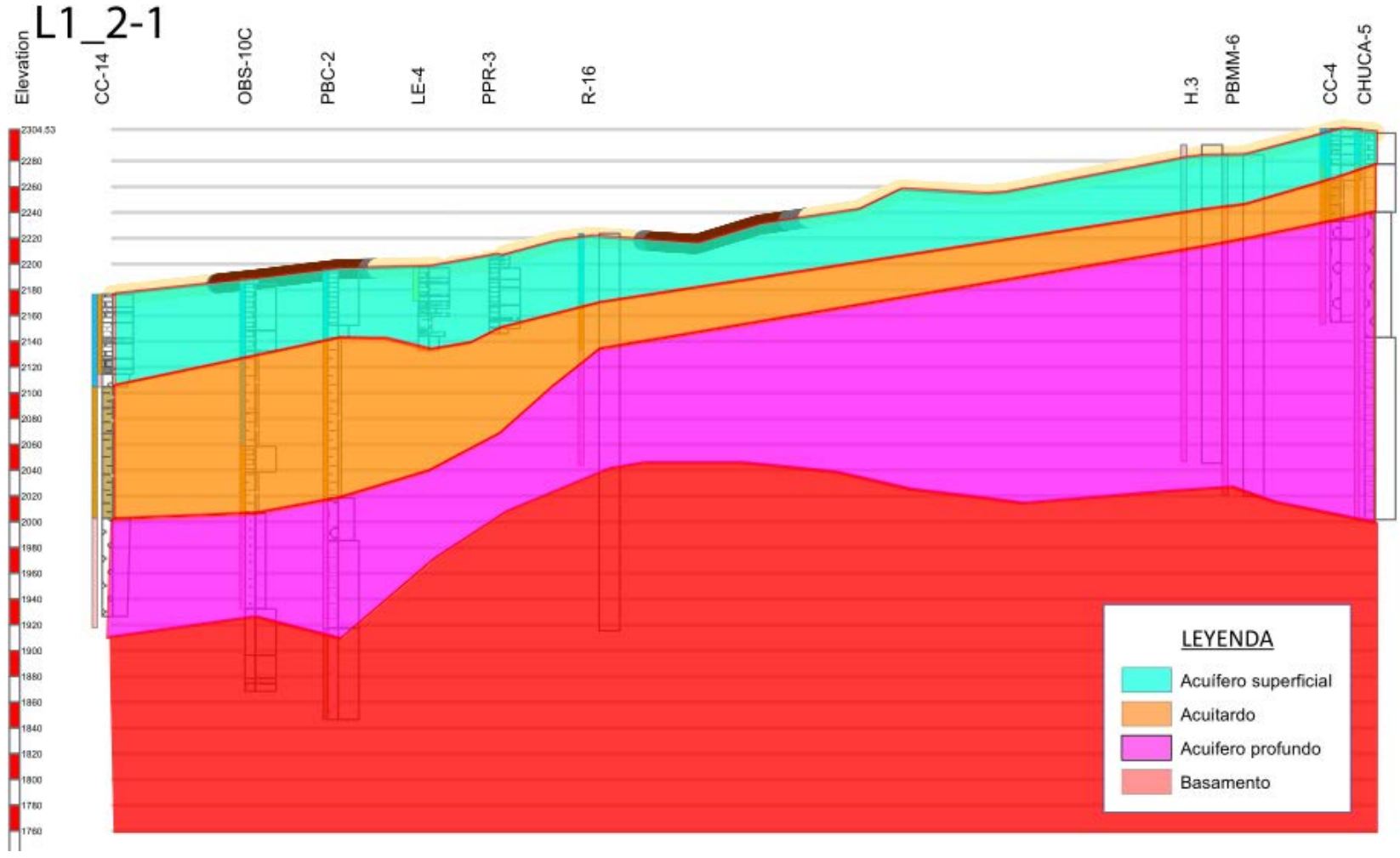
L1_2-1
Elevation
CC-14
OBS-10C
PBC-2
LE-4
PPR-3
R-16
H.3
PBMM-6
CC-4
CHUCA-5
2304.53
2280
2260
2240
2220
2200
2180
2160
2140
2120
2100
2080
2060
2040
2020
2000
1980
1960
1940
1920
1900
1880
1860
1840
1820
1800
1780
1760
LEYENDA
Acuífero superficial
Acuitardo
Acuifero profundo
Basamento

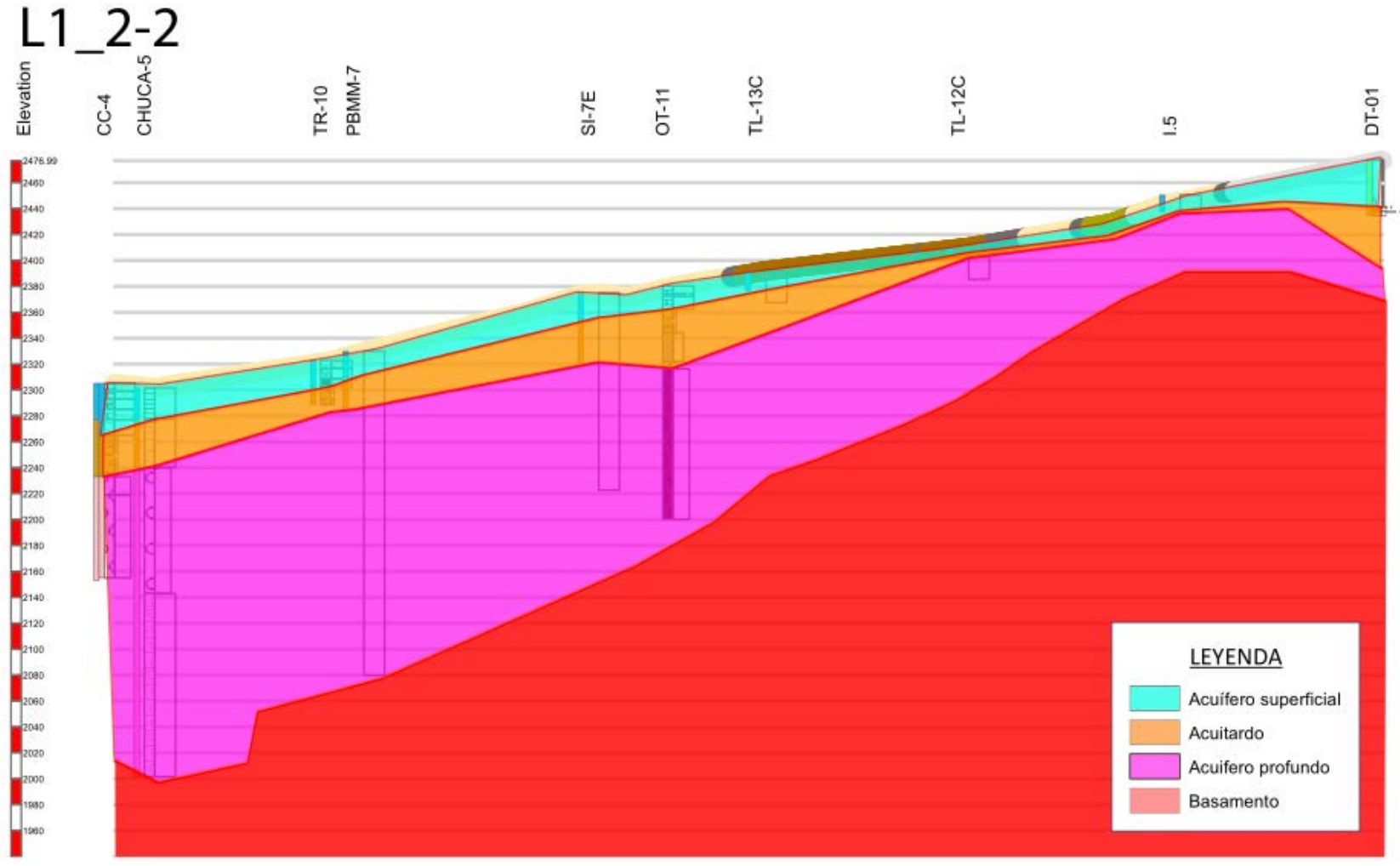
L1_2-2
Elevation
CC-4
CHUCA-5
TR-10
PBMM-7
SI-7E
OT-11
TL-13C
TL-12C
I.5
DT-01
2478.99
2460
2440
2420
2400
2380
2360
2340
2320
2300
2280
2260
2240
2220
2200
2180
2160
2140
2120
2100
2080
2060
2040
2020
2000
1980
1960
LEYENDA
Acuífero superficial
Acuitardo
Acuífero profundo
Basamento

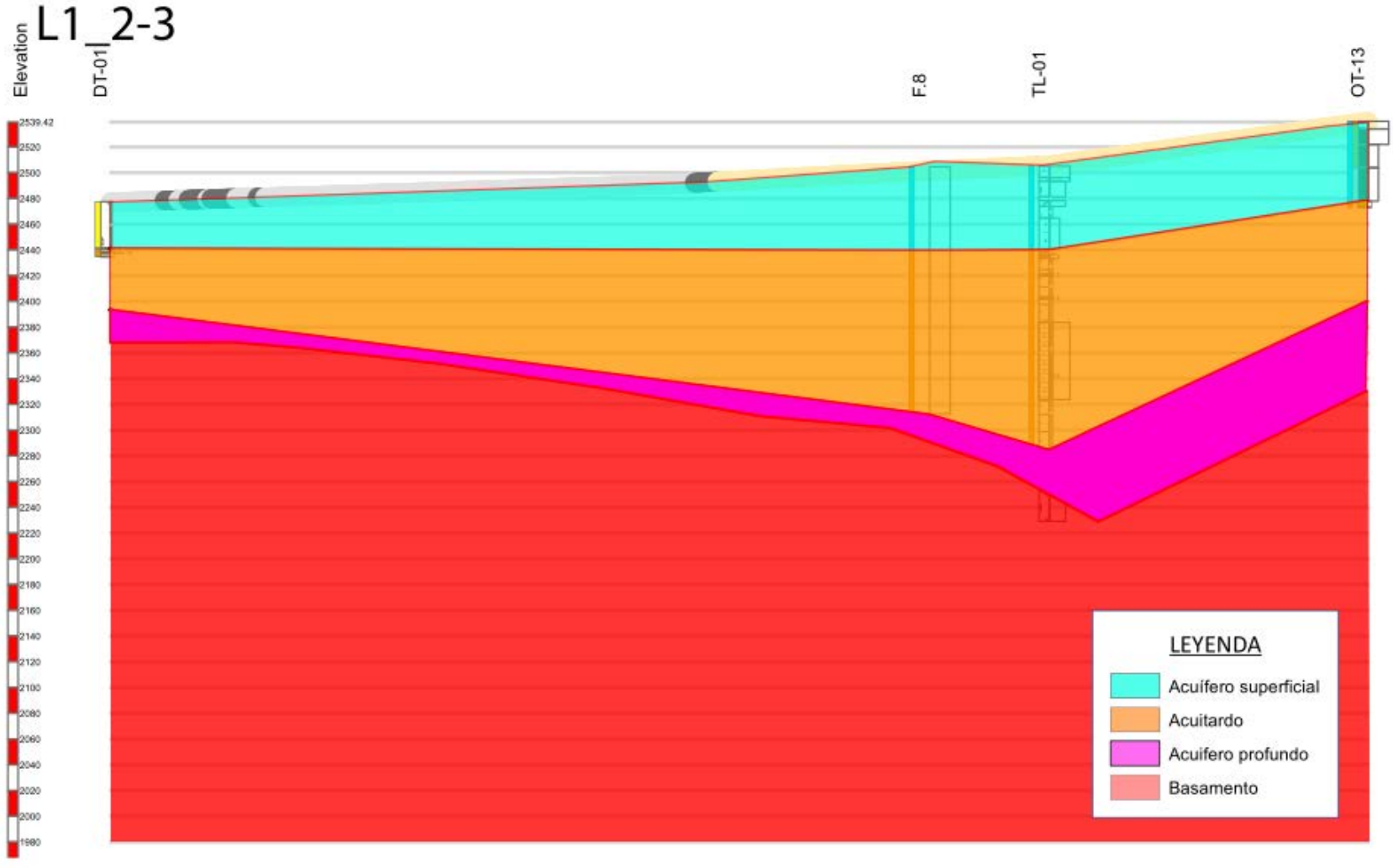
L1_2-3
Elevation
DT-01
F.8
TL-01
OT-13
2539.42
2520
2500
2480
2460
2440
2420
2400
2380
2360
2340
2320
2300
2280
2260
2240
2220
2200
2180
2160
2140
2120
2100
2080
2060
2040
2020
2000
1980
LEYENDA
Acuífero superficial
Acuitardo
Acuífero profundo
Basamento

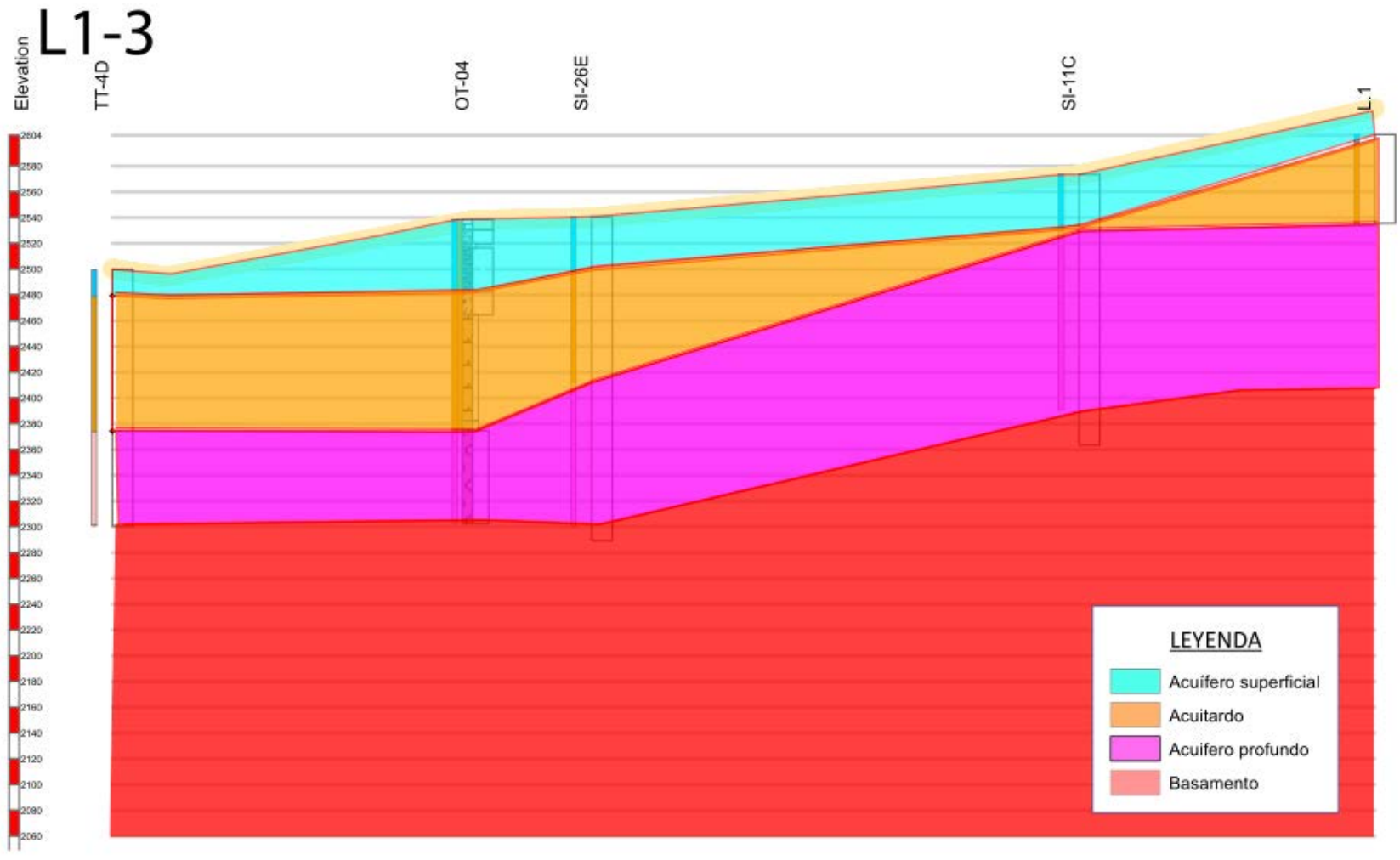
L1-3
Elevation
TT-4D
OT-04
SI-26E
SI-11C
L.1
2600
2580
2560
2540
2520
2500
2480
2460
2440
2420
2400
2380
2360
2340
2320
2300
2280
2260
2240
2220
2200
2180
2160
2140
2120
2100
2080
2060
LEYENDA
Acuífero superficial
Acuitardo
Acuífero profundo
Basamento

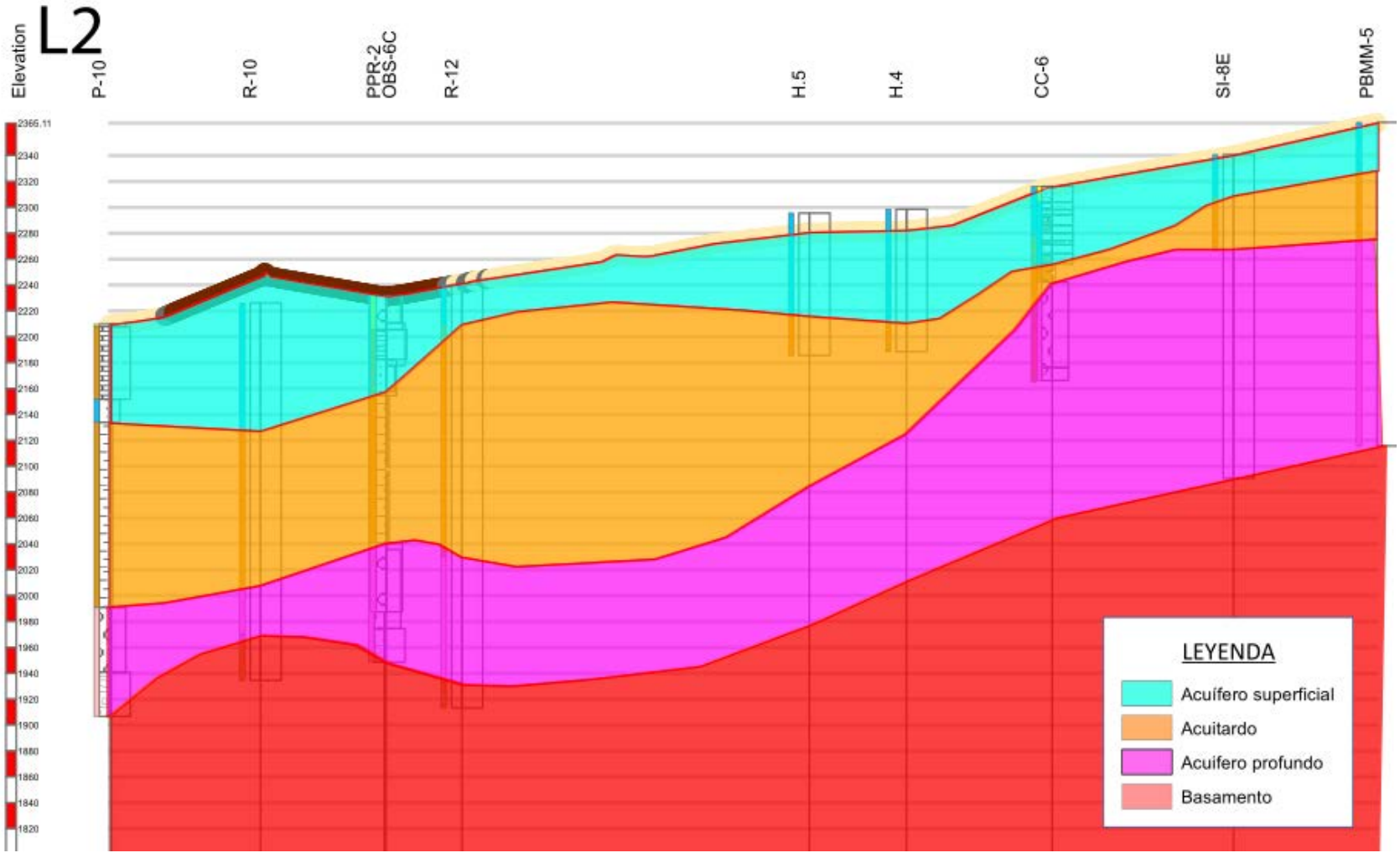
L2
Elevation
P-10
R-10
PPR-2
OBS-6C
R-12
H.5
H.4
CC-6
SI-8E
PBMM-5
2365.11
2340
2320
2300
2280
2260
2240
2220
2200
2180
2160
2140
2120
2100
2080
2060
2040
2020
2000
1980
1960
1940
1920
1900
1880
1860
1840
1820
LEYENDA
Acuífero superficial
Acuitardo
Acuífero profundo
Basamento

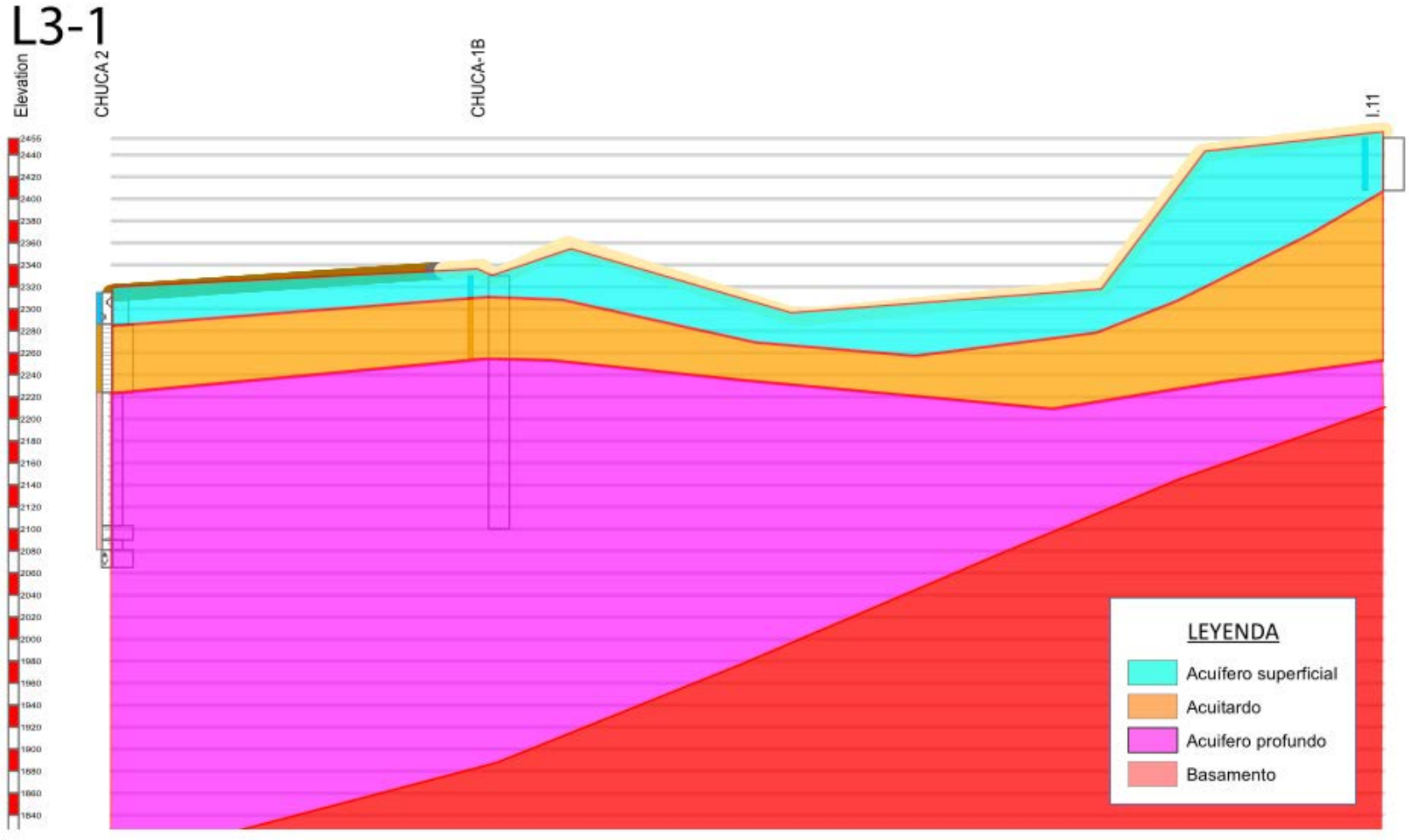
L3-1
Elevation
CHUCA 2
CHUCA-1B
I.11
LEYENDA
Acuífero superficial
Acuitardo
Acuífero profundo
Basamento

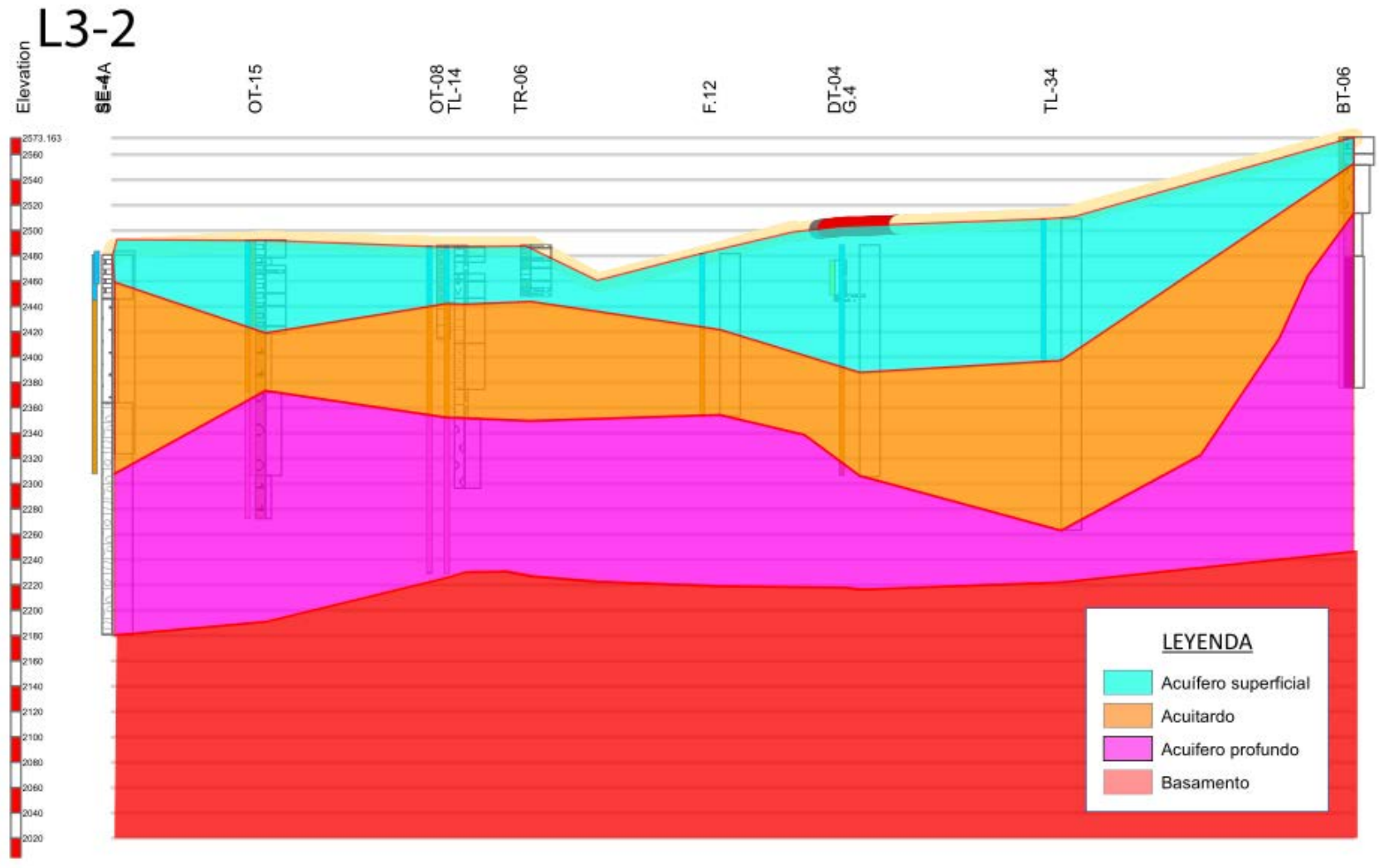
L3-2
Elevation
SE-4A
OT-15
OT-08
TL-14
TR-06
F.12
DT-04
G.4
TL-34
BT-06
2573.163
2560
2540
2520
2500
2480
2460
2440
2420
2400
2380
2360
2340
2320
2300
2280
2260
2240
2220
2200
2180
2160
2140
2120
2100
2080
2060
2040
2020
LEYENDA
Acuífero superficial
Acuitardo
Acuifero profundo
Basamento

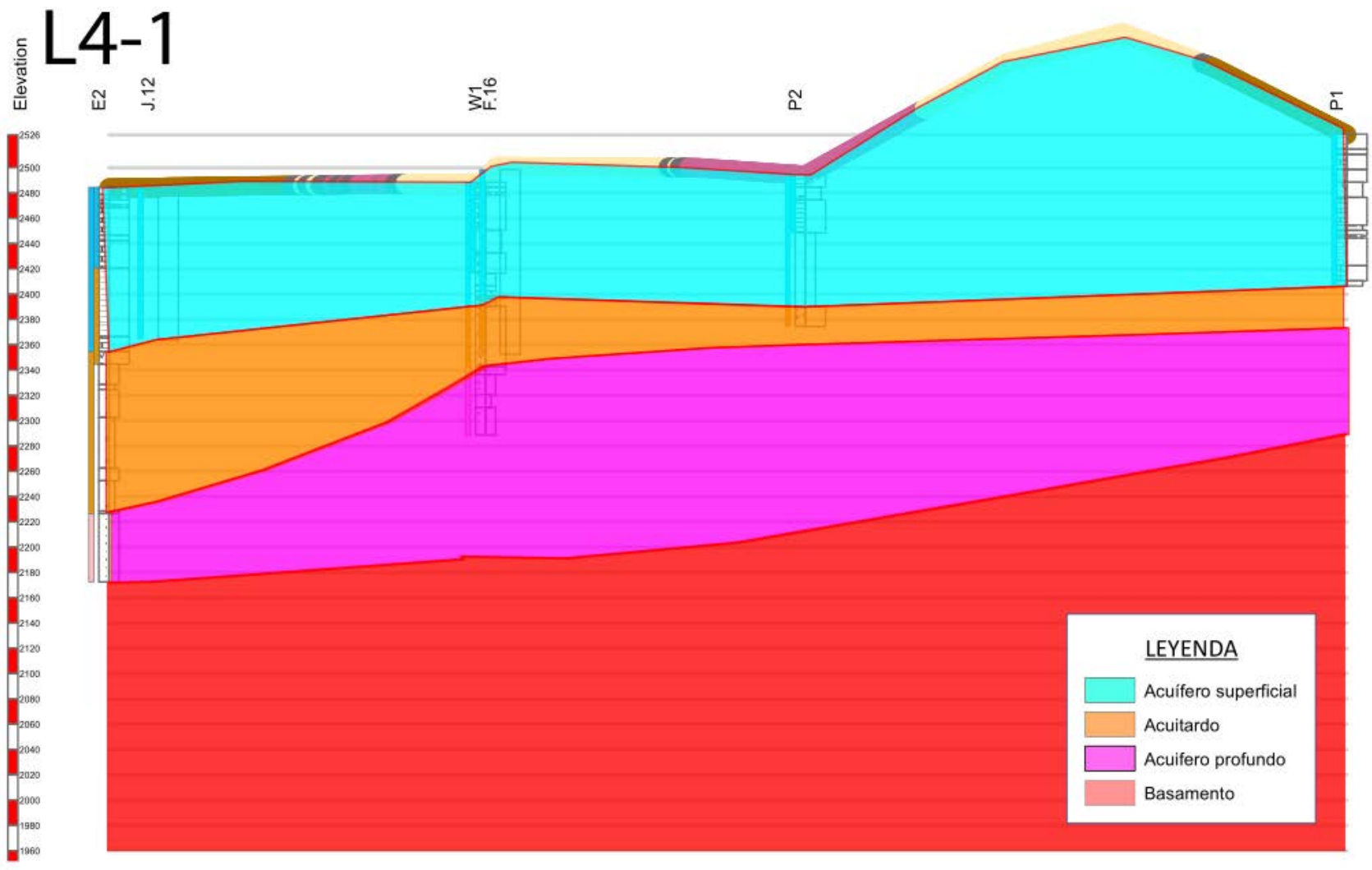
L4-1
Elevation
E2
J.12
W1
F.16
P2
P1
2526
2500
2480
2460
2440
2420
2400
2380
2360
2340
2320
2300
2280
2260
2240
2220
2200
2180
2160
2140
2120
2100
2080
2060
2040
2020
2000
1980
1960
LEYENDA
Acuífero superficial
Acuitardo
Acuifero profundo
Basamento

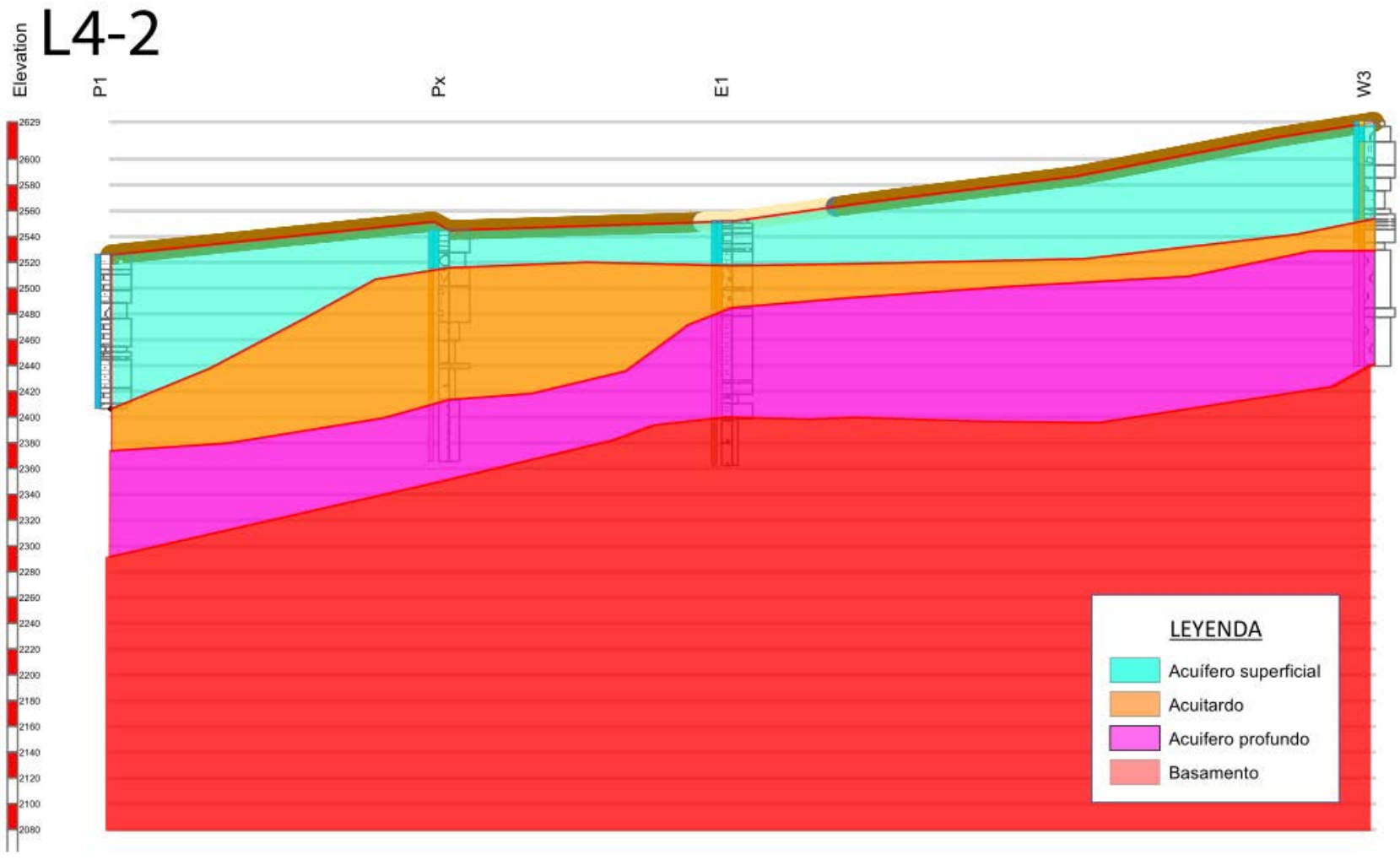
L4-2
Elevation
P1
Px
E1
W3
2629
2600
2580
2560
2540
2520
2500
2480
2460
2440
2420
2400
2380
2360
2340
2320
2300
2280
2260
2240
2220
2200
2180
2160
2140
2120
2100
2080
LEYENDA
Acuífero superficial
Acuitardo
Acuífero profundo
Basamento

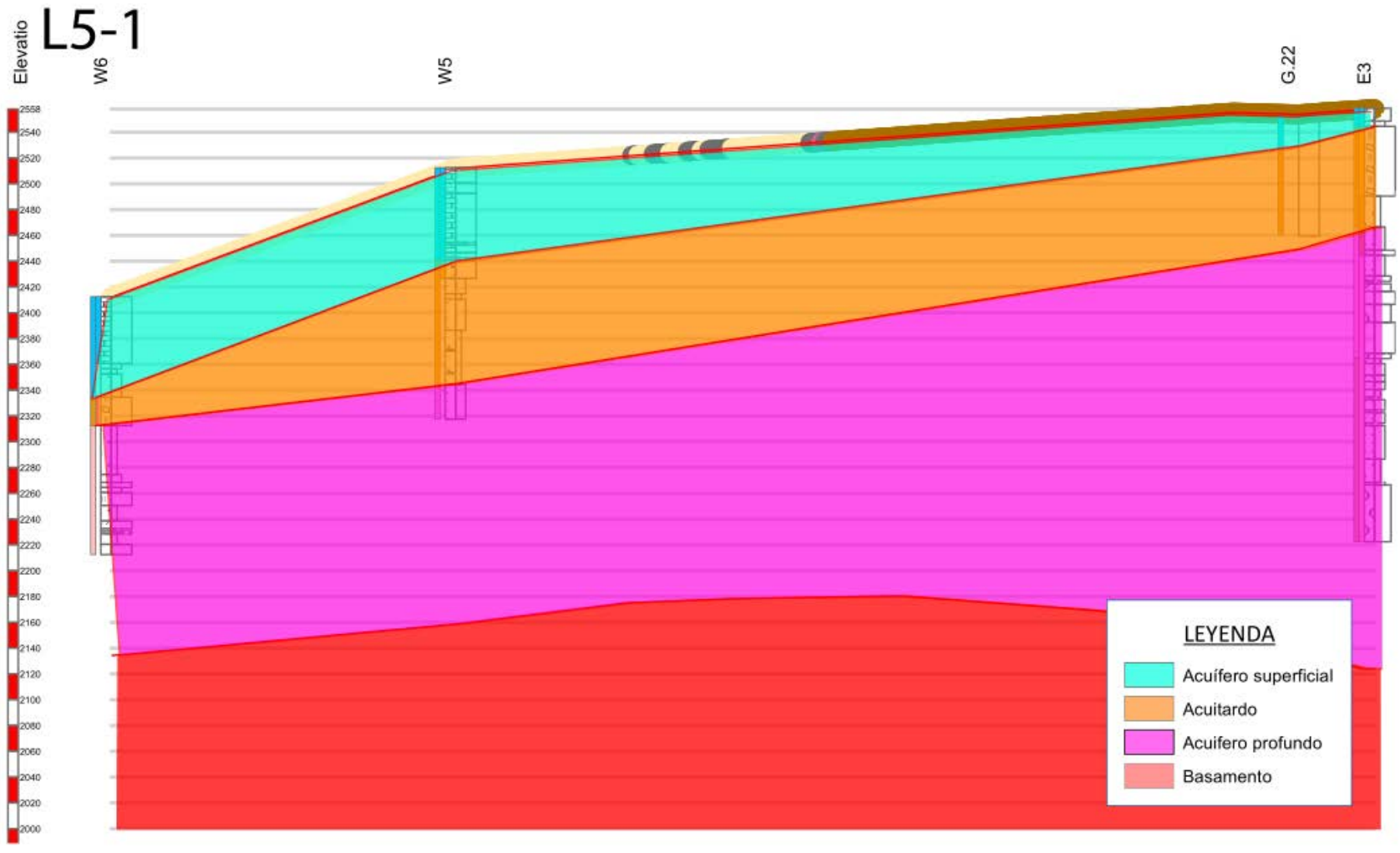
L5-1
Elevatio
W6
W5
G.22
E3
2558
2540
2520
2500
2480
2460
2440
2420
2400
2380
2360
2340
2320
2300
2280
2260
2240
2220
2200
2180
2160
2140
2120
2100
2080
2060
2040
2020
2000
LEYENDA
Acuífero superficial
Acuitardo
Acuifero profundo
Basamento

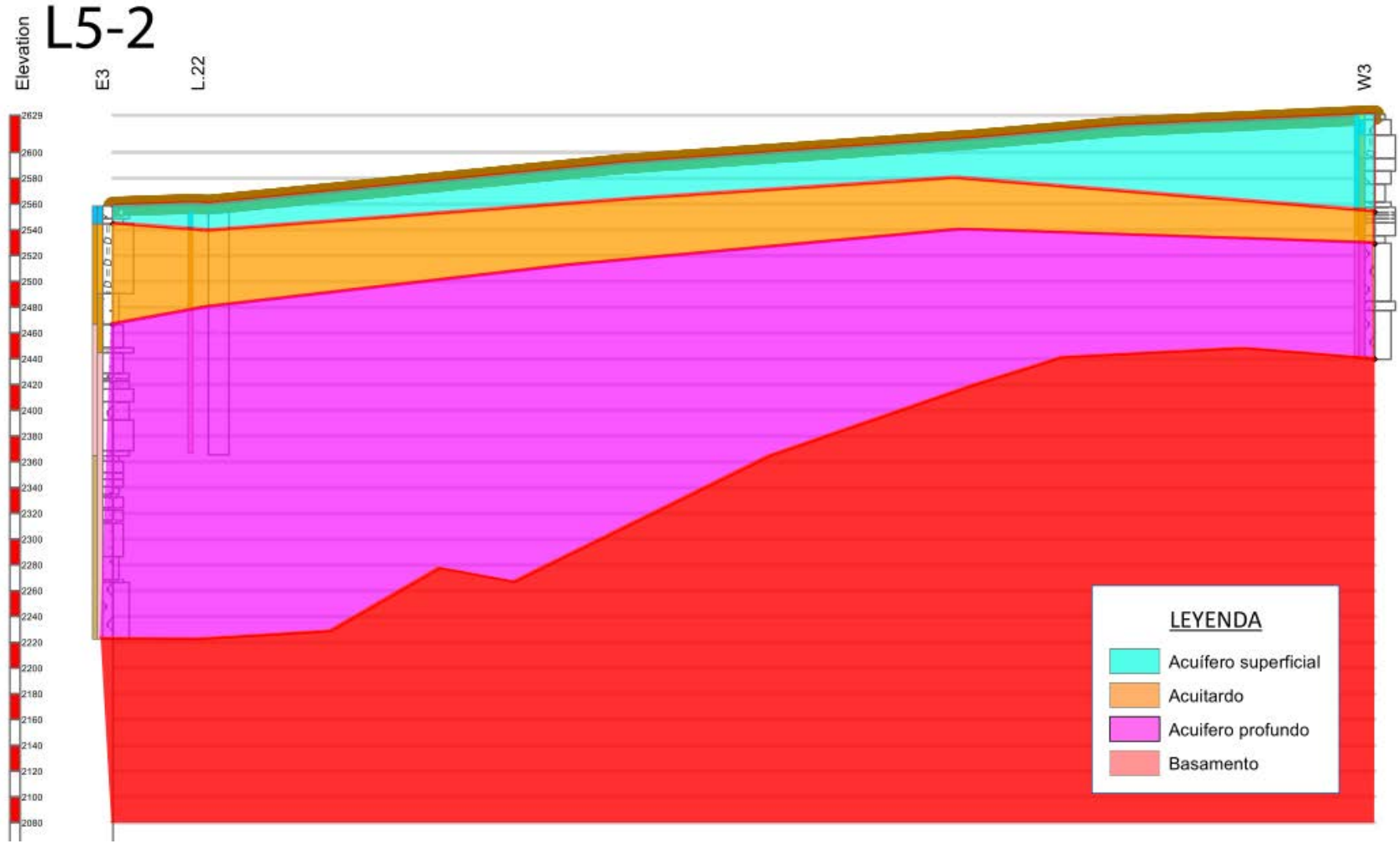
L5-2
Elevation
E3
L.22
W3
2620
2600
2580
2560
2540
2520
2500
2480
2460
2440
2420
2400
2380
2360
2340
2320
2300
2280
2260
2240
2220
2200
2180
2160
2140
2120
2100
2080
LEYENDA
Acuífero superficial
Acuitardo
Acuifero profundo
Basamento

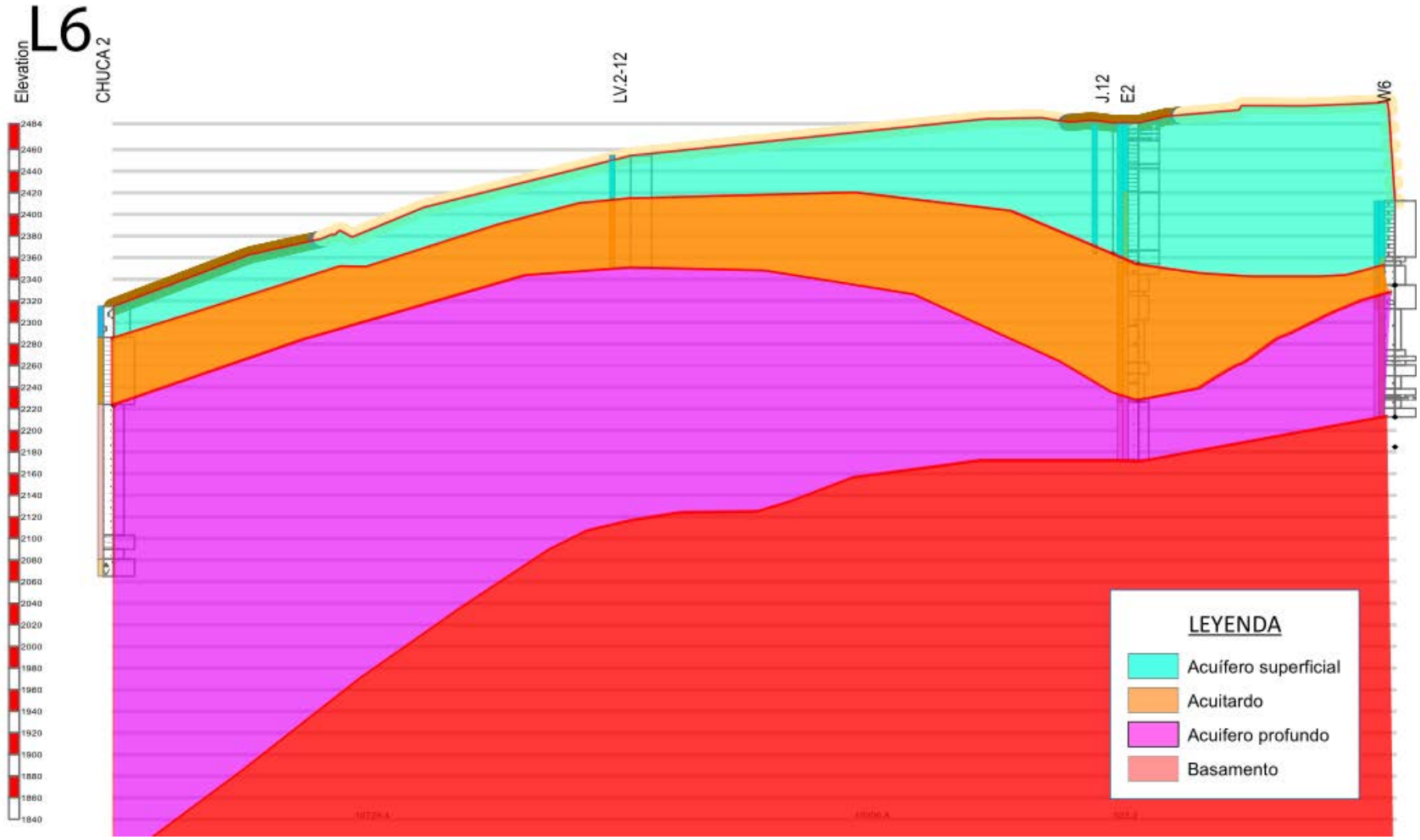
L6
Elevation
CHUCA 2
LV.2-12
J.12
E2
W6
2484
2460
2440
2420
2400
2380
2360
2340
2320
2300
2280
2260
2240
2220
2200
2180
2160
2140
2120
2100
2080
2060
2040
2020
2000
1980
1960
1940
1920
1900
1880
1860
1840
LEYENDA
Acuífero superficial
Acuitardo
Acuifero profundo
Basamento

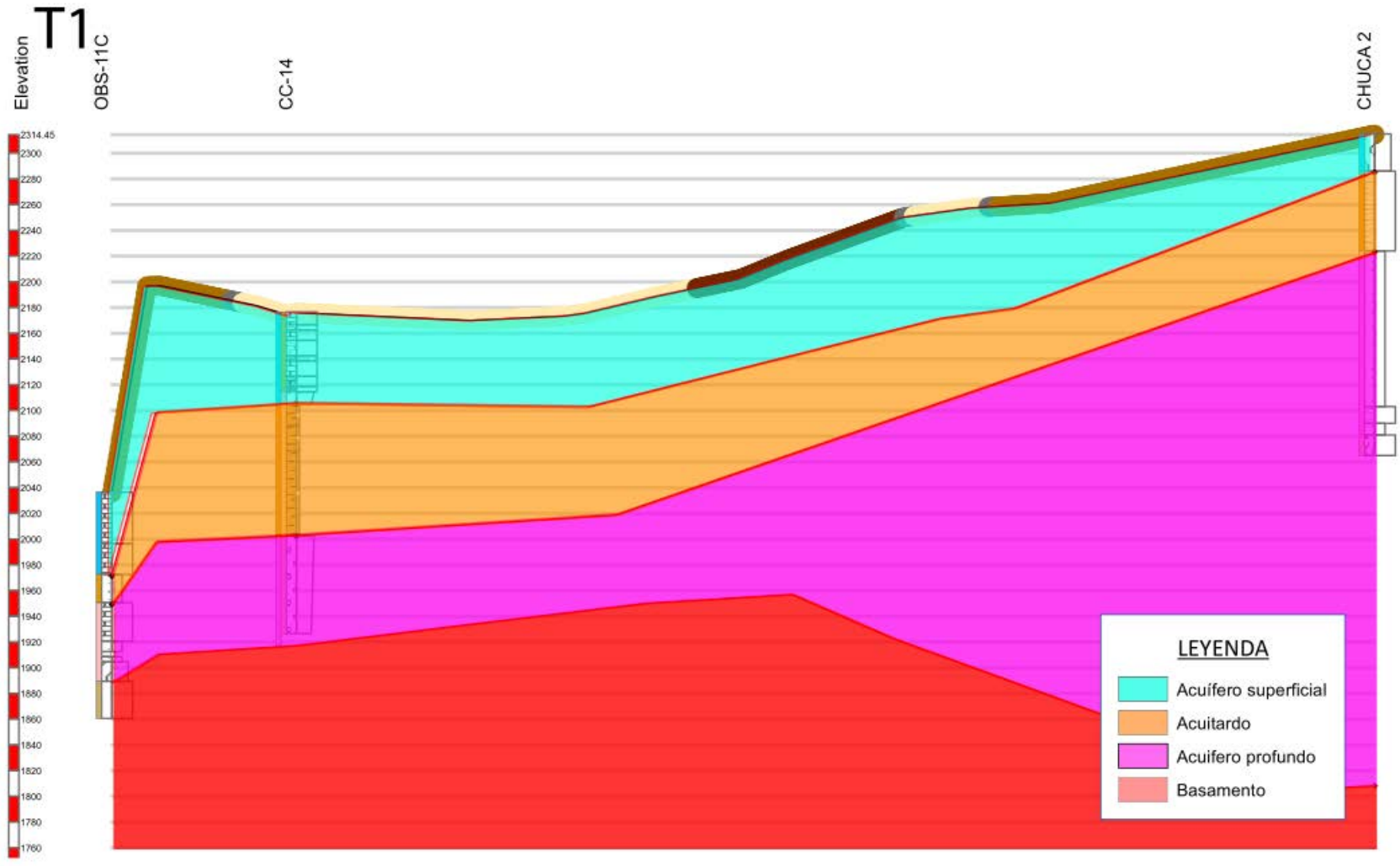
T1
Elevation
OBS-11C
CC-14
CHUCA 2
2314.45
2300
2280
2260
2240
2220
2200
2180
2160
2140
2120
2100
2080
2060
2040
2020
2000
1980
1960
1940
1920
1900
1880
1860
1840
1820
1800
1780
1760
LEYENDA
Acuífero superficial
Acuitardo
Acuífero profundo
Basamento

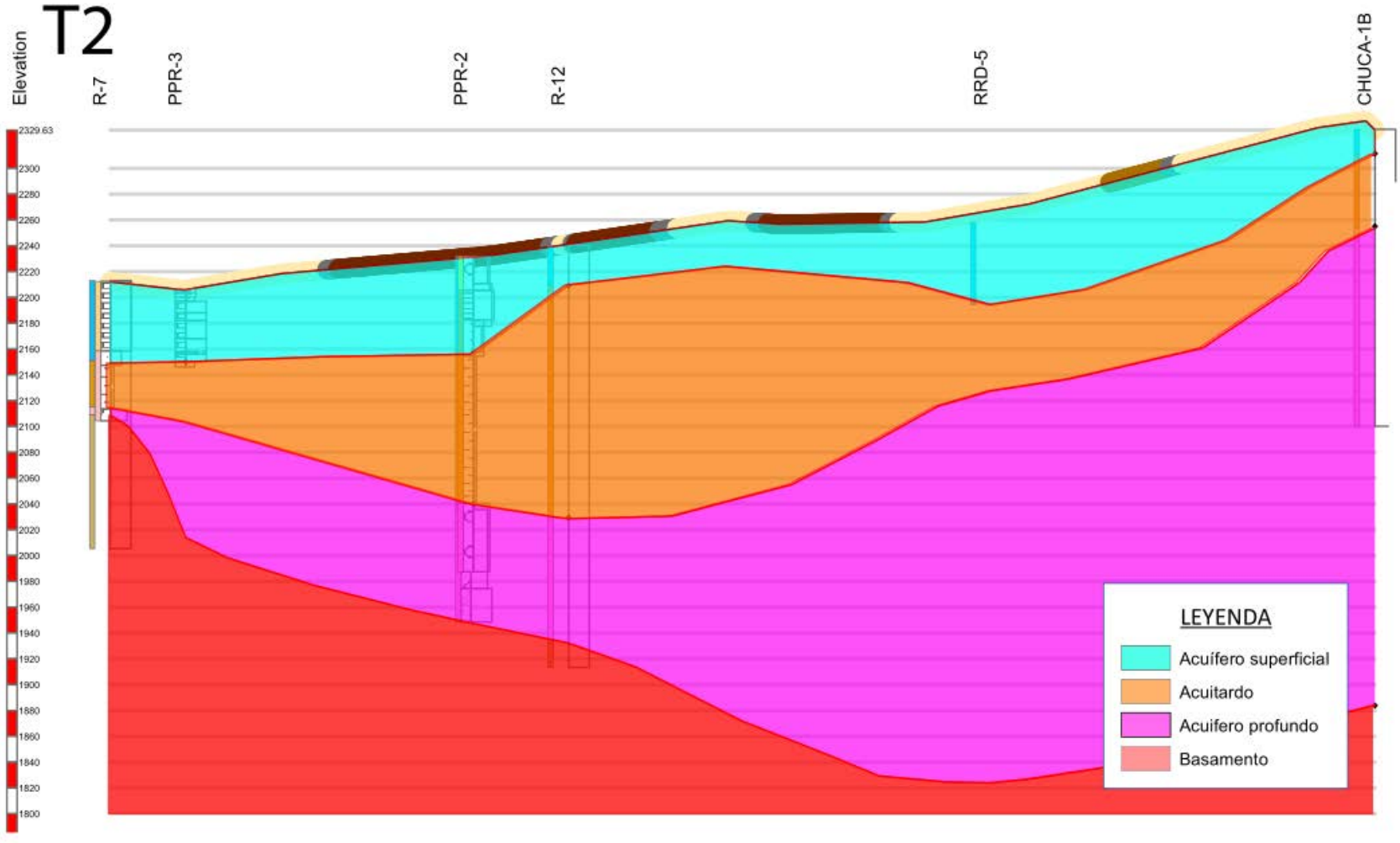
T2
Elevation
R-7
PPR-3
PPR-2
R-12
RRD-5
CHUCA-1B
2329.63
2300
2280
2260
2240
2220
2200
2180
2160
2140
2120
2100
2080
2060
2040
2020
2000
1980
1960
1940
1920
1900
1880
1860
1840
1820
1800
LEYENDA
Acuífero superficial
Acuitardo
Acuifero profundo
Basamento

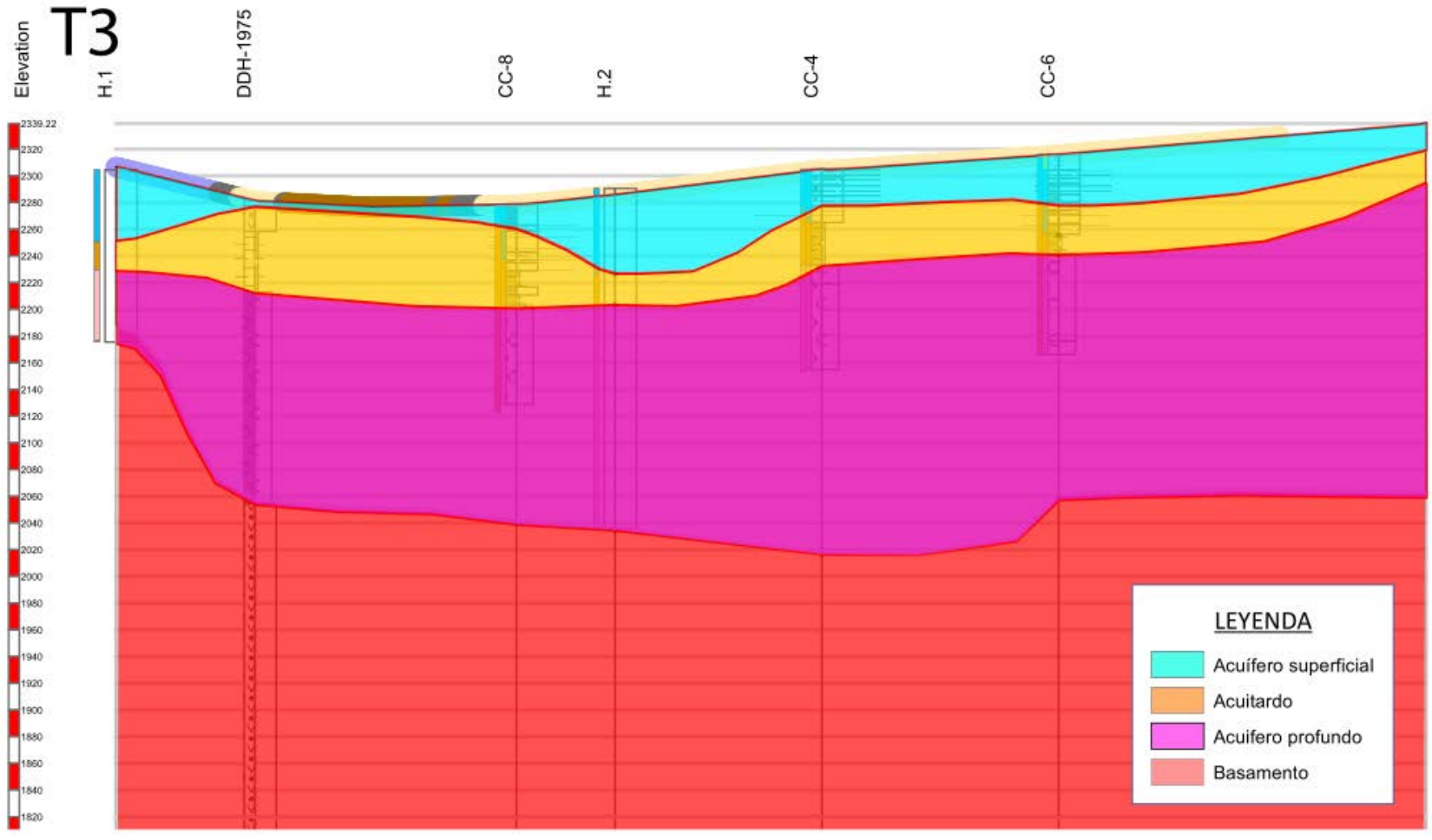
T3
Elevation
H.1
DDH-1975
CC-8
H.2
CC-4
CC-6
2339.22
2320
2300
2280
2260
2240
2220
2200
2180
2160
2140
2120
2100
2080
2060
2040
2020
2000
1980
1960
1940
1920
1900
1880
1860
1840
1820
LEYENDA
Acuífero superficial
Acuitardo
Acuífero profundo
Basamento

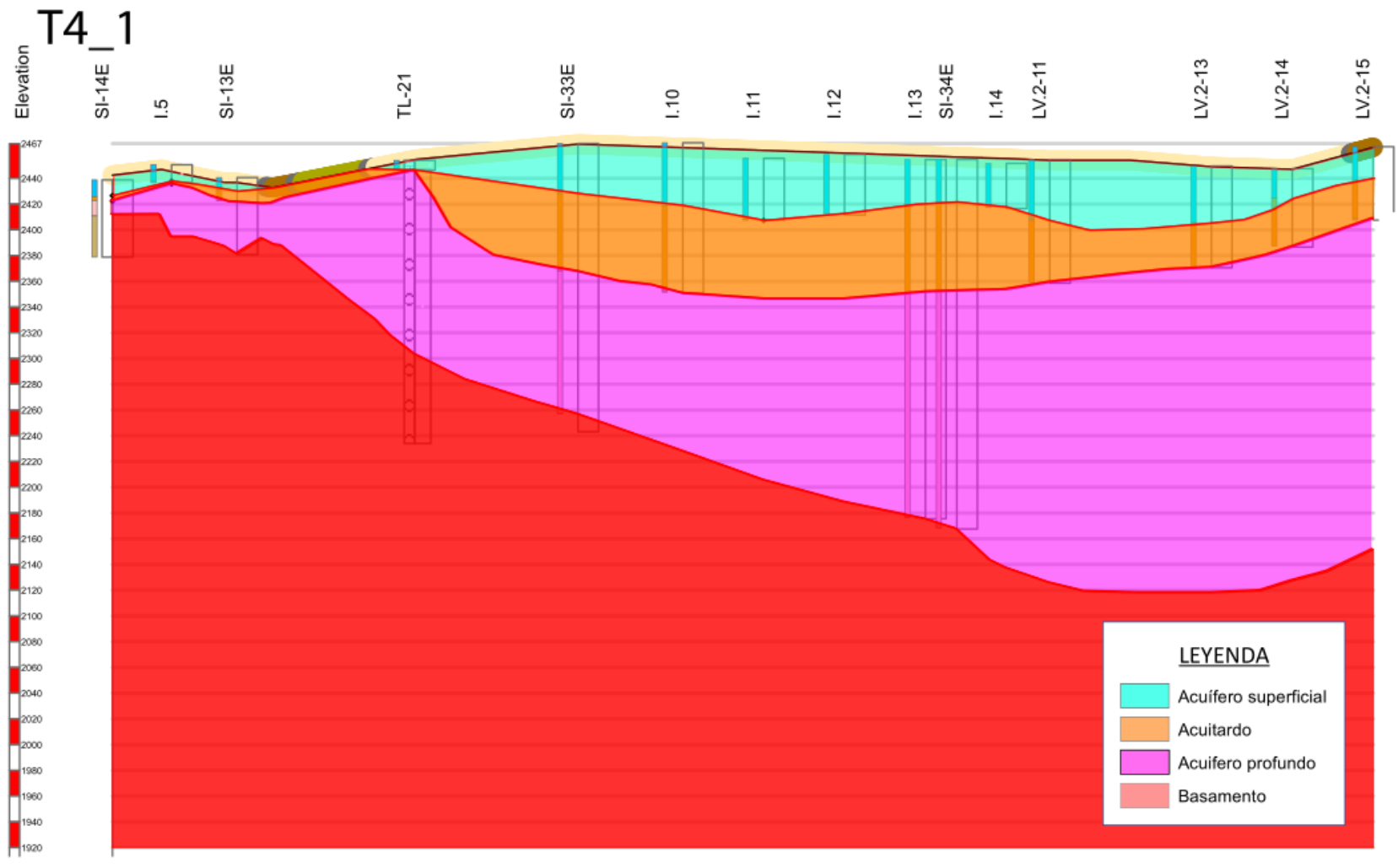
T4_1
Elevation
SI-14E
I.5
SI-13E
TL-21
SI-33E
I.10
I.11
I.12
I.13
SI-34E
I.14
LV.2-11
LV.2-13
LV.2-14
LV.2-15
2467
2440
2420
2400
2380
2360
2340
2320
2300
2280
2260
2240
2220
2200
2180
2160
2140
2120
2100
2080
2060
2040
2020
2000
1980
1960
1940
1920
LEYENDA
Acuífero superficial
Acuitardo
Acuifero profundo
Basamento

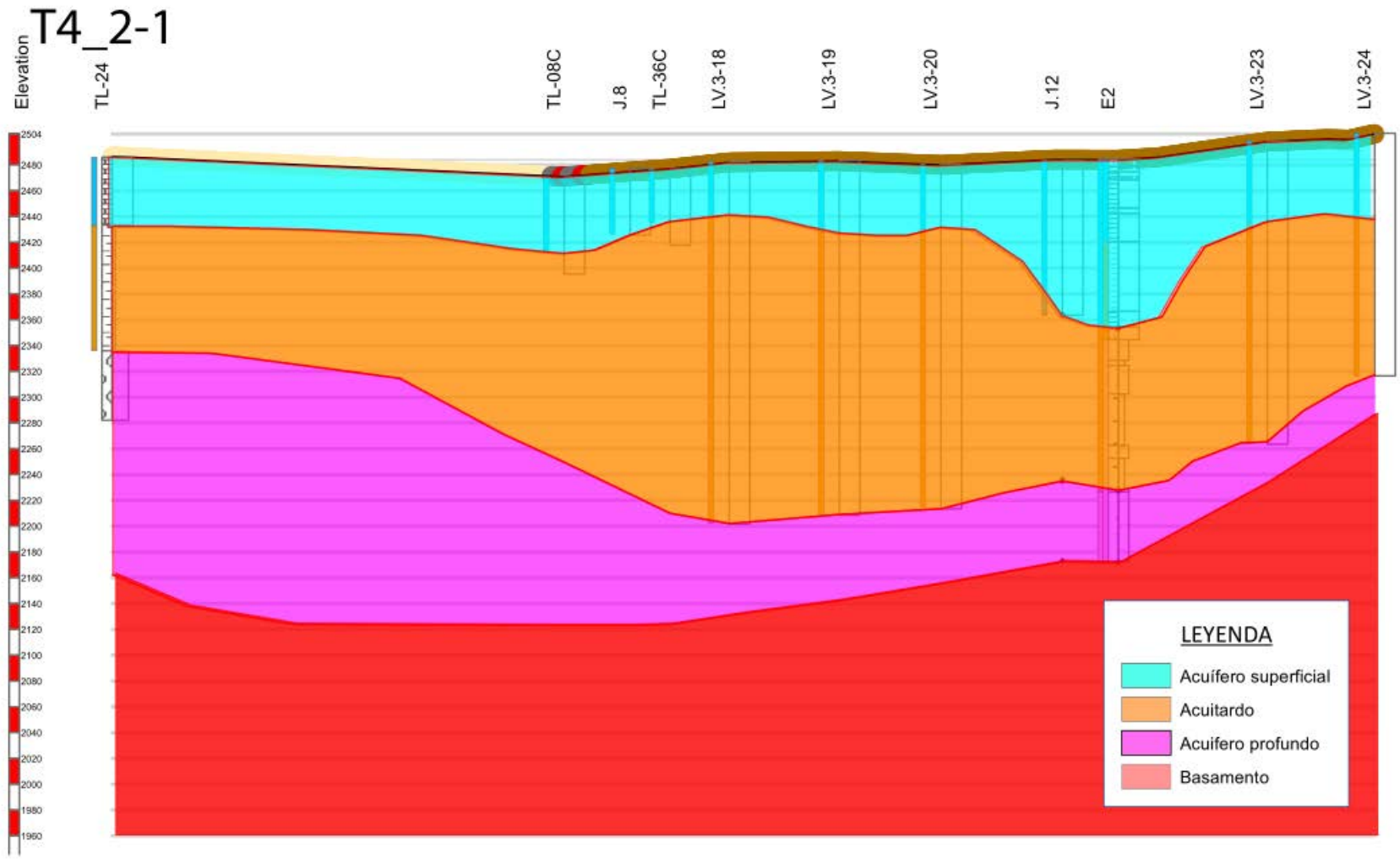
T4_2-1
Elevation
TL-24
TL-08C
J.8
TL-36C
LV.3-18
LV.3-19
LV.3-20
J.12
E2
LV.3-23
LV.3-24
2504
2480
2460
2440
2420
2400
2380
2360
2340
2320
2300
2280
2260
2240
2220
2200
2180
2160
2140
2120
2100
2080
2060
2040
2020
2000
1980
1960
LEYENDA
Acuífero superficial
Acuitardo
Acuifero profundo
Basamento

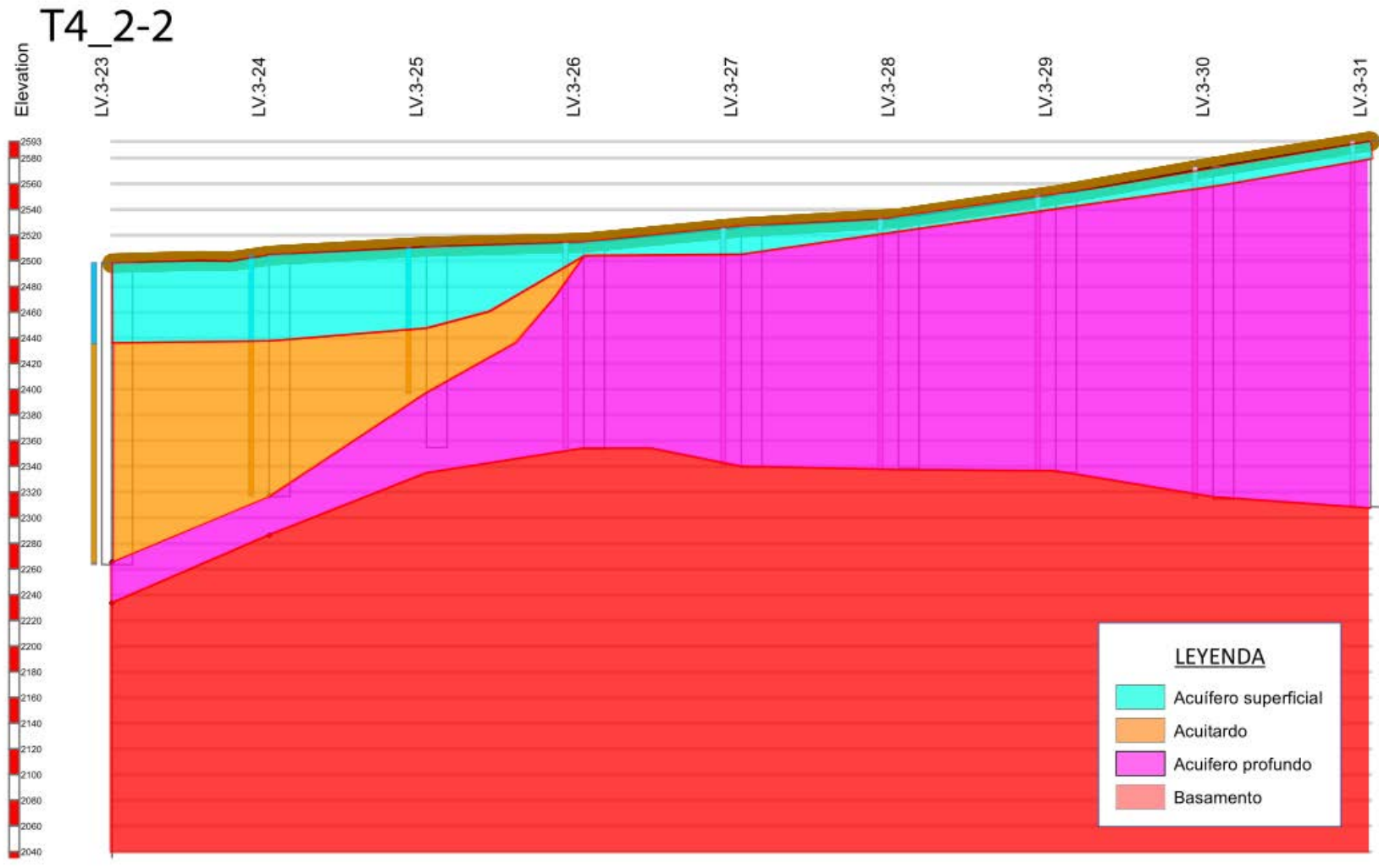
T4_2-2
Elevation
LV.3-23
LV.3-24
LV.3-25
LV.3-26
LV.3-27
LV.3-28
LV.3-29
LV.3-30
LV.3-31
2593
2580
2560
2540
2520
2500
2480
2460
2440
2420
2400
2380
2360
2340
2320
2300
2280
2260
2240
2220
2200
2180
2160
2140
2120
2100
2080
2060
2040
LEYENDA
Acuífero superficial
Acuitardo
Acuífero profundo
Basamento

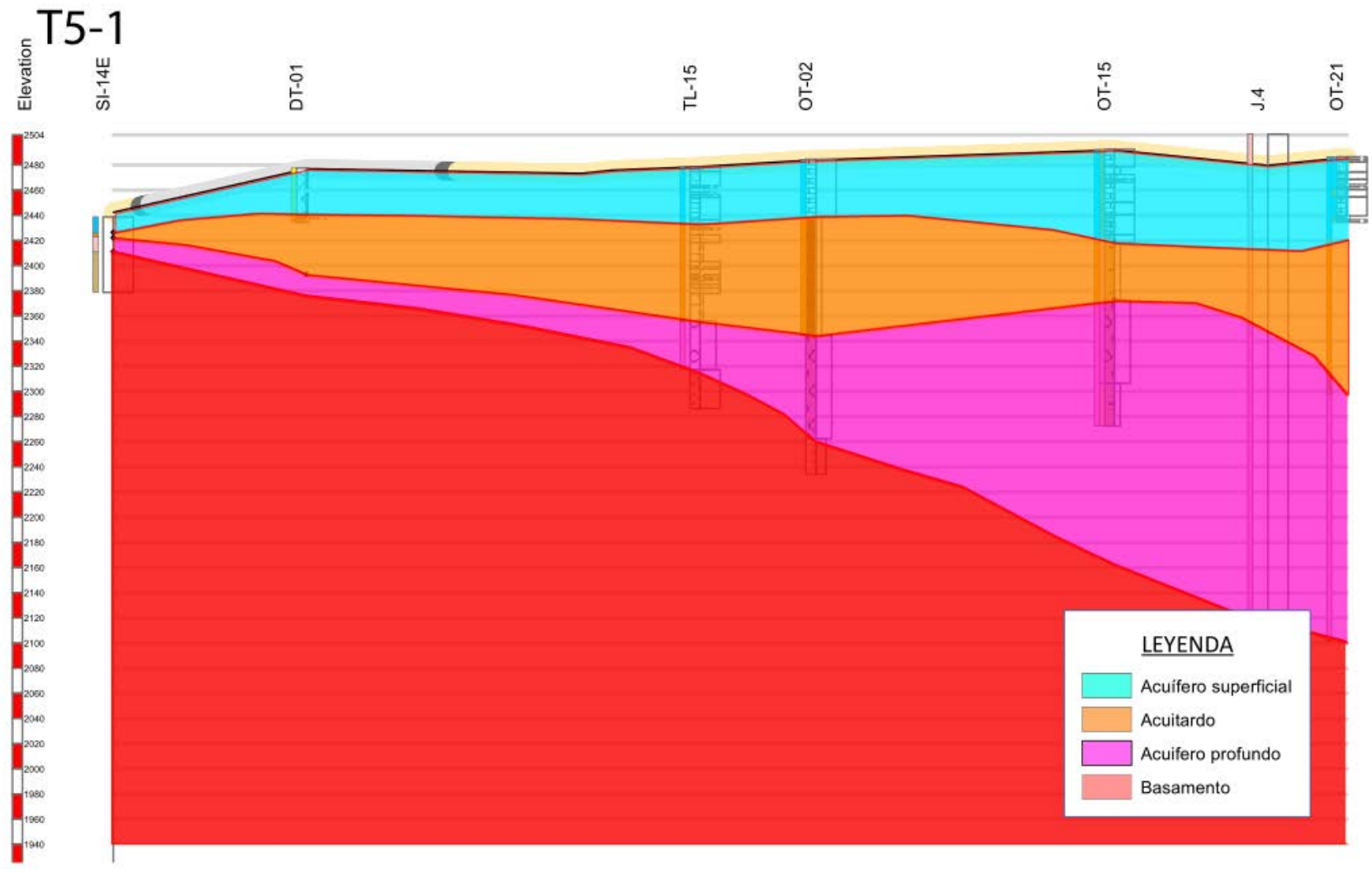
T5-1
Elevation
SI-14E
DT-01
TL-15
OT-02
OT-15
J.4
OT-21
2504
2480
2460
2440
2420
2400
2380
2360
2340
2320
2300
2280
2260
2240
2220
2200
2180
2160
2140
2120
2100
2080
2060
2040
2020
2000
1980
1960
1940
LEYENDA
Acuífero superficial
Acuitardo
Acuífero profundo
Basamento

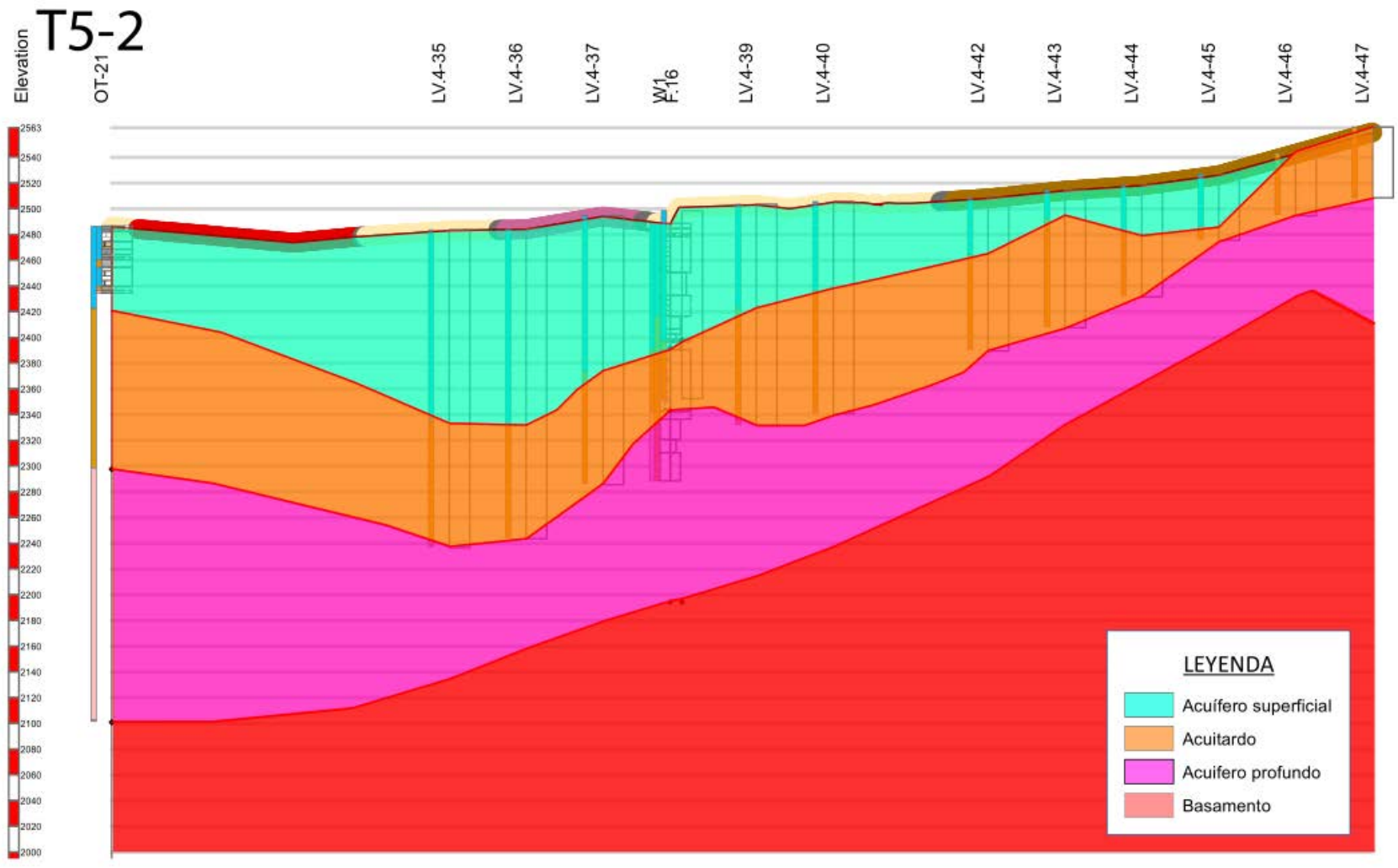
T5-2
Elevation
OT-21
LV.4-35
LV.4-36
LV.4-37
W1
P.16
LV.4-39
LV.4-40
LV.4-42
LV.4-43
LV.4-44
LV.4-45
LV.4-46
LV.4-47
2563
2540
2520
2500
2480
2460
2440
2420
2400
2380
2360
2340
2320
2300
2280
2260
2240
2220
2200
2180
2160
2140
2120
2100
2080
2060
2040
2020
2000
LEYENDA
Acuífero superficial
Acuitardo
Acuífero profundo
Basamento

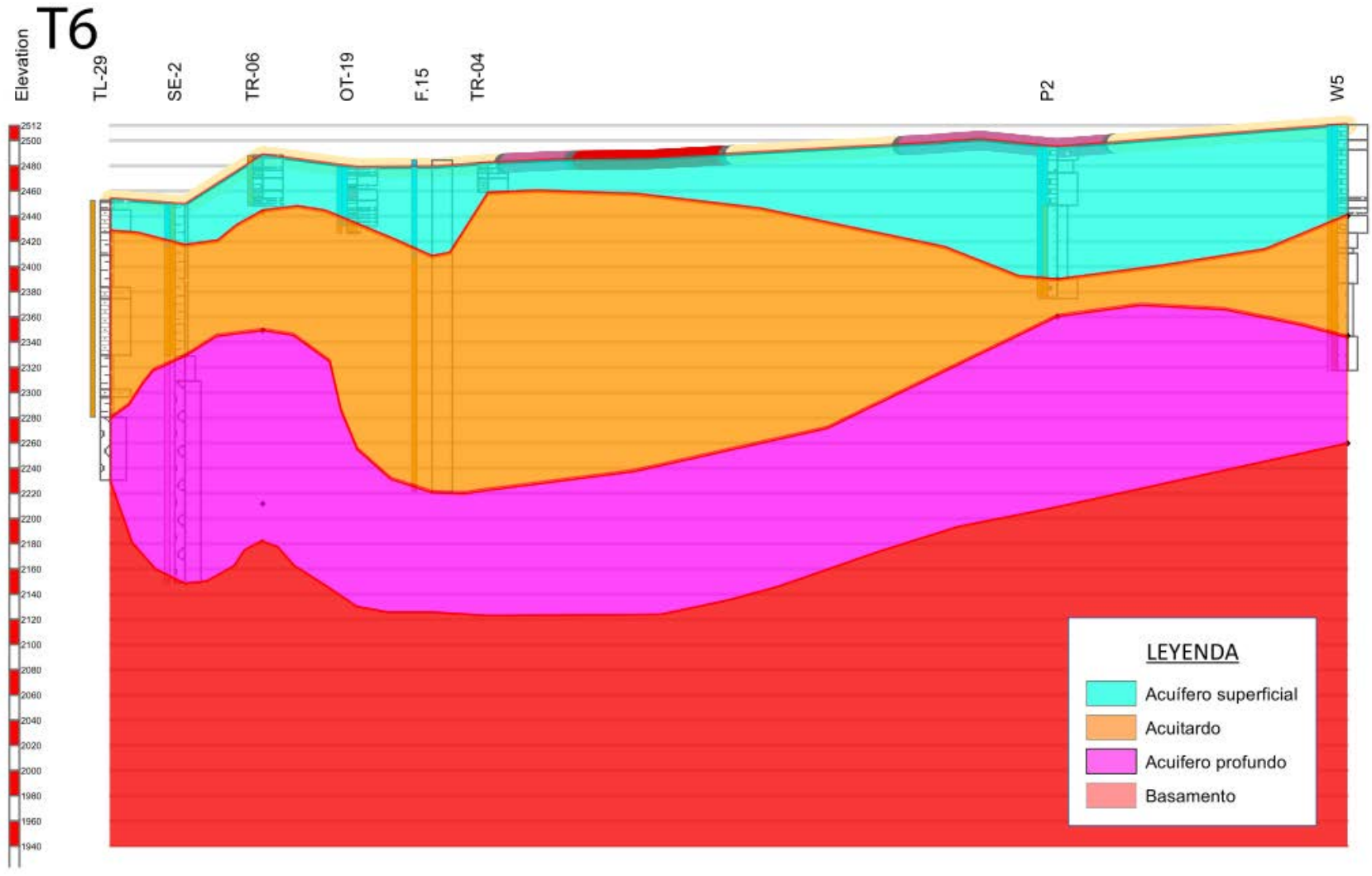
T6
Elevation
TL-29
SE-2
TR-06
OT-19
F.15
TR-04
P2
W5
2512
2500
2480
2460
2440
2420
2400
2380
2360
2340
2320
2300
2280
2260
2240
2220
2200
2180
2160
2140
2120
2100
2080
2060
2040
2020
2000
1980
1960
1940
LEYENDA
Acuífero superficial
Acuitardo
Acuífero profundo
Basamento

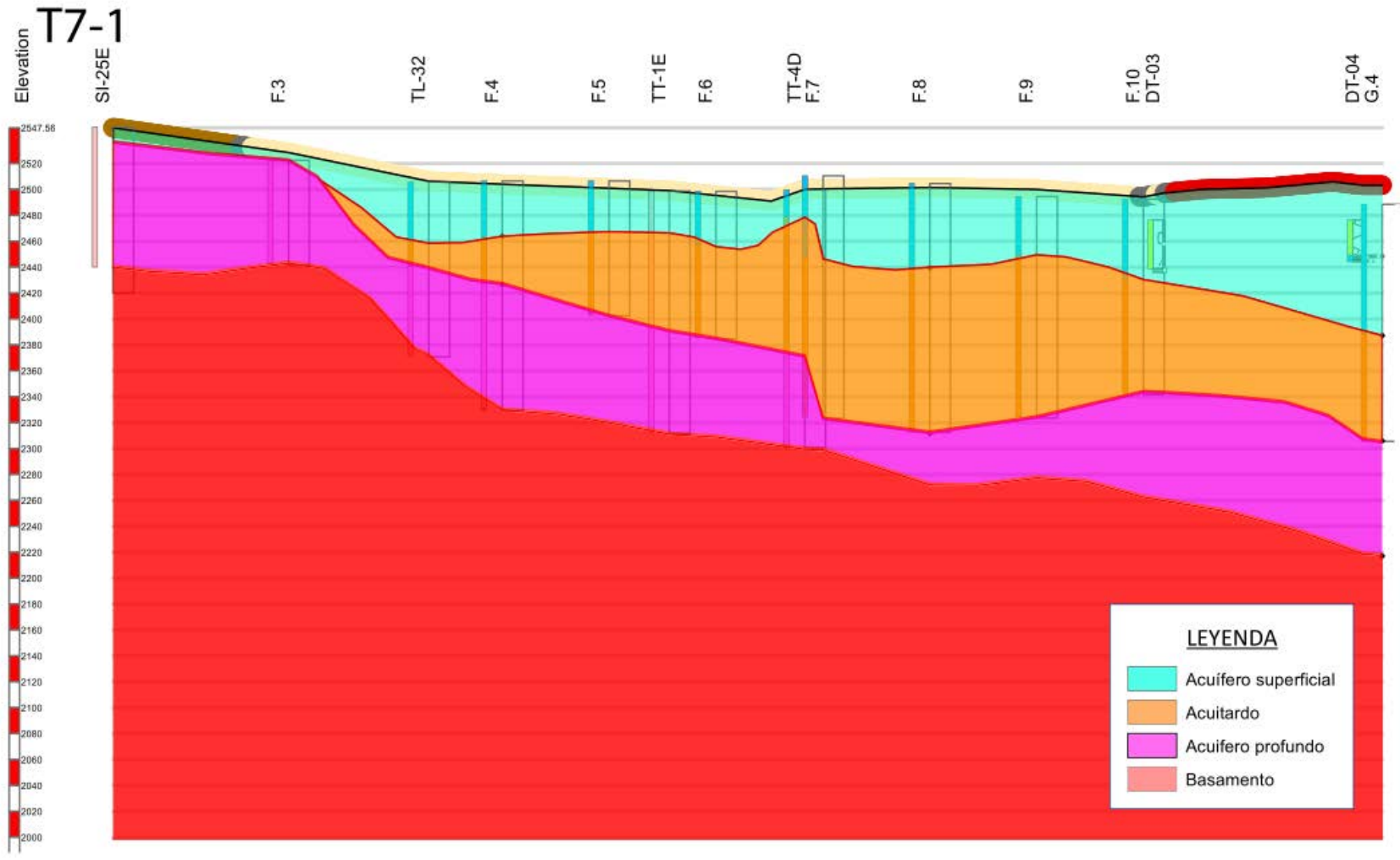
T7-1
Elevation
SI-25E
F.3
TL-32
F.4
F.5
TT-1E
F.6
TT-4D
F.7
F.8
F.9
F.10
DT-03
DT-04
G.4
2547.56
2520
2500
2480
2460
2440
2420
2400
2380
2360
2340
2320
2300
2280
2260
2240
2220
2200
2180
2160
2140
2120
2100
2080
2060
2040
2020
2000
LEYENDA
Acuífero superficial
Acuitardo
Acuifero profundo
Basamento

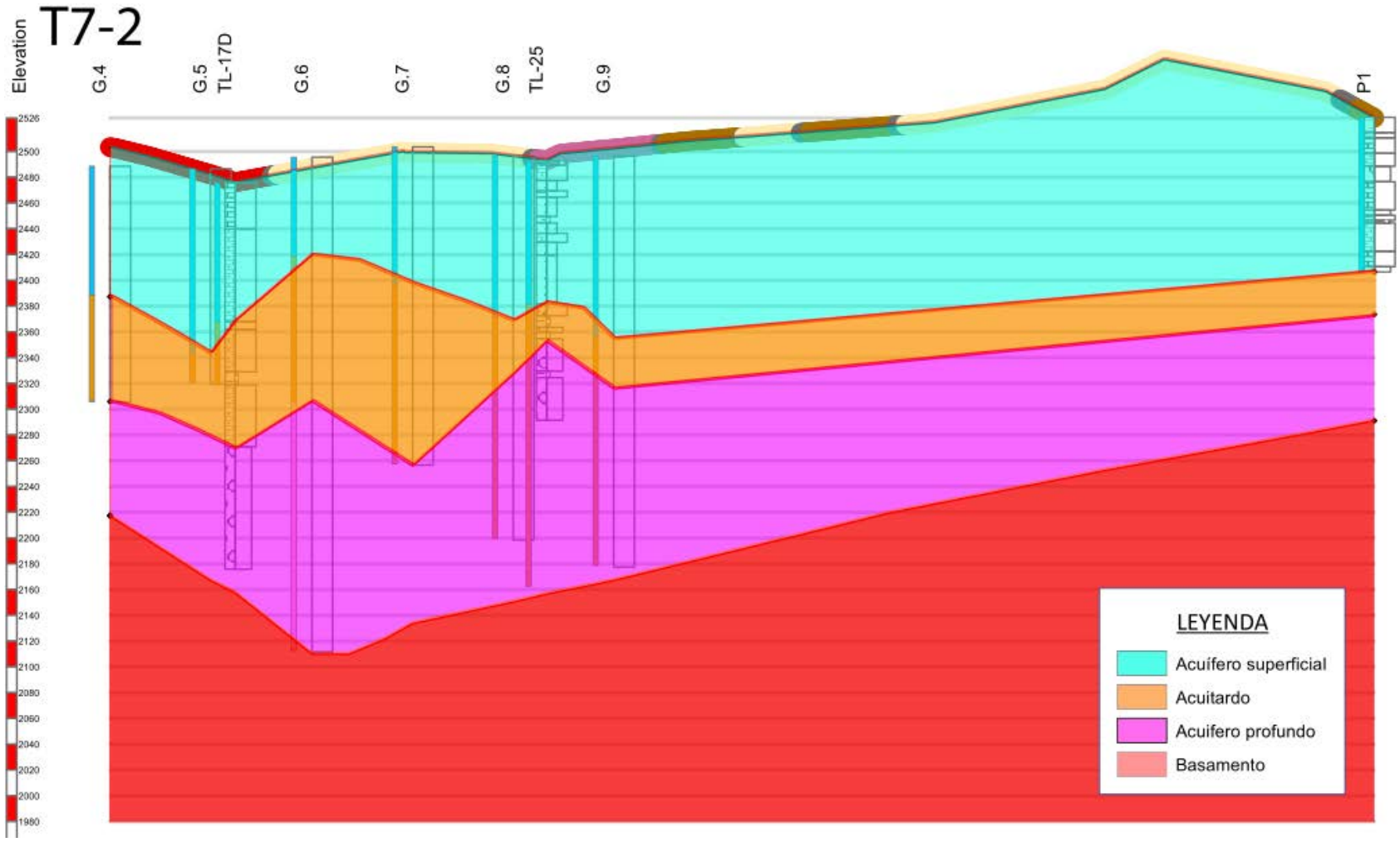
T7-2
Elevation
G.4
G.5
TL-17D
G.6
G.7
G.8
TL-25
G.9
P1
2526
2500
2480
2460
2440
2420
2400
2380
2360
2340
2320
2300
2280
2260
2240
2220
2200
2180
2160
2140
2120
2100
2080
2060
2040
2020
2000
1980
LEYENDA
Acuífero superficial
Acuitardo
Acuífero profundo
Basamento

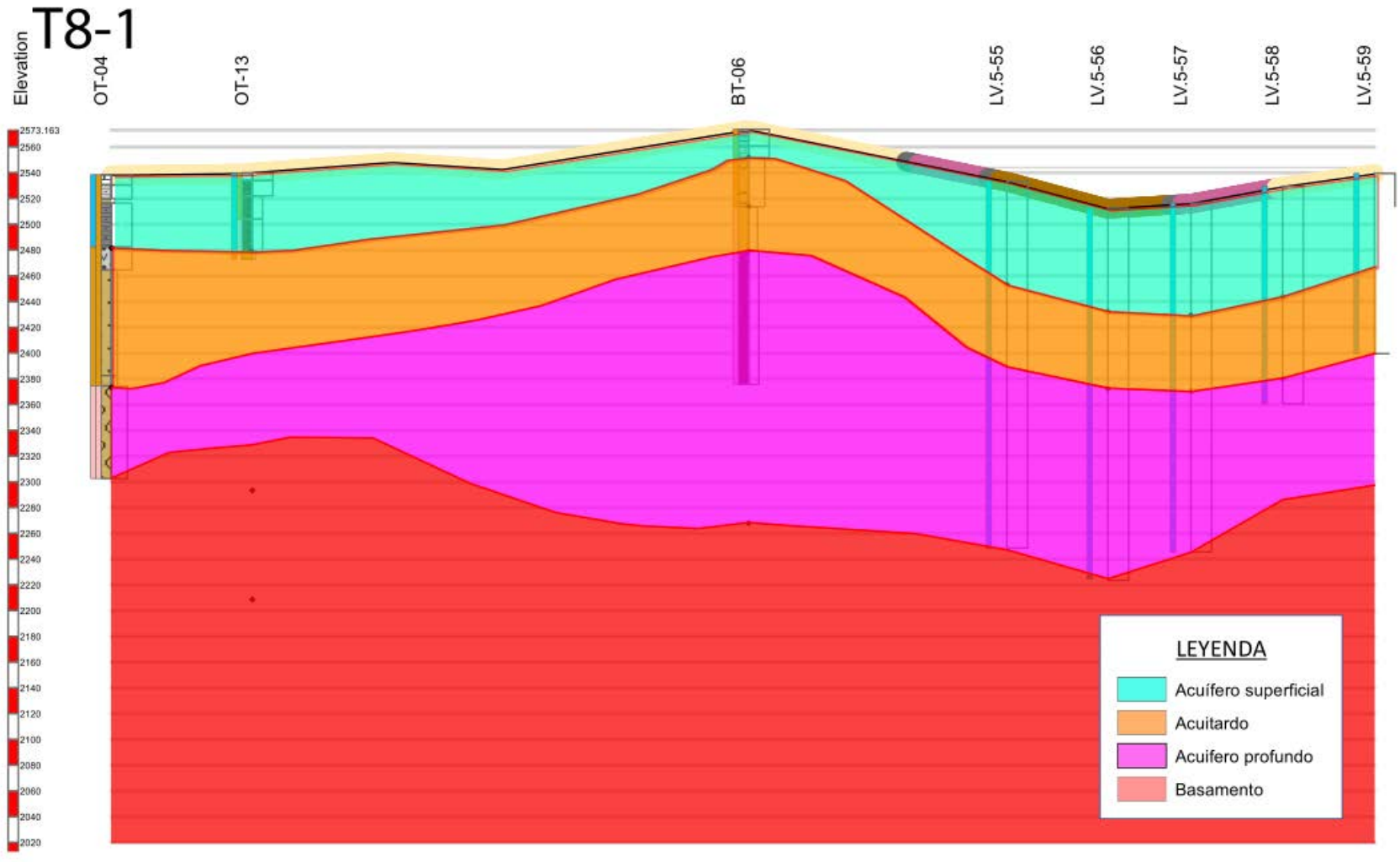
T8-1
Elevation
OT-04
OT-13
BT-06
LV.5-55
LV.5-56
LV.5-57
LV.5-58
LV.5-59
2573.163
2560
2540
2520
2500
2480
2460
2440
2420
2400
2380
2360
2340
2320
2300
2280
2260
2240
2220
2200
2180
2160
2140
2120
2100
2080
2060
2040
2020
LEYENDA
Acuífero superficial
Acuitardo
Acuífero profundo
Basamento

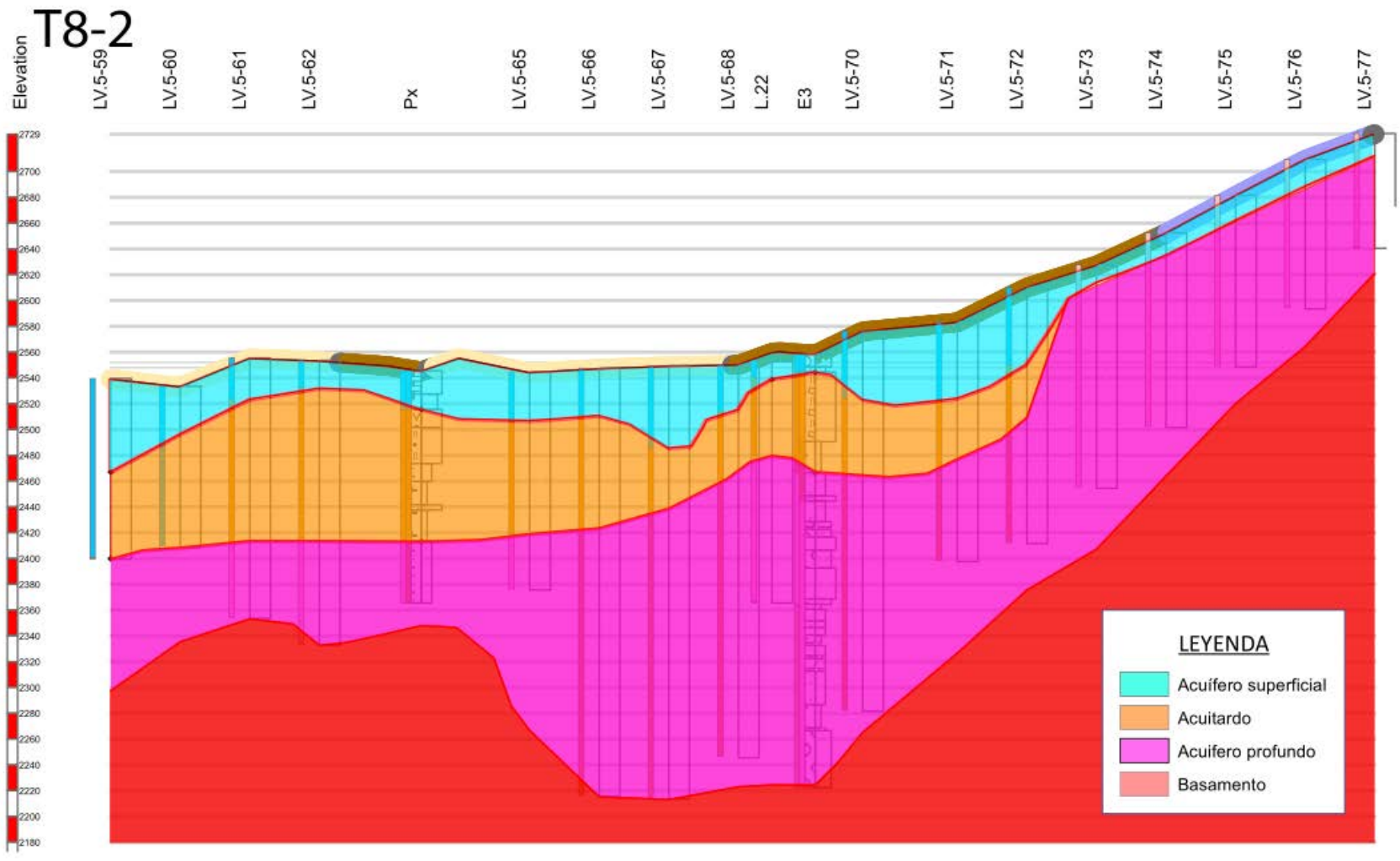
T8-2
Elevation
LV.5-59
LV.5-60
LV.5-61
LV.5-62
Px
LV.5-65
LV.5-66
LV.5-67
LV.5-68
L.22
E3
LV.5-70
LV.5-71
LV.5-72
LV.5-73
LV.5-74
LV.5-75
LV.5-76
LV.5-77
2729
2700
2680
2660
2640
2620
2600
2580
2560
2540
2520
2500
2480
2460
2440
2420
2400
2380
2360
2340
2320
2300
2280
2260
2240
2220
2200
2180
LEYENDA
Acuífero superficial
Acuitardo
Acuifero profundo
Basamento

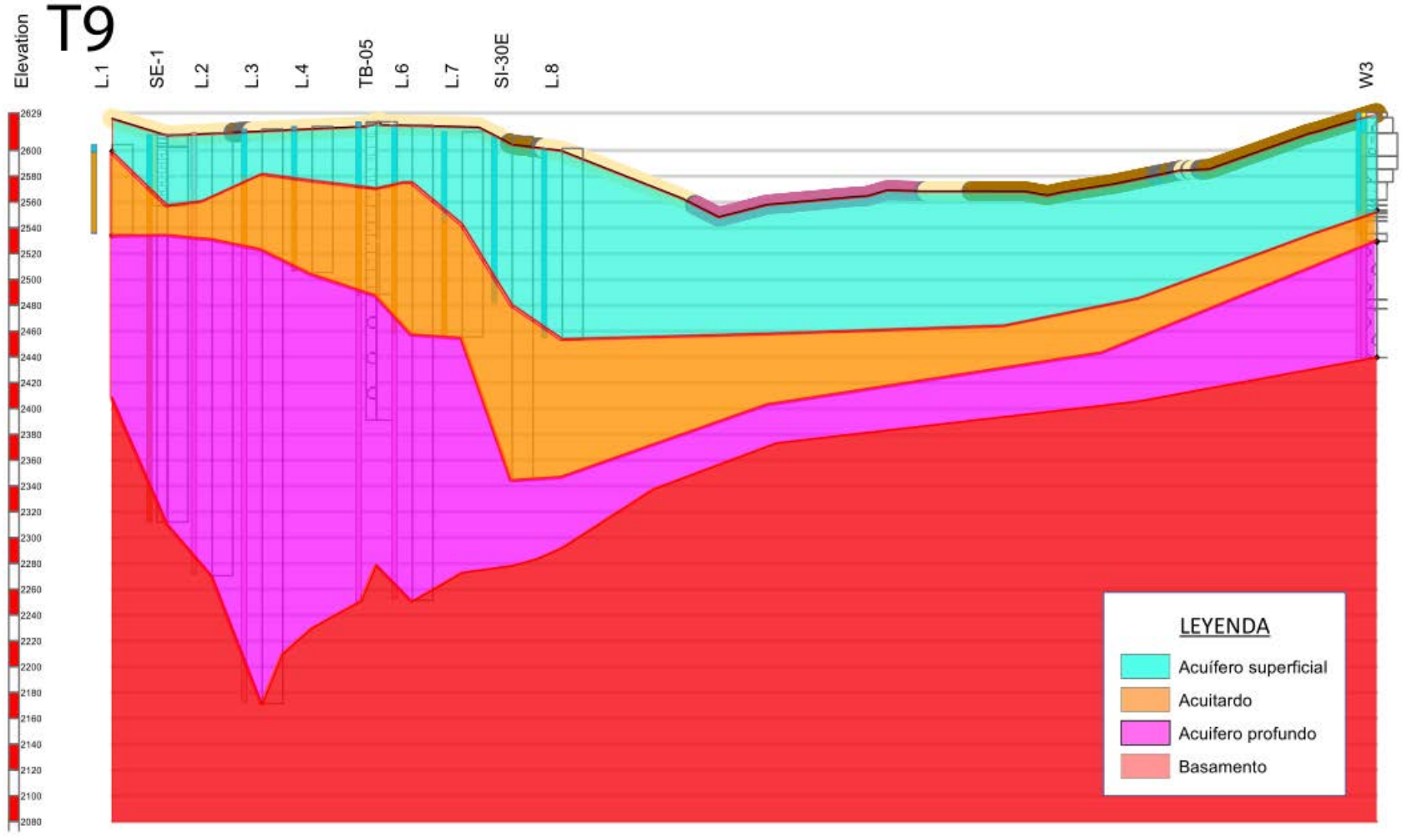
T9
Elevation
2629
2600
2580
2560
2540
2520
2500
2480
2460
2440
2420
2400
2380
2360
2340
2320
2300
2280
2260
2240
2220
2200
2180
2160
2140
2120
2100
2080
L.1
SE-1
L.2
L.3
L.4
TB-05
L.6
L.7
SI-30E
L.8
W3
LEYENDA
Acuífero superficial
Acuitardo
Acuifero profundo
Basamento